2-2019

A Study of the Impact of the Physical Properties of Blood on the Interpretation of Bloodstain Patterns in Forensic Investigations

Ira S. DuBey
The Graduate Center, City University of New York

How does access to this work benefit you? Let us know!

A Study of the Impact of the Physical Properties of Blood

on the Interpretation of Bloodstain Patterns in

Forensic Investigations

By

IRA SCOTT DUBEY

A dissertation submitted to the graduate faculty in criminal justice in partial
fulfillment of the requirements for the degree of Doctor of Philosophy, The City University
of New York

2019

ii

**A Study of the Impact of the Physical Properties of Blood on the Interpretation of
Bloodstain Patterns in Forensic Investigations**

By

Ira Scott DuBey

The manuscript has been read and accepted for the Graduate Faculty in Criminal Justice
in satisfaction of the dissertation requirements for the degree of Doctor of Philosophy.

_____   _____

Date   Thomas A. Kubic, J.D., Ph.D.

                                        Chair of Examining Committee

_____   _____

Date   Deborah Koetzle, Ph.D.

                                        Executive Officer

Supervisory Committee

Nicholas Petraco, MS

John A. Reffner, Ph.D.

Yale Caplan, Ph.D.

Janine Cook, Ph.D.

THE CITY UNIVERSITY OF NEW YORK

iii

ABSTRACT

A Study of the Impact of the Physical Properties of Blood on the Interpretation of

Bloodstain Patterns in Forensic Investigations

By

Ira Scott DuBey

Advisor: Thomas A. Kubic, J.D., Ph.D.

There are many situations when the value of the physical characteristics of blood far

outweighs the information gained from DNA analysis of the bloodstain (Brodbeck, 2012;

Raymond, Smith and Liesegang, 1996). Analysis of bloodstain patterns at crime scenes or on

clothing often provides significant information and serves both as investigative aids and as

evidence presented in court. There has been limited work done to evaluate the potential impact of

variation in the physical properties of blood on the interpretation of blood spatter patterns. This

dissertation will expand on previous work and investigate how changes in the physical properties

of blood, specifically those characteristics that influence flight characteristics and the non-

Newtonian properties of the blood, may affect the bloodstain patterns and therefore the

interpretation of these patterns during crime scene reconstruction. These properties include

surface tension, viscosity, and density (Raymond et al, 1996).

ACKNOWLEDGEMENTS

This dissertation is dedicated to my parents Edward and Berenice DuBey, who always wanted to say "my son the doctor."

My sincerest thank you to all of the dedicated individuals who assisted and guided me through this long, challenging journey.

To my family, Renee, Michael & David, who provided unwavering support and encouragement including assisting me with shooting simulations, administrative review and especially keeping me motivated during difficult times. My brother, Ken DuBey, for taking the time to "debug" my computer issues and keeping me sane at the same time.

A special thank you to friends including Daniel Weir who worked tirelessly as my "wing man" assisting me with never-ending blood spatter simulations and calculations, Dr. Mike Cook who graciously allowed me to use his property for shooting simulations and Susan Weymouth for her superb computer skills, especially with formatting pictures.

My deepest appreciation and gratitude to Dr. Janine Cook's continuous guidance on formatting and assisting with viscosity experiments. Your expertise, unwavering support, patience and constantly positive attitude was invaluable to me and I will always be thankful for all that you have done to support me through this project.

To my Dissertation Committee members, a sincere thank you to Dr. John Reffner for your helpful guidance and support especially during challenging times and Nick Petraco for graciously stepping in when Dr. DeForest was unable to be on the committee for health reasons.

Dr. Yale Caplan and Dr. Peter DeForest for their ongoing encouragement and guidance.

Lastly, I must express my profound gratitude to Dr. Thom Kubic. You have been a true

mentor to me in every sense of the word, for your dedication and countless hours of

guidance, advice, counseling and motivating discussions. This accomplishment would not

have been possible with you.

TABLE OF CONTENTS

List of Tables

xiii

List of Figures

xviii

Chapter 1. The Problem

Crime scene reconstruction, especially in crimes of violence, often relies on an interpretation of blood spatter patterns at a crime scene. The patterns may help in determining the sequence of events as well as the location of the perpetrator(s) relative to the victim(s). This interpretation is typically based on the blood spatter pattern that is produced when blood is cast off of a weapon and onto a surface, which is a dynamic situation, or when blood comes directly from a primary source onto a surface, a passive situation. Bloodstain pattern analysis takes into consideration how the bloodstains were formed and makes assumptions regarding the physical characteristics of human blood. The information provided by an evaluation of bloodstain patterns may include the nature of the weapon that was used, the number of blows sustained by the victim(s), the position of and the movements of the victim(s) and assailant(s) during and after the attack, the sequence of wounds, whether there is more than one crime scene, and other information. When this information is combined with all of the available physical evidence, it may allow for a reconstruction of the events prior to, during, and following the event. Bloodstain pattern analysis is a scientific endeavor employing the principles of biology, physics, and mathematics in the analysis.

The three basic categories of bloodstain groups were classified by MacDonell in 1971 and were based on the correlation between the velocity of the impacting force generating the blood droplets and the size of the resulting bloodstains.

1. Low velocity impact spatter is created when a source of liquid blood is subject to a force with a velocity of up to 5.0 ft/s. Primary stains measuring 3.0 mm or greater in diameter are indicative of gravitational force only.

1

2. In medium velocity impact spatter, bloodstains are created when a source of liquid blood is subject to a force with a velocity between 5.0 and 25.0 ft/s. Primary stains have a diameter between 1.0 and 3.0 mm and are indicative of blunt force trauma.

3. In high velocity impact spatter, bloodstains are created when a source of liquid blood is subject to a force with a velocity greater than 100.0 ft/s. The primaries stains measure 1.0 mm or less in diameter and are indicative of firearms, explosions, and high speed machinery (MacDonell, 1971). This classification based on velocity is no longer used; it has been replaced by the taxonomy described below.

James in 2005 developed a logically configured taxonomic key for bloodstain patterns (James et al., 2005). The primary bloodstain pattern categories are as follows: passive/gravity, spatter, and altered. The sub-categories for these are:

- Passive/Gravity: contact, drop(s), flow, saturation/pooling, and free falling volume. All of these bloodstain patterns are formed under the influence of gravity.

- Spatter: impact, secondary, and projection mechanisms. The bloodstains in this category result from active events such as gunshot and cast-off from an object, such as a knife or bat (Brodbeck, 2012).

- Altered: clotted, diluted, dried, diffused, insect artefacts, sequencing and void patterns (James et al., 2005)

There is a further refinement of the spatter mechanisms as follows:

- Spatter – secondary mechanisms: satellite spatter;

- Spatter – impact mechanisms: gunshot, beating/stabbing, power tools, etc.; and

- Spatter – projection mechanisms: cast-off, arterial and expired (James, et al., 2005).

The interpretation of blood pattern spatter relies upon the pattern that the blood makes when it impacts a surface. The contact surface characteristics may render the pattern to be of little or no value in reconstruction and is an important consideration in evaluating which stains are useful for this purpose. The angle of impact is calculated based on a trigonometric calculation of the arcsine of the width divided by the length of a blood spatter. An investigator would determine these angles from a number of blood spatters and then reconstruct by triangulation of the trajectories to determine the point at which those blood spatters originated, for example the position of a knife or bat from which the blood was cast off at the time it changed direction. The assumptions are based on "normal" blood's physical and biological parameters.

The use of blood spatter analysis (BSA) as an aid in the reconstruction of crime scenes was used by Dr. Paul Kirk in the State of Ohio vs. Samuel Sheppard murder case in 1955. In his affidavit, Dr. Kirk described the position of the accused and the victim at the time the blood spatter was produced (Bevel & Gardner, 2002; James et al., 2005). In 1971, Herbert Leon MacDonell co-authored *Flight Characteristics and Stain Parameters of Human Blood* with Bialousz (MacDonell & Bialousz, 1971). The research for the book was funded by a Law Enforcement Assistance Administration (LEAA) grant. Also in 1971, MacDonell authored Interpretation of Bloodstains – Physical Considerations in Legal Medicine (MacDonell, 1971). In 2002, the Federal Bureau of Investigation (FBI) funded the formation of a scientific working group on bloodstain pattern analysis, SWGSTAIN (James et al., 2005).

Blood is a fluid with a suspension of solid particles in the plasma liquid component (Ciofalo et al., 2002). There are three types of formed cellular elements in blood - red blood cells (erythrocytes), white blood cells (leukocytes), and platelets (thrombocytes). The cellular potion of the blood is approximately 45% of the total blood volume and the plasma portion is

3

approximately 55% (Rodak, 2002). Erythrocytes contain hemoglobin and transport oxygen from the lungs throughout the body. There are about 30 trillion erythrocytes circulating in the normal human blood at any given time. Leukocytes serve to defend the body against bacteria, viruses, and microorganisms. Leukocytes can be divided into granulocytes and nongranulocytes. Granulocytes are further divided into neutrophils, eosinophils, and basophils. Nongranuloctes include lymphocytes and monocytes (Dailey, 2001). There are about 430 billion leukocytes circulating in the normal human blood at any given time. Thrombocytes play a major role in hemostasis and control bleeding by blood clot formation. Plasma provides the medium for circulation of the cellular components of blood as well as other solutes. Plasma is comprised of approximately 90% water, 8% soluble protein, and 1% organic acids and salts (Bevel & Gardner, 2002). Albumin accounts for 60% of the plasma protein and contributes to osmotic pressure (Marieb, 2003). If the cellular component of blood is removed, the plasma can be regarded as a Newtonian fluid and has a viscosity of about 1.6 times that of water (Ciofalo et al., 2002).

Biorheology is the study of the fluid dynamics of biological fluid. Vogel defines blood as a complex, multidimensional continuum of a non-Newtonian fluid and viscoelastic solids (Vogel, 1996). A Newtonian fluid shows a linear relationship between applied shear stress and strain rate. In non-Newtonian fluids, the shear stress and strain rate are nonlinear; therefore, there is no constant coefficient for viscosity (Vogel, 1996). Blood is a non-Newtonian fluid with its suspension of cells in plasma and a dynamic viscosity that is not dependent on shear strain rate; therefore, the shear stress is not proportional to the shear rate (Eckmann et al., 2000). Blood exhibits viscoelasticity, elasticity, thixotropic response, and shear thinning. The microdynamics of the erythrocytes account for the viscoelasticity, thixotropic, and shear thinning of blood (Ciofalo et al., 1999).

4

Drop formation of a non-Newtonian fluid can be attributed to surface tension, cohesion, and viscosity (Wonder, 2001). In the absence of any opposing forces, surface tension will form a drop of liquid into a sphere, which offers the smallest surface area for a specific volume and prevents the droplet from separating (Dillard & Goldberg, 1978). The flight of the blood droplet through air and the shape of the stain on the receiving surface are directly influenced by surface tension (Raymond, 1997). Relative density (d, specific gravity) for a fluid is the measure of its weight per unit volume, expressed as $d = m/v$, where m = mass and v = volume. Whole human blood has a density of 1.060 g/cm^3, which is 6% greater than water (James et al., 2005). The frictional force that exists between adjacent layers of fluids as they move past one another creates the resistance to flow. A deformation (shear strain) occurs when force (shear stress) is applied to a volume of material (Chaplin, 2007). Increasing the concentration of a dissolved substance in a fluid generally increases the viscosity. For example, an increase in the number of erythrocytes in a volume of plasma makes the blood thicker and increases its viscosity (Chaplin, 2007).

Hematocrit or packed cell volume is the percentage of the volume of red blood cells in relation to the volume of plasma (Rodak, 2002). "Normal" adult hematocrit values range from 35% to 54% (Dailey, 2001). Hematocrit value is important because blood viscosity is considered to be a function of the hematocrit value (Raymond, 1997; Bevel et al., 2002). As the hematocrit value increases, there is a disproportional increase in blood viscosity; a 50% increase in the hematocrit value can result in a 100% increase in viscosity (Kalbunde, 2005).

Plasma is the portion of the blood in which the cellular elements are suspended. A change in plasma viscosity affects blood viscosity regardless of the hematocrit. Plasma is a Newtonian fluid; its viscosity is independent of shear rate. The level of plasma viscosity is increased in

pathophysiological conditions and is closely related to the protein content of plasma (Baskurt et al., 2003).

The use of bloodstain pattern analysis as an aid in crime scene reconstruction may provide much useful information, including areas of convergence and origin of bloodstains, type and direction of impact, and mechanisms by which bloodstains and patterns were produced. This information affords an understanding on how blood was deposited onto particular items; the position of the victim, assailant, and items located within the scene relative to one another during the event; and possibly the movement of the victim, assailant, or other items post event. This additional information, along with post mortem findings, will support or contradict statements. The evaluation of the information determined from the bloodstain pattern analysis must be further evaluated in conjunction with all other physical evidence before concluding the sequence of events and the crime scene reconstruction (Raymond et al., 2001; Bevel & Gardner, 2002; James et al., 2005).

There has been little work done on how changes in the physical properties of blood may have an impact on bloodstain patterns. Physical properties of blood may change when an individual has a blood disorder or disease or when an individual is taking certain therapeutics. In an aging population, the incidence of individuals developing blood disorders increases, and likewise, more individuals are prescribed therapeutics for these conditions. Additionally, it is reasonable to assume that some victims of violent crime will fall into this category.

This research study evaluated changes in the physical characteristics of blood and how this impacted the interpretation of bloodstain patterns in forensic investigations. The principal question is whether the blood spatter pattern calculations are valid in situations where the physical properties of blood are different from what is typically classified as normal. That is, do

6

changes in the physical and biological characteristics of the donor's blood cause the blood spatter pattern to be modified, whereby the angle calculations and interpretation of the scene are incorrect, possibly resulting in an erroneous conclusion as to the reconstruction of events by the crime scene investigator?

The Significance of the Problem

The conclusions that a crime scene investigator makes regarding blood spatter patterns are based on the assumption that the physical properties of blood are constant or normal. The question of whether blood was not in the normal range of physical parameters, possibly as a result of disease or therapeutic agents, has yet to be considered and reported thereon. Could these factors have an influence on the bloodstain patterns produced by the blood and therefore on the forensic interpretation of the patterns?

Examples of diseases that impact the physical properties of blood are described below. Hyperviscosity syndrome (HVS) is manifested by increased plasma viscosity typically as a result of increased circulating serum immunoglobulins. HVS can also result from increased cellular blood components, whether white or red blood cells, in a hyper-proliferative state (Hemingway, 2014). In general, hyperviscosity occurs from pathologic changes of the cellular or protein fractions of the blood. Examples of this syndrome include polycythemias, multiple myeloma, leukemia, Waldenstrom macroglobulinemia, sepsis, monoclonal gammapathies, rouleau formation, post splenectomy, altered shape of erythrocytes, antibody-mediated erythrocyte damage, increased leukocyte count, thrombocytosis, hyperlipoproteinemia, hyperfibrinogenemia, hypercyrofibrogenemia, macroglobulinemia, myeloma, amyloidosis, polyclonal hyperviscosity syndrome, Sjogren's syndrome, SLE, lymphoproliferative disorders, hyperglobulinemia

7

associated with cirrhosis, chronic active hepatitis, acute burns, and sickle cell anemia (Adams et al., 2009; Wu, 2006).

Polycythemia, which literally translates into "too many cells in the blood," is a disease state in which the proportion of blood volume that is occupied by red blood cells increases. It can be due to an increase in the number of red blood cells, which is absolute polycythemia, or to a decrease in plasma volume, which is relative polycythemia (Tefferi, 2003).

With rheumatic diseases, increased plasma viscosity has been identified, such as in patients with rheumatoid arthritis. The average increase in plasma viscosity in active chronic cases was 11%, 30% in subactive cases, and 60% in acute cases (Walitza, 1980).

Elevations in plasma viscosity also correlate to the progression of coronary and peripheral artery diseases (Kesmarky, et al., 2008).

Though not a focus of my research, studies on therapeutic agents that alter blood physical characteristics can provide insight because research on disease states with altered blood physical characteristics is limited. Examples of therapeutic agents that have an effect on the physical properties of blood are described below.

Warfarin is a widely prescribed drug used to prevent the formation and migration of blood clots. It is the most extensively prescribed anticoagulant drug in North America with annual prescriptions in the United States of approximately 2 million (Holbrook et al., 2005). Warfarin inhibits the vitamin K-dependent synthesis of biologically active forms of the calcium-dependent clotting factors II, VII, IX, and X, as well as the regulatory factors protein C, protein S, and protein Z. Warfarin does not affect the viscosity of blood (Ansell et al., 2008; Freedman, 1992).

Erythropoietin (EPO) is a naturally occurring hormone that stimulates red blood cell production. Recombinant EPO (rEPO) is a synthetic version of this hormone (Waite & Fine, 2007). EPO therapy is utilized in a number of medical conditions, including anemia and platelet disorders, where it is thought that EPO may increase platelet numbers (Harmening, 1997).

The effect of changes in the physical properties of blood and the possible impact of blood disorders on blood pattern analysis is an underexplored area within the field of forensic science and requires further scientific investigation due to bloodstain analysis' inclusion in legal proceedings (Brownson & Banks, 2010). This research studied the physical properties of blood and the potential impact of variations in the physical properties on bloodstain patterns in forensic investigations. The significance of the problem could be great if blood that is outside the normal range of physical properties behaves in a manner such that incorrect conclusions could be made from crime scene investigations utilizing blood spatter patterns.

Past Work Related to the Problem

There have been a number of papers published that discuss the droplet flight and impact dynamics of blood; however, none mention the potential errors introduced into the calculations by uncertainties in the biological and physical properties of blood (Rogers, 2009). Rogers reached the following conclusions based on her hematocrit research. There is a significant difference between the determination of x, y, and z coordinate blood spatter values for the varying blood hematocrit values. The calculated coordinate values are within "acceptable industry limits" (Carter et al., 2006). The hematocrit value was found to affect the width and length of the resultant bloodstain; however, a proportional relationship exists such that the hematocrit value does not affect the width to length ratio, and therefore, the calculated impact angle (Rogers, 2009). As the hematocrit value decreased, stain width and length both increased.

9

The effect of hematocrit value on impact angle calculations is statistically significant, but there is close agreement between the known and calculated impact angles irrespective of the hematocrit value. Rogers found that the error associated with impact angle calculations for bloodstains created using a blood hematocrit range of 11.2% to 68.9% falls within variation stated in the literature (Rogers, 2009; Laturnus, 1994; Berel & Gardner, 2002; James et al., 2005). Rogers concluded that the hematocrit value significantly affects the bloodstains length and width (Rogers, 2009).

Further study is required to evaluate the distribution and size of bloodstains as a function of hematocrit value and applied force and to determine what the impact of changes in the physical properties of blood would have on resultant spatter from a gunshot.

Because there is limited work related to the problem of how changes in the physical properties of blood may impact bloodstain pattern analysis, investigators have studied certain therapeutic agents and illicit drugs for their ability to produce altered blood physical characteristics. The addition of amphetamine to blood at therapeutic to potentially lethal doses resulted in a decrease in its dynamic viscosity over the range of 0.5 to 11.0%, respectively (Brownson & Banks, 2010). The conclusions from this study were that the physical parameters of blood that are presumed to be constant within forensic applications of bloodstain pattern analysis play a large role in their interpretation and may have implications in pattern analysis (Brownson & Banks, 2010).

El-Sayed, Brownson, and Banks have studied the effect of warfarin, an anticoagulant that is used to prevent thrombosis and embolism, on bloodstain pattern analysis (El-Sayed et al., 2011). In their study, blood samples were spiked with varying concentrations of warfarin and the dynamic viscosities were measured (El-Sayed, 2011). The study concluded that "it is evident that

10

the inclusion of warfarin results in a change in blood viscosity and surface tension, resulting in changes to the calculated angles, heights, and impact velocities of resulting bloodstains when utilizing bloodstain pattern analysis to construe such information; however, the alterations incurred appear insignificant in our case, thus in terms of an observable alteration in the interpretation of bloodstain pattern analysis, this is likely highly improbable." (El-Sayed, 2011). Since blood is a non-Newtonian fluid, the reduction in viscosity from the presence of warfarin will change the way blood flows and this may have implications in spatter or droplets that result from a gunshot (El-Sayed, 2011).

The potential impact of changes in the physical properties of blood and how this may impact the interpretation of blood spatter produced from the impact of a projectile fired from a firearm into tissue was investigated as part of this research study. The El-Sayed paper notes that the energy transfer from a bullet striking a blood source causes the blood to disintegrate into small droplets. Changes in blood surface tension and viscosity could alter this disintegration process and the droplet size.

The full implications of changes in the physical properties of blood, including alterations in blood viscosity, surface tension, and density, require further investigation to understand what impact there would be on the interpretation of bloodstain patterns.

Research Approach

This research expanded upon previous work that evaluated how certain biological variations in blood impacted the physical characteristics of blood, and therefore, modify resultant blood spatter patterns. The physical characteristics evaluated were hematocrit, complete blood count, viscosity, contact angle, and relative density. Other evaluations included the concentration, type, and frequency of cellular components and protein concentrations.

11

Components of the study.

The physical properties of blood were be modified by changing the cellular and/or plasma portion of blood samples. Human blood containing an anti-coagulant, sodium heparin, was used in this study. Pizzola and De Forest compared blood containing heparin to freshly drawn blood without heparin; no statistically significant difference was noted with regards to density, surface tension, or viscosity (Pizzola, Roth, & De Forest, 1986).

Blood spatter studies.

For blood spatter studies, human blood specimens of very high density, high density, normal, low density, and very low density were used. These specimens were used in all of the evaluations. Additional specimens were added based on the need to further refine the values.

Instrumentation.

The ADVIA® 120 System hematology analyzer (Siemens Healthineers, Erlangen, Germany) was used for the measurement of hematocrit, complete blood count, differentials, and other cellular components. An Anton Paar DMA 35 density meter (Anton Paar, Graz, Austria) was used for the measurement of the relative density of the blood samples (Rosencranz & Bogen, 2006). An Anton Paar MCR 302 rheometer was used to measure viscosity of the blood samples.

Software for BSA.

Virtual stringing methods to determine the area of convergence or region of origin are equivalent to manual stringing methods transposed onto a computer. The HemoSpat® (FORidnet Software, Ottawa, ON, Canada) bloodstain pattern analysis software and digital measurements of bloodstains was utilized in this study (Hakim & Liscio, 2015; Carter et al., 2006).

Passive/Gravity.

12

The first evaluation consisted of allowing a drop of blood formed using a serological pipette to fall only under the influence of gravity onto a smooth paper target. Blood was dropped from a height of 150 cm to avoid any issues associated with oscillating blood droplets because oscillations have been reported to dampen after 40 cm for passive drops (Raymond et al., 1996). The target was adjusted to the following angles: 10, 25, 40, 55, 70, and 90°. The five human blood specimens of varying densities were used to form spatter patterns at each target angle with an N of 10 for a total of 300 determinations. The extreme situations were initially evaluated and any impact on blood spatter patterns evaluated. Each bloodstain was measured using a digital caliper and all of the bloodstains were photographed to document their patterns. A statistical analysis was conducted to evaluate any differences in the angels of impact between the different blood densities.

Spatter: impact/cast-off.

The five blood specimens of varying densities were utilized in a simulation of a bat striking the point of origin. Each simulation was repeated five times with blood spatter patterns being evaluated for each event. A minimum of 10 bloodstains were created for each simulation and trajectories determined from these. This evaluation included both manual and digital measuring. The process for digital measurements is as follows. A numerical scale was affixed to the wall adjacent to the bloodstain to be measured and the bloodstain was photographed with a digital camera. The digital image was downloaded into the HemoSpat® computer program and the picture was cropped to include the bloodstain and the scale. The middle of the bloodstain was identified. The software program measured the bloodstain, and the resultant data was used for the angle of impact calculations. A statistical analysis was conducted to evaluate any differences between normal blood density and the various high and low blood density spatter patterns on the

13

areas of origin. Statistical evaluation compared calculated areas of origin using a manual string method to the computer generated areas of origin and further compared to the actual areas of origin for each event. This phase of the study required 25 events (simulations) for blood source evaluation for a total of 250 bloodstain evaluations.

Spatter: gunshot.

The five blood specimens of varying densities were used in the gunshot blood spatter phase of the study. A 0.38 caliber S and W Model 15 revolver (Smith & Wesson, Springfield, MA) was used to simulate a gunshot to the head. Each blood specimen was used in each of 10 simulations for a total of 50 simulations. The primary evaluation was the distance the spatter produced from the gunshot travels. Other patterns were also studied. The extent of evaluation depended on the geometry of the bloodstain patterns produced. Statistical analysis and comparison of the normal blood to the other blood specimens were conducted.

Quality assurance.

Quality assurance (QA) of crime scene analysis is a complicated task given the range of potential evidence and the variety of potential scenes. There is no "standard" crime scene or evidence, and items may have been subjected to a variety of factors, environmental and others, prior to the scene being discovered. "Physical evidence cannot be wrong, it cannot perjure itself, it cannot be wholly absent. Only human failure to find it, study and understand it can diminish its value." (Thornton & Kirk, 1974). This thesis recommended an approach to ensure quality assurance during the crime scene investigation and evidence recovery process. In particular, a QA process around bloodstain pattern analysis and documentation was detailed.

Statistical analysis.

A component of this research involved the comparison of manual measurements of the BSA process to digital measurements. The analysis of the data generated from this research was used to determine the impact of the physical properties of blood on the interpretation of bloodstain patterns in forensic investigations. What are the differences and are they statistically significant? Under what conditions or circumstances do they occur? This was related to possible implications of blood disorders on bloodstain pattern interpretation.

Additional areas for research.

An element of scene reconstruction may be evaluating whether disease state blood is present. Is it possible to test the dry bloodstains to evaluate the disease state of the blood donor? One option may be to test bloodstains for the presence of therapeutic drugs used to treat the targeted disease states to elucidate the underlying disease of the victim or source of the bloodstain.

Research Process

The following activities were undertaken in order to accomplish this research study:

1. Obtain human blood components

2. Prepare blood samples for testing

3. Obtain instrumentation for density measurements

4. Utilize instrumentation for cellular component analysis

5. Construct device to be used in passive bloodstain experiments (Study 1)

6. Obtain bloodstain analysis software package

7. Conduct Study 1

8. Data and statistical analysis of Study 1 data

9. Construct room for blood spatter experiments (Study 2)

10. Construct device to produce blood spatter

11. Obtain additional human blood components

12. Prepare blood samples for Study 2 testing

13. Conduct Study 2

14. Data analysis of the manual string method and computer modeling

15. Statistical analysis of data

16. Construct bloodstain collection unit for gunshot experiments (Study 3)

17. Conduct Study 3

18. Data and statistical analysis

19. Discussion and conclusions

Chapter 2. Study 1: Passive/Gravity

The purpose of this study was to analyze the statistical relationship between the changes in the physical properties of blood, bloodstain geometry, and angle of impact determinations. Five different blood samples were utilized and the angles of impact were calculated at the following target angles: 10, 25, 40, 55, 70, and 90°.

Preparation of Blood Samples

Human blood components were purchased from BioreclamationIVT (BioIVT, Hicksville, NY) and consisted of the following:

- 50 mL of human whole blood with sodium heparin added as anticoagulant (Figure 1),

- 25 mL of human red blood cells with sodium heparin added as an anticoagulant (Figure 2), and

16

- 25 mL of unfiltered human serum (Figure 3).

All of the human blood components were tested and found to be negative for the following: HIV 1/2 Ab, HCV Ab (hepatitis C), non-reactive for HBsAg (hepatitis B), HIV-1 RNA, HCV RNA (hepatitis C), HBV DNA, WNV RNA, ANTI-T CRUZI, and STS (syphilis). (Certificates of analysis are contained in the Appendix.) All blood was stored at 4 $^{\circ}$C until use.

Figure 1. Human whole blood

Figure 2. Human red blood cells

17
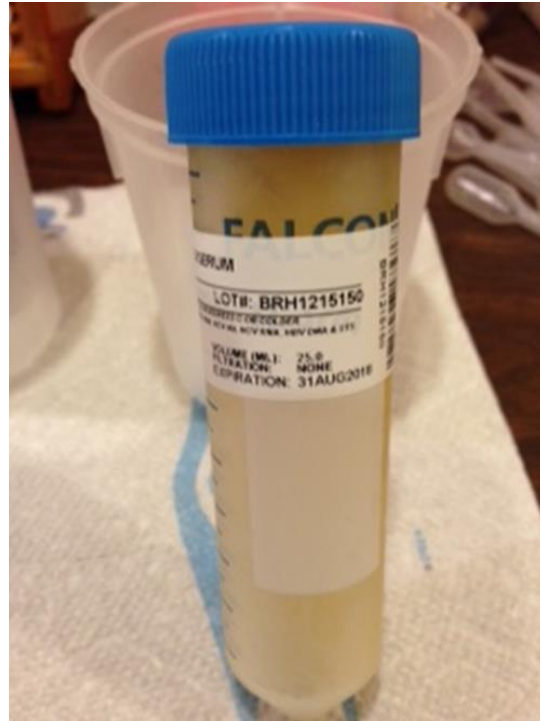
Figure 3. Human serum

The whole blood was centrifuged to separate the cellular components from the plasma using a Model 614B Drucker Laboratory centrifuge (Drucker Diagnostics, Port Matilda, PA). A total of nine blood samples were prepared by combining the cellular whole blood components with serum in the proportions noted in Table 1.

Table 1. Blood sample preparation for Study 1

Sample #	Cells, %	Cells, mL	Serum, %	Serum, mL
1	5	0.5	95	9.5
2	10	1.0	90	9.0
3	15	1.5	85	8.5
4	20	2.0	80	8.0

18

5	40	4.0	60	6.0
6	80	8.0	20	2.0
7	85	8.5	15	1.5
8	90	9.0	10	1.0
9	95	9.5	5	0.5

Hematocrit

For each of the nine samples, the hematocrit (HCT) was determined using the ADVIA 120 Siemens hematology analyzer (Figure 4 and Table 2). The HCT or packed cell volume (PCV) is the volume of red blood cells in relation to the volume of plasma (Rodak, 2002). The instrument data printouts are included in the Appendix.

Figure 4. Siemens ADVIA® hematology analyzer

19

Table 2. HCT determinations of the prepared blood samples

Sample number	HCT, %
1	4.4%
2	8.0%
3	11.7%
4	15.4%
5	32.5%
6	67.0%
7	73.0%
8	Measurements not available for 8 and 9
9	Instrument filter issues

Density

For each of the nine blood samples, the density was determined by using an Anton Paar DMA 35® density meter (Figure 5). The density meter utilizes Anton Paar's oscillating U-tube technology. The sample is introduced into a U-shaped borosilicate glass tube using a disposable syringe. The tube is excited to vibrate electronically at its characteristic frequency. The characteristic frequency changes depending on the density of the sample (Anton Paar, 2012). The density measurements, as shown in Table 3, were taken at 37 ºC.

20

Figure 5. Anton Paar Portable Density Meter DMA 35

Table 3. Density determinations

Sample Number	Density, g/cm³ at 37 ºC Mean , N=3	Standard Deviation (SD)
1	1.0272	0.0001
2	1.0274	0.0001
3	1.0299	0.0007
4	1.0339	0.0027
5	1.0455	0.0005
6	1.0677	0.0003
7	1.0710	0.0020

Five blood samples were selected from the prepared samples to be used in Studies 1-3.

The sample designations are listed in Table 4.

21

Table 4. Sample density designations

Sample number	Sample Designation - Density
1	VL: very low
3	L: low
5	N: normal
6	H: high
7	VH: very high

Viscosity

Viscosity measurements of the five blood samples of varying density were carried out using a MCR 302 Rheometer (Anton Paar, USA) (Figure 6). The samples were loaded onto the bottom plate using disposable Pasteur pipettes (Figure 7). The temperature was set at 37 ^{o}C and maintained at this temperature using the peltier temperature-controlled plate. The rheometer uses a cone-plate system, and the rotational test was carried out at a shear rate range from 5 s^{-1} to 500 s^{-1} at a constant temperature of 37 ^{o}C (Figure 8). The data are presented in Figure 9; the blood samples labelled 1 through 5 correspond to (1) very low density, (2) low density, (3) normal density, (4) high density, and (5) very high density. To properly characterize the blood samples at all five densities, two measuring systems were utilized - a cone with a 50 mm diameter for the less dense samples (1, 2, and 3) and a plate with a 25 mm diameter for the more dense samples (4 and 5). For the flow curve, the viscosity is measured as a function of shear. Blood is a non-Newtonian fluid and it is shear thinning; as shear increases the viscosity decreases. The results of the analysis clearly show that the higher the density, the higher the viscosity. All five blood samples showed a decrease in viscosity as the shear increased.

22

Figure 6. The MCR 302 Rheometer by Anton Paar
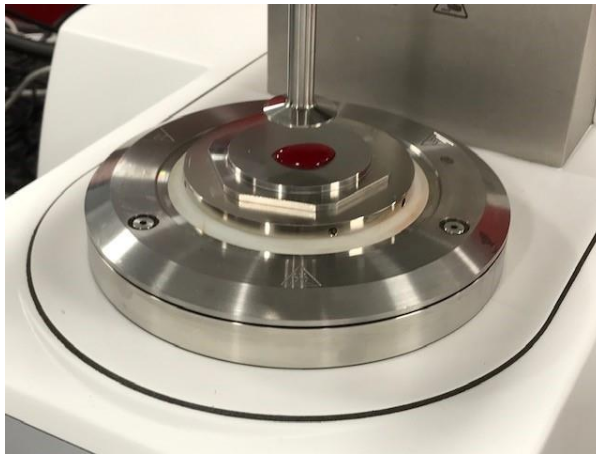
Figure 7. Close up of the spindle with blood drop applied to the MCR 302 Rheometer
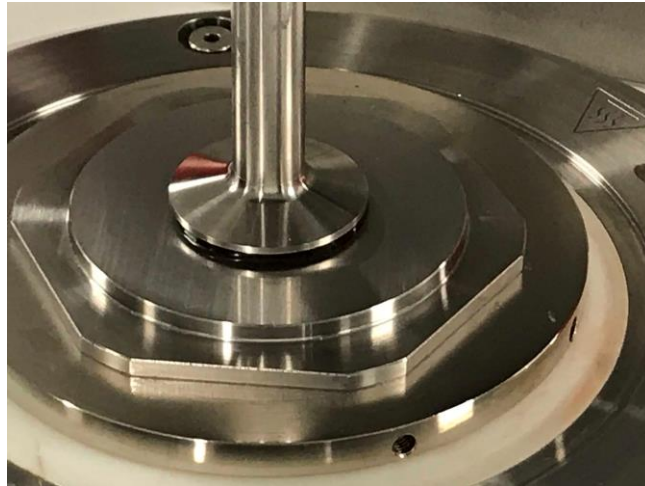
Figure 8. Rheometer in operation
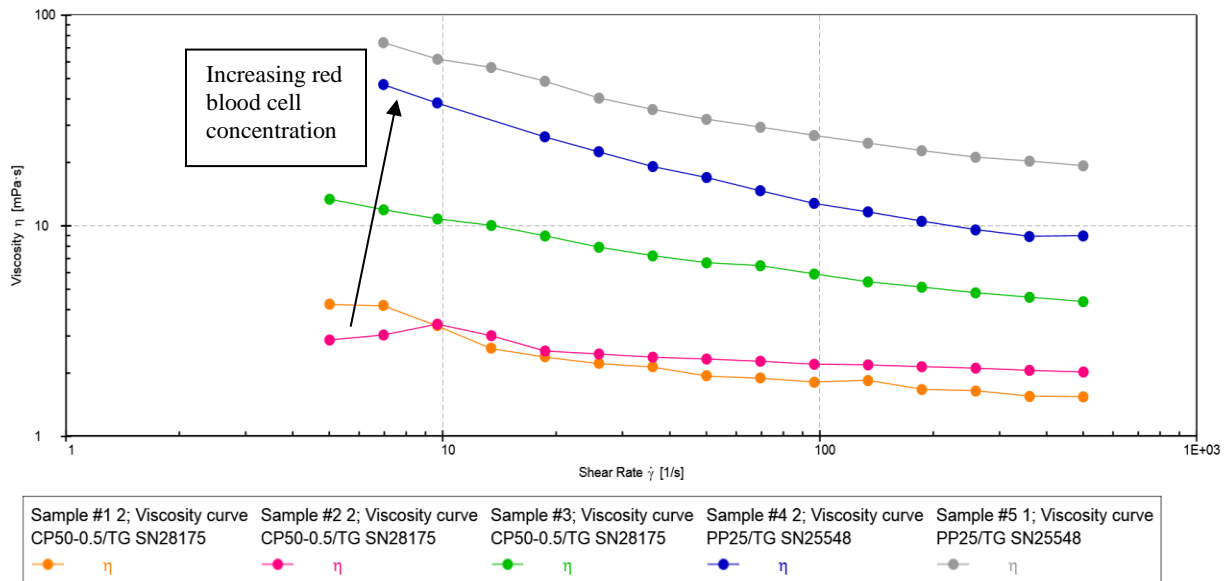
Figure 9. Viscosity of the five blood samples of varying densities at increasing shear rates

Relationship Between Hematocrit, Density, and Viscosity

For Figures 10, 11, 12 and 13, the data points are the five blood samples that were prepared for Study 1. From left to right in the graphs, they are designated as per Table 4 as follows: (1) very low density, (3) low density, (5) normal density, (6) high density and (7) very high density. The corresponding HCT percentages are contained in Table 2. Figure 10 shows the relationship between the density of the blood samples and the HCT of the blood samples. The hematocrit is defined as the volume occupied by erythrocytes in a given volume of blood and is usually expressed as a percentage of the volume of the whole blood sample. (Harmening, 1997) As the HCT increases, the density increases. The R^2 value is 0.9928.

Figure 11 shows the relationship between viscosity at a shear rate of 96.7 s^{-1} to HCT. The viscosity increases significantly above a HCT value of 65%. The R^2 value is 0.9578.

Figure 12 shows the relationship between viscosity at a shear rate of 96.7 s^{-1} to density. The viscosity increases significantly above a density of 1.06 g/cm^3, which corresponds with blood sample number six of the study, which has a density of 1.0677 g/cm^3 (see Table 3). The R^2 value is 0.9774.

Figure 13 shows the relationship between the log of viscosity at a shear rate of 96.7 s^{-1} to density. The R^2 value is 1.0.
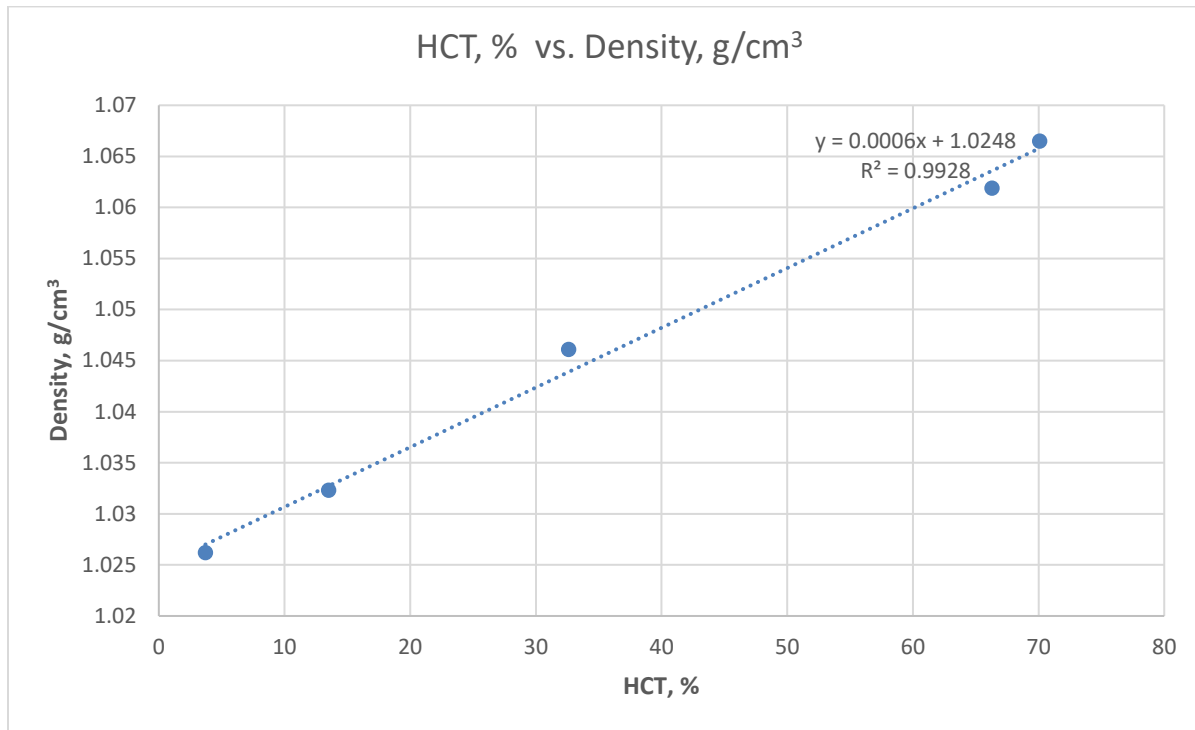
Figure 10. Relationship between density and HCT (hematocrit)
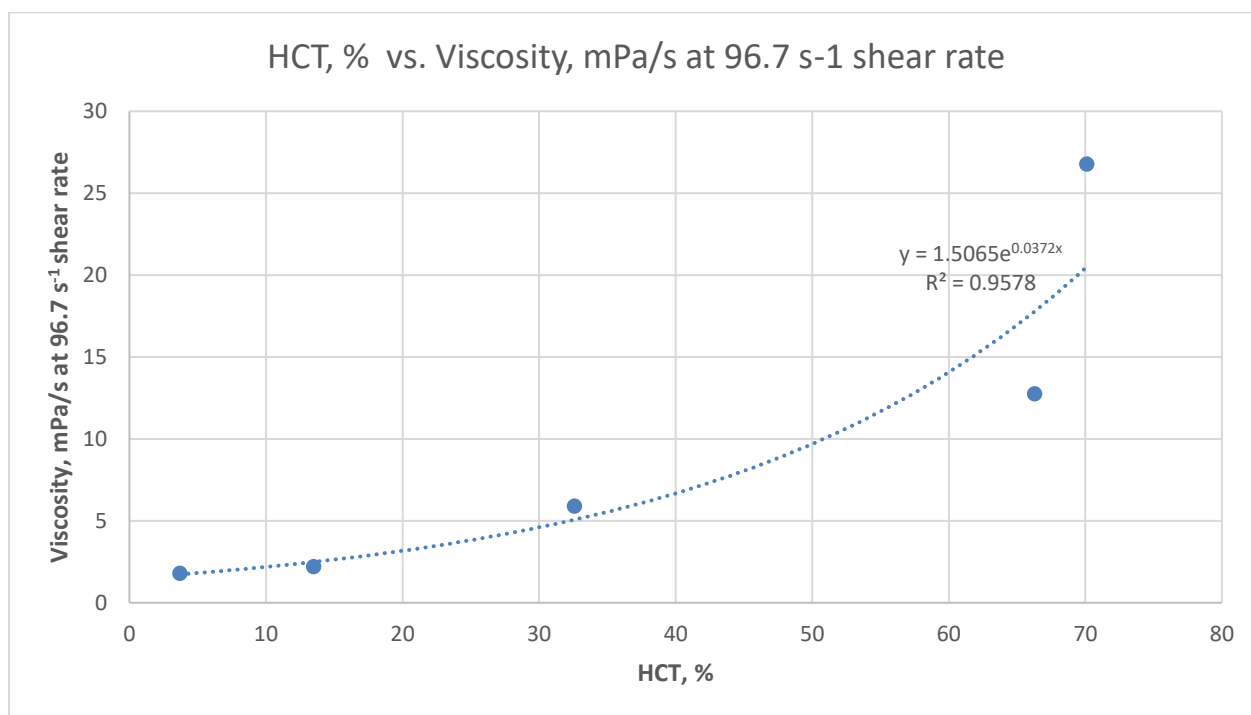
Figure 11. Relationship between hematocrit and viscosity.
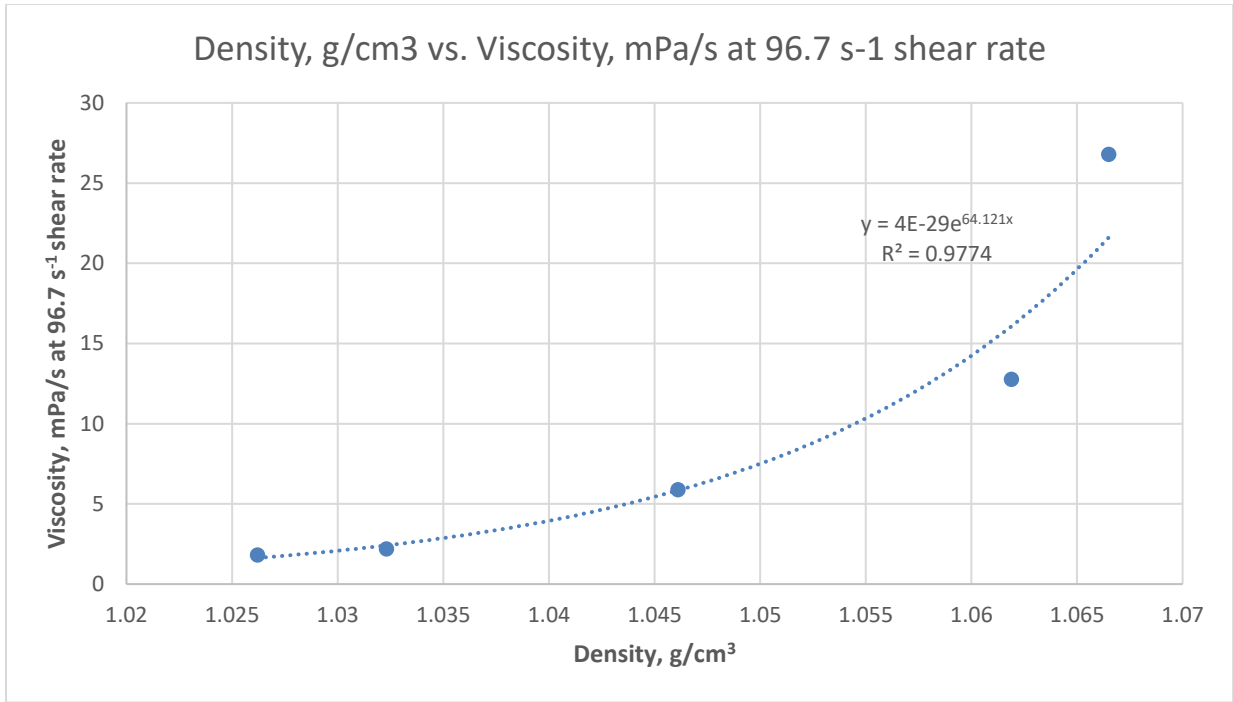
Figure 12. Relationship between density and viscosity
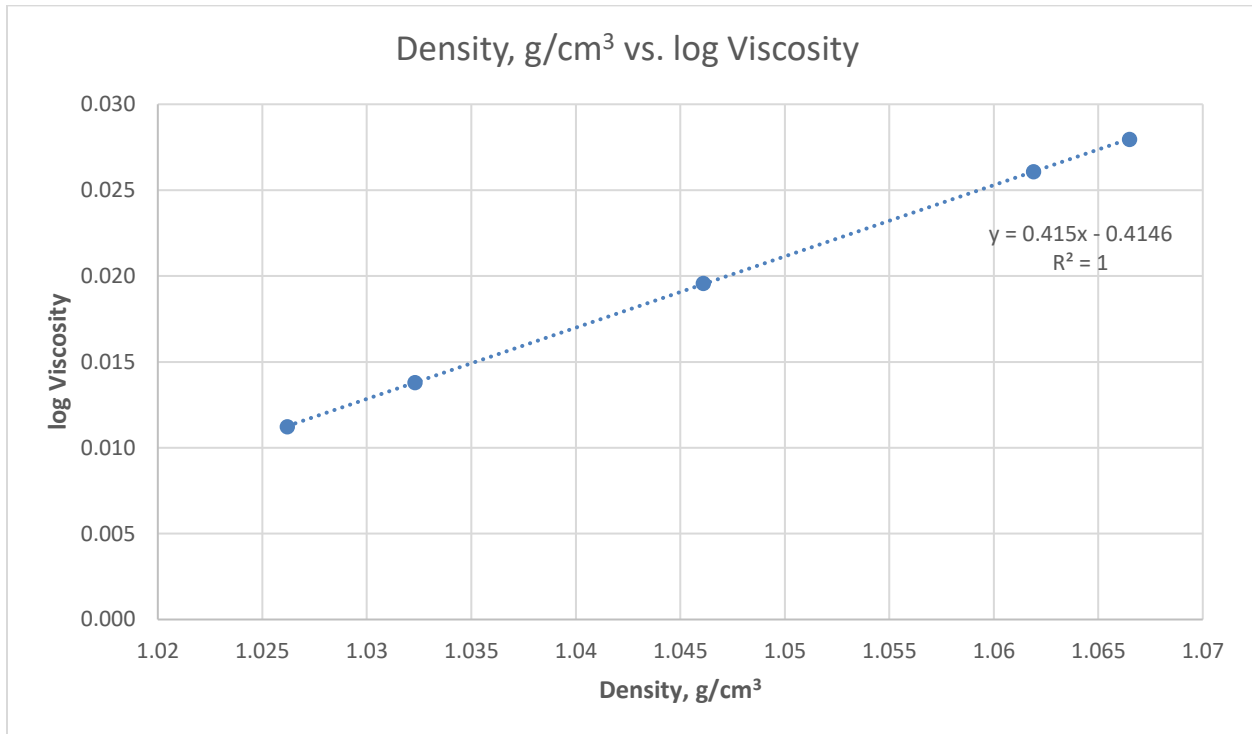
Figure 13. Relationship between log viscosity and density

27

Contact Angle and Surface Tension

Surface tension is the force acting on the surface of a liquid, tending to minimize the surface area. It is often observed as the formation of a meniscus in containers or as the formation of droplets or bubbles on a surface (Mukherjee et al, 2005). Surface tension is an important physical property of blood when evaluating blood spatter, however the surface tension of patient's blood is not assessed in common medical practice (Hrncir & Rosina, 1997). There are a number of approaches to determine surface tension. The capillary rise method determines the surface tension of a liquid by using capillary tubes. When a capillary tube is placed in a fluid, the liquid level in it rises above the normal liquid level. This elevation in the liquid level is a function of the surface tension. Capillary action occurs when adhesion to the wall is stronger than the cohesive forces between the liquid molecules (Mukherjee, 2005). A second method is bubble pressure tensiometry which is based on the measurement of the maximum pressure in a bubble growing at the tip of a capillary immersed into the liquid under study. The pressure required for the separation of the air bubble from the capillary tip, which drops at the air-liquid interfaces, is directly proportional to the surface tension (Zaitsev, 2018). The third method is the drop weight method. In this method the drop weights from any one tip are proportional to surface tensions, it is only necessary to measure the weight of the falling drop. (Woodward, 1912).

The contact angle is a quantitative measure of the wetting of a solid by a liquid. It is defined as the angle formed by a liquid at the three-phase boundary where a liquid, gas, and solid intersect. The Young equation describes the balance at the three phase contact of solid-liquid and gas.

$$Ysv = Ysl + Ylv \cos \Theta y$$

28

The interfacial tensions, which measure the free energy (per unit area) Ysv, Ysl and Ylv

form the equilibrium contact angle of wetting, Θy (Adamson & Gast, 1997). Measurements of

the contact angle of the five blood samples of varying density were obtained on three different

surfaces: polyethylene, acrylic (PMMA), and Teflon (PTFE). The FTIR scans of the materials

are contained in the Appendix (see Table 5).

In order to measure the contact angles of the five blood samples, the following procedure

was followed. The data collection set up consisted of a Cannon EOS 60D camera with a Cannon

180 mm L macro lens on a tripod, which was used to photograph a single drop of blood on a

specific surface (Figure 14).
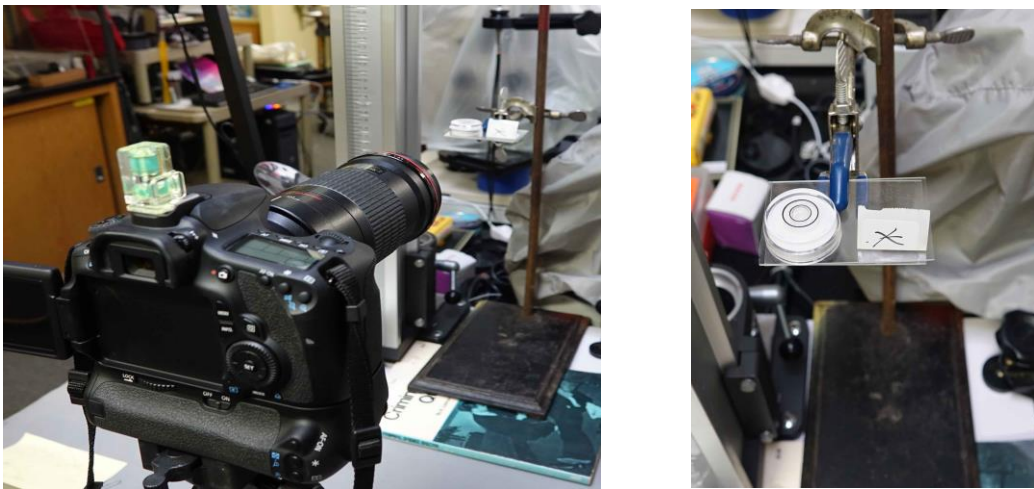
Figure 14. Data collection equipment, showing camera (left) with 180 mm lens aligned to target. Note spirit level and target area bubble level to ensure proper alignment.

The camera was set at auto light balance ASA 400 and halogen lights were utilized on a camera

stand. The camera was focused on a stand that held the approximately 3 inch x 3 inch section of

material upon which the blood drops were placed (Figure 15).

29
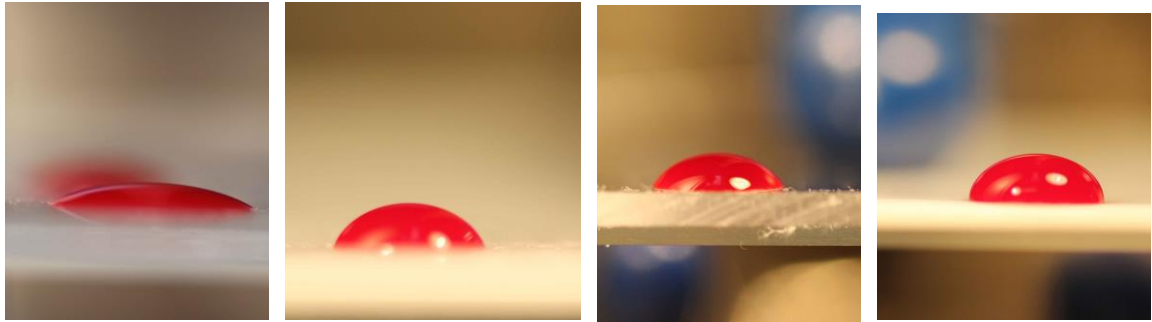
Figure 15. Sample images of blood contact angle (left to right): uncleaned glass slide, acrylic, HDPE, and PTFE. All polymers were precleaned with acetone, followed by detergent in water, followed by water rinse, and drying with clean wipes.

The blood samples were heated in a water bath to 37 ºC prior to being dropped onto specific surfaces and five drops were placed on each surface and photographed. The total number of drops photographed was 5 for each surface on 3 different surfaces for each of the 5 blood samples of varying density, for a total of 75 blood drop pictures measured. The measurement of the contact angles was made on the computer monitor utilizing a calibrated protractor (Figures 16-17). The calibration angle data are contained in the Appendix.
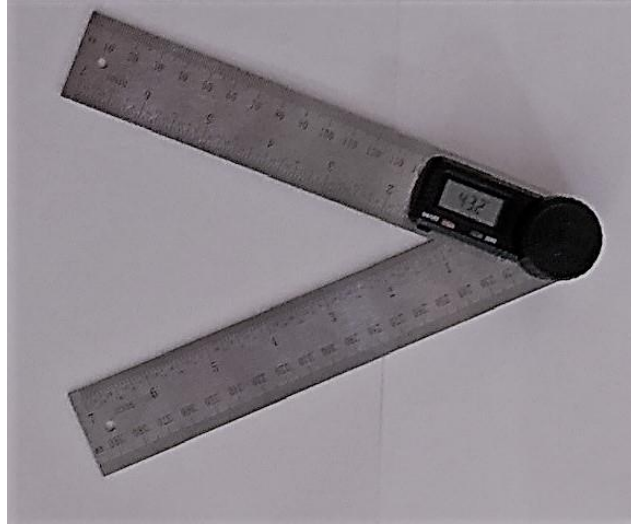
Figure 16. Calibrated protractor
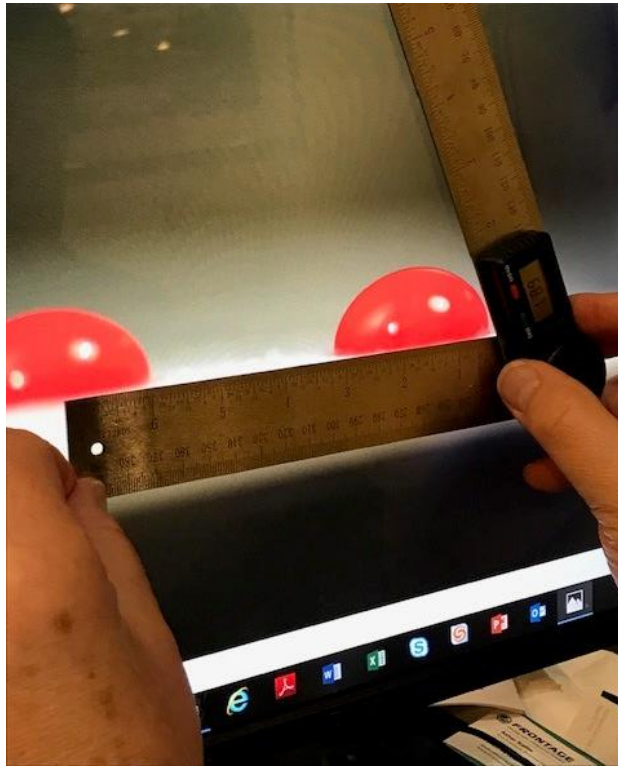
Figure 17. Measuring contact angle of blood drop on monitor using calibrated protractor

31

Figure 18 is a schematic of measuring the contact angle when the angle is acute (right drawing) which indicates a hydrophilic surface and when the angle is obtuse (left drawing) which indicates a hydrophobic surface.
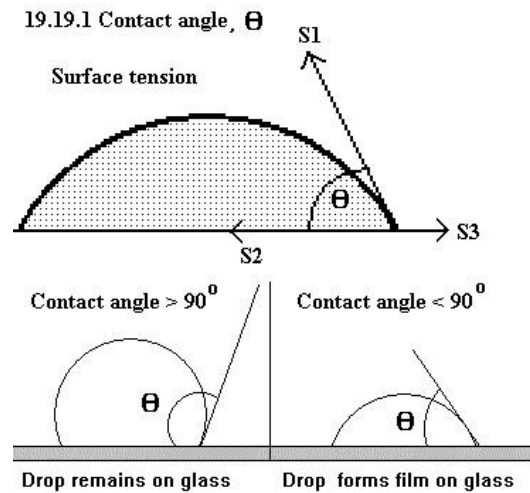
Figure 18. Contact angle measurement

Table 5 shows as the surface material is more hydrophobic the contact angle increases across all blood densities. Increasing contact angles from acrylic (PMMA) to polyethylene (HDPE) to Teflon (PTFE). See list of polymers and contact angles in the Appendix.

32

Table 5. Contact angle measurements of blood of varying densities on polyethylene, acrylic, and Teflon surfaces. Each measurement is the mean of n=5.

CONTACT ANGLES									
		POLYETHYLENE			ACRYLIC PMMA			TEFLON PTFE	
BLOOD DENSITY		MEAN	SD		MEAN	SD		MEAN	SD
very low		68.8	2.31		73.6	3.01		84.7	1.52
low		73.9	4.58		73.4	3.31		85.8	1.26
normal		75.8	1.76		73.4	1.28		83.2	0.69
high		78.7	1.70		73.3	0.19		83.4	1.08
very high		81.7	0.78		74.2	2.50		84.6	0.98
MEAN		75.8			73.6			84.3	
SD		4.37			0.32			0.94	

Passive Blood Drop Device Construction

A device was fabricated to be used for the Study 1 passive blood drops. The purpose of this device was to simulate a drop of blood from a fixed height striking a target surface at a specific angle. The device was constructed from acrylic panes with a base that measures 24 inches by 24 inches, 3 walls composed of the same material, and a bottom pane that was hinged to allow to movement to specific fixed angles (Figures 19-20). The angles were determined by use of a protractor, and holes were drilled in the acrylic panes for the following angles: 10, 25, 40, 55, 70, and 90°. A total of six angles were used for this phase of the study. Acrylic rods were placed in the holes to hold the movable acrylic pane in place at each angle during the testing.

33

Figure 19. Passive blood drop collection device

Pipette

Sheet of paper with blood stain pattern

Holes drilled at specific angles

Protractor

Acrylic pane
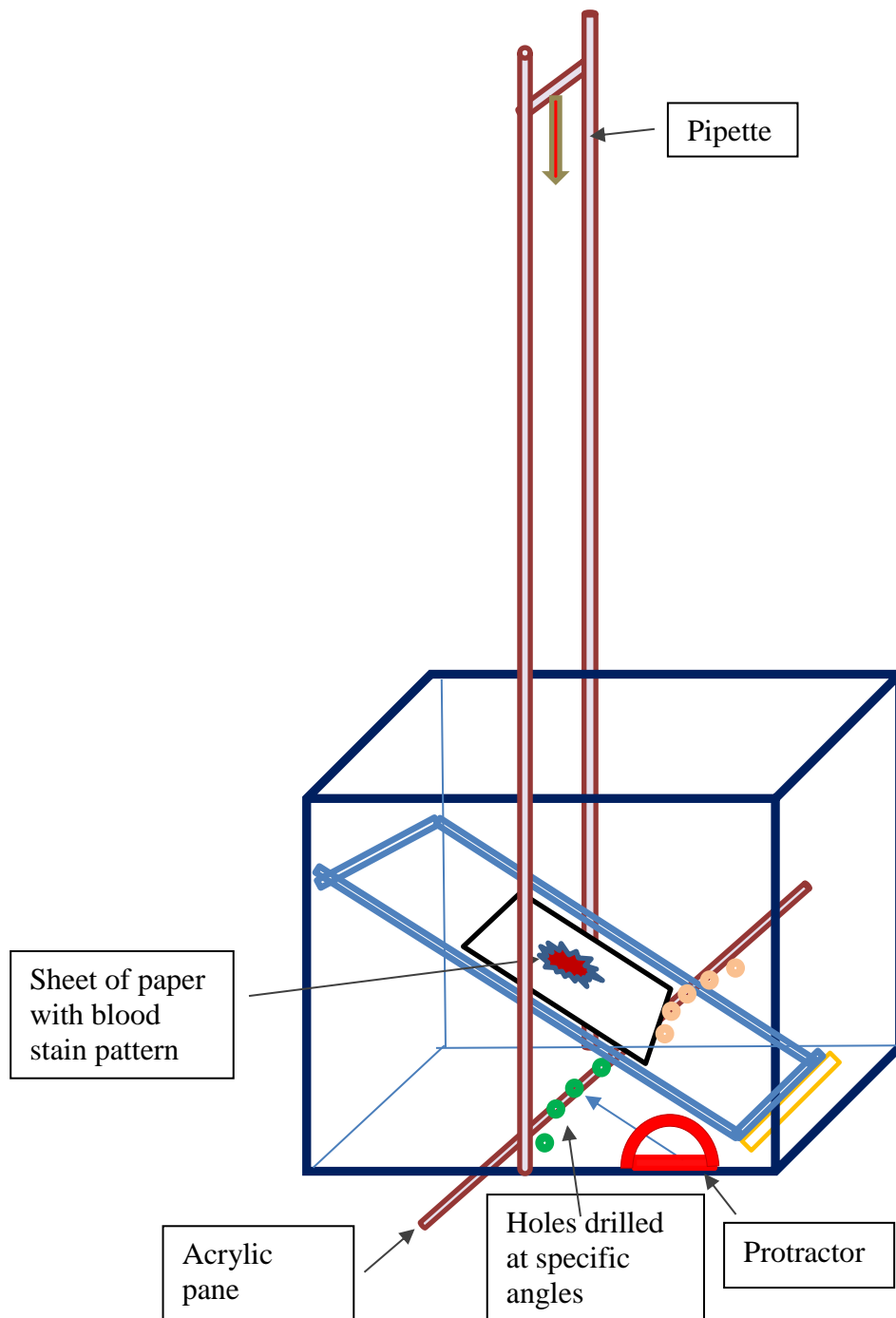
Figure 20. Schematic of the passive blood drop collection device

All of the blood samples utilized in the study were maintained at 37 °C in a Precision 280® series water bath (Thermo Fisher Scientific, Waltham, MA) prior to use. All of the blood samples were dropped from a height of 150 cm to eliminate distortion due to oscillation, which causes blood droplets to deviate from their spherical shape (Pizzola et al., 1986; Pizzola et al., 1986a; Raymond et al., 1996a). For free falling droplets, no detectable oscillation was present after 40 cm (Raymond et al., 1996a).

Using a disposable serological pipette containing sample, a drop was allowed to form and released for each determination. Each blood sample drop was repeated with a sample size (N) of 10 for each angle and for each of the 5 densities, for a total of 300 bloodstain determinations. The target for this study was premium multipurpose office paper, which is plain, white, smooth surface 8 ½ x 11 inch sheet. Pictures of all of the bloodstains are contained in the Appendix; below are representative bloodstain pictures (Figures 21-37).

Figure 21. Very high density blood sample dropped at a 10° angle.

Figure 22. Normal density blood sample dropped at a 10° angle.

Figure 23. Normal density blood sample dropped at a 10º angle.

37
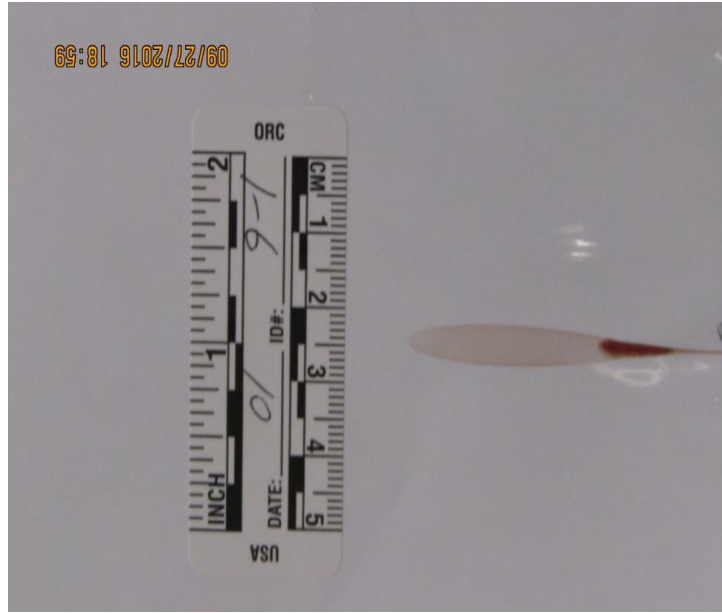
Figure 24. Very low density blood sample dropped at a 10º angle.

Figure 25. Very low density blood sample dropped at a 25º angle.

38

Figure 26. Normal density blood sample dropped at a 25º angle.

Figure 27. Very high density blood sample dropped at a 25º angle.

39
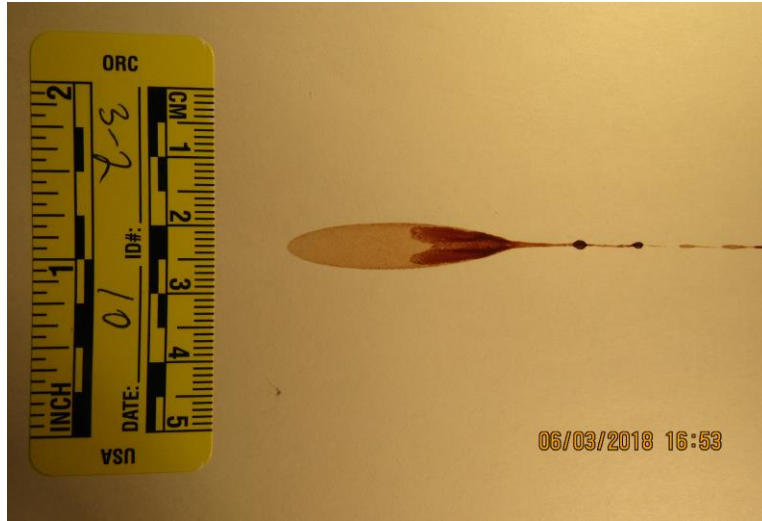
Figure 28. Bloodstain 3 (low density) at a 10° angle.
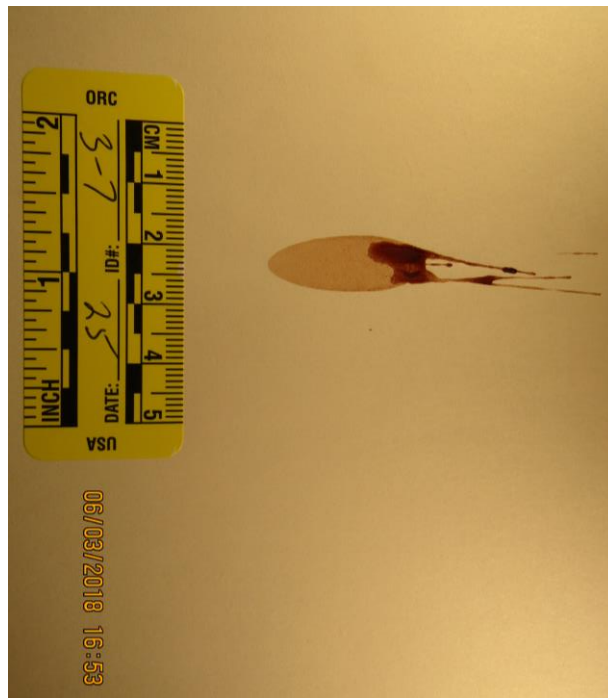
Figure 29. Bloodstain 3 (low density) at a 25° angle.

المنارة للاستشارات

www.manaraa.com

Figure 30. Bloodstain 3 (low density) at a 40° angle.
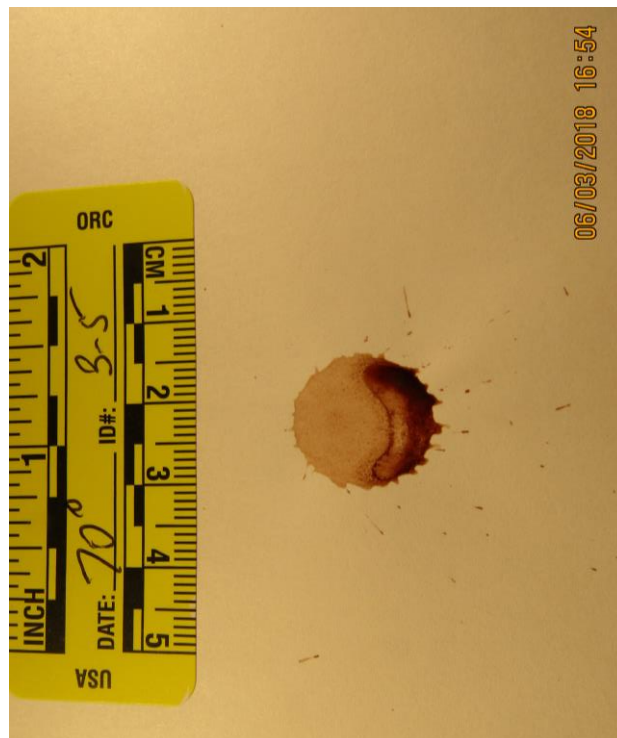
Figure 31. Bloodstain 3 (low density) at a 70° angle.

41

Figure 32. Bloodstain 3 (low density) at a 90° angle
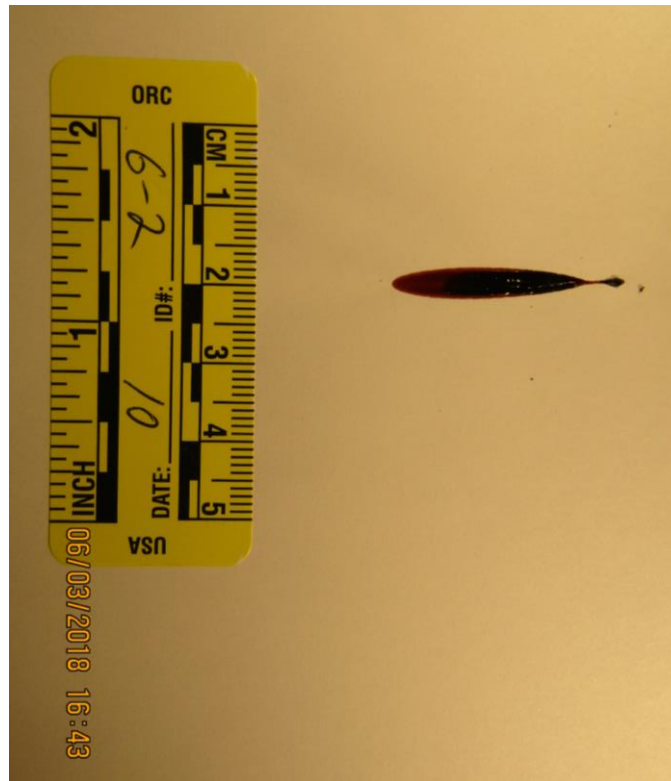
Figure 33. Bloodstain 6 (high density) at a 10° angle.

Figure 34. Bloodstain 6 (high density) at a 25° angle.
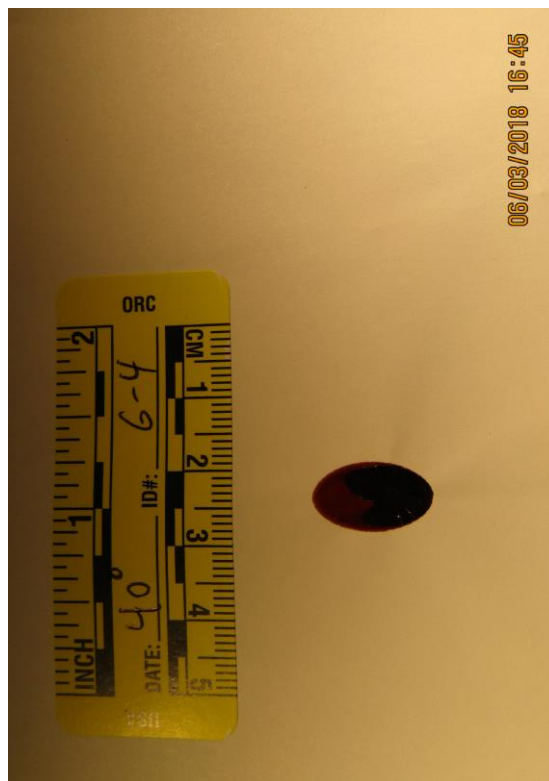
Figure 35. Bloodstain 6 (high density) at a 40° angle.

Figure 36. Bloodstain 6 (high density) at a 55° angle.

Figure 37. Bloodstain 6 (high density) at a 90° angle.

44

Observations on Bloodstain Geometry

A summary of the bloodstain observations is presented in Table 6.

Table 6. Observations on the geometry of the bloodstains

Bloodstain number, (n)/angle	Observations
3 at 10°	Elongated tail and secondary tailing
3 all angles	Light red color
3 at 25°	Length and width increased, multiple tails, light red color, cellular material concentrated in direction of travel
3 at 40°	Same comments as 25°
3 at 70°	Directionality not clear, dark red zone of cellular material in direction of travel
3 at 90°	No directionality, cells separate from serum and form banding pattern, color not uniform
6 at 10°	Dark red color, tail present
6 at 25°	No tail
6 at 40°	No tail, difficult to determine directionality, concentration of cellular material at one end indicates direction of travel
6 at 55°	Very small tail, dark red color, cellular material concentrated in direction of travel
6 at 90°	Uniform color throughout bloodstain

Bloodstain Measurements

An evaluation was conducted to determine the best approach to the measurement (length and width determinations) of the bloodstains for Study 1. First, a stainless steel scale that meets the Japanese Industrial Standard (JIS) grade 1 of JIS B 7516-2005 was considered. The scale has graduations to 0.5mm (see Appendix for metal rule specifications). A second option to measure

45

the bloodstains was the use of a digital caliper that measures to 0.01mm (see digital caliper specifications in the Appendix). An evaluation of the two measuring devices was conducted to compare their accuracy and precision. The digital caliper and the steel scale were utilized to make ten measurements of 4.5 mm and ten measurements of 120 mm. The results of the measurements are contained in Table 7. The measurements of 4.5 mm using the digital caliper had an error of 5.78% compared to the steel rule which had an error of 11.11%. The measurements of 120 mm using the digital caliper had an error of 0.27% compared to the steel rule which had an error of 0.33%. Overall, the digital caliper had better accuracy and precision. The digital caliper was used for all of the bloodstain measurements in Study 1. The next evaluation was to determine the best approach to measuring the bloodstains, the first option was to measure the bloodstain directly using magnification in order to clearly see the margins of the bloodstains. For this determination, a fingerprint magnifier was used with the bloodstain on a flat surface. The other option was to measure the digital image of the enlarged bloodstain, approximately 4X on a computer monitor. The measurements for both approaches utilized the digital caliper. Nine different bloodstains were selected for the comparison analysis between these two approaches (see Table 8). Table 8 lists the bloodstains from Study 1 that were utilized for the evaluation of accuracy and precision. Very low density bloodstain is indicated by 1, and the actual sample is the next number; therefore, 1.2 is a bloodstain with very low density and is the second of ten bloodstains in this group. The angle indicates the angle of impact for the bloodstain, for example 90 degrees. The same nomenclature is used for all of the bloodstains in Study 1. Each of the nine bloodstains was measured ten times using each measuring approach for a total of ninety determinations for bloodstain measurements with the digital caliper directly on the bloodstain and ninety determinations for bloodstain measurements with the digital caliper

46

measuring off of the enlarged bloodstain image on the computer monitor (see all data on

comparison of measurements in the Appendix). A summary of the comparison is contained in

Table 9. The pooled SD for bloodstains measured directly was 0.0159 and the pooled SD for

enlarged bloodstains was 0.0118. The F statistic was calculated, and it was determined with 95%

confidence that the difference in SD are due to random error; therefore, measuring directly or

measuring the enlarged bloodstain are equally precise. It is probable that using a software

package that would allow for measurements on the computer monitor without the need to utilize

the digital caliper would significantly increase precision.

All of the bloodstains for Study 1 were measured (width and length) directly from the

bloodstains using magnification with the digital caliper to 0.01 mm (see Tables 11, 12, 13, 14,

and 15 for all bloodstain measurements). Figure 38 shows the digital caliper being used to

measure the length of a bloodstain.

Table 7. Measurements using metal scale and linear caliper for comparison

	measurements using scale and linear caliper					
	target measurement 4.5mm		scale - caliper	target measurement 120mm		scale - caliper
	scale	caliper	delta	scale	caliper	delta
1	5.25	4.24	1.01	121.0	120.28	0.72
2	5.0	5.18	-0.18	120.5	120.45	0.05
3	5.0	4.41	0.59	120.5	120.65	-0.15
4	5.5	5.06	0.44	120.0	120.41	-0.41
5	5.25	5.18	0.07	120.5	120.16	0.34
6	5.0	5.35	-0.35	120.5	120.53	-0.03
7	5.0	4.59	0.41	120.5	119.87	0.63
8	4.5	4.33	0.17	120.0	120.33	-0.33
9	4.5	4.43	0.07	120.5	120.30	0.20
10	5.0	4.86	0.14	120.0	120.24	-0.24
mean	5.0	4.76	0.34	120.4	120.32	0.31
Sd	0.311	0.410		0.316	0.214	
RSD	6.24%	8.62%		0.26%	0.18%	
(% error) or accuracy	11.11%	5.78%		0.33%	0.27%	
	The scale is a metal calibrated rule, at low numbers the caliper has a much lower error than the rule 5.78% compared to 11.11%					
	all measurements were made with the aid of a 5X magnifier and for the rule I could estimate to .25mm, the scale markings were to .5					
	at higher measurements the percent errors between the rule and the caliper are very close, 0.33% compared to 0.27%					

Figure 38. Linear caliper used to measure bloodstains

The angle of impact or impact angle was used for all of the bloodstain angle determinations in this dissertation. The angles of impact were measured with respect to the plane of the surface and were determined from the arc sin of W/L. An alternative approach is to determine the angle of incidence, calculated from the arc cosine of W/L. The angle of incidence is measured with respect to the normal to the surface, rather than to the surface itself. A drop of blood impacting a level surface straight on would have an angle of incidence of 0° and an angle of impact of 90°. (DeForest et al.,1983)

48

Table 8. Bloodstains used for comparison and evaluation of linear caliper

Bloodstains used for comparison evaluations

	90 degrees	55 degrees	10 degrees
very low density	1.2	1.4	1.5
normal density	5.5	5.3	5.1
very high density	7.1	7.1	7.1

Table 9. Average ratios and RSD comparing linear caliper alone to approximately 4X

enlargement of bloodstain measured with linear caliper.

average ratios and RSD comparing caliper alone to 4X measurements

stain	caliper alone avg ratio	RSD	4X measurement avg ratio	RSD
10 degrees				
VH 1	0.14	3.59%	0.13	4.94%
N 2	0.16	4.17%	0.14	8.25%
VL 3	0.12	4.69%	0.14	4.58%
55 degree				
VH 4	0.81	3.47%	0.79	1.67%
N 5	0.79	2.23%	0.76	1.58%
VL 6	0.80	2.70%	0.78	1.95%
90 degree				
VH 7	0.97	1.47%	0.97	1.60%
N 8	0.98	1.48%	0.98	1.45%
VL 9	0.98	1.47%	0.98	1.00%

Study 1 Bloodstain Analysis Data

For each bloodstain (N = 300), the width (W) and length (L) were determined and the angle of impact was calculated as W/L = arcsine of angle of impact (MacDonell & Bialousz, 1971).

The width, length, W/L, and angle of impact of each bloodstain grouping at each predetermined angle are contained in Tables 10 through 14.

Table 10. Study 1, sample 1 very low density bloodstain measurements.

BLOOD SAMPLE #1 (VERY LOW DENSITY)

10 Degrees		W	L	W/L	Angle				55 Degrees		W	L	W/L	Angle
1.1		6.01	39.44	0.15	8.62				1.1		15.32	17.80	0.86	59.31
1.2		5.44	41.02	0.13	7.46				1.2		15.14	18.37	0.82	55.08
1.3		5.50	34.10	0.16	9.20				1.3		14.93	18.73	0.80	53.13
1.4		5.37	37.70	0.14	8.04				1.4		13.79	17.38	0.79	52.18
1.5		4.69	40.24	0.12	6.89				1.5		13.85	18.16	0.76	49.46
1.6		5.96	42.42	0.14	8.04				1.6		13.51	17.33	0.78	51.26
1.7		5.43	32.54	0.17	9.78				1.7		13.43	18.06	0.74	47.73
1.8		5.31	33.63	0.16	9.20				1.8		13.76	17.57	0.78	51.26
1.9		4.77	36.45	0.13	7.46				1.9		15.30	18.77	0.82	55.08
1.10		5.32	36.64	0.15	8.62				1.10		13.62	17.55	0.78	51.26
	mean	5.38	37.42		8.33					mean	14.27	17.97		52.57
	SD	0.40	3.17		0.92					SD	0.75	0.50		3.27
25 Degrees									**70 Degrees**					
1.1		11.53	33.87	0.34	19.87				1.1		19.00	20.23	0.94	70.05
1.2		10.27	24.91	0.41	24.20				1.2		15.83	17.65	0.90	64.15
1.3		8.82	24.26	0.36	21.10				1.3		13.98	16.45	0.85	58.21
1.4		8.76	31.81	0.28	16.26				1.4		14.37	16.15	0.89	62.87
1.5		*							1.5		14.70	16.20	0.91	65.50
1.6		9.41	26.90	0.35	20.48				1.6		14.17	15.98	0.89	62.87
1.7		9.94	30.25	0.33	19.26				1.7		16.35	17.80	0.92	66.92
1.8		*							1.8		16.81	18.10	0.93	68.43
1.9		9.84	28.74	0.34	19.87				1.9		15.82	16.92	0.93	68.43
1.10		9.25	28.76	0.32	18.66				1.10		14.81	17.11	0.87	60.45
	mean	9.73	28.69		19.96					mean	15.58	17.26		64.78
	SD	0.84	3.08		2.24					SD	1.45	1.21		3.78
40 Degrees									**90 Degrees**					
1.1		14.25	23.96	0.59	36.15				1.1		17.36	17.68	0.98	78.52
1.2		14.90	25.09	0.59	36.15				1.2		17.74	17.84	0.99	81.89
1.3		15.15	25.33	0.60	36.86				1.3		17.78	18.77	0.95	71.80
1.4		15.26	25.18	0.61	37.58				1.4		18.21	18.51	0.98	78.52
1.5		14.20	23.55	0.60	36.86				1.5		17.41	18.40	0.95	71.80
1.6		14.51	24.19	0.60	36.86				1.6		17.95	18.47	0.97	75.93
1.7		16.27	25.07	0.65	40.54				1.7		17.46	18.16	0.96	73.73
1.8		14.50	22.38	0.65	40.54				1.8		17.93	18.21	0.98	78.52
1.9		14.84	23.55	0.63	39.05				1.9		16.38	17.04	0.96	73.73
1.10		15.09	23.64	0.64	39.79				1.10		16.64	17.88	0.93	68.43
	mean	14.90	24.19		38.03					mean	17.49	18.10		75.28
	SD	0.57	0.91		1.76					SD	0.55	0.47		4.10
	* bloodstain geometry not clear													

Table 11. Study 1, sample 3 low density bloodstain measurements

BLOOD SAMPLE #3 (LOW DENSITY)

10 Degrees		W	L	W/L	Angle		55 Degrees		W	L	W/L	Angle
3.1		5.86	36.44	0.16	9.20		3.1		15.76	19.56	0.81	54.09
3.2		7.29	34.10	0.21	12.12		3.2		14.39	18.98	0.76	49.46
3.3		7.35	40.33	0.18	10.36		3.3		14.08	18.59	0.76	49.46
3.4		6.02	42.13	0.14	8.04		3.4		15.26	18.18	0.84	57.14
3.5		6.57	44.54	0.15	8.62		3.5		15.41	18.93	0.81	54.09
3.6		7.55	36.73	0.21	12.12		3.6		14.91	19.23	0.78	51.26
3.7		7.13	37.19	0.19	10.95		3.7		15.50	18.86	0.82	55.08
3.8		7.37	41.87	0.18	10.36		3.8		13.53	17.38	0.78	51.26
3.9		6.47	45.11	0.14	8.04		3.9		14.37	18.08	0.79	52.18
3.10		6.86	42.04	0.16	9.20		3.10		13.94	17.62	0.79	52.18
	mean	6.85	40.05		9.91			mean	14.72	18.54		52.62
	SD	0.56	3.53		1.52			SD	0.71	0.67		2.46
25 Degrees							**70 Degrees**					
3.1		11.59	28.22	0.41	24.20		3.1		15.11	16.19	0.93	68.43
3.2		12.24	32.47	0.38	22.33		3.2		16.55	17.56	0.94	70.05
3.3		12.00	28.14	0.43	25.46		3.3		14.28	15.71	0.91	65.50
3.4		11.74	25.14	0.47	28.03		3.4		14.52	15.87	0.91	65.50
3.5		*					3.5		15.63	17.14	0.91	65.50
3.6		9.97	27.70	0.36	21.10		3.6		16.65	17.72	0.94	70.05
3.7		10.12	27.96	0.36	21.10		3.7		15.66	17.26	0.91	65.50
3.8		11.11	26.02	0.43	25.46		3.8		14.87	16.79	0.89	62.87
3.9		11.06	25.94	0.43	25.46		3.9		15.22	16.46	0.92	66.92
3.10		10.08	26.52	0.38	22.33		3.10		15.91	16.90	0.94	70.05
	mean	11.1	27.57		23.94			mean	15.44	16.76		67.03
	SD	0.81	2.02		2.37			SD	0.75	0.65		2.49
40 Degrees							**90 Degrees**					
3.1		12.55	18.58	0.68	42.84		3.1		16.18	16.77	0.96	73.73
3.2		13.66	19.70	0.69	43.63		3.2		15.13	15.24	0.99	81.89
3.3		13.93	20.64	0.67	42.06		3.3		14.99	15.64	0.96	73.73
3.4		13.05	20.09	0.65	40.54		3.4		15.39	15.96	0.96	73.73
3.5		13.73	17.42	0.79	52.18		3.5		16.02	16.17	0.99	81.89
3.6		15.03	19.00	0.79	52.18		3.6		*			
3.7		13.28	20.64	0.64	39.79		3.7		15.89	16.12	0.99	81.89
3.8		11.91	17.69	0.67	42.06		3.8		15.55	15.94	0.98	78.52
3.9		12.44	19.99	0.62	38.31		3.9		15.46	15.55	0.99	81.89
3.10		13.44	20.34	0.66	41.29		3.10		15.61	15.57	1.00	90.00
	mean	13.3	19.41		43.48			mean	15.58	15.88		79.69
	SD	0.83	1.12		4.82			SD	0.37	0.42		5.40
	* bloodstain geometry not clear											

Table 12. Study 1, sample 5 normal density bloodstain measurements

BLOOD SAMPLE #5 (NORMAL DENSITY)													
10 Degrees	**W**	**L**	**W/L**	**Angle**				**55 Degrees**		**W**	**L**	**W/L**	**Angle**
5.1	5.41	31.45	0.17	9.78				5.1		15.24	19.62	0.78	51.26
5.2	5.91	39.39	0.15	8.62				5.2		14.95	19.56	0.76	49.46
5.3	5.15	34.87	0.15	8.62				5.3		14.80	19.39	0.76	49.46
5.4	5.03	39.73	0.13	7.46				5.4		15.60	19.13	0.82	55.08
5.5	6.14	33.64	0.18	10.36				5.5		13.96	18.18	0.77	50.35
5.6	5.06	37.49	0.13	7.46				5.6		13.85	18.40	0.75	48.59
5.7	5.40	31.18	0.17	9.78				5.7		15.44	20.02	0.77	50.35
5.8	5.75	39.33	0.15	8.62				5.8		15.06	19.12	0.79	52.18
5.9	5.81	40.03	0.15	8.62				5.9		15.54	19.53	0.80	53.13
5.10	5.32	37.48	0.14	8.04				5.10		15.02	19.02	0.79	52.18
mean	5.50	36.46		8.73					mean	14.95	19.20		51.21
SD	0.36	3.25		0.97					SD	0.57	0.53		1.97
25 Degrees								**70 Degrees**					
5.1	9.53	25.12	0.38	22.33				5.1		16.62	17.61	0.94	70.05
5.2	8.47	29.75	0.28	16.26				5.2		17.29	18.80	0.92	66.92
5.3	9.55	28.40	0.34	19.87				5.3		13.42	15.16	0.89	62.87
5.4	9.08	29.28	0.31	18.05				5.4		16.49	17.58	0.94	70.05
5.5	9.88	30.08	0.33	19.26				5.5		16.14	17.38	0.93	68.43
5.6	8.92	33.46	0.27	15.66				5.6		16.32	17.39	0.94	70.05
5.7	8.76	25.62	0.34	19.87				5.7		17.35	18.48	0.94	70.05
5.8	9.13	29.14	0.31	18.05				5.8		15.99	17.69	0.90	64.15
5.9	9.47	26.65	0.36	21.10				5.9		15.60	17.01	0.92	66.92
5.10	8.92	28.01	0.32	18.66				5.10		15.67	17.64	0.89	62.87
mean	9.17	28.55		18.91					mean	16.09	17.47		67.23
SD	0.40	2.30		2.04					SD	1.05	0.91		2.99
40 Degrees								**90 Degrees**					
5.1	13.50	21.22	0.64	39.79				5.1		15.63	15.61	1.00	90.00
5.2	13.00	20.72	0.63	39.05				5.2		16.40	17.05	0.96	73.73
5.3	12.61	20.33	0.62	38.31				5.3		14.76	15.31	0.96	73.73
5.4	12.42	20.63	0.60	36.86				5.4		17.57	17.49	1.00	90.00
5.5	12.64	20.29	0.62	38.31				5.5		16.14	16.27	0.99	81.89
5.6	13.20	21.87	0.60	36.86				5.6		16.21	16.63	0.97	75.93
5.7	13.73	21.48	0.64	39.79				5.7		16.07	16.91	0.95	71.80
5.8	13.19	20.65	0.64	39.79				5.8		16.37	16.59	0.99	81.89
5.9	13.15	20.04	0.66	41.29				5.9		16.61	16.53	1.00	90.00
5.10	12.00	19.07	0.63	39.05				5.10		15.60	15.65	1.00	90.00
mean	12.94	20.63		38.91					mean	16.14	16.40		81.89
SD	0.49	0.74		1.38					SD	0.69	0.66		7.69

52

Table 13. Study 1, sample 6 high density bloodstain measurements

BLOOD SAMPLE #6 (HIGH DENSITY)

10 Degrees		W	L	W/L	Angle				55 Degrees		W	L	W/L	Angle
6.1		4.28	28.24	0.15	8.62				6.1		12.29	13.63	0.90	64.15
6.2		4.35	24.49	0.18	10.36				6.2		10.77	13.77	0.78	51.26
6.3		4.76	28.80	0.17	9.78				6.3		10.41	13.32	0.78	51.26
6.4		4.75	25.62	0.19	10.95				6.4		11.21	14.07	0.80	53.13
6.5		5.02	29.95	0.17	9.78				6.5		*			
6.6		4.11	33.57	0.12	6.89				6.6		11.80	14.38	0.82	55.08
6.7		4.77	30.71	0.16	9.20				6.7		10.77	13.10	0.82	55.08
6.8		5.36	29.32	0.18	10.36				6.8		10.82	13.63	0.79	52.18
6.9		5.29	26.66	0.20	11.53				6.9		9.58	13.07	0.73	46.88
6.10		*							6.10		10.45	13.42	0.78	51.26
	mean	4.27	25.74		9.71					mean	10.90	13.60		53.36
	SD	0.41	2.60		1.37					SD	0.75	0.40		4.73
25 Degrees									**70 Degrees**					
6.1		8.10	19.42	0.42	24.83				6.1		10.84	13.71	0.79	52.18
6.2		7.82	19.50	0.40	23.57				6.2		10.76	11.91	0.90	64.15
6.3		8.02	18.78	0.43	25.46				6.3		9.24	11.99	0.77	50.35
6.4		8.04	18.93	0.42	24.83				6.4		11.56	12.52	0.92	66.92
6.5		*							6.5		*			
6.6		6.92	17.56	0.39	22.95				6.6		11.96	13.99	0.85	58.21
6.7		7.32	19.04	0.38	22.33				6.7		11.89	14.94	0.80	53.13
6.8		7.55	18.74	0.40	23.57				6.8		11.83	13.03	0.91	65.50
6.9		6.93	17.17	0.40	23.57				6.9		11.40	12.23	0.93	68.43
6.10		7.33	18.29	0.40	23.57				6.10		11.91	12.55	0.95	71.80
	mean	7.56	18.60		23.85					mean	11.27	12.99		61.18
	SD	0.43	0.74		0.99					SD	0.83	0.97		7.88
40 Degrees									**90 Degrees**					
6.1		9.96	14.65	0.68	42.84				6.1		12.22	12.65	0.97	75.93
6.2		10.45	12.83	0.81	54.09				6.2		12.20	12.53	0.97	75.93
6.3		9.54	14.56	0.64	39.79				6.3		12.38	12.33	1.00	90.00
6.4		9.94	16.18	0.61	37.58				6.4		*			
6.5		*							6.5		10.07	10.40	0.97	75.93
6.6		10.07	14.84	0.68	42.84				6.6		12.35	12.74	0.97	75.93
6.7		9.53	15.97	0.60	36.86				6.7		10.92	11.23	0.97	75.93
6.8		10.68	16.74	0.64	39.79				6.8		9.34	10.04	0.93	68.43
6.9		10.87	16.63	0.65	40.54				6.9		11.63	12.26	0.95	71.80
6.10		10.55	16.14	0.65	40.54				6.10		11.80	12.03	0.98	78.52
	mean	10.18	15.39		42.25					mean	11.43	11.80		76.48
	SD	0.45	1.20		5.08					SD	1.03	0.94		5.86
	*bloodstain geometry not clear													

53

Table 14. Study 1, sample 7 very high density bloodstain measurements

BLOOD SAMPLE #7 (VERY HIGH DENSITY)

10 Degrees		W	L	W/L	Angle					55 Degrees		W	L	W/L	Angle
7.1		4.45	29.70	0.15	8.62					7.1		11.71	14.20	0.82	55.08
7.2*	7.4A	6.38	33.87	0.19	10.95					7.2		10.99	13.40	0.82	55.08
7.3		5.26	30.15	0.17	9.78					7.3		11.17	13.98	0.80	53.13
7.4		5.24	33.02	0.16	9.20					7.4		11.09	13.02	0.85	58.21
7.5		5.93	32.74	0.18	10.36					7.5		11.08	12.54	0.88	61.64
7.6		5.61	27.48	0.20	11.53					7.6		11.26	13.48	0.84	57.14
7.7		5.74	30.90	0.19	10.95					7.7		10.72	13.46	0.80	53.13
7.8		5.57	33.83	0.16	9.20					7.8		11.56	13.09	0.88	61.64
7.9		5.62	29.05	0.19	10.95					7.9		11.35	13.91	0.82	55.08
7.10		5.44	28.89	0.19	10.95					7.10		10.81	13.33	0.81	54.09
	mean	5.52	30.96		10.24						mean	11.17	13.44		56.42
	SD	0.47	2.15		0.98						SD	0.29	0.47		3.17
25 Degrees										**70 Degrees**					
7.1		8.16	19.60	0.42	24.83					7.1		12.50	13.48	0.93	68.43
7.2		7.94	18.78	0.42	24.83					7.2		*			
7.3		7.63	19.89	0.38	22.33					7.3		12.09	13.32	0.91	65.50
7.4		8.44	20.87	0.40	23.57					7.4		12.18	13.48	0.90	64.15
7.5		7.87	20.22	0.39	22.95					7.5		10.82	12.42	0.87	60.45
7.6		8.23	19.44	0.42	24.83					7.6		10.41	12.05	0.86	59.31
7.7		8.71	20.77	0.42	24.83					7.7		12.65	13.41	0.94	70.05
7.8		7.89	20.28	0.39	22.95					7.8		*			
7.9		7.99	20.70	0.39	22.95					7.9		12.25	13.76	0.89	62.87
7.10		8.04	18.80	0.43	25.46					7.10		11.02	12.33	0.89	62.87
	mean	8.09	19.94		23.95						mean	11.74	13.03		64.21
	SD	0.29	0.73		1.11						SD	0.79	0.61		3.69
40 Degrees										**90 Degrees**					
7.1		10.32	17.40	0.59	36.15					7.1		13.82	13.84	1.00	90.00
7.2		10.85	17.67	0.61	37.58					7.2		12.90	12.63	1.02	90.00
7.3		10.67	17.03	0.63	39.05					7.3		12.56	13.20	0.95	71.80
7.4		10.13	15.65	0.65	40.54					7.4		12.80	12.77	1.00	90.00
7.5		9.74	15.85	0.61	37.58					7.5		12.54	12.78	0.98	78.52
7.6		9.69	15.12	0.64	39.79					7.6		13.43	13.37	1.00	90.00
7.7		9.79	15.79	0.62	38.31					7.7		11.60	12.17	0.95	71.80
7.8		10.24	16.78	0.61	37.58					7.8		11.16	11.49	0.97	75.93
7.9		10.91	17.76	0.61	37.58					7.9		11.25	11.56	0.97	75.93
7.10		9.24	15.25	0.61	37.58					7.10		11.50	11.84	0.97	75.93
	mean	10.16	16.43		38.17						mean	12.35	12.56		80.99
	SD	0.52	0.95		1.28						SD	0.88	0.74		8.00
	* bloodstain geometry not clear														
	7.4A substituted for 7.2														

Data Analysis Approach

For Studies 1, 2, and 3, the hypotheses were tested by the computation and examination of 95% CIs (CI) as described by Kock (2015) and by the interpretation of effect sizes, as recommended by Ferguson (2009) and Sullivan & Feinn (2012). The statistical analysis was conducted with Minitab v. 17.3 software (Minitab Inc., State College, PA), using the protocols described by Peck et al. (2016).

Interval plot with mean ± 95% confidence interval (CI)

Interval plots (otherwise known as error bar charts) were constructed using Minitab 17.3 software to provide graphical summaries that visually compared the mean values of a numerical variable sampled from a known population of data (e.g., the angle of impact and the location of the volume of origin of the blood spatter) classified into specified groups (e.g., five levels of blood density). The mean value of each group of data was represented by a circular symbol. The 95% CI of each mean value was symbolized by a vertical bar (Hampton & Havel, 2014; Minitab, 2016; Peck et al., 2016).

The 95% CI encompasses the range of values that should theoretically contain the true mean value of the population of data in 95 out of 100 samples (assuming that a representative sample has been drawn from the population). The researcher can be 95% confident that the true mean value of the data in a specified group is captured within the lower and upper limit of the CI for that group. The difference between values of two group means is probably significant (at the $p = 0.05$ level of statistical significance) when the interval bars do not overlap with each other (Kock, 2015).

The 95% CI not only provides information on the variability of the mean value in an observed sample of data (i.e., the precision of the mean) but also provides information on the

55

probable relationship of the sample mean to the true value of the mean in the population from which the sample was drawn (i.e., the accuracy of the mean). A CI calculated to measure the effects of a treatment indicates the range within which the true effect of the treatment is likely to be captured. CIs aid the interpretation of experimental data by putting upper and lower limits on the likely size of any true effect of a treatment (Davies & Crombie, 2009).

The formula to calculate a 95% CI is:

$$M \pm t_{(N-1)} \times SE$$

where M = mean value of a sample of data; $t_{(N-1)}$ is the critical value of the *t* statistic at $p = 0.05$ when the sample size is N; and SE is the standard error of the mean, given by $\sigma/\sqrt{N}$, (where σ = standard deviation of the sample of data).

Research Questions and Research Hypotheses

The purpose of Study 1 was to analyze the statistical relationship between blood density, angle of impact, and the geometry of the bloodstains.

The four research questions are:

- RQ1a: To what extent is blood density correlated with the geometry (i.e., width and length) of the bloodstain?

- RQ1b: To what extent is blood density correlated with the pre-defined angle of impact?

- RQ1c: To what extent does the pre-defined angle of impact act as a mediator in the correlation between blood density and the geometry of the bloodstain?

- RQ1d: To what extent is there a difference between the pre-defined angles of impact and the calculated angles of impact?

The four associated research hypotheses are:

- H1a: Blood density is correlated with the geometry (i.e., width and length) of the bloodstain.

56

- H1b: The angle of impact is correlated with the geometry of the bloodstain.

- H1c: The angle of impact acts as a moderator, altering the strength and/or direction of the correlation between blood density and the geometry of the bloodstain.

- H1d: There is no difference between the pre-defined angles of impact and the calculated angles of impact of the bloodstains (Fisher, R., personal communication 4/30/ 2018).

Data Analysis

Moderation analysis.

The generic moderation model to test H1a to H1c is illustrated in Figure 39, where the rectangular symbols represent the variables, and the arrows represent the correlations between the variables. The interaction term to identify the moderating effect is the product of the predictor x the moderator.
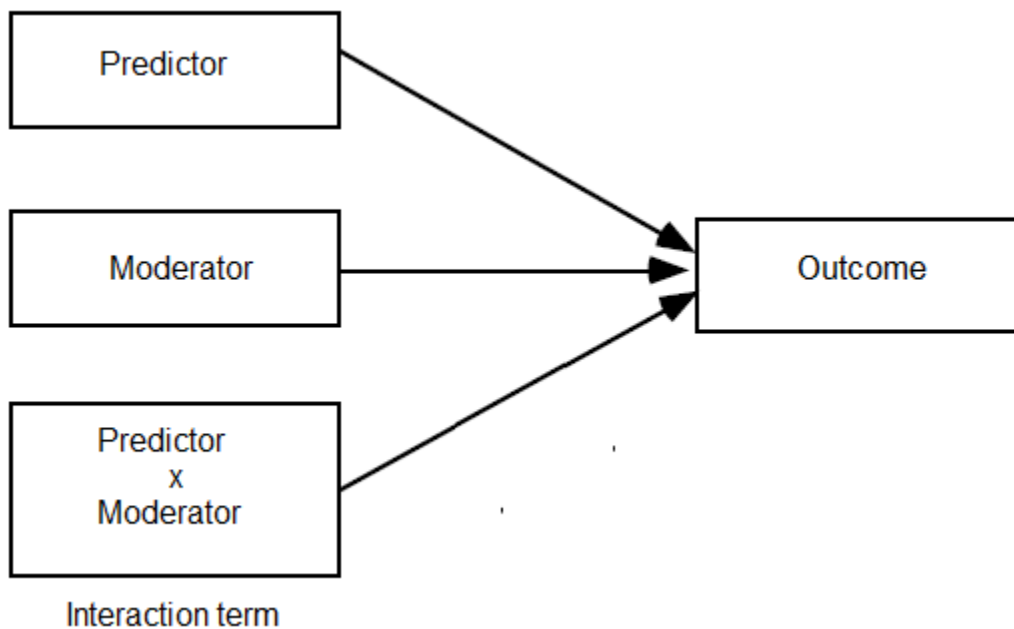
Figure 39. Generic moderator model (adapted from Baron & Kenny, 1986).

The testing of H1a to H1c assumed that a moderator (i.e., the pre-defined angle of impact) altered the strength and/or direction of the correlation between the predictor variable

(i.e., the blood density) and the outcome variable (i.e., the geometry of the bloodstain). Moderation meant that the correlation between blood density and the geometry of the bloodstain was not consistent with respect to all angles of incidence. The correlation between blood density and the geometry of the bloodstain might be weak at certain angles of impact, but the correlation may be strong at other angles of impact.

Hypotheses involving the evaluation of moderating effects have, for over 30 years, been tested by regression analysis based on the computation or ordinary least squares (OLS) (Baron & Kenny, 1986; Hayes, 2013). However, in the last decade, more modern techniques, including moderated path analysis, based on the computation of partial least squares (PLS) have been developed (Aimram et al., 2015; Edwards & Lambert, 2007; Fassot et al., 2016; Wong, 2016). Figure 40 illustrates the path diagram to test H1a, H1b, and H1c using moderated path analysis. The oval symbols represent the variables, and the arrows represent the hypotheses, proposing correlations between the variables. The interaction term to identify the moderating effect is angle of impact x blood density.
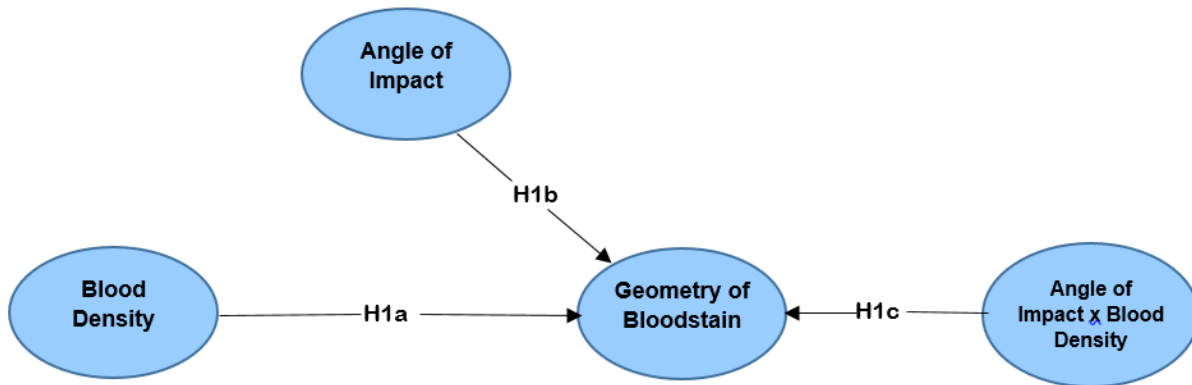
Figure 40. Path diagram to illustrate H1a, H1b, and H1c.

58

The advantages of using PLS path analysis over OLS regression as discussed by Hair et al. (2017) are as follows:

- PLS is a non-parametric method, therefore, unlike OLS regression, it does not assume that the variables are normally distributed;

- unlike OLS regression, PLS operates with variables having all types of measurement and distributional characteristics (e.g., nominal, ordinal, and interval level); and

- unlike OLS regression, PLS achieves a high level of statistical power with small sample sizes because the correlations (path coefficients) between the variables and the statistical significance of the path coefficients are computed by bootstrapping.

The bootstrapping procedure samples and resamples the data to collect a total of 5000 random sub samples. The Monte Carlo algorithm for subsampling is used for the bootstrap, meaning that the data are shuffled like a pack of cards in a casino before each sub-sample is drawn from the data set. The bootstrapped mean, standard error, and 95% CI for each path coefficient are computed. H1a, H1b, and H1c are supported if:

- the 95% CIs of the path coefficients do not include zero; and

- the effect size, indicated by R^2 = the proportion of the variance explained, is large enough to reflect practical significance. The criterion of Ferguson (2009) was applied that the absolute minimum effect size to indicate a practically significant effect is $R^2 = 0.04$ (i.e., 4% of the variance is explained).

The limitation of using PLS path analysis to examine moderation is that the magnitude and significance of the path coefficient between the moderating effect (i.e., blood density x the geometry of the bloodstain) and the dependent variable (i.e., geometry of bloodstain) symbolized by the arrow labelled H1c in Figure 40 does not fully characterize the moderating effect (Jose,

2013). A graphical analysis was therefore conducted to provide a visual method of examining how the correlation between the blood density and the width and length of the blood stain changed in strength and/or direction with respect to different levels of the pre-defined angle of impact. Linear trend lines were fitted to the scatterplots of the geometry of the bloodstain and the blood density. Moderating effects were visualized by the slopes of the fitted linear trend lines changing systematically across the six pre-defined angles of impact (i.e., 10, 25, 40, 55, 70, and 90°).

H1d, proposing no difference between the pre-defined angles of impact and the computed angles of impact (derived from the width divided by the length of the bloodstain), was tested by determining if the pre-defined angles of impact (i.e., 10, 25, 40, 55, 70, and 90°) were captured within the lower and upper limits of the 95% CI of the computed angles of impact.

This section provides the results of moderation analysis to address the research questions RQ1a, RQ1b, and RQ1c and test the associated hypotheses H1a, H1b, and H1c. Figure 41 presents the path diagram output by SmartPLS® (SmartPLS GmbH, Hamburg, Germany) to illustrate the relationships between the blood density (predictor), the pre-defined angle of impact (moderator), the width of the bloodstain (outcome), and the moderating effect (blood density x angle of impact) when the blood density was increased using an ordinal scale ranging from very low (1) to very high (7). The R^2 value = 0.769 (i.e., 76.9% of the variance in the width of bloodstain was explained) was well above the minimum effect size of 0.04 required to reflect a strong practically significant effect (Fisher, R. personal communication 5/2/ 2018).

60

Figure 41. Path analysis of the moderating effect of angle of impact on the correlation between blood density and width of bloodstain.

The negative path coefficient between the blood density and the width of bloodstain ($\beta =$ -0.342, 95% CI = -0.311, -0.373) was less than zero. Consequently, when the blood density increased, the width of bloodstain decreased. The path coefficient between the angle of impact and the width of bloodstain ($\beta = 0.792$, 95% CI = 0.768, 0.815) was significantly greater than zero (because the positive 95% CI did not capture zero). Consequently, when the angle of impact increased, the width of bloodstain also increased. Figure 42 illustrates the positive correlation between the angle of impact and the width of bloodstain using a fitted linear trend line.

Figure 42. Correlation between angle of impact and width of bloodstain.

The path coefficient for the moderating effect (blood density x angle of impact) (β = - 0.129, 95% CI = -0.096, -0.162) was significantly less than zero. Consequently, the angle of impact was identified as a significant moderator, and the moderating effect was negative.

Figure 43 illustrates the negative moderating effect of angle of impact on the linear correlation between the width of bloodstain and blood density. When the angle of impact was 10°, the linear trend line fitted to the data was almost horizontal, reflecting little or no correlation between blood density and width of bloodstain. However, when the angle of impact was increased progressively to 25, 40, 55, and 70°, the downward sloping fitted linear trend lines became progressively steeper. The steepest linear trend line was when the angle of impact = 90°. Consequently, the moderating effect of angle of impact was to systematically decrease the width

62

of bloodstain when the blood density was increased from very low (1), through low (3), normal (5), and high (6) to very high (7).

Figure 43.Visual analysis of the moderating effect of angle of impact on the correlation between blood density and width of bloodstain.

Figure 44 presents the path diagram output by SmartPLS to illustrate the relationships between the blood density (predictor) the pre-defined angle of impact (moderator), the length of the bloodstain (outcome), and the moderating effect (blood density x angle of impact). The R^2 value = 0.722 (72.2% of the variance in the length of bloodstain was explained) was well above the minimum effect size of 0.04 required to indicate a strong and practically significant effect.
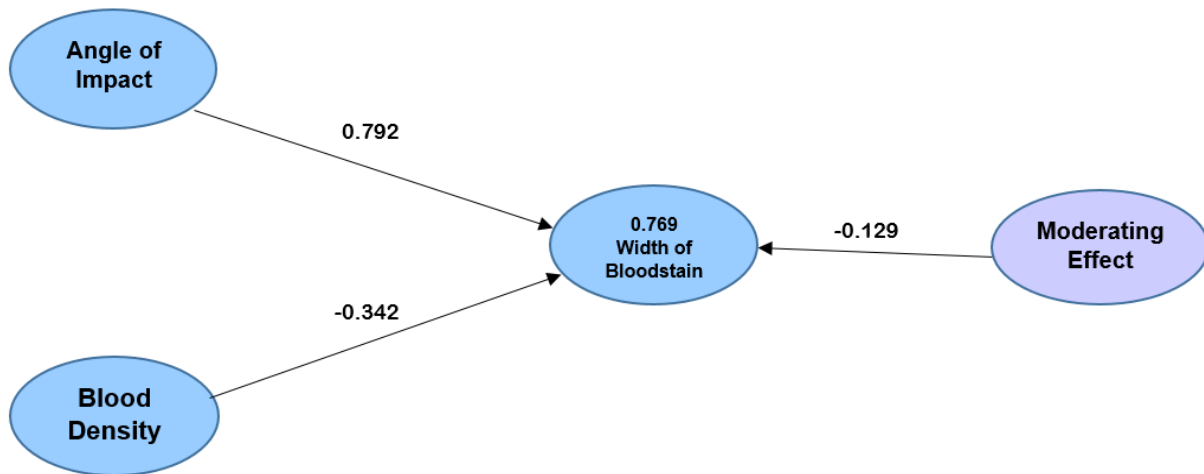
Figure 44. Path analysis of the moderating effect of angle of impact on the correlation between blood density and length of bloodstain.

The negative path coefficient between the blood density and the length of Bloodstain (β = -0.455, 95% CI = -0.389, -0.520) was significantly less than zero. Consequently, when the blood density increased, the length of bloodstain decreased. The negative path coefficient between the angle of impact and the length of bloodstain (β = -0.953, 95% CI = -0.897, -1.008) was significantly less than zero (because the negative 95% CI did not capture zero). Consequently, when the angle of impact increased, the length of bloodstain decreased. Figure 45 illustrates the negative correlation between the angle of impact and the length of bloodstain using a fitted linear trend line.

64
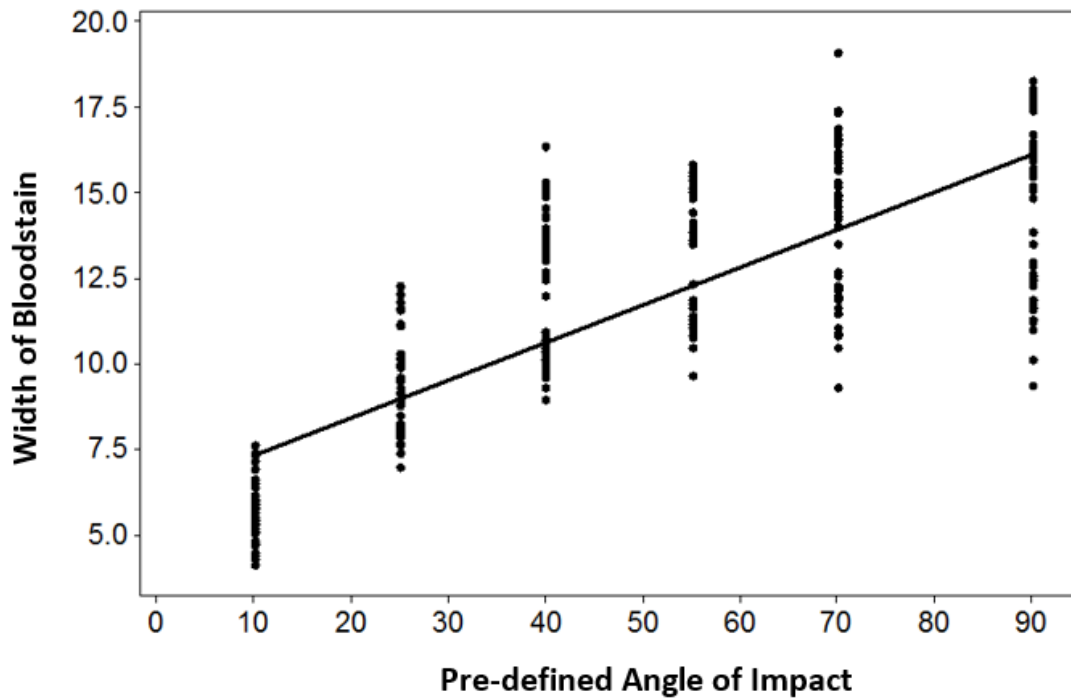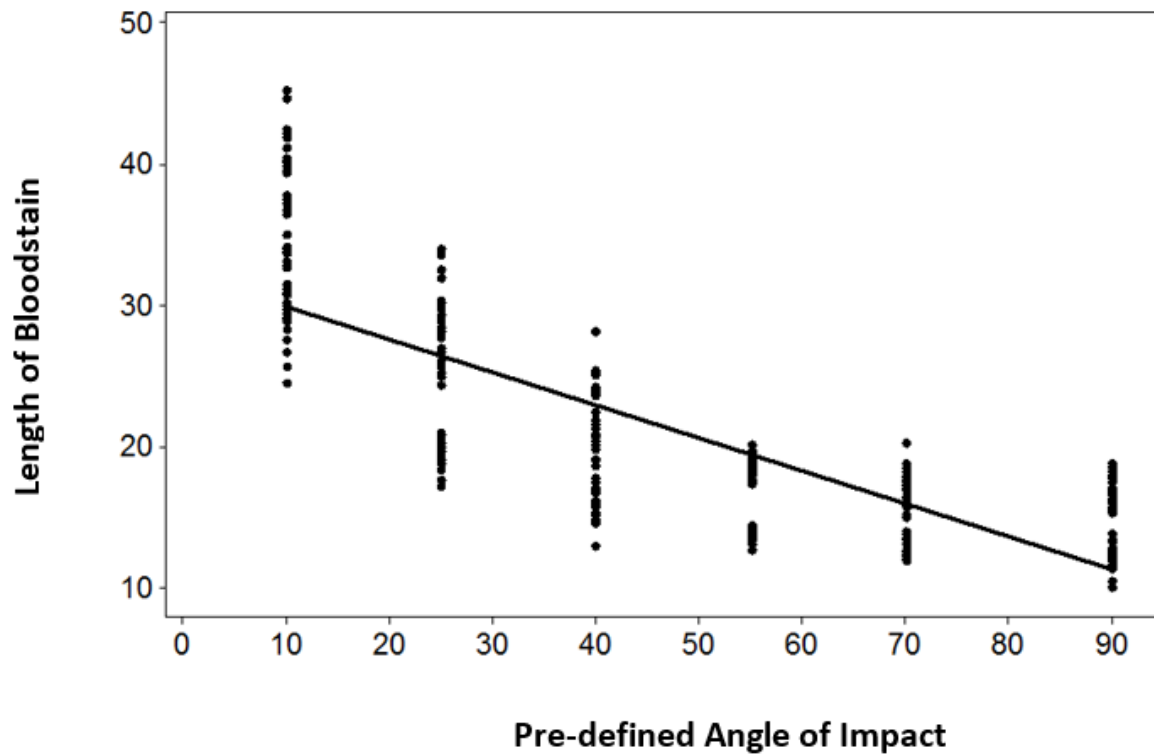
Figure 45. Correlation between angle of impact and length of bloodstain.

The path coefficient for the moderating effect ($\beta = 0.299$, 95% CI = 0.181, 0.417) was significantly greater than zero. Consequently, the angle of impact was identified as a moderator and the moderating effect was positive. Figure 46 illustrates the effect of angle of impact on the linear correlation between the length of bloodstain and blood density. When the angle of impact was 10 degrees, the linear trend line fitted to the data sloped downward, reflecting the negative correlation between blood density and length of bloodstain. When the angle of impact was increased progressively to 25, 40, 55, and 70°, the fitted linear trend lines tended to be less steep. The linear trend line with the lowest slope occurred when the angle of impact was 90°. Consequently, there was a systematic moderating effect of angle of impact on the length of bloodstain when the blood density increased from very low to very high.
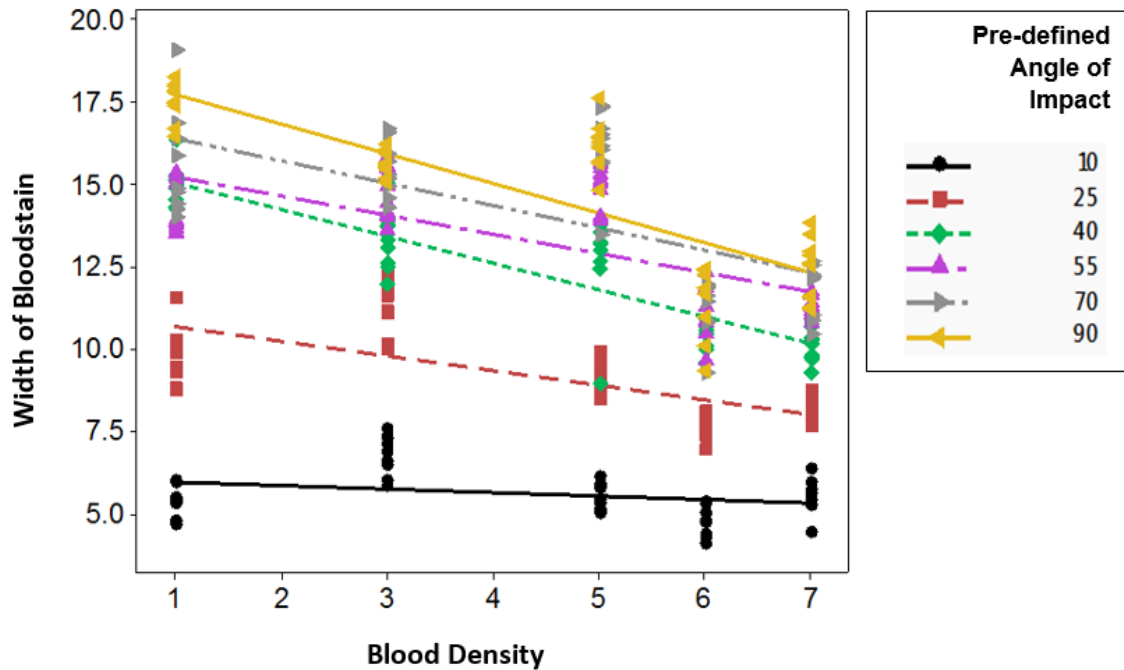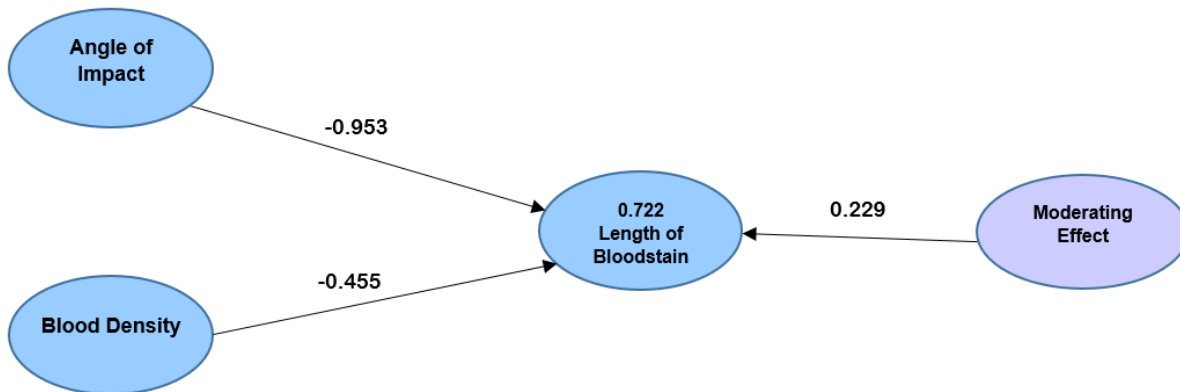
65
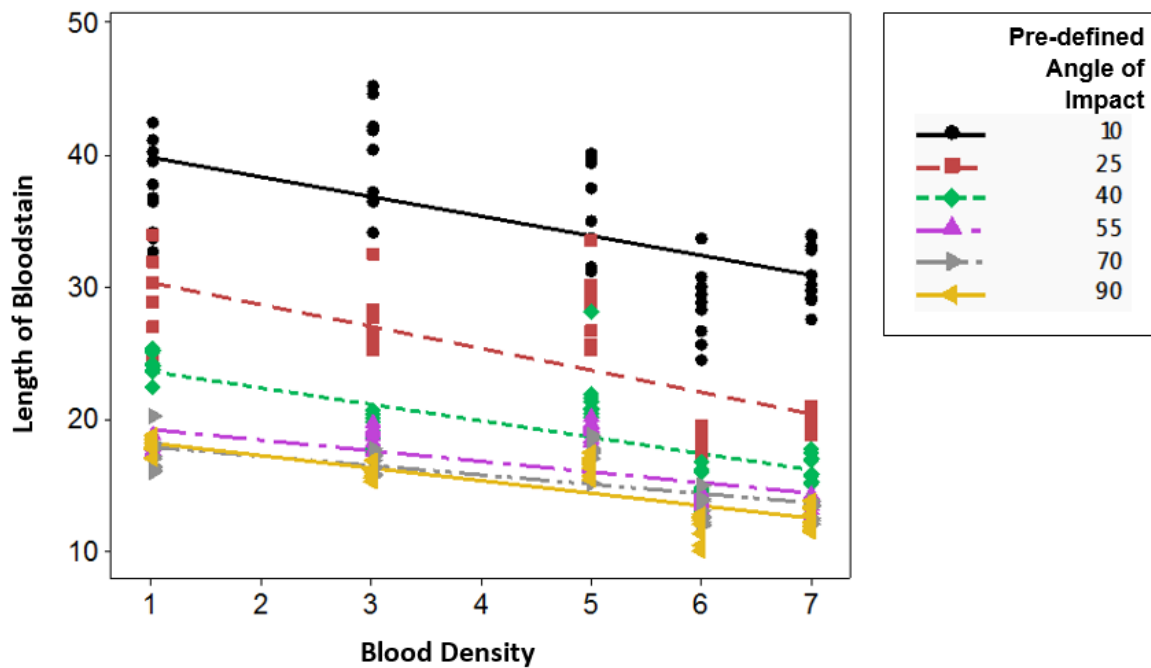
Figure 46. Visual analysis of the moderating effect of angle of impact on the correlation between blood density and length of bloodstain.

The summarized results of the testing of hypotheses H1a, H1b, and H1c, based on the moderation analysis presented above, are that:

- H1a: Blood density is correlated with the width and the length of the bloodstain;

- H1b: The angle of impact is correlated with the geometry (i.e., the width and length) of the bloodstain, and

- H1c: The angle of impact acted as a moderator, by altering the strength and/or direction of the correlation between the blood density and the width and length of the bloodstain.

- Hid: there is no difference between the pre-defined angles of impact and the calculated angles of impact was tested by comparing the pre-defined angles of impact (i.e. 10, 25, 40, 55, 70, and 90 degrees) with the 95% confidence intervals of the computed mean angles of

66

impact. Figures 47–52 present the results. The mean calculated angles of impact are represented by circular symbols and the lower and upper bounds of the 95% CI are represented by I symbols. Differences between the pre-defined and calculated angles were indicated if the pre-defined angles did not strongly overlap with the lower and upper boundaries of the 95% CI of the calculated angles. Figure 47 shows that when the blood density was very low (1) and normal (5) the mean calculated angles (8.33 and 8.74 degrees) were lower than the pre-defined angle (10 degrees). Figure 48 shows that the mean calculated angles (18.94 and 23.95 degrees) were consistently lower than the pre-determined angle (25 degrees) at all levels of blood density. Figure 49 shows that when the blood density was very low (1), normal (5), and very high (7) the mean calculated angles (38.04, 36.87 and 38.17 degrees) were lower than the pre-defined angle (40 degrees). Figure 50 shows that the mean calculated angles (52.58 to 53.36 degrees) were consistently lower than the pre-determined angle (55 degrees) when the blood density was very low (1), low (3), normal (5), and high (6), but greater than the 55 degrees (56.42 degrees) when the blood density was very high (7). Figure 51 shows that the mean calculated angles (61.19 to 67.24 degrees) were consistently lower than the pre-determined angle (70 degrees) at all levels of blood density. Figure 52 also shows that the mean calculated angles (75.29 to 81.89 degrees) were consistently lower than the pre-determined angle (90 degrees) at all levels of blood density.

Figure 47. Comparison of pre-defined angle of impact (10°) vs. mean and 95% CI of calculated angles of impact. Mean calculated angles of impact are represented by circular symbols and the lower and upper bounds of the 95% CI are represented by I symbols.
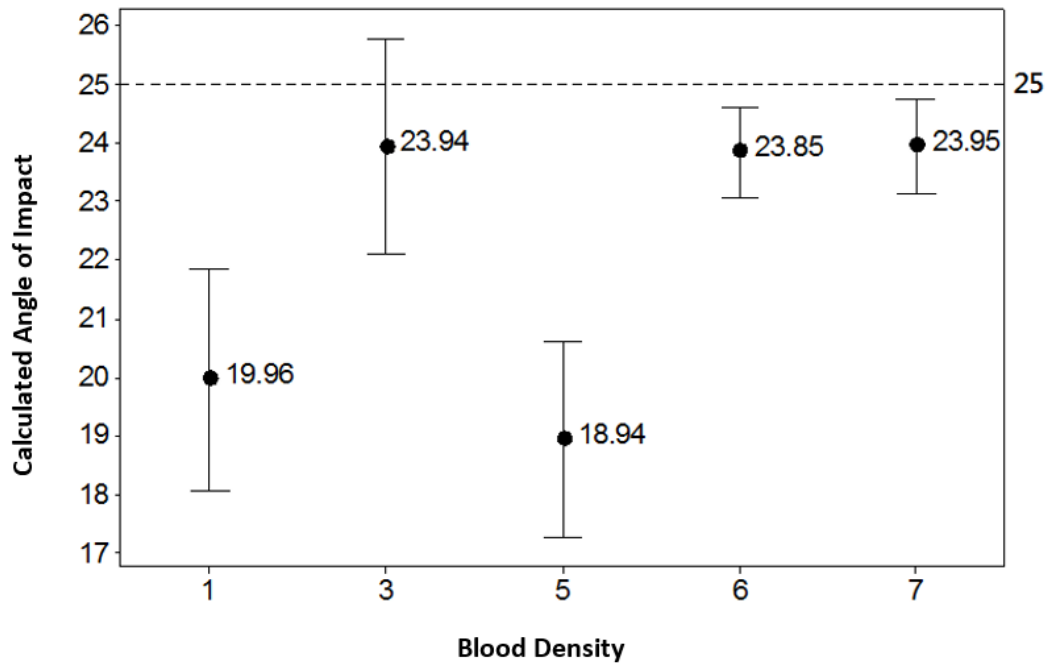
Figure 48. Comparison of pre-defined angle of incidence (25º) vs. mean and 95% CI of calculated angles of impact. Mean calculated angles of impact are represented by circular symbols and the lower and upper bounds of the 95% CI are represented by I symbols.
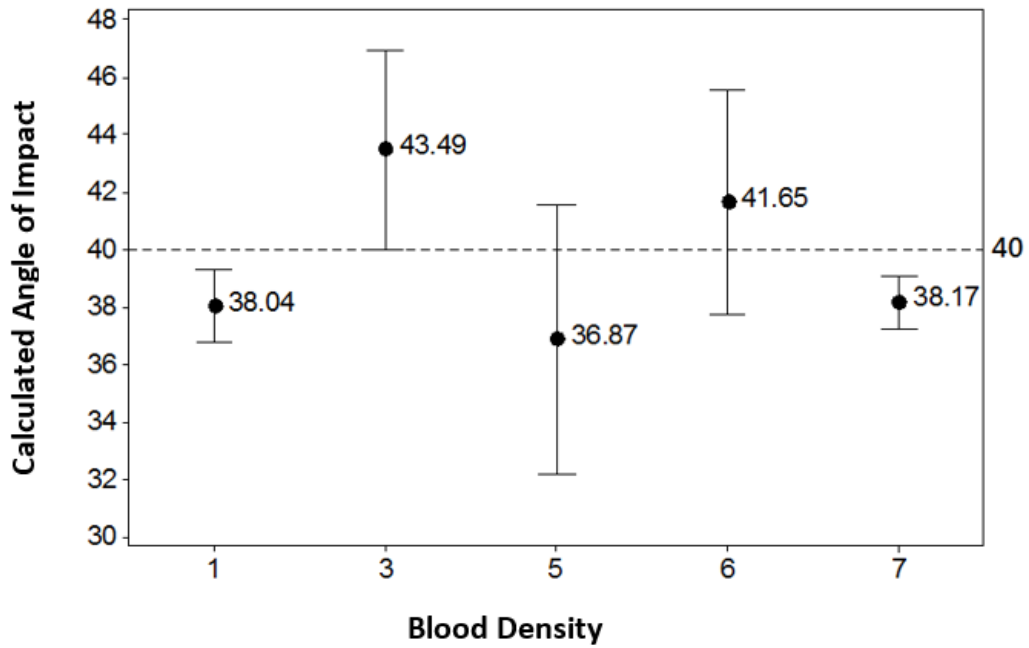
Figure 49. Comparison of pre-defined angle of impact (40°) vs. mean and 95% CI of calculated angles of impact. Mean calculated angles of impact are represented by circular symbols and the lower and upper bounds of the 95% CI are represented by I symbols.
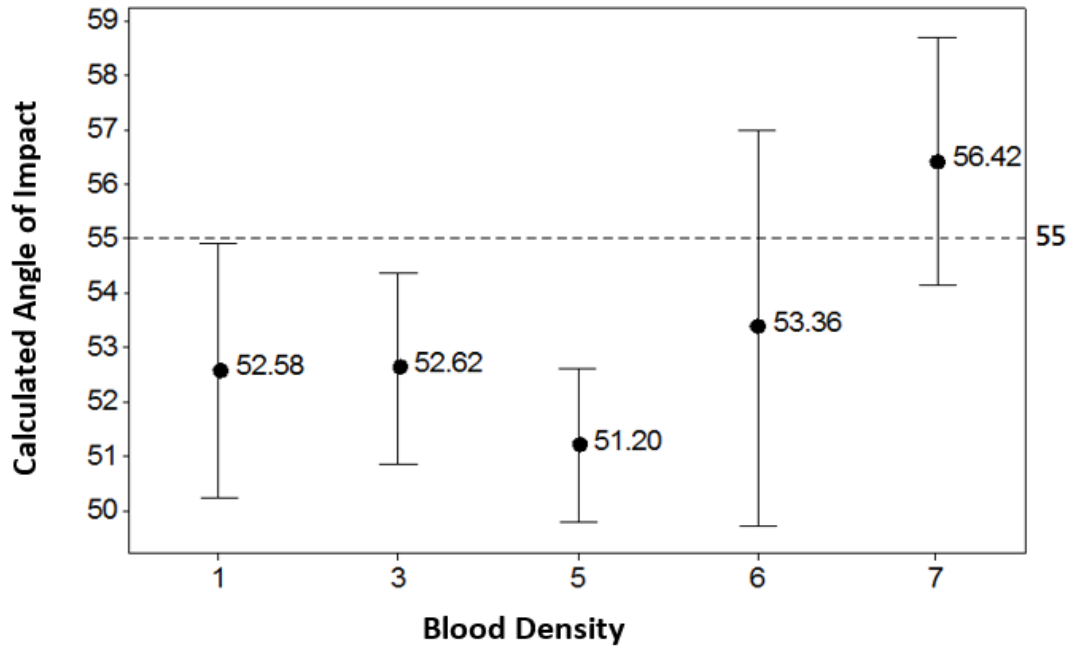
Figure 50. Comparison of pre-defined angle of impact (55º) vs. mean and 95% CI of calculated

angles of impact. Mean calculated angles of impact are represented by circular symbols and the

lower and upper bounds of the 95% CI are represented by I symbols.

71
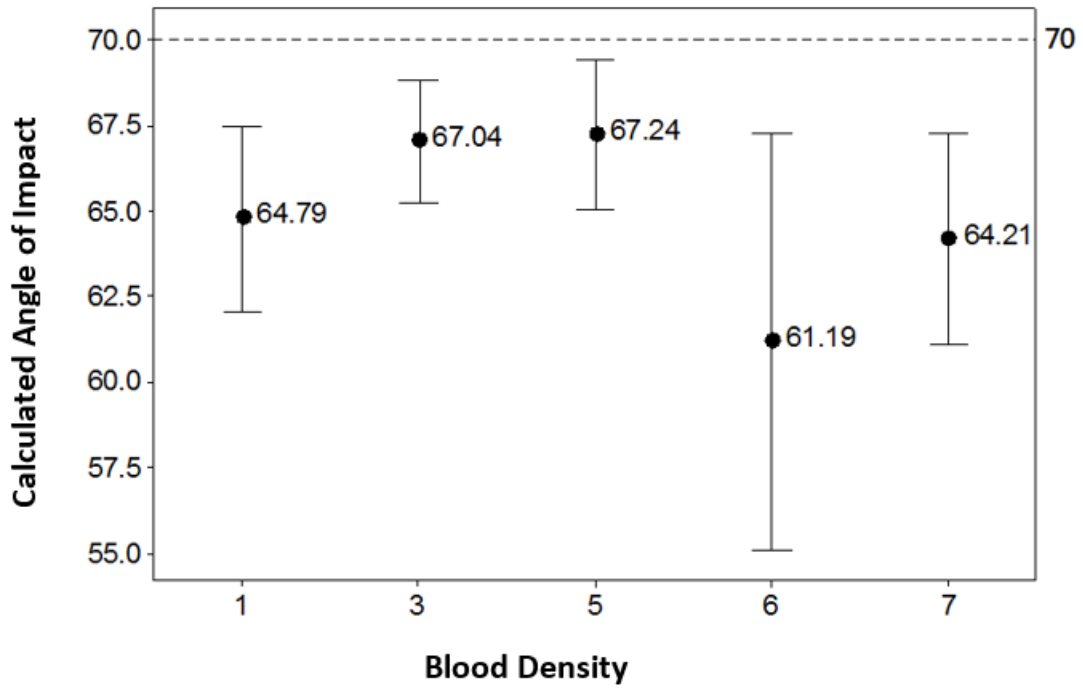
Figure 51. Comparison of pre-defined angle of impact (70°) vs. mean and 95% CI of calculated

angles of impact. Mean calculated angles of impact are represented by circular symbols and the

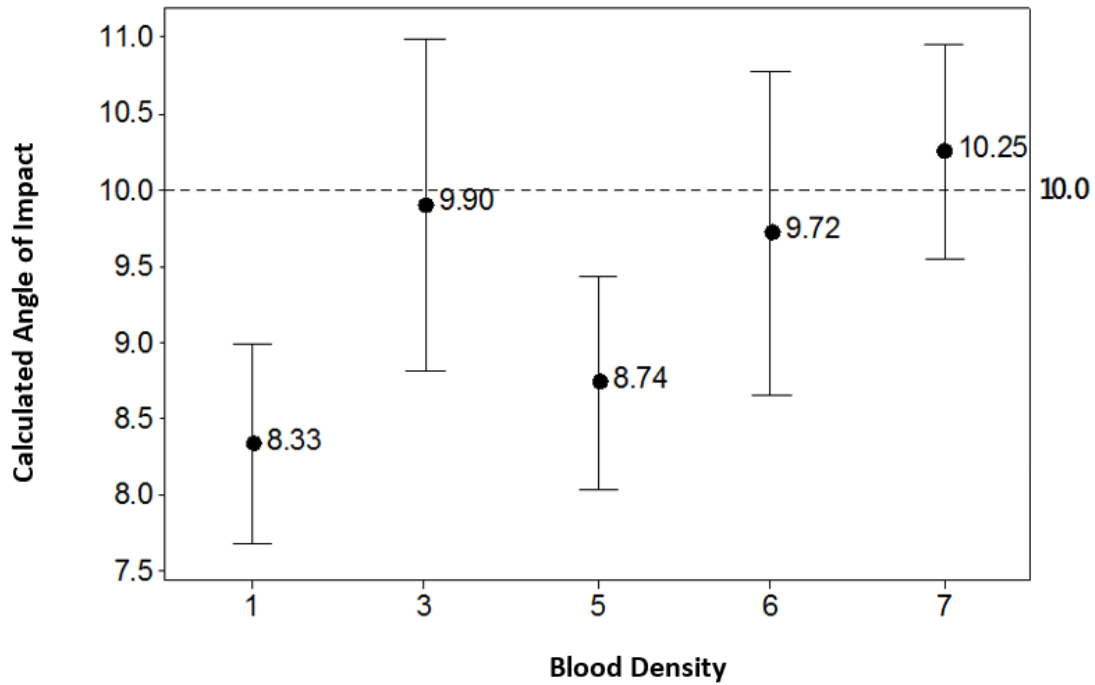*lower and upper bounds of the 95% CI are represented by I symbols.*
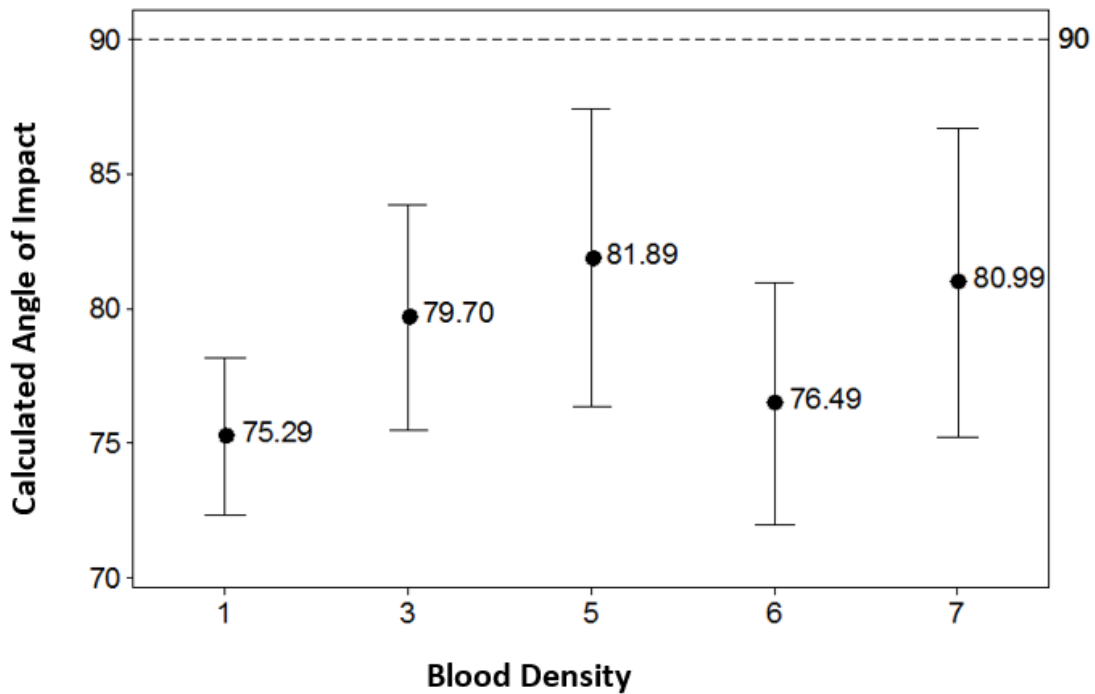
Figure 52. Comparison of pre-defined angle of impact (90°) vs. mean and 95% CI of calculated angles of impact. Mean calculated angles of impact are represented by circular symbols and the lower and upper bounds of the 95% CI are represented by I symbols.

The hypothesis H1d was rejected. When the pre-defined angles of impact were higher (55 to 90 degrees), then the calculated angles of impact at all levels of blood density were lower than the pre-defined angles. At lower pre-defined angles of impact, there appeared to be no systematic effects of blood density on the differences between the pre-determined and calculated angles of impact.

Conclusions

Blood density is correlated with the width and the length of the bloodstains. The angle of impact is correlated with the geometry (W and L) of the bloodstain. The angle of impact acts as a moderator by altering the strength and/or direction of the correlation between blood density and

the width and length of the bloodstain. The moderating effect was negative for the width and positive for the length of the bloodstain. The result is that the change in density of the blood does not alter the angle of impact but does have an effect on other characteristics of the bloodstain.

The bloodstains produced by the low density blood were either very light red or light red in color and had multiple tails. This seems to indicate that there are multiple breaks in the surface tension upon striking a surface as compared to a bloodstain with a single tail. High density samples were dark red in color with a single shorter tail as compared to normal density bloodstains. The difference in color and geometry do not effect the angle of impact determinations as the tail portion of the bloodstain is not used in calculations (Fisher, R, personal communication 5/3/18).

Chapter 3. Study 2: Impact – Area of Origin Determination

Purpose and Study Plan

The purpose of Study 2 was to conduct simulations to compare the known area of origin (intersection, convergence) of bloodstains to the calculated areas of origin of bloodstains using a manual string approach and a commercially available computer program (HemoSpat®) with five blood samples of varying densities. Five simulations for each blood sample provided 25 simulations and 10 bloodstains were examined in each simulation for a total of 250 blood spatter examinations.

Construction of Device to Simulate Blood Spatter

To complete Study 2, a device had to be fabricated that could be used to generate the blood spatter for all of the simulations and a room had to be constructed to carry out the blood spatter study.

Device construction.

A device was fabricated which would have the ability to generate blood spatter on the walls of the simulation room. A Rawlings R 25 inch, 12 oz metal alloy bat (Rawlings Sporting Goods, St. Louis, MO) was chosen as the "weapon" that would be used to strike a target. Metal was chosen over a wooden bat as it was easier to clean the metal bat between simulations. The device to hold the bat and allow it to rotate on its axis was constructed from perforated metal sections bolted to an acrylic base. A hole was drilled through the base of the bat allowing a threaded metal rod to pass through it and act as the axis for rotation of the bat. The bat was 25 inches in length. The testing of the bat falling under its own weight onto a target saturated with synthetic blood (Arrowhead Forensics, Lenexa, KS) failed to produce adequate blood spatter. A 1-lb weight was attached to the bat to determine if the additional weight would resolve this situation, but it was not effective. It was decided to add two Everbilt $^5/_8$ inch x 6½ inch extension springs to increase the rate of motion of the bat towards the target and produce a uniform impact. Figure 38 depicts springs and with added weight in place. The device allows the bat to rotate while staying in a rigid plane. In this manner, the target location relative to the bat stays constant.
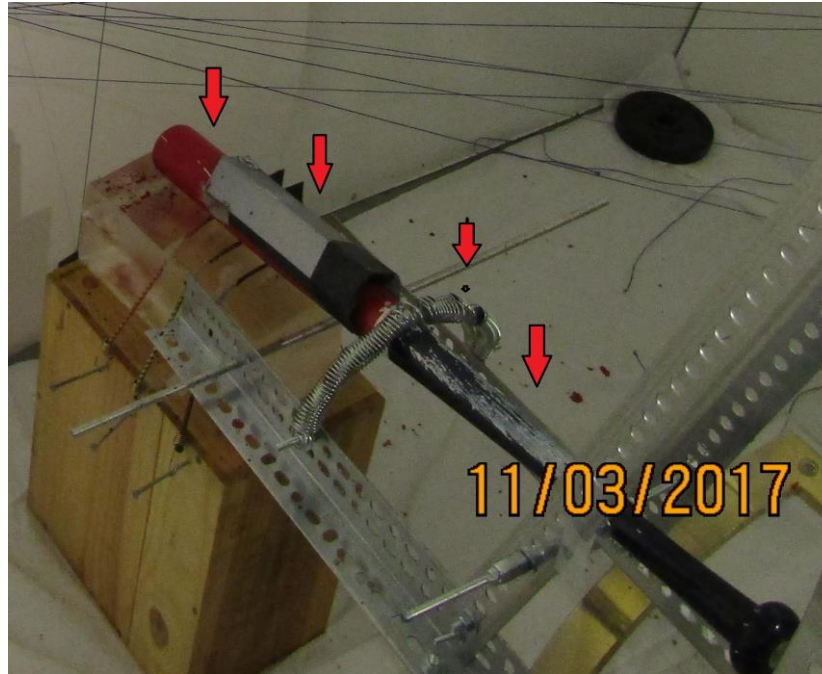
Figure 53. Close up of the blood spatter device and ballistic gel. Arrows left to right show: end of bat striking ballistic gel target, extra weights, springs and bat shaft with rotation rod.

A 10% ballistic gelatin block from Clear Ballistics (Clear Ballistics LLC, Fort Smith, AR) was used as the target in order to simulate the bat striking an individual. The ballistic block measured 22.5 cm in length, 10 cm in width, and 10 cm in depth. A variety of items were evaluated for holding a fixed amount of blood in place on the ballistic gel for the bat to strike. These items included the following:

1. Studio 35 Beauty latex free cosmetic wedges, measuring 4.2 cm x 2.4 cm with the depth varying from 1.5 cm to 0.4 cm.

2. Studio 35 Beauty textured cotton rounds, measuring 5.5 cm in diameter, with a depth of 0.2 cm. This item was tested with a single round, 2 rounds together, and 3 rounds together.

3. Studio 35 Beauty quilted cotton squares, measuring 5.8 cm x 5.2 cm x 0.3 cm. This item was tested with a single square, 2 squares together, and 3 squares together.

4. 3M Ocelo sponge, a section of the sponge was cut out measuring 3 cm x 4 cm x 1.8 cm. See Figure 54S.

Figure 54. Materials tested to hold blood samples for blood spatter simulations.

All of the above initial evaluation testing was conducted using synthetic blood obtained from Arrowhead Forensics. Synthetic blood is a proprietary dilute aqueous mixture containing hemoglobin, amino acids, protein, and other components (MSDSs in the Appendix).

Each of the 4 materials listed above had a total of 1 mL (20 drops from a VWR disposable glass Pasteur pipet) dropped onto it.

All of the initial testing of the device was conducted in an empty farm house (Figure 55) with permission of the owner. This farm house, which is located in a remote area, was later used for Study 3 ballistics testing. Since, the farm house had no electricity experiments were limited to daylight hours and the synthetic blood was evaluated at room temperature rather than at 37 ºC.

77

All of the subsequent testing was conducted in either a room built for this purpose or at the farm house but with the use of a generator to power lights and a water bath.

Figure 55. Farm house for preliminary testing of Study 2.

Each of the 4 materials was evaluated, and none provided a sufficient number of bloodstains for analysis, which were at least 10 bloodstains with a suitable geometry for angle of impact determination. The final evaluation was to cut out a section of the ballistic gel that was suitable for holding 1 mL of blood and not using any absorbent material to hold the blood. The section that was cut out measured 2.5 cm x 2.0 cm x 0.2 cm. This simulated what would be the second strike to the head (exposed skin area) of an individual as blood was already on the surface of the skin as a result of the first strike. This approach was successful in generating a sufficient number of bloodstains to allow for utilization of the string method and the computer generated approach of area of origin determination simulations. See Figures 56 and 57. A head made from

78

ballistic gel was evaluated for use as a target, but problems with keeping a blood sample of constant volume in place to conduct the simulations was unfortunately not feasible. See Figures 58 and 59.

Figure 56. Ballistic gel target with cut out for blood samples.
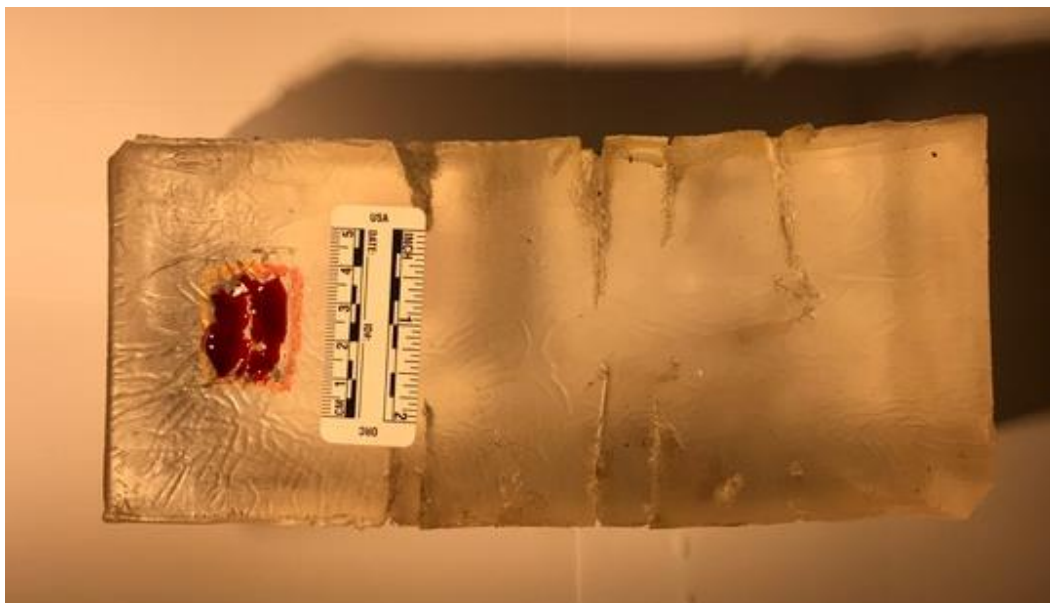
Figure 57. Ballistic gel target with 1 mL of synthetic blood in cut out.

79

Figure 58. Ballistic gel head as possible target.
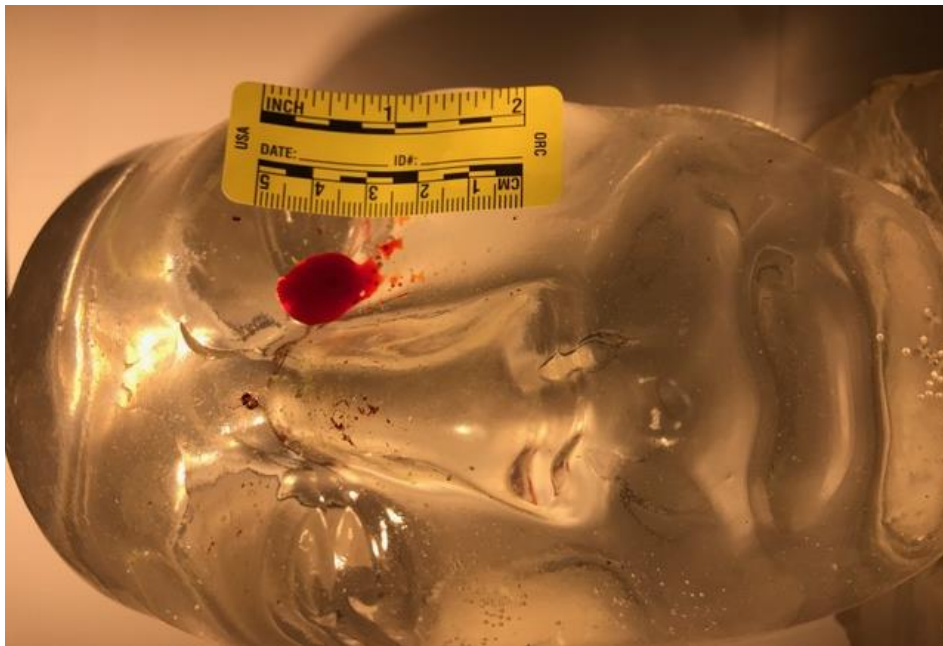
Figure 59. Ballistic gel head with synthetic blood for testing.

Room Construction for Blood Spatter Simulations

       The next phase required the building of a room in which to carry out the simulations. The

room was constructed from Charlotte Pipe (Charlotte Pipe, Charlotte, NC) 1 inch PVC piping

and wall board material that had a smooth surface. The surface was easily cleaned between

simulations and the smooth surface allowed for bloodstains with clear geometry without surface-

induced distortions. The room measured as follows: height 209 cm, width 214 cm, and length

240 cm. See Figures 60-62 for completed room for simulations.

Figure 60. Room construction for blood spatter simulations.

Figure 61. Room construction for blood spatter simulations.

Figure 62. Completed room.

Once the room construction was completed, the first testing of the device in the simulation room was with synthetic blood at 37 $^{\circ}$C. This was followed with the simulations utilizing the five blood samples of varying densities.

Preparation of Blood Samples

Human blood components were purchased from BioIVT and consisted of the following:

- 100 mL of human whole blood with sodium heparin added as anticoagulant,

- 75 mL of human red blood cells with sodium heparin added as an anticoagulant, and

- 100 mL of unfiltered human serum.

All of the human blood components were tested and found to be negative for the following: HIV 1/2 Ab, HCV Ab (hepatitis C), non-reactive for HBsAg (hepatitis B), HIV-1 RNA, HCV RNA (hepatitis C), HBV DNA, WNV RNA, ANTI-T CRUZI, and STS (syphilis) (certificates of analysis are contained in the Appendix).The blood samples were prepared as described in Table 15, and the density and HCT were determined for each (Tables 16-17).

Table 15. Preparation matrix for the blood samples

Sample Number	Serum, %	Serum, mL	Cells, %	Cells, mL
1	95	38	5	2
2	85	34	15	6
3	60	24	40	16
4	20	8	80	32
5	15	6	85	34

Table 16. Sample density determinations

Sample Number	Density, g/cm^3 at 37 ºC
1	1.0267
2	1.0312
3	1.0442
4	1.0619
5	1.0699

Table 17. Sample hematocrit determinations

Sample Number	HCT
1	7.25%
2	12.4%
3	34.0%
4	68.0%
5	73.25%

Manual String Process

Manual string method.

For each bloodstain, the manual string method was utilized whereby each bloodstain was measured for length and width and the angle of impact was calculated using the equation arc sine = W/L. Once the angle of impact was calculated, a zero-edge protractor, in which the scale goes to the surface, is used in conjunction with a string to determine where the source of the blood was located at the time the blood spatter being analyzed was produced. First, the direction of the blood spatter must be determined based on the shape of the bloodstain (Figure 63).

84
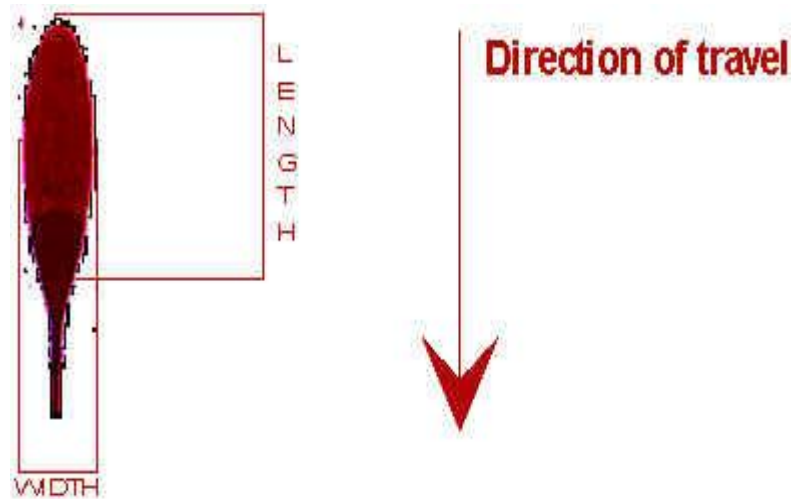
Figure 63. Directionality of blood spatter.(http://www.bloodspatter.com/bloodstain-tutorial-2)

The protractor was placed at the point where the blood spatter impacted the surface (Figure 64). A string was secured to the surface by tape, pin, or adhesive clips (used in this study) (Figure 65). The string was then projected back in the same direction as the blood spatter would have originated and at the angle that the blood spatter impacted the surface. The string was pulled taut and secured on another wall or other object. The location of the blood spatter in the room was documented. For each blood spatter, the process was repeated – blood spatter width and length was measured, the angle of impact was calculated, directionality was determined, and the blood spatter was located in the room using a protractor and secured string. The site where the strings intersect is the area of origin of those blood spatters. The coordinates of the area of origin were documented and used as part of the crime scene reconstruction. This is one part of the reconstruction, and all of the evidence must be considered in order to reconstruct the sequence of events; it is a complex and time consuming endeavor.

85
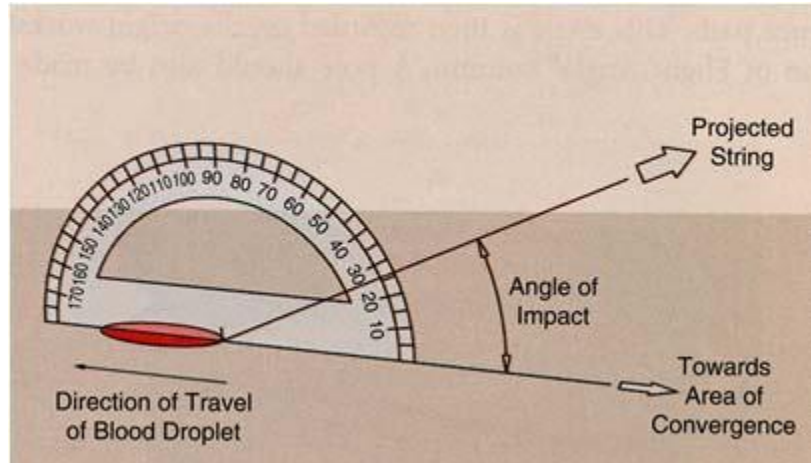
Figure 64. Zero edge protractor placement for string method.

Figure 65. Strings used for manual string process. Note the use of different color strings.

Computer Program and Digital Photographs

In addition to the manual string approach to determine the area of origin, a computer

program was utilized. The program was the HemoSpat® software, version 1.10, released

11/10/2016 (HemoSpat®, 2016). The process included digital photographs of each bloodstain

and data entry of all of the coordinates for each bloodstain into the software. The digital

photographs were obtained with a Canon SX420 IS digital camera (Canon U.S.A, Inc.,

Arlington, VA). The manual and computer-generated areas of origin were compared to the actual

areas of origin for each blood density simulation. The steps to enter the digital photograph and

associated location coordinates are given in Figure 65.

<div style="border: 1px solid black; padding: 1em;">

HemoSpat® Bloodstain Pattern Analysis Software

HemoSpat® Program Steps for collection of bloodstain data once digital

photograph of bloodstain has been obtained

Open program

Click on "Create Project"

Add values for walls, the front wall being the default wall the program measures the

bloodstains.

Open the document source of the bloodstain photos.

INSERT IMAGES: Drag first bloodstain photo from their source and drag them into the

green box stating "drop your stain images here." Alternatively, the "File" button in the upper

left-hand corner has an "import images" feature. Drag subsequent bloodstain photos onto the first

bloodstain photo.

Click on the bloodstain to be analyzed. Set the scaling to fit the screen as necessary.

CROP: The program automatically sets the cursor to begin cropping. Click and hold to

draw a box around both the spatter and the scale. When finished, press the lock icon to lock the

cropped picture.

</div>

87

SELECT STAIN: Click the middle of the blood stain and the program measures the stain. If the outline of the computer's recognition of the stain is incorrect press ESC, and click the middle of the stain again. When satisfied, press the lock button.

SCALE: Drag and hold the mouse to draw a box around the metric side of the scale. When satisfied click the lock button.

PLUM LINE: To orient the stain with regard to the plum line, click the middle of the picture and drag the digital plum line until it follows the plum line drawn on the scale.

For each photo:

Set the scale to 50 mm

Record the Y and Z value in the program

Orient the stain to the "front wall" using the drag-down drop box.

Analysis:

Click "View" in the upper left-hand corner. Click "2D VIEWS."

To export the analysis, click "File" in the upper left-hand corner. Click "export" and select the file type to be exported. ".txt" is the default analysis that opens in "Notepad," and "Comma Separated" saves the data in Excel format.

Figure 65. HemoSpat® program steps.

Blood Spatter Simulations Process

The first step was to create the blood spatter patterns that will be evaluated. 1 mL aliquot of the blood sample, maintained at 37 ºC, was pipetted into the cut out in the ballistic gelatin block (Figure 66). The bat was in the upright position with no spring tension on it (Figure 67).

Figure 66. Blood spatter device testing impact material.

Figure 67 Blood spatter device testing.

The bat was rotated until the springs are engaged and then released and allowed to strike

the target producing blood spatter on the walls of the simulation room (Figure 68). Between each

simulation, the bat was cleaned of any blood residue. The target location was re-established in

89

case it had moved from the previous simulation, and the x, y, and z measurements were documented (Figures 69-70). For each simulation, 10 bloodstains were identified and a 5 cm adhesive photographic scale was affixed next to each bloodstain and labeled with the bloodstain number. A plum line was dropped next to each bloodstain, and the line is traced on to the photographic scale associated with each bloodstain. The location of each bloodstain is documented by measuring the distance from the left wall (y), the distance from the floor (z), and the distance out from the front wall (x), if applicable. The measurements of each bloodstain were then determined; the width and the length were recorded. The next step was photographing each bloodstain with a digital camera. The pictures were downloaded into the HemoSpat software for the computer-generated analysis. Once the photography is completed, the task of completing the manual string analysis continued. From the width and length numbers, the arcsine was calculated and the angle of impact determined for each bloodstain. Using a zero edge protractor adjacent to the point where the bloodstain impacted the wall, a string was attached by means of an adhesive clip to the wall. The string was lined up with the appropriate angle of impact for the bloodstain from the protractor, and the string was extended back away from the stain until it was affixed to another wall or object. The string now approximated the path that this blood spatter followed from its origin until it impacted the wall. Different colored strings were used to help distinguish between bloodstains or simulations if the strings remained in place, creating a very complicated scenario. The strings for each simulation, after being documented, were removed before the next simulation took place. The process described above was repeated for each of the 10 bloodstains used in each simulation. The area(s) where the strings intersected (cross) represented the origin, the area (x, y, and z) where the source of the bloodstains was located at the time the specific

90

bloodstains were produced on the walls of the room. Once the manual string process was

completed, the computer-generated process was followed as outlined in Figure 50.

Figure 68. Test of blood spatter device in simulation room.
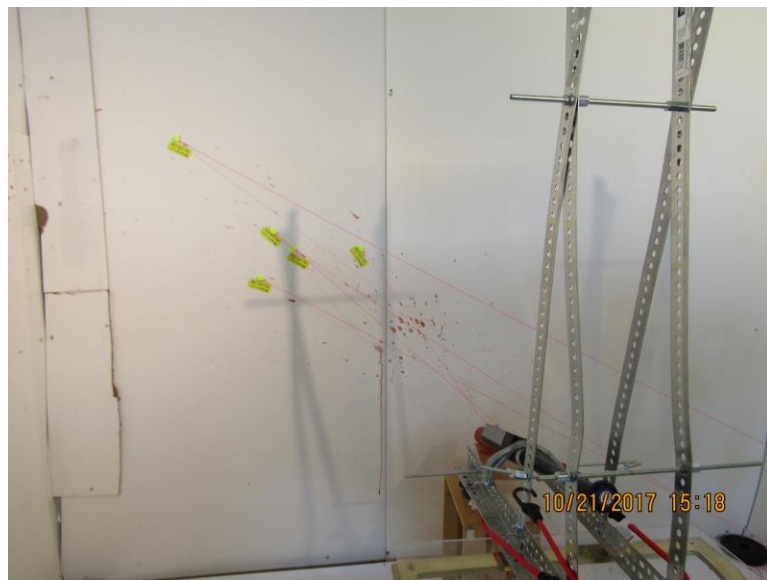
Figure 69. Spatter test using synthetic blood and strings.

91

Figure 70. Room and spatter device set up for simulations.

The entire process was repeated for each simulation utilizing the 5 different blood samples for a total of 25 simulations. Both the string method and the computer-generated method were very tedious and required a significant amount of diligence and expertise to be performed correctly and accurately. Each simulation took a minimum of 4 hours; therefore, the 25 simulations required a minimum of 100 hours labor.

Simulations Data Collection

The tables that follow contain the data collected for each simulation (Tables 18-42). The figures (Figures 71, 74, 76-77, 80, 82-83, 85, 87, 89, 91, 93-94, 96, 98, 100, 102, 105-106, 108, 111, 114, 116, 118-119, 121, 123, 125, 127, and 129) that follow are the computer generated simulations from the data in the tables and pictures (Figures 72-73, 75, 78-79, 81, 84, 86, 88, 90, 92, 95, 97 ,99, 101, 103-104, 107, 109-110, 112-113, 115, 117, 120, 122, 124, 126, and 128) of the manual string method showing the strings and areas of origin. The statistics pertaining to the

simulations, as calculated by the manual string and software methods, are presented in Tables
43-44.

Table 18. Simulation 1.1 stain coordinate data

SIMULATION #1.1 - STAIN COORDINATE DATA							LOCATION	
VERY LOW DENSITY BLOOD								
BLOOD STAIN		W	L	W/L	ANGLE		X	Y	Z
1		1.5	6	0.25	14.48			154	102
2		4	9	0.44	26.1			169	103
3		4	8	0.5	30			181	109
4		2.5	6	0.42	24.83			193	92
5		4	11	0.36	21.1			179	96
6		2.5	5	0.5	30			204	132
7		2	5	0.4	23.58			191	140
8		2.5	4	0.63	29.05			163	107
9		4	8	0.5	30			183	88
10		5	13	0.38	22.33			208	186
			KNOWN AREA OF ORIGIN			31	119	45
			STRING METHOD AREA OF ORIGIN			17	132	78
			HEMOSPAT CALCULATED			28.9	123.1	91.6
			*all numbers are in centimeters					

In the above table under location, X is the distance out from the front wall, Y is the distance from
the left wall and Z is the distance from the floor. For the known area of origin and the string
method area of origin, X, Y, and Z were manually measured. For the HemoSpat® calculated area
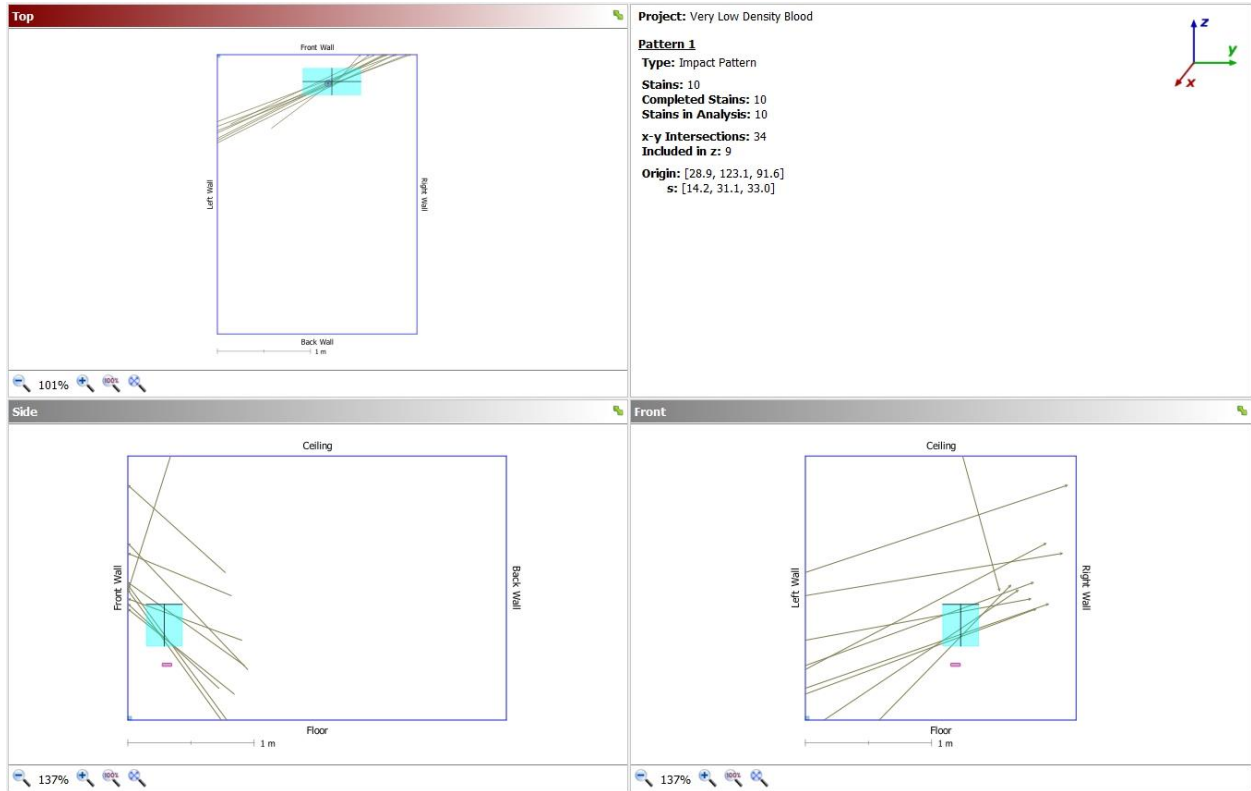of origin, X, Y, and Z were computer generated.
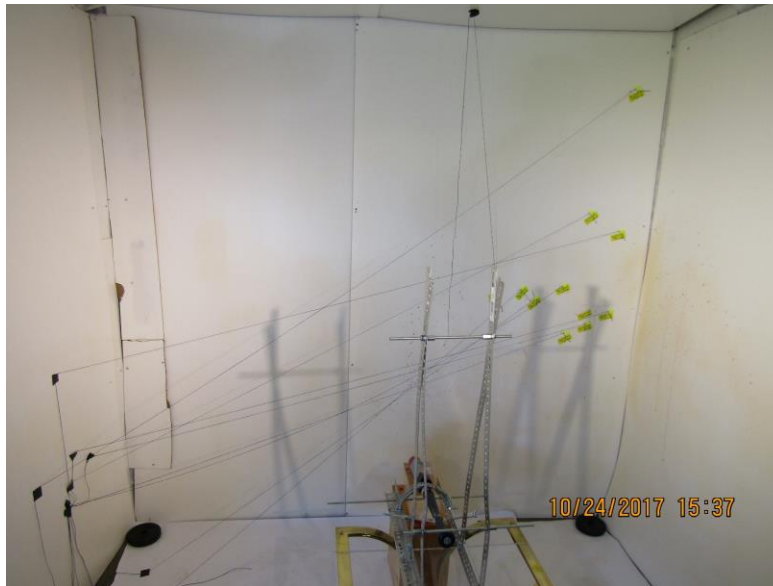
93

Figure 71. Simulation 1.1 computer-generated data.

Figure 72. Simulation 1.1 string method construction.

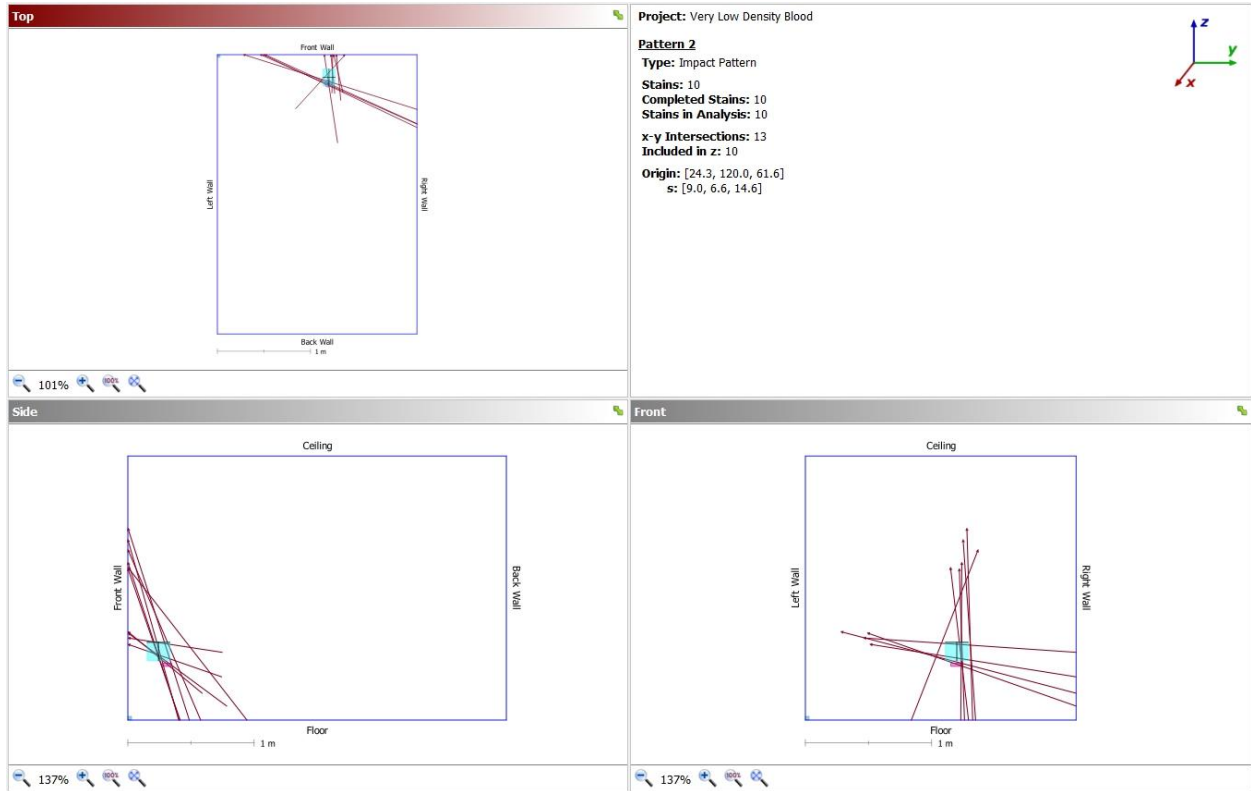*Figure 73. Simulation 1.1 string method construction.*
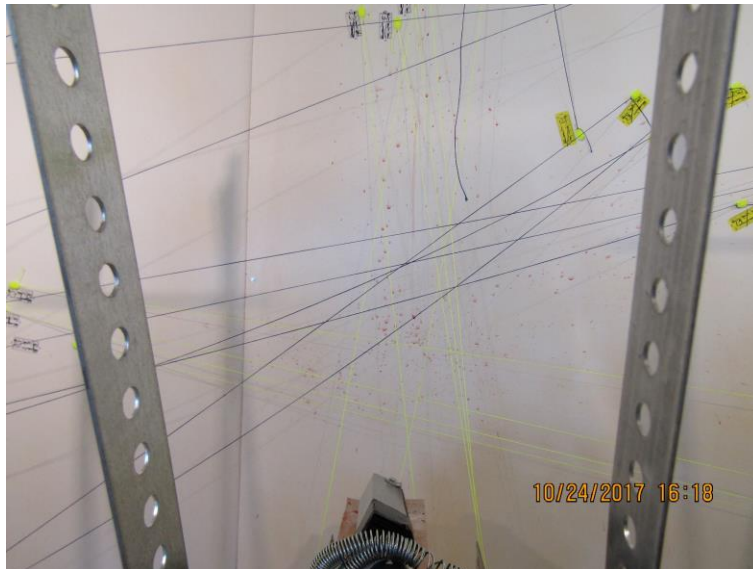
Table 19. Simulation 1.2 stain coordinate data

| SIMULATION 1.2 - STAIN COORDINATE DATA | | | | | | | LOCATION | |
| VERY LOW DENSITY BLOOD | | | | | | | | |
BLOOD STAIN		W	L	W/L	ANGLE		X	Y	Z
1		1	4	0.25	14.5			51	60
2		1.5	4	0.38	22.3			46	65
3		1	3	0.33	19.3			28	70
4		2	6.5	0.31	18.1			49	69
5		3	5	0.6	36.9			115	121
6		4	9	0.44	26.1			122	120
7		4	9	0.44	26.1			124	125
8		4	10	0.4	23.6			125	143
9		2	4	0.5	30			137	135
10		3	8	0.38	22.3			128	152
				KNOWN AREA OF ORIGIN			31	119	45
				STRING METHOD AREA OF ORIGIN			16	128	76
				HEMOSPAT CALCULATED			24.3	120	61.6
				*all numbers are in centimeters					

In the above table under location, X is the distance out from the front wall, Y is the distance from the left wall and Z is the distance from the floor. For the known area of origin and the string method area of origin, X, Y, and Z were manually measured. For the HemoSpat® calculated area of origin, X, Y, and Z were computer generated.

Figure 74. Simulation 1.2 computer-generated data.

Figure 75. Simulation 1.2 string method construction.

Table 20. Simulation 1.3 stain coordinate data

BLOOD STAIN		W	L	W/L	ANGLE		LOCATION		
SIMULATION #1.3 - STAIN COORDINATE DATA									
VERY LOW DENSITY BLOOD									
							X	Y	Z
1		3	7	0.43	25.5			201	181
2		3	9	0.33	19.3			185	152
3		3	9	0.33	19.3			182	147
4		2	5	0.4	23.6			180	124
5		4	8	0.5	30			207	169
6		2	5	0.46	23.6			156	150
7		1	4	0.25	14.5			162	162
8		2	4	0.5	30			157	137
9		1.5	4	0.38	22.3			169	165
10		5	12	0.42	24.8			191	148
			KNOWN AREA OF ORIGIN				28	119	46
			STRING METHOD AREA OF ORIGIN				18	129	87
			HEMOSPAT CALCULATED				31.1	127.6	27.3
			*all numbers are in centimeters						

In the above table under location, X is the distance out from the front wall, Y is the distance from the left wall and Z is the distance from the floor. For the known area of origin and the string method area of origin, X, Y, and Z were manually measured. For the HemoSpat® calculated area of origin, X, Y, and Z were computer generated.
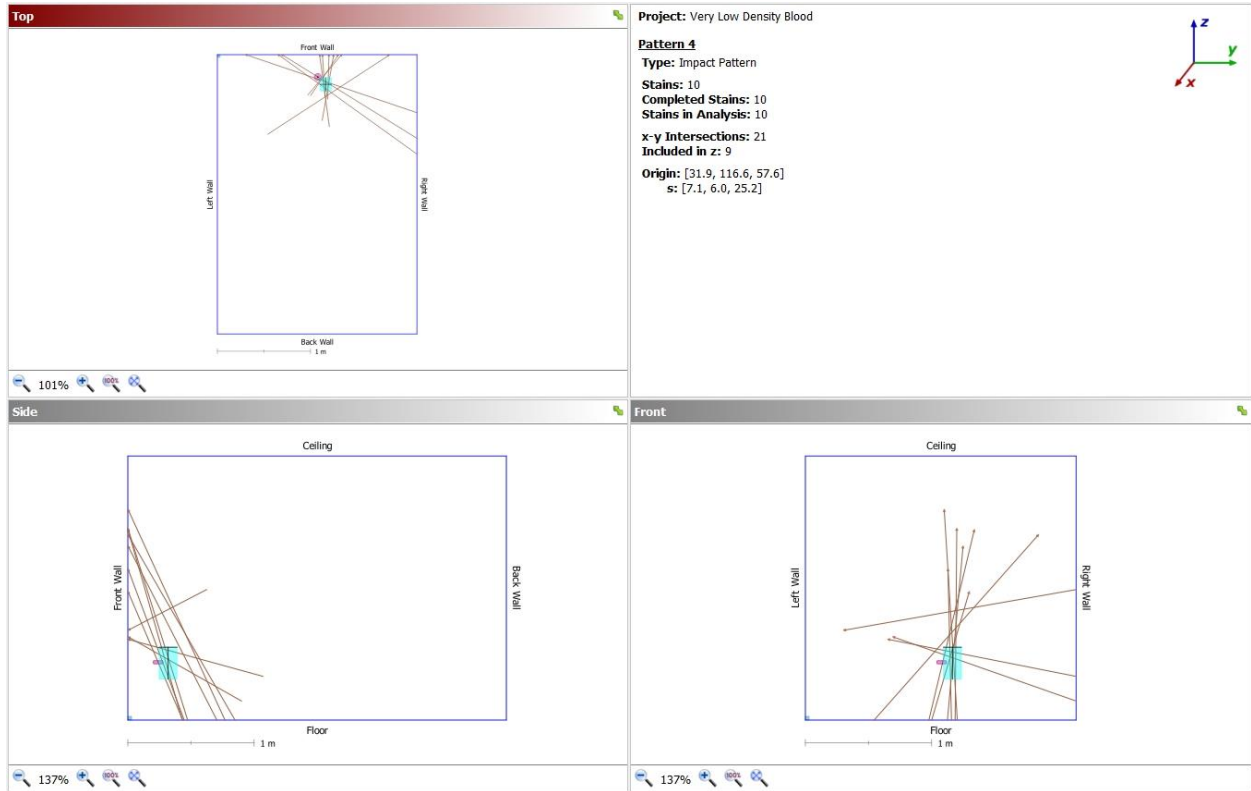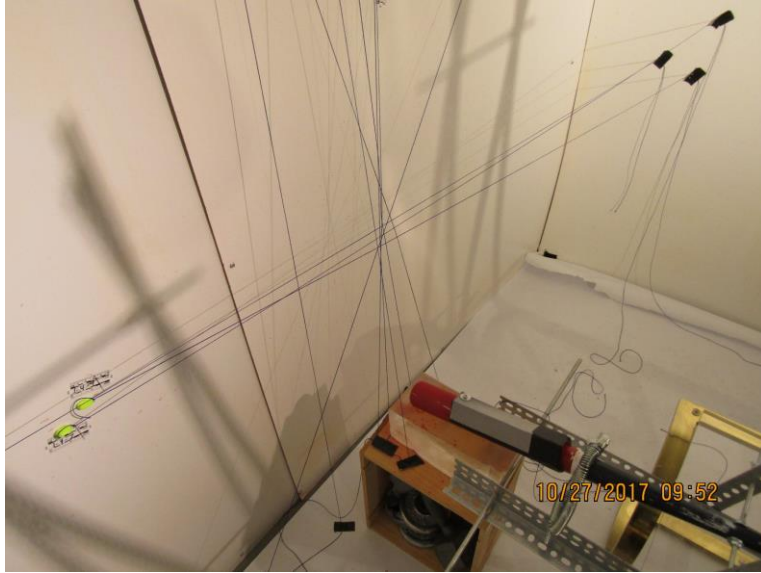
98

Figure 76. Simulation 1.3 computer-generated data.

Table 21. Simulation 1.4 stain coordinate data

SIMULATION	#1.4 - STAIN COORDINATE DATA						LOCATION	
VERY LOW DENSITY BLOOD								
BLOOD STAIN		W	L	W/L	ANGLE	X	Y	Z
1		3	10	0.3	17.5		125	138
2		1	5	0.2	11.5		134	151
3		2	10	0.2	11.5		120	152
4		4	13	0.31	18.1		110	167
5		1.5	4	0.38	22.3		130	102
6		1	5	0.2	11.5		30	71
7		2	4	0.5	30		65	64
8		2	10	0.2	11.5		185	147
9		3	5	0.6	36.9		69	66
10		1	4	0.25	14.5		113	120
			KNOWN AREA OF ORIGIN			24	108	47
			STRING METHOD AREA OF ORIGIN			15	117	72
			HEMOSPAT CALCULATED			31.9	116.6	57.6
			*all numbers are in centimeters					

In the above table under location, X is the distance out from the front wall, Y is the distance from the left wall and Z is the distance from the floor. For the known area of origin and the string method area of origin, X, Y, and Z were manually measured. For the HemoSpat® calculated area of origin, X, Y, and Z were computer generated.
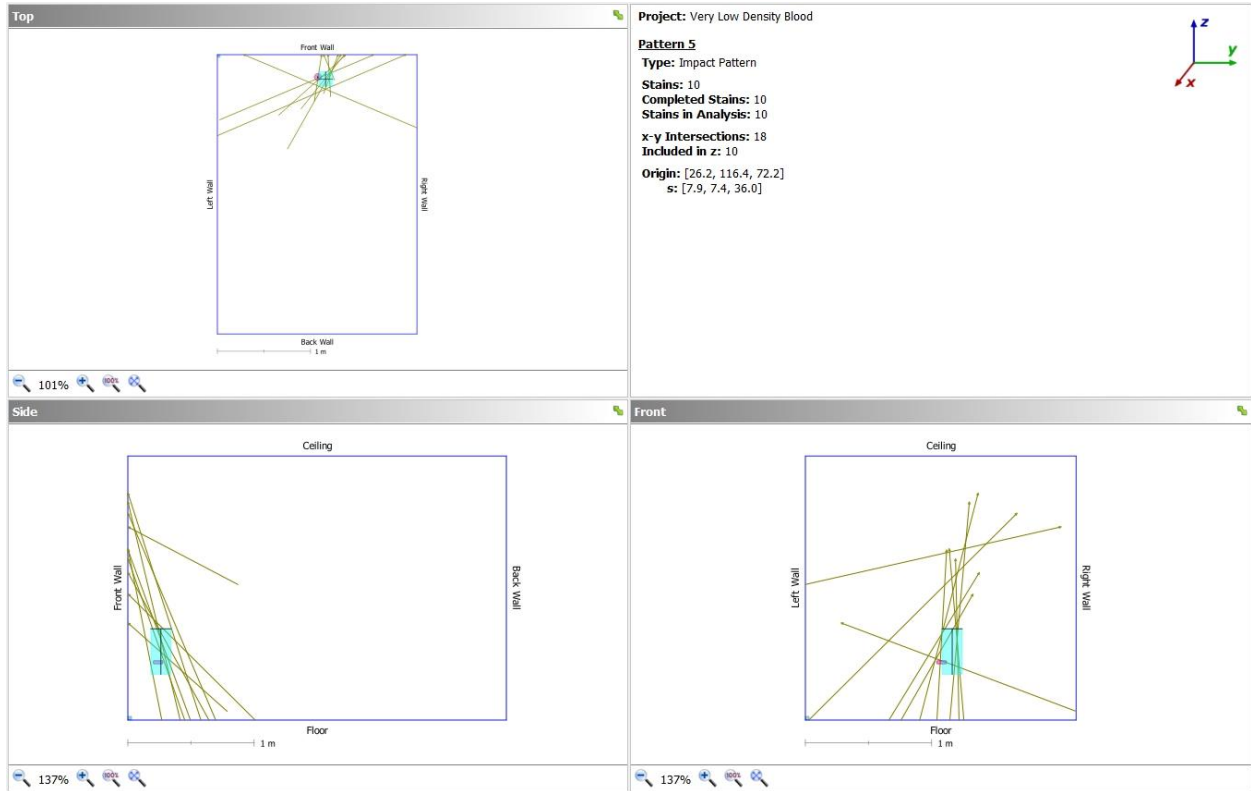
100

Figure 77. Simulation 1.4 computer-generated data.

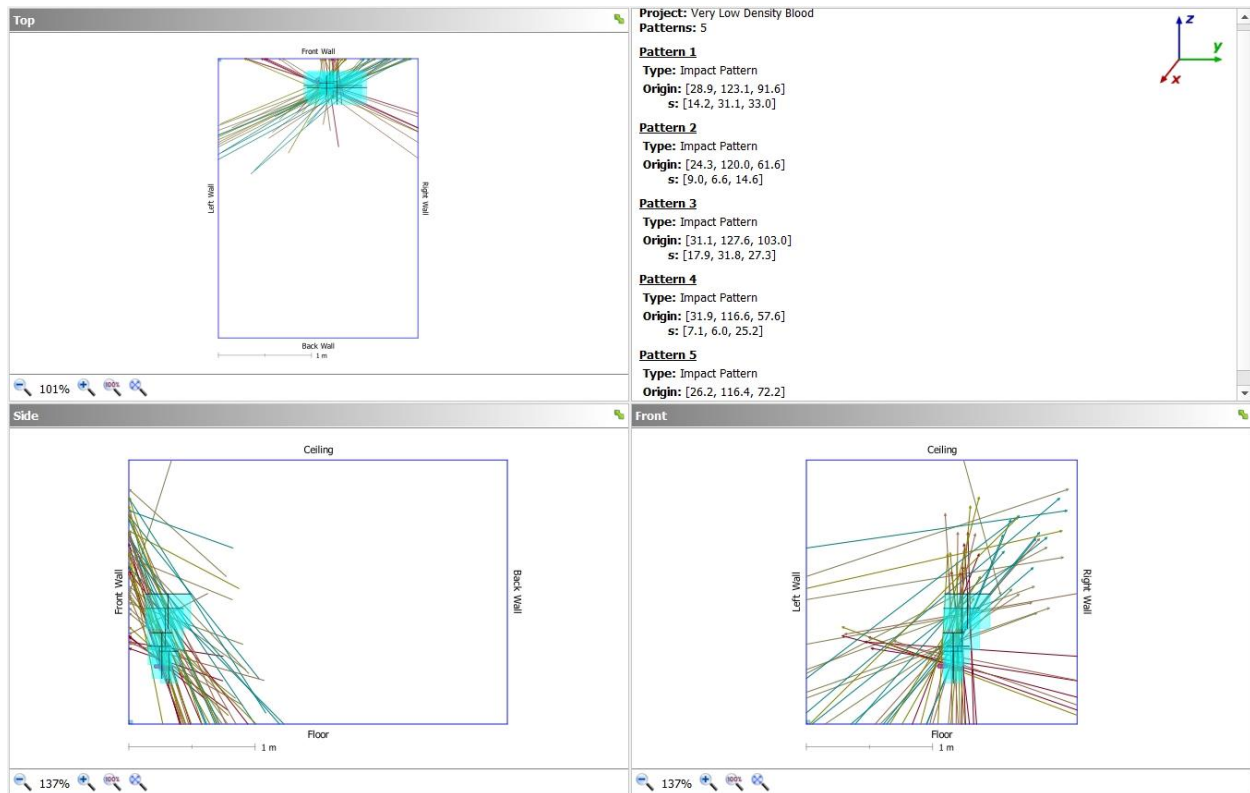*Figure 78. Simulation 1.4 string method construction.*

Figure 79. Simulation 1.4 string method construction.

Table 22. Simulation 1.5 stain coordinate data

SIMULATION #1.5 - STAIN COORDINATE DATA							LOCATION	
VERY LOW DENSITY BLOOD								
BLOOD STAIN	W	L	W/L	ANGLE		X	Y	Z
1	4	15	0.27	15.7			114	136
2	2	7	0.29	16.9			112	135
3	3	5	0.6	36.9			133	100
4	3	5	0.6	36.9			138	117
5	1	4	0.25	14.5			168	164
6	1	5	0.2	11.5			203	153
7	1	4	0.25	14.5			119	128
8	1	5	0.2	11.5			137	180
9	1	5	0.2	11.5			130	173
10	1	4	0.25	14.5			28	77
			KNOWN AREA OF ORIGIN			24	108	47
			STRING METHOD AREA OF ORIGIN			20	111	69.5
			HEMOSPAT CALCULATED			26.2	116.4	72.2
			*all numbers are in centimeters					

In the above table under location, X is the distance out from the front wall, Y is the distance from the left wall and Z is the distance from the floor. For the known area of origin and the string method area of origin, X, Y, and Z were manually measured. For the HemoSpat® calculated area of origin, X, Y, and Z were computer generated.
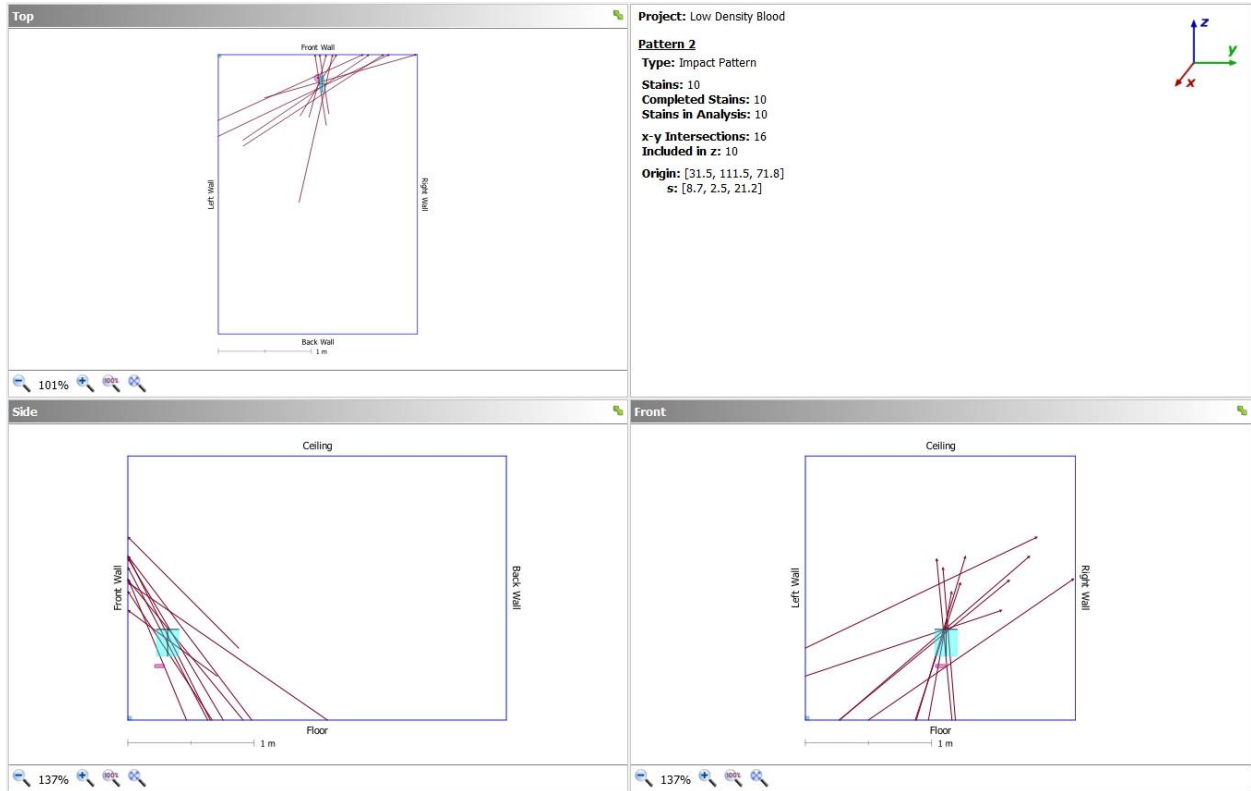
103

Figure 80. Simulation 1.5 computer-generated data.

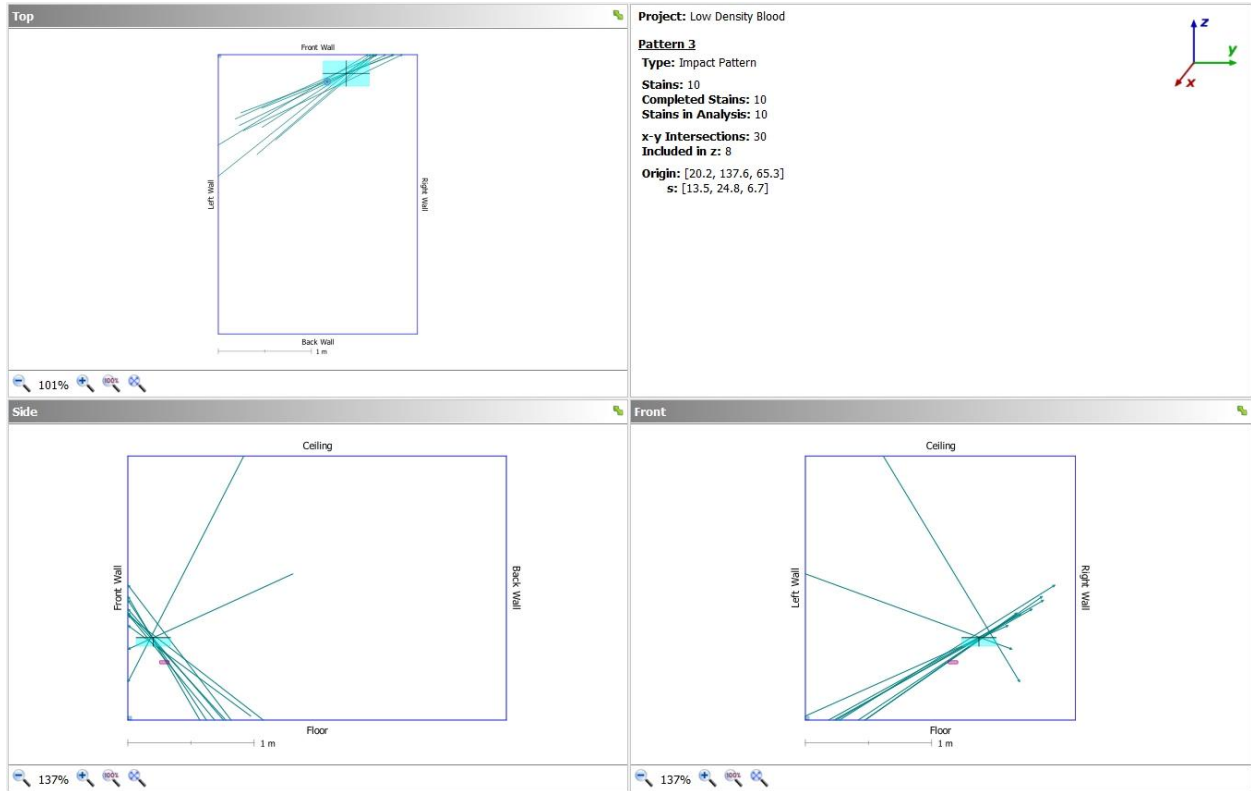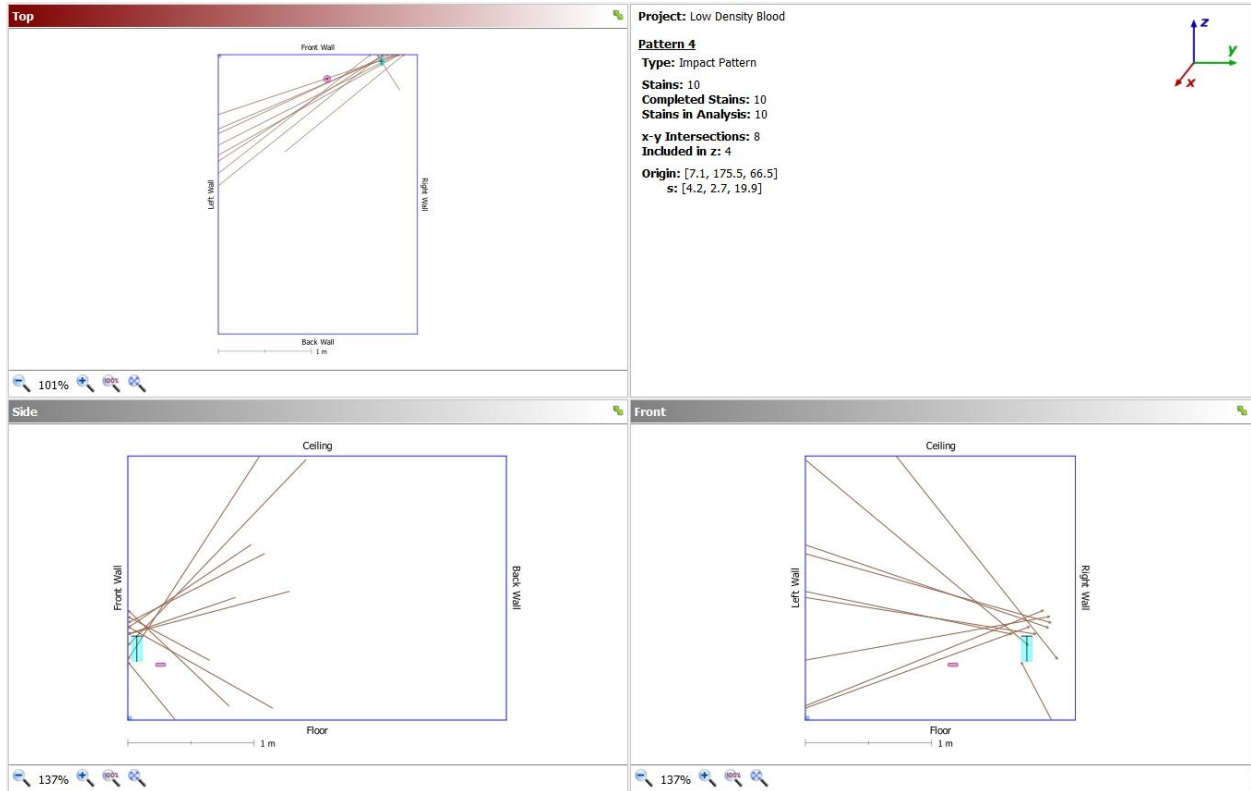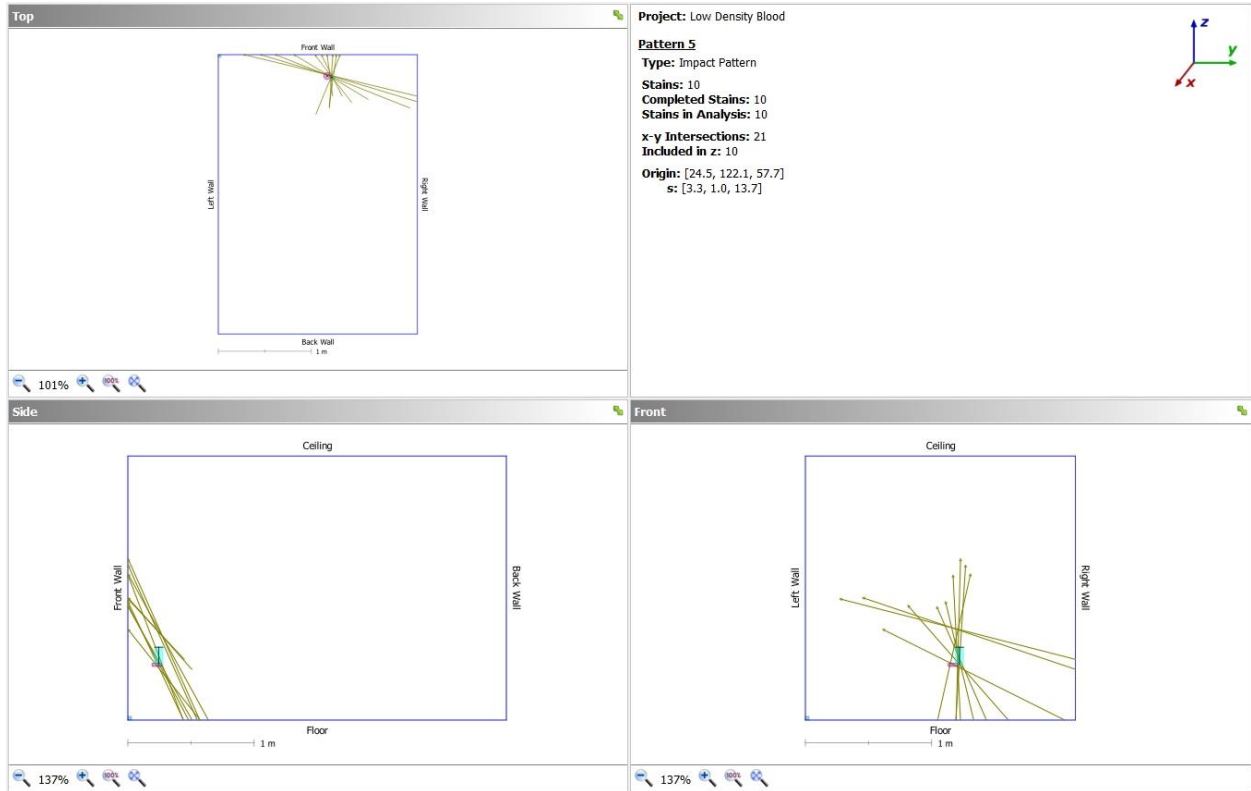*Figure 81. Simulation 1.5 string method construction.*

Figure 82. Very Low Density Blood group simulation data.

Table 23. Simulation 2.1 stain coordinate data

SIMULATION #2.1 - STAIN COORDINATE DATA							LOCATION	
LOW DENSITY BLOOD								
BLOOD STAIN	W	L	W/L	ANGLE		X	Y	Z
1	2	6	0.33	19.3			75	104
2	2	4	0.5	30			126	106
3	1	3	0.33	19.3			159	97
4	1	4	0.25	14.6			172	94
5	1.5	3	0.5	30			151	83
6	2	5	0.4	14.7			130	101
7	1	3	0.33	19.3			197	105
8	2	4	0.5	30			100	96
9	2	4	0.5	30			116	113
10	2	3	0.67	42.1			92	106
			KNOWN AREA OF ORIGIN		25	107	44	
			STRING METHOD AREA OF ORIGIN		16	106	80	
			HEMOSPAT CALCULATED		34	108	53.4	
			*all numbers are in centimeters					

In the above table under location, X is the distance out from the front wall, Y is the distance from the left wall and Z is the distance from the floor. For the known area of origin and the string method area of origin, X, Y, and Z were manually measured. For the HemoSpat® calculated area of origin, X, Y, and Z were computer generated.

Figure 83. Simulation 2.1 computer-generated data.

Figure 84. Simulation 2.1 string method construction.
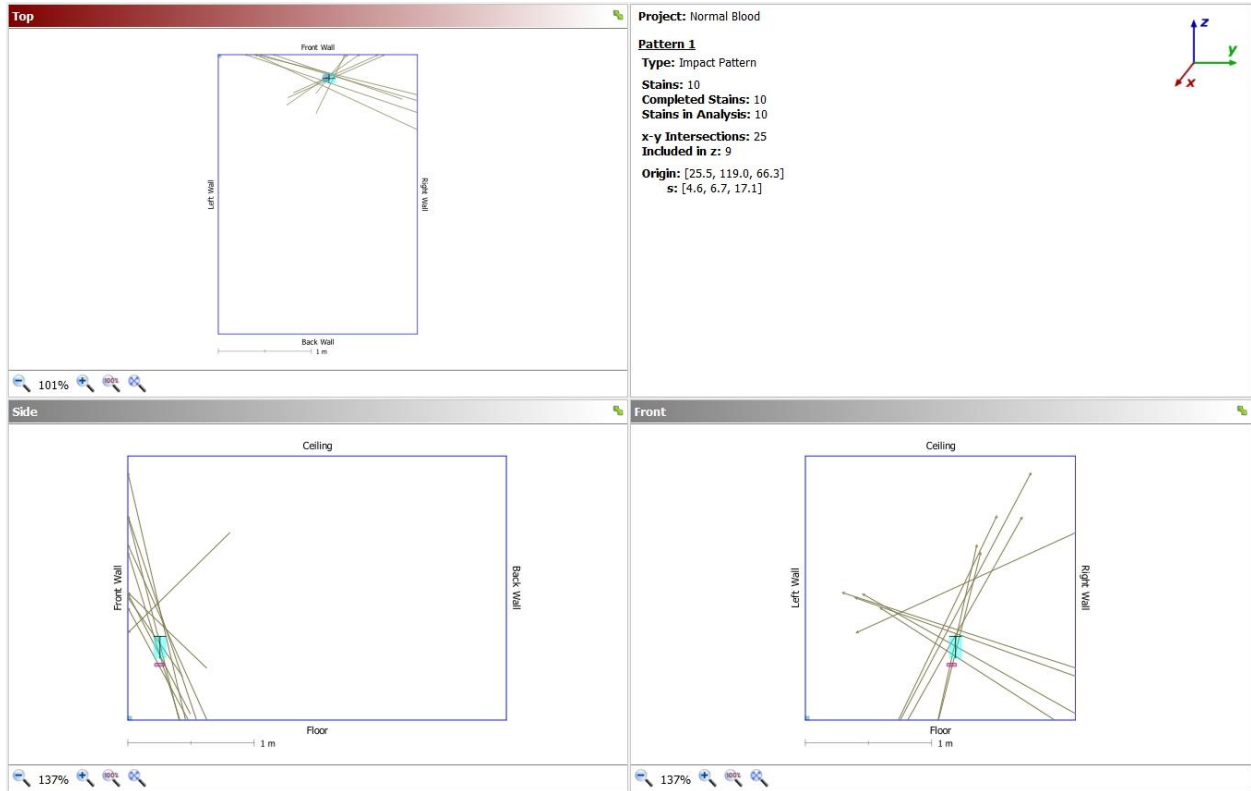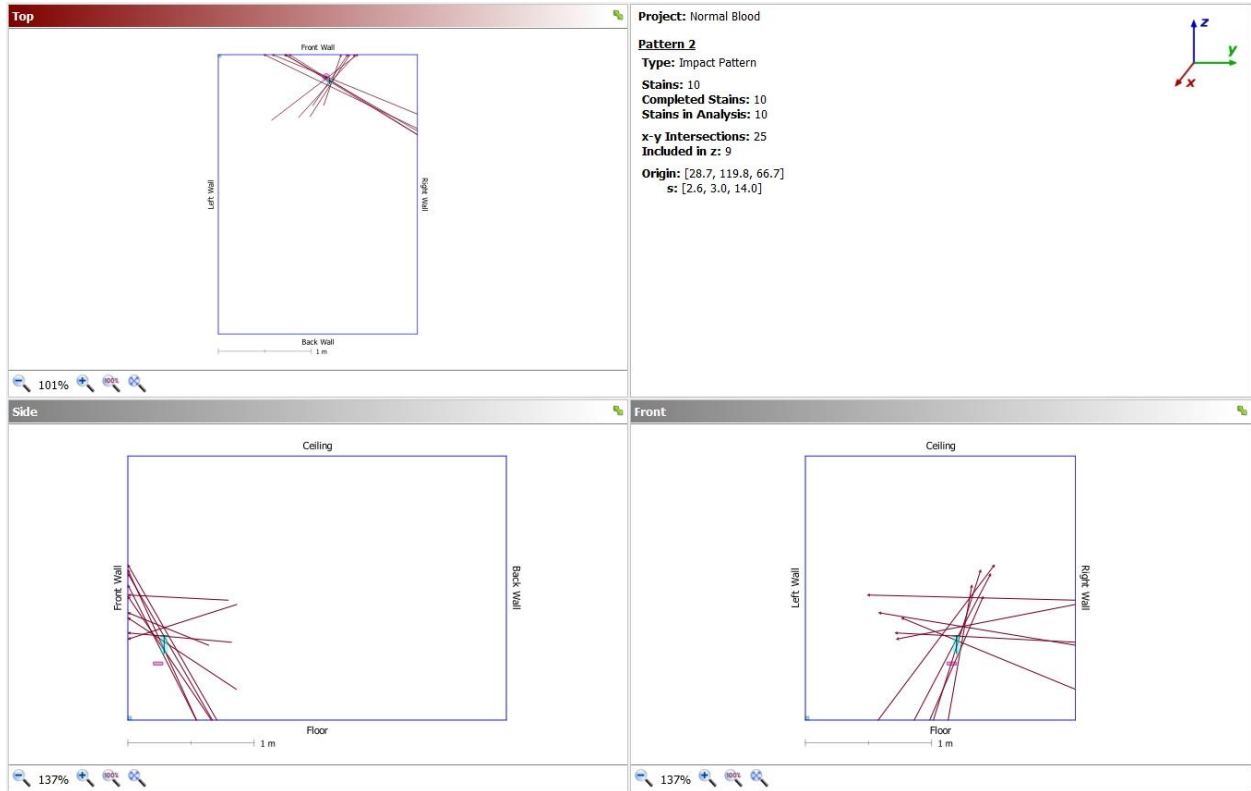
Table 24. Simulation 2.2 stain coordinate data

SIMULATION	#2.2 - STAIN COORDINATE DATA						LOCATION	
LOW DENSITY BLOOD								
BLOOD STAIN		W	L	W/L	ANGLE	X	Y	Z
1		2	12	0.17	9.8		178	130
2		2	5	0.4	23.6		184	145
3		2	5	0.4	23.6		127	130
4		2	4	0.5	30		109	121
5		2	4	0.5	30		123	109
6		1	5	0.2	11.5		213	112
7		1	3	0.3	19.3		162	111
8		3	5	0.6	36.9		104	128
9		2	4	0.5	30		116	102
10		3	7	0.43	25.5		156	87
			KNOWN AREA OF ORIGIN			25	107	44
			STRING METHOD AREA OF ORIGIN			19	114	83
			HEMOSPAT CALCULATED			31.5	111	71.8
			*all numbers are in centimeters					

In the above table under location, X is the distance out from the front wall, Y is the distance from the left wall and Z is the distance from the floor. For the known area of origin and the string method area of origin, X, Y, and Z were manually measured. For the HemoSpat® calculated area of origin, X, Y, and Z were computer generated.

108

Figure 85. Simulation 2.2 computer-generated data.

Figure 86. Simulation 2.2 string method construction.

Table 25. Simulation 2.3 stain coordinate data

SIMULATION #2.3 - STAIN COORDINATE DATA							LOCATION	
LOW DENSITY BLOOD								
BLOOD STAIN	W	L	W/L	ANGLE		X	Y	Z
1	2	9	0.22	12.7			198	107
2	1	3	0.33	19.3			189	95
3	1	3	0.33	19.3			171	84
4	1	4	0.25	14.5			161	75
5	3	4	0.75	48.6			164	56
6	2	4	0.5	30			168	85
7	1	3	0.33	19.3			180	88
8	2	5	0.4	23.6			188	98
9	2	4	0.5	30			170	30
10	2	4	0.5	30			167	83
			KNOWN AREA OF ORIGIN			29	117	47
			STRING METHOD AREA OF ORIGIN			22	115	63
			HEMOSPAT CALCULATED			20.2	137.6	65.3
			*all numbers are in centimeters					

In the above table under location, X is the distance out from the front wall, Y is the distance from the left wall and Z is the distance from the floor. For the known area of origin and the string method area of origin, X, Y, and Z were manually measured. For the HemoSpat® calculated area of origin, X, Y, and Z were computer generated.
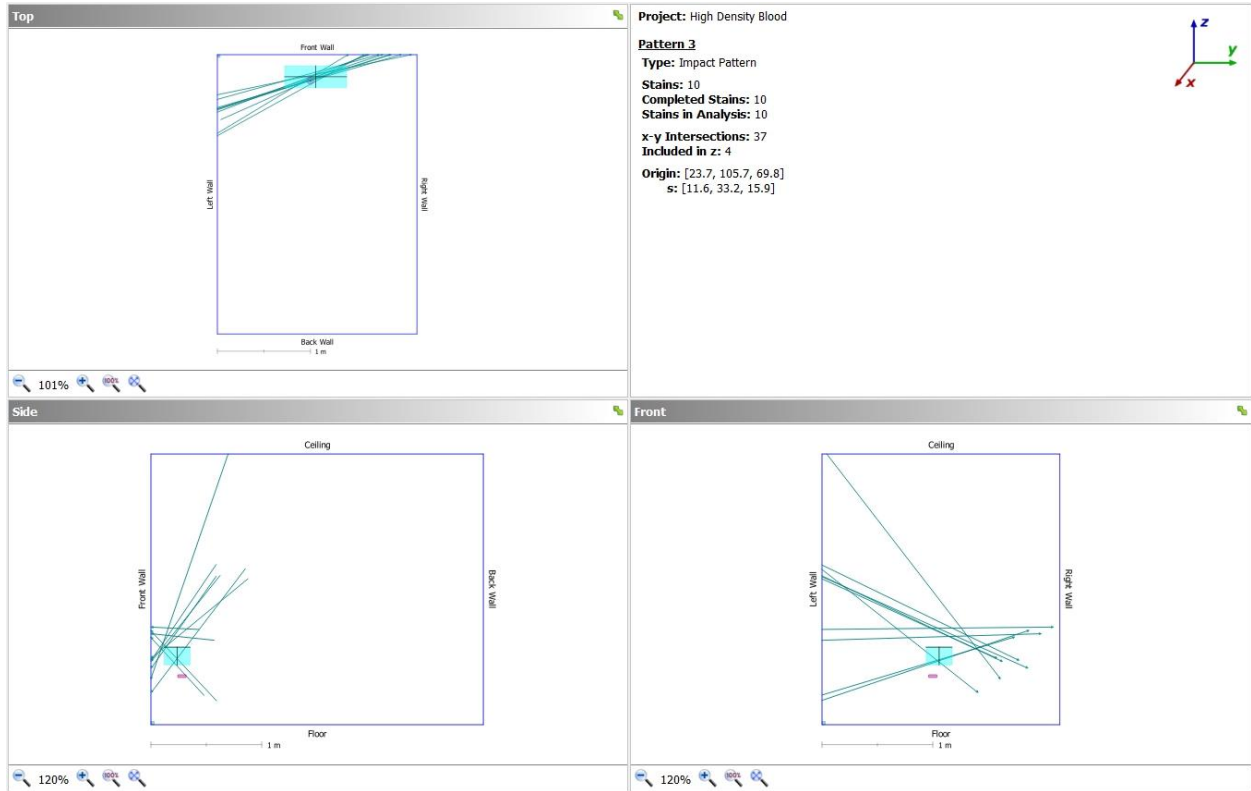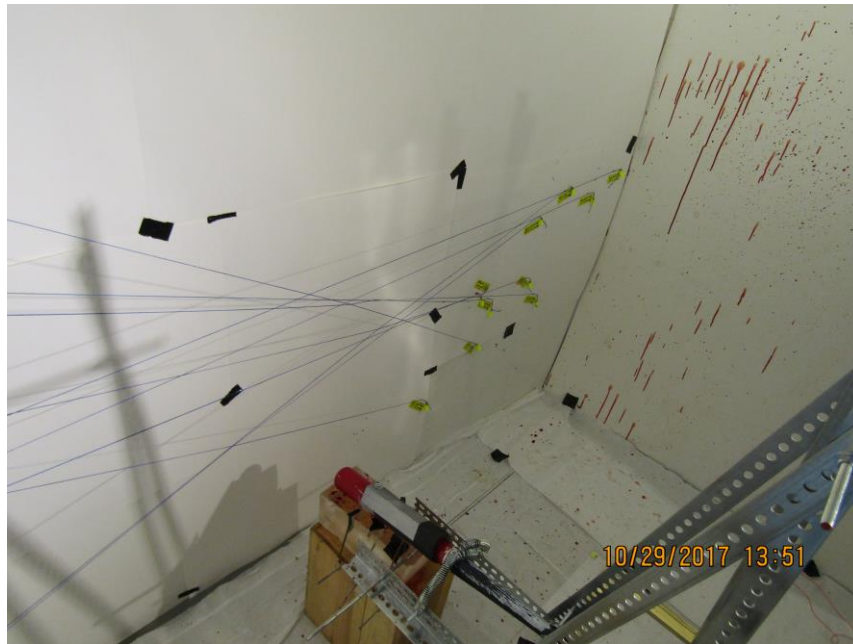
110

Figure 87. Simulation 2.3 computer-generated data.
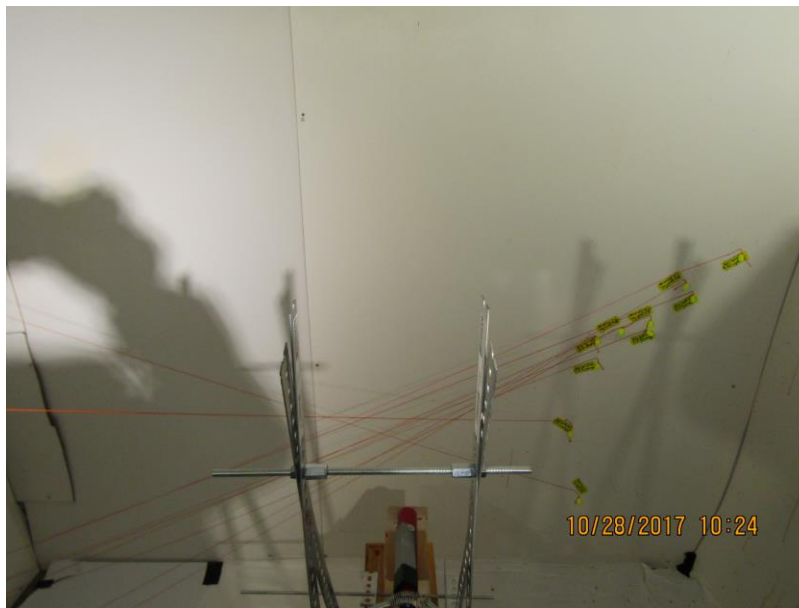
Figure 88. Simulation 2.3 string method construction.

111

Table 26. Simulation 2.4 stain coordinate data

SIMULATION #2.4 - STAIN COORDINATE DATA							LOCATION	
LOW DENSITY BLOOD								
BLOOD STAIN	W	L	W/L	ANGLE		X	Y	Z
1	3	5	0.6	36.9			164	68
2	1	4	0.25	14.5			177	59
3	2	4	0.5	30			183	68
4	2	4	0.5	30			193	73
5	2.5	8	0.31	18.1			194	82
6	2	7	0.29	16.9			189	87
7	1	4	0.25	14.5			200	48
8	1	4	0.25	14.5			195	77
9	1	3	0.33	19.3			171	46
10	1	3	0.33	19.3			178	74
			KNOWN AREA OF ORIGIN			26	117	45
			STRING METHOD AREA OF ORIGIN			17	145	77
			HEMOSPAT CALCULATED			7	175.5	66.5
			*all numbers are in centimeters					

In the above table under location, X is the distance out from the front wall, Y is the distance from
the left wall and Z is the distance from the floor. For the known area of origin and the string
method area of origin, X, Y, and Z were manually measured. For the HemoSpat® calculated area
of origin, X, Y, and Z were computer generated.

112

Figure 89. Simulation 2.4 computer-generated data.
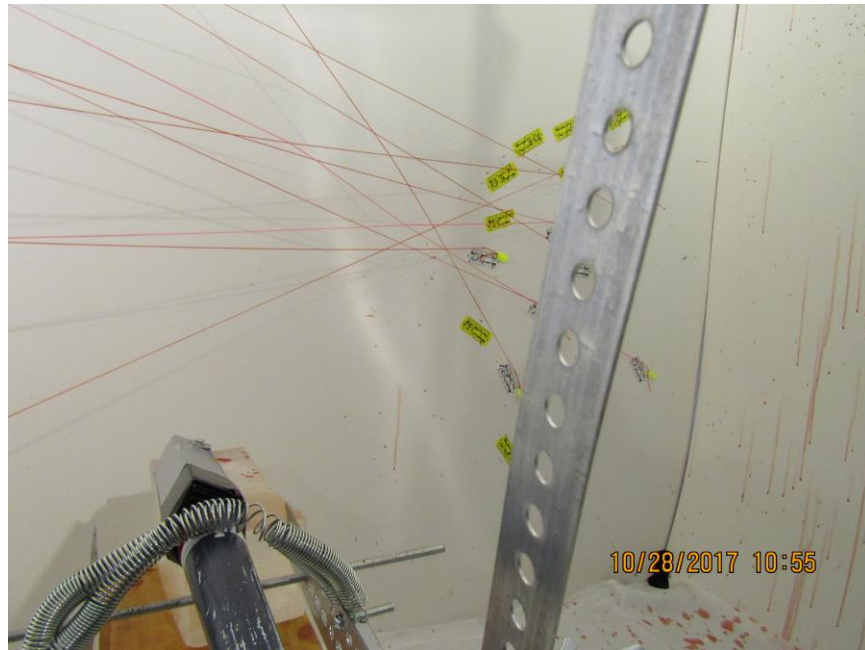
Figure 90. Simulation 2.4 string method construction.

113
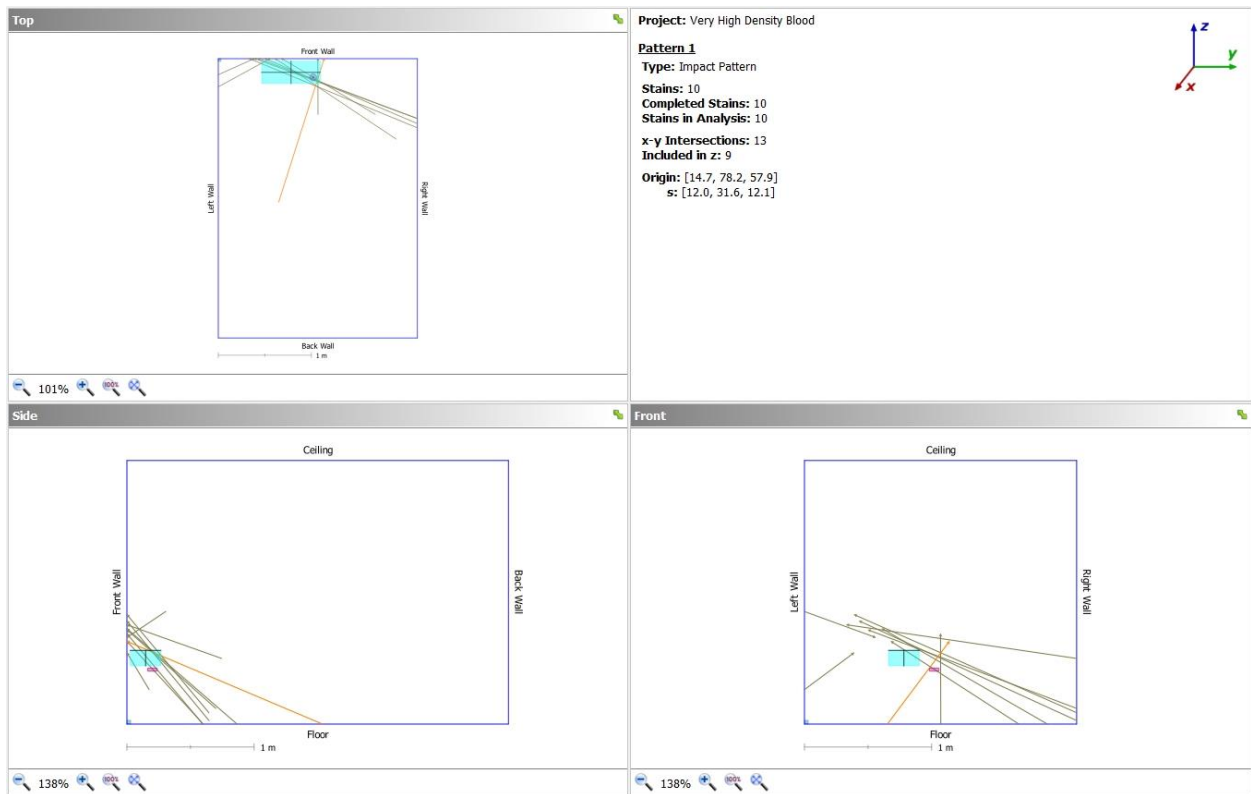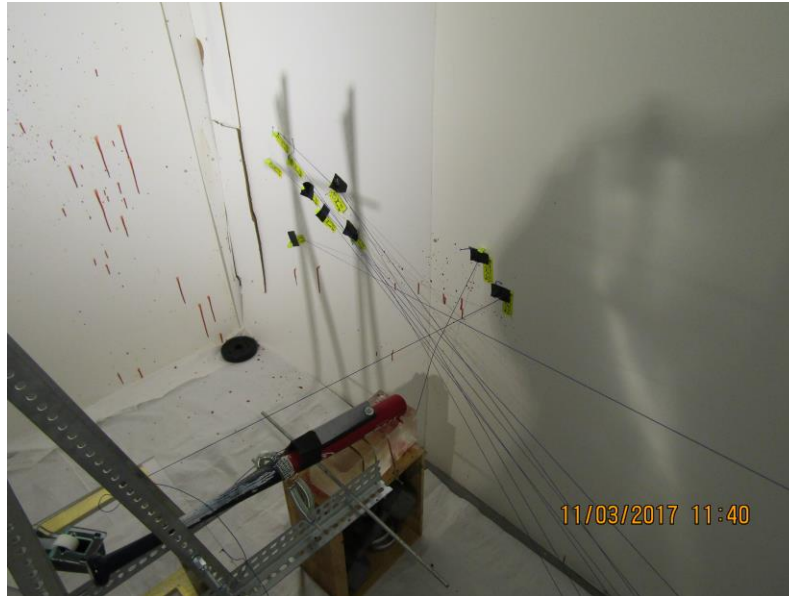
Table 27. Simulation 2.5 stain coordinate data

| SIMULATION #2.5 - STAIN COORDINATE DATA | | | | | | LOCATION | |
| LOW DENSITY BLOOD | | | | | | | |
BLOOD STAIN	W	L	W/L	ANGLE	X	Y	Z
1	2	4	0.5	30		123	128
2	1	5	0.2	11.5		117	115
3	1.5	5	0.3	17.5		111	94
4	1	5	0.2	11.5		45	97
5	1	5	0.2	11.5		27	96
6	1.5	5	0.3	17.5		61	72
7	1	4	0.25	14.5		81	91
8	2	4	0.5	30		104	90
9	1.5	6	0.25	14.5		131	116
10	1.5	5	0.3	30		127	123
			KNOWN AREA OF ORIGIN		23	117	45
			STRING METHOD AREA OF ORIGIN		16	115	78
			HEMOSPAT CALCULATED		24.5	122.1	57.7
			*all numbers are in centimeters				

In the above table under location, X is the distance out from the front wall, Y is the distance from the left wall and Z is the distance from the floor. For the known area of origin and the string method area of origin, X, Y, and Z were manually measured. For the HemoSpat® calculated area of origin, X, Y, and Z were computer generated.
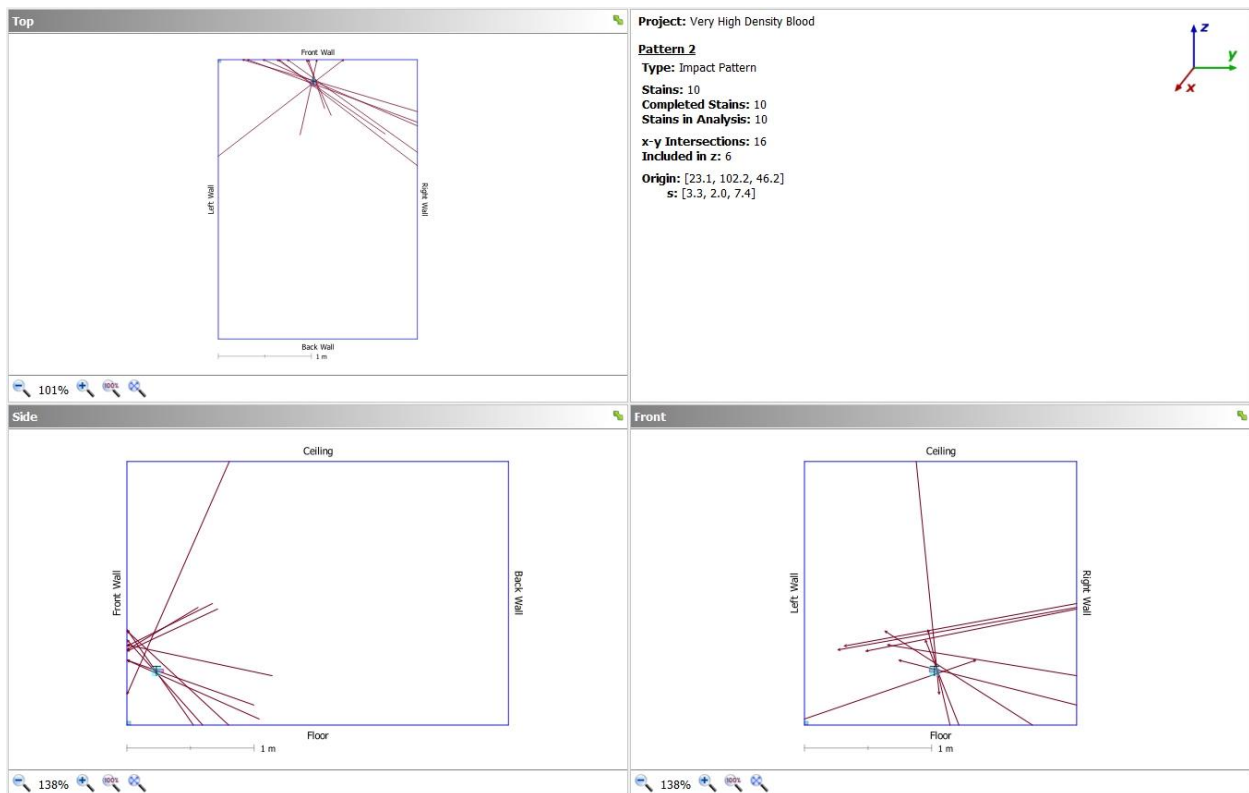
Figure 91. Simulation 2.5 computer-generated data.

Figure 92. Simulation 2.5 string method construction.

115

Figure 93. Low density blood group computer-generated data.

Table 28. Simulation 3.1 stain coordinate data

| SIMULATION #3.1 - STAIN COORDINATE DATA | | | | | | | LOCATION | |
| NORMAL DENSITY BLOOD | | | | | | | | |
BLOOD STAIN		W	L	W/L	ANGLE		X	Y	Z
1		1	10	0.1	5.7			45	100
2		1	4	0.25	14.5			40	69
3		1.5	5	0.3	17.5			39	97
4		1	4	0.25	14.5			29	101
5		1	3	0.33	19.3			136	139
6		1	4	0.25	14.5			139	133
7		1	4	0.25	14.5			172	161
8		2	5	0.4	23.6			152	162
9		1	7	0.14	8			179	196
10		1.5	4	0.38	22.3			59	89
		KNOWN AREA OF ORIGIN					25	116	45
		STRING METHOD AREA OF ORIGIN					20	117	80
		HEMOSPAT CALCULATED					25.5	119	66.3
		*all numbers are in centimeters							

In the above table under location, X is the distance out from the front wall, Y is the distance from the left wall and Z is the distance from the floor. For the known area of origin and the string method area of origin, X, Y, and Z were manually measured. For the HemoSpat® calculated area of origin, X, Y, and Z were computer generated.
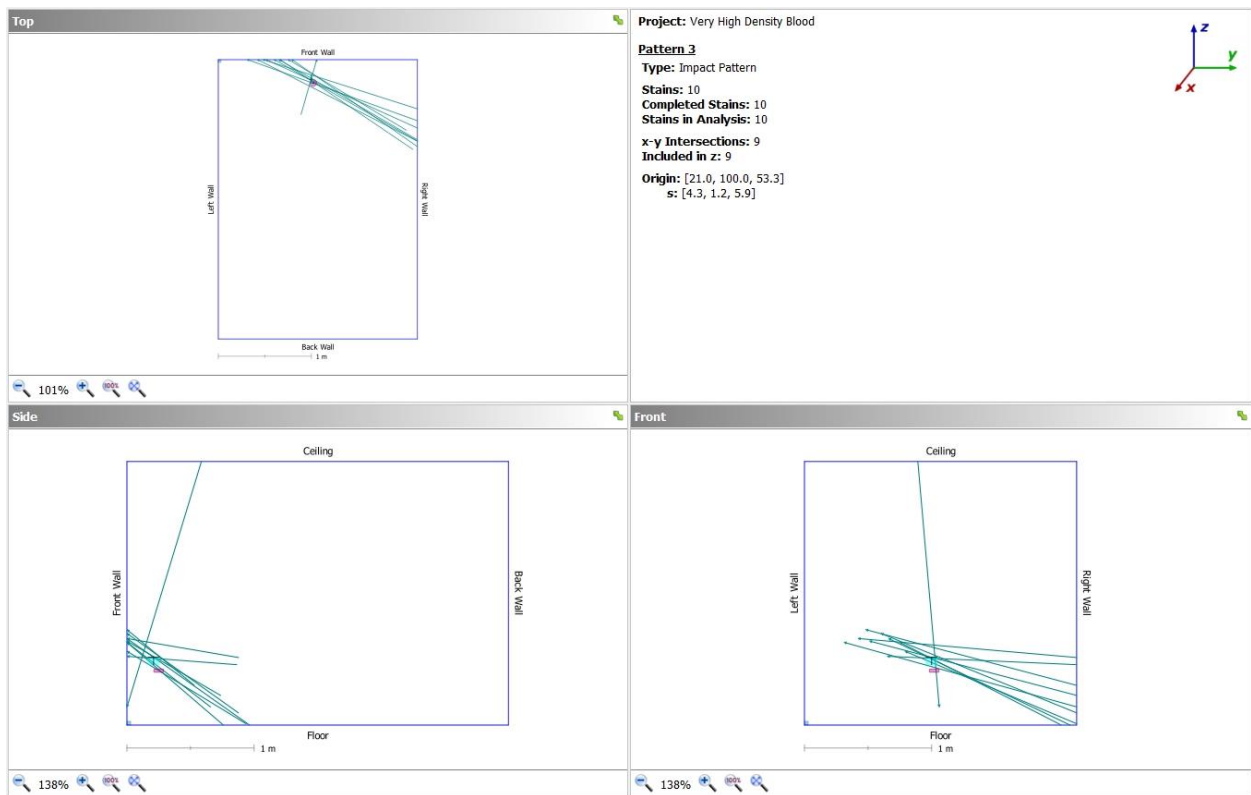
117

Figure 94. Simulation 3.1 computer-generated data.

Figure 95. Simulation 3.1 string method construction.

Table 29. Simulation 3.2 stain coordinate data

BLOOD STAIN		W	L	W/L	ANGLE		X	LOCATION Y	Z
SIMULATION #3.2 - STAIN COORDINATE DATA									
NORMAL DENSITY BLOOD									
1		1.5	5	0.3	17.5			147	116
2		2	4	0.5	30			141	98
3		2	4	0.5	30			139	119
4		1	4	0.25	14.5			132	107
5		2.5	4	0.63	39.1			72	64
6		3	7	0.43	25.1			71	69
7		1.5	4	0.38	22.3			58	85
8		2	4	0.5	30			49	99
9		2	4	0.5	30			76	81
10		1	3	0.33	19.3			150	123
			KNOWN AREA OF ORIGIN				24	116	46
			STRING METHOD AREA OF ORIGIN				16	124	80
			HEMOSPAT CALCULATED				28.7	119.8	66.7
			*all numbers are in centimeters						

In the above table under location, X is the distance out from the front wall, Y is the distance from the left wall and Z is the distance from the floor. For the known area of origin and the string method area of origin, X, Y, and Z were manually measured. For the HemoSpat® calculated area of origin, X, Y, and Z were computer generated.
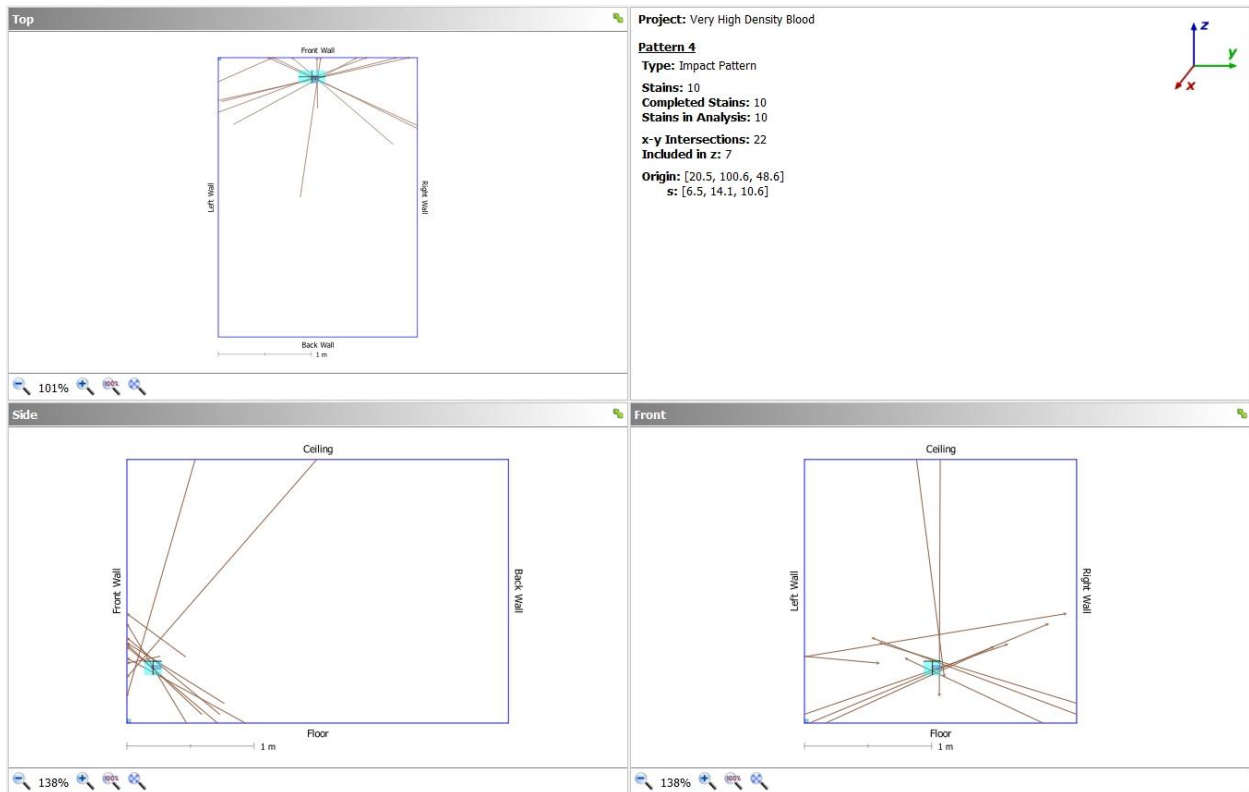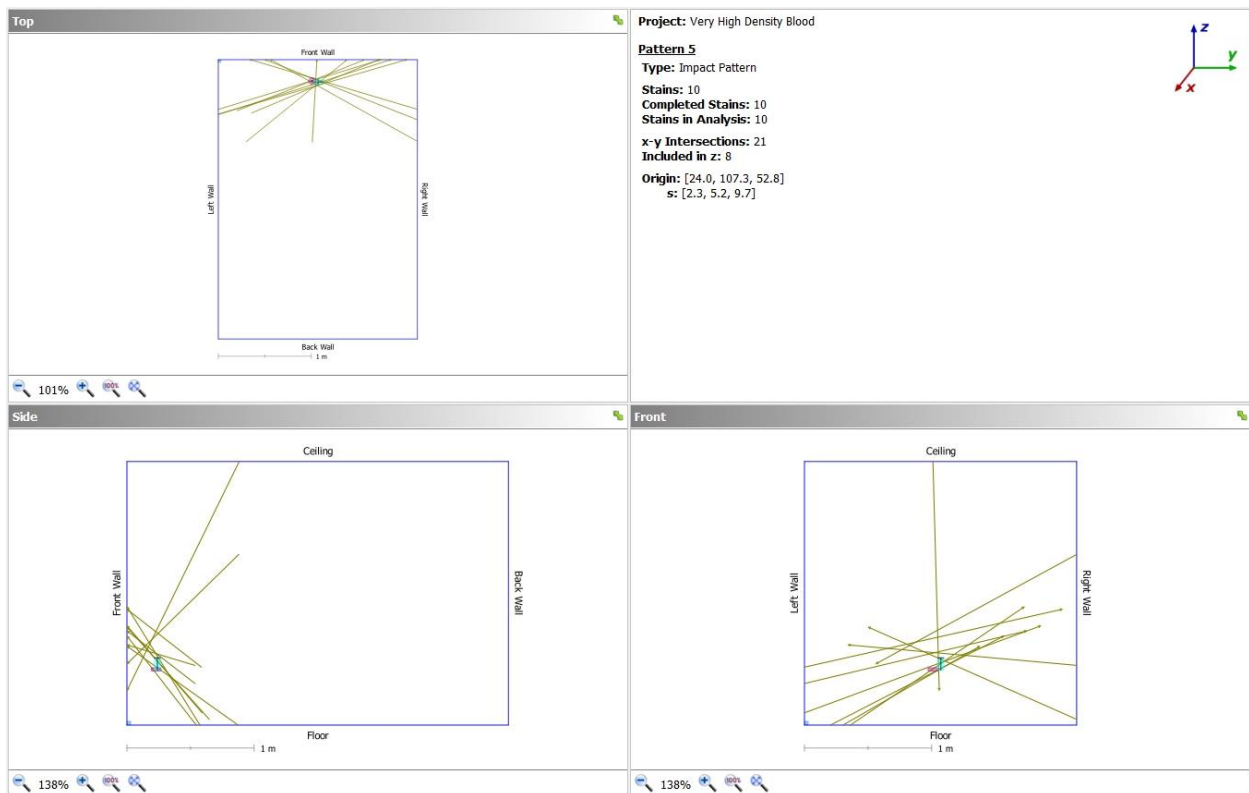
Figure 96. Simulation 3.2 computer-generated data.

*Figure 97. Simulation 3.2 string method construction.*

Table 30. Simulation 3.3 stain coordinate data

SIMULATION #3.3 - STAIN COORDINATE DATA							LOCATION	
NORMAL DENSITY BLOOD								
BLOOD STAIN		W	L	W/L	ANGLE	X	Y	Z
1		1	6	0.17	9.8		44	92
2		1.5	6	0.25	14.5		48	96
3		1	4	0.25	14.5		22	79
4		1	3	0.33	19.3		34	109
5		1	3	0.33	19.3		43	86
6		1.5	4	0.38	22.3		142	114
7		1	4	0.25	14.5		40	91
8		1	3	0.33	19.3		51	82
9		1	3	0.33	19.3		66	82
10		1	3.5	0.29	16.9		45	54
			KNOWN AREA OF ORIGIN		24	116	46	
			STRING METHOD AREA OF ORIGIN		13	87	68	
			HEMOSPAT CALCULATED		32.4	124.6	48.6	
			*all numbers are in centimeters					

In the above table under location, X is the distance out from the front wall, Y is the distance from the left wall and Z is the distance from the floor. For the known area of origin and the string method area of origin, X, Y, and Z were manually measured. For the HemoSpat® calculated area of origin, X, Y, and Z were computer generated.

121

Figure 98. Simulation 3.3 computer-generated data.

Figure 99. Simulation 3.3 string method construction.

122

Table 31. Simulation 3.4 stain coordinate data

SIMULATION #3.4 - STAIN COORDINATE DATA							LOCATION	
NORMAL DENSITY BLOOD								
BLOOD STAIN		W	L	W/L	ANGLE	X	Y	Z
1		2.5	6	0.42	24.8		133	130
2		3	11	0.27	15.7		108	152
3		1.5	6	0.25	14.5		130	117
4		2	5	0.4	23.6		129	97
5		2	5	0.4	23.6		181	85
6		1	3	0.33	19.3		192	95
7		2	3	0.67	42.1		125	90
8		1	3	0.33	19.3		128	89
9		2	3	0.67	42.1		122	124
10		2	5	0.4	23.6		128	122
			KNOWN AREA OF ORIGIN			20	117	44
			STRING METHOD AREA OF ORIGIN			20	115	75
			HEMOSPAT CALCULATED			43.1	110.6	44.2
			*all numbers are in centimeters					

In the above table under location, X is the distance out from the front wall, Y is the distance from the left wall and Z is the distance from the floor. For the known area of origin and the string method area of origin, X, Y, and Z were manually measured. For the HemoSpat® calculated area of origin, X, Y, and Z were computer generated.

123

Figure 100. Simulation 3.4 computer-generated data.

Figure 101. Simulation 3.4 string method construction.

Table 32. Simulation 3.5 stain data coordinate

SIMULATION #3.5 - STAIN COORDINATE DATA						LOCATION	
NORMAL DENSITY BLOOD							
						LOCATION	
BLOOD STAIN	W	L	W/L	ANGLE	X	Y	Z
1	1	9	0.11	6.3		191	126
2	1.5	6	0.25	14.5		187	148
3	1	7	0.14	8		161	121
4	1.5	5	0.3	17.5		136	135
5	2	9	0.22	12.7		127	150
6	1.5	6	0.25	14.5		116	125
7	2	5	0.4	23.6		135	100
8	1	3	0.33	19.3		74	94
9	1.5	3	0.5	30		76	84
10	1.5	4	0.38	22.3		163	91
			KNOWN AREA OF ORIGIN		20	117	44
			STRING METHOD AREA OF ORIGIN		17	113	77
			HEMOSPAT CALCULATED		27.1	116.5	61.4
			*all numbers are in centimeters				

In the above table under location, X is the distance out from the front wall, Y is the distance from the left wall and Z is the distance from the floor. For the known area of origin and the string method area of origin, X, Y, and Z were manually measured. For the HemoSpat® calculated area of origin, X, Y, and Z were computer generated.

Figure 102. Simulation 3.5 computer-generated data.

Figure 103. Simulation 3.5 string method construction.

126

Figure 104. Simulation 3.5 string method construction.
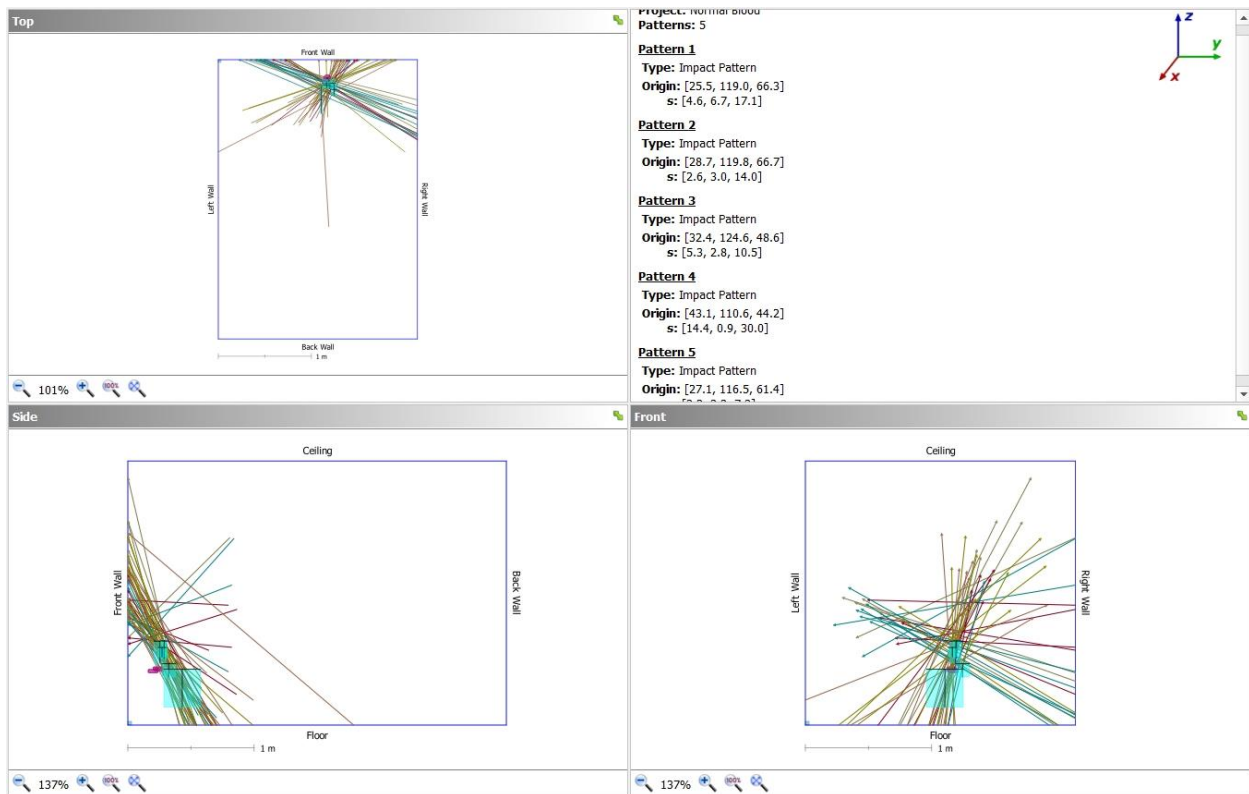
Figure 105. Normal blood group computer-generated data.

127

Table 33. Simulation 4.1 stain coordinate data

SIMULATION #4.1 - STAIN COORDINATE DATA							LOCATION		
HIGH DENSITY BLOOD									
BLOOD STAIN		W	L	W/L	ANGLE		X	Y	Z
1		2	9	0.22	12.7			67	123
2		3	12	0.25	14.5			77	129
3		1	5	0.2	11.5			61	137
4		3	3	0.33	19.3			190	77
5		3	4	0.75	49			49	82
6		1	9	0.33	19.3			213	120
7		1	8	0.13	7.5			197	103
8		1	7	0.14	8			204	94
9		1	4	0.25	14.5			179	73
10		1	5	0.2	11.5			58	146
			KNOWN AREA OF ORIGIN				25	101	44
			STRING METHOD AREA OF ORIGIN				14.5	104	61
			HEMOSPAT CALCULATED				24.5	104.6	52.4
			*all numbers are in centimeters						

In the above table under location, X is the distance out from the front wall, Y is the distance from the left wall and Z is the distance from the floor. For the known area of origin and the string method area of origin, X, Y, and Z were manually measured. For the HemoSpat® calculated area of origin, X, Y, and Z were computer generated.

128

Figure 106. Simulation 4.1 computer-generated data.

Figure 107. Simulation 4.1 string method construction.

129

Table 34. Simulation 4.2 stain coordinate data

| SIMULATION #4.2 - STAIN COORDINATE DATA | | | | | | LOCATION | | |
| HIGH DENSITY BLOOD | | | | | | | | |
BLOOD STAIN	W	L	W/L	ANGLE		X	Y	Z
1	1.5	5	0.3	17.5			162	135
2	1.5	5	0.3	17.5			154	130
3	1.5	5	0.3	17.5			144	134
4	2	4	0.5	30			142	143
5	2.5	5	0.5	30			129	109
6	1	4	0.25	14.5			109	79
7	1	4	0.25	14.5			30	54
8	1	3	0.33	19.3			29	57
9	2	4	0.5	30			126	126
10	1.5	3	0.5	30			173	132
			KNOWN AREA OF ORIGIN			25	101	44
			STRING METHOD AREA OF ORIGIN			20	102	60
			HEMOSPAT CALCULATED			33.8	106	60.4
			*all numbers are in centimeters					

In the above table under location, X is the distance out from the front wall, Y is the distance from the left wall and Z is the distance from the floor. For the known area of origin and the string method area of origin, X, Y, and Z were manually measured. For the HemoSpat® calculated area of origin, X, Y, and Z were computer generated.

130

Figure 108. Simulation 4.2 computer-generated data.

Figure 109. Simulation 4.2 string method construction.

131

Figure 110. Simulation 4.2 string method construction.

Table 35. Simulation 4.3 stain coordinate data

| SIMULATION #4.3 - STAIN COORDINATE DATA | | | | | | | LOCATION | |
| HIGH DENSITY BLOOD | | | | | | | | |
BLOOD STAIN		W	L	W/L	ANGLE		X	Y	Z
1		3	12	0.25	14.5			209	88
2		1	5	0.2	11.5			187	85
3		2	8	0.25	14.5			198	82
4		1	4	0.25	14.5			178	58
5		1	4	0.25	14.5			174	79
6		1.5	4	0.38	22.3			163	57
7		4	10	0.4	23.6			158	60
8		1.5	6	0.25	14.5			186	51
9		1.5	4	0.38	22.3			141	29
10		1	4	0.25	14.5			161	41
			KNOWN AREA OF ORIGIN				28	100	45
			STRING METHOD AREA OF ORIGIN				15	121	70
			HEMOSPAT CALCULATED				23.7	105.7	69.8
			*all numbers are in centimeters						

In the above table under location, X is the distance out from the front wall, Y is the distance from the left wall and Z is the distance from the floor. For the known area of origin and the string method area of origin, X, Y, and Z were manually measured. For the HemoSpat® calculated area of origin, X, Y, and Z were computer generated.

133

Figure 111. Simulation 4.3 computer-generated data.

Figure 112. Simulation 4.3 string method construction.

134

Figure 113. Simulation 4.3 string method construction.

Table 36. Simulation 4.4 stain coordinate data

| SIMULATION #4.4 - STAIN COORDINATE DATA | | | | | | | LOCATION | |
| HIGH DENSITY BLOOD | | | | | | | | |
BLOOD STAIN	W	L	W/L	ANGLE		X	Y	Z
1	1	4	0.25	14.5			105	110
2	3.5	7	0.5	23.6			103	99
3	3	8	0.38	22.3			110	100
4	1	3	0.33	19.3			188	121
5	1.5	4	0.38	22.3			100	93
6	1	6	0.17	9.8			170	117
7	2	8	0.25	14.5			204	135
8	2	10	0.2	11.5			209	143
9	1.5	5	0.3	17.5			160	92
10	1	4	0.25	14.5			178	91
		KNOWN AREA OF ORIGIN				24	100	45
		STRING METHOD AREA OF ORIGIN				20	102	77
		HEMOSPAT CALCULATED				23.9	102.4	58.7
		*all numbers are in centimeters						

In the above table under location, X is the distance out from the front wall, Y is the distance from the left wall and Z is the distance from the floor. For the known area of origin and the string method area of origin, X, Y, and Z were manually measured. For the HemoSpat® calculated area of origin, X, Y, and Z were computer generated.

Figure 114. Simulation 4.4 computer-generated data.

Figure 115. Simulation 4.4 string method construction.

Table 37. Simulation 4.5 stain coordinate data

SIMULATION #4.5 - STAIN COORDINATE DATA						LOCATION		
HIGH DENSITY BLOOD								
BLOOD STAIN		W	L	W/L	ANGLE	X	Y	Z
1		2	6	0.33	19.3		140	46
2		4	6	0.67	42.1		128	71
3		1.5	4	0.38	22.3		169	73
4		1	4	0.25	14.5		187	75
5		2	4	0.5	30		106	119
6		1	4	0.25	14.5		46	76
7		1	4	0.25	14.5		38	72
8		3	16	0.19	10.9		84	12
9		1.5	5	0.3	17.5		150	69
10		1.5	5	0.3	17.5		206	80
			KNOWN AREA OF ORIGIN			24	100	45
			STRING METHOD AREA OF ORIGIN			13	122	60
			HEMOSPAT CALCULATED			24.1	100.8	54.5
			*all numbers are in centimeters					

In the above table under location, X is the distance out from the front wall, Y is the distance from the left wall and Z is the distance from the floor. For the known area of origin and the string method area of origin, X, Y, and Z were manually measured. For the HemoSpat® calculated area of origin, X, Y, and Z were computer generated.

Figure 116. Simulation 4.5 computer-generated data.
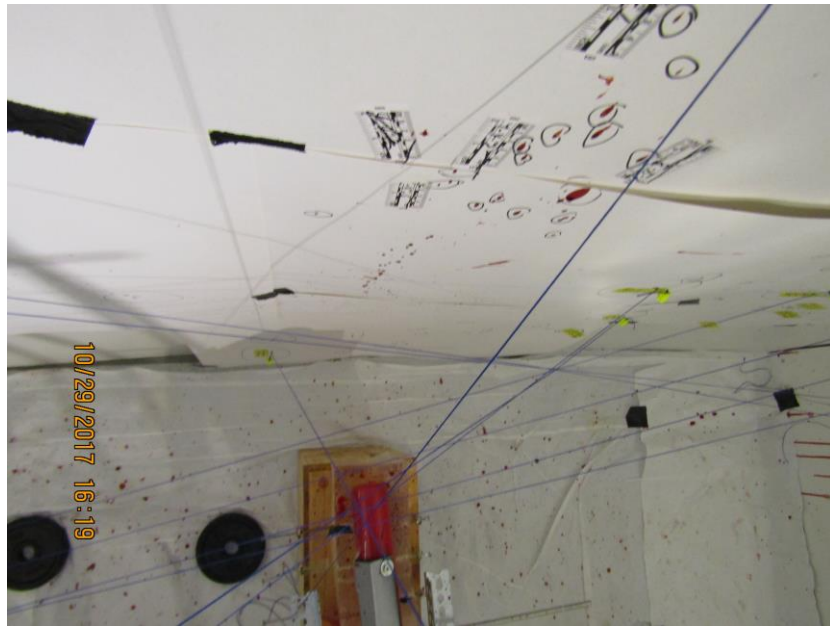
Figure 117. Simulation 4.5 string method construction.

www.manaraa.com
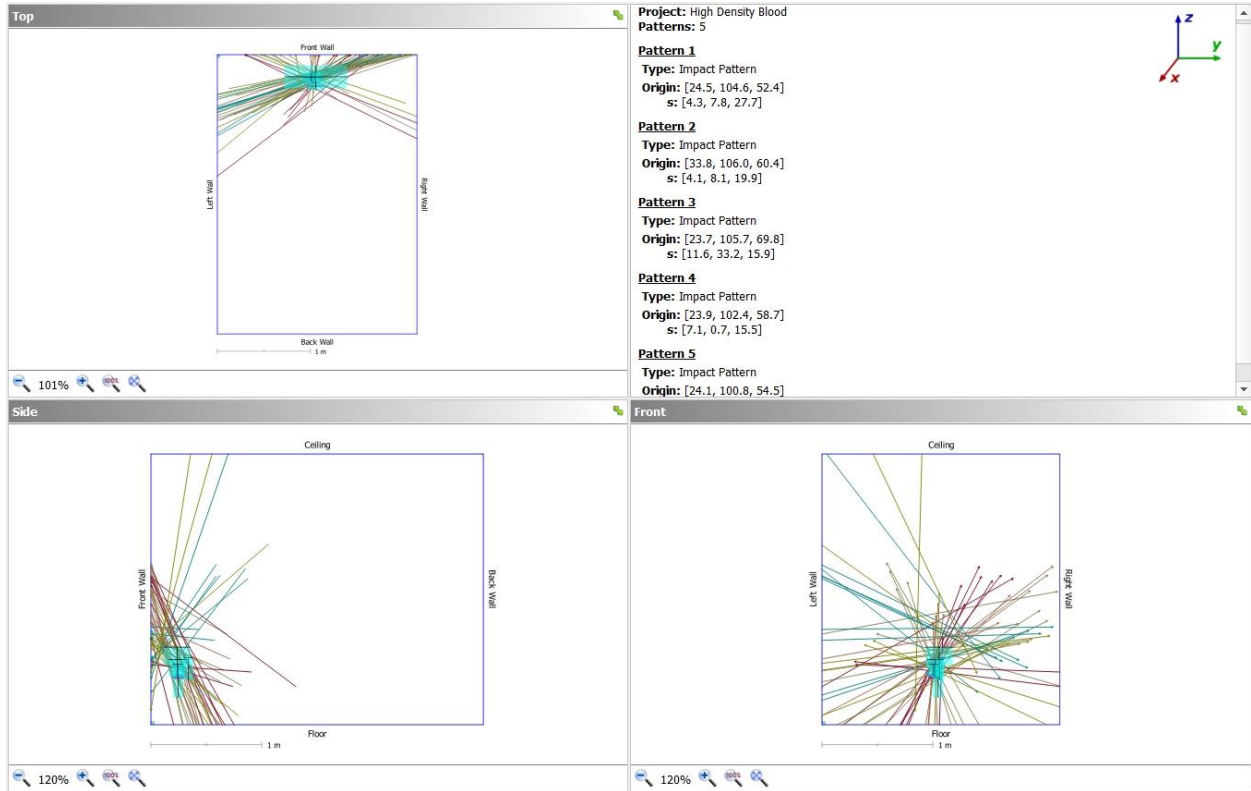
Figure 118. High density blood group computer-generated data.

Table 38. Simulation 5.1 stain coordinate data

SIMULATION #5.1 - STAIN COORDINATE BLOOD							LOCATION	
VERY HIGH DENSITY BLOOD								
BLOOD STAIN		W	L	W/L	ANGLE	X	Y	Z
1		1.5	5	0.3	17.5		39	86
2		1	3	0.33	19.3		33	78
3		1.5	4	0.38	22.3		43	81
4		1	3	0.33	19.3		50	74
5		2	3	0.67	42.1		61	75
6		1	3	0.33	19.3		68	65
7		2.5	3.5	0.71	45.2		107	71
8		2	2	1	90		114	65
9		1	3	0.33	19.3		39	56
10		1	3	0.33	19.3		56	68
			KNOWN AREA OF ORIGIN		25	102	44	
			STRING METHOD AREA OF ORIGIN		17	105	56	
			HEMOSPAT CALCULATED		14.7	78.2	57.9	
			*all numbers are in centimeters					

In the above table under location, X is the distance out from the front wall, Y is the distance from the left wall and Z is the distance from the floor. For the known area of origin and the string method area of origin, X, Y, and Z were manually measured. For the HemoSpat® calculated area of origin, X, Y, and Z were computer generated.

Figure 119. Simulation 5.1 computer-generated data.

Figure 120. Simulation 5.1 string method construction.

Table 39. Simulation 5.2 stain coordinate data

SIMULATION #5.2 - STAIN COORDINATE DATA								
VERY HIGH DENSITY BLOOD								
							LOCATION	
BLOOD STAIN		W	L	W/L	ANGLE		X	Y	Z
1		2	5	0.4	23.6			26	59
2		1.5	3.5	0.43	25.5			31	62
3		1.5	3.5	0.43	25.5			48	58
4		1.5	3	0.5	30			63	74
5		2	3.5	0.57	34.8			65	63
6		1.5	3	0.5	30			74	51
7		2.5	3	0.2	11.5			75	67
8		1.5	3	0.5	30			97	75
9		3	4.5	0.67	42.1			106	24
10		1	3	0.33	19.3			135	51
			KNOWN AREA OF ORIGIN			25	102	44
			STRING METHOD AREA OF ORIGIN			18	101	62
			HEMOSPAT CALCULATED			23.1	102.1	46.2
			*all numbers are in centimeters					

143

In the above table under location, X is the distance out from the front wall, Y is the distance from the left wall and Z is the distance from the floor. For the known area of origin and the string method area of origin, X, Y, and Z were manually measured. For the HemoSpat® calculated area of origin, X, Y, and Z were computer generated.

Figure 121. Simulation 5.2 computer-generated data.

144
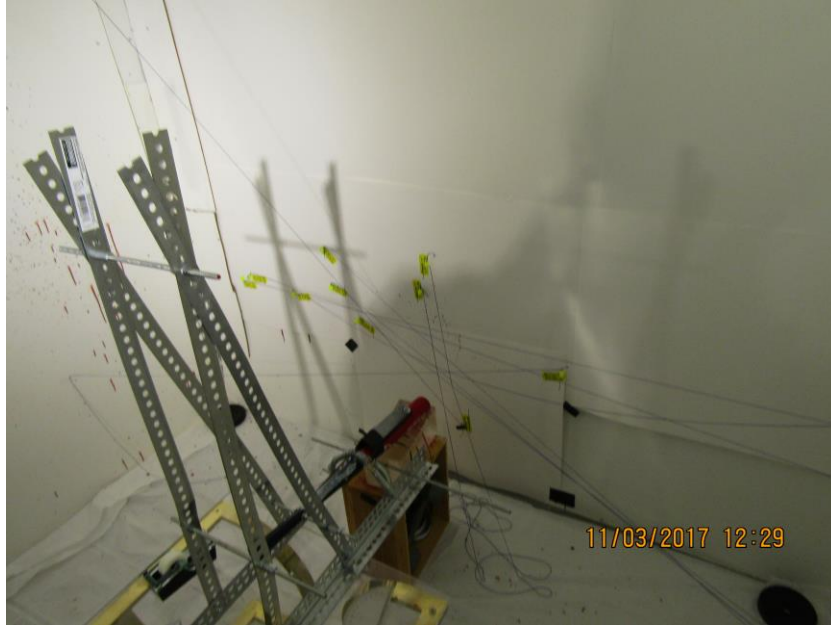
Figure 122. Simulation 5.2 string method construction.

Table 40. Simulation 5.3 stain coordinate data

SIMULATION #5.3 - STAIN COORDINATE DATA							LOCATION	
VERY HIGH DENSITY BLOOD								
BLOOD STAIN	W	L	W/L	ANGLE		X	Y	Z
1	1	4	0.25	14.5			31	65
2	1.5	3	0.43	25.5			42	68
3	1	3	0.33	19.3			48	75
4	1	2.5	0.4	23.6			51	66
5	1.5	3	0.5	30			60	72
6	1	2.5	0.4	23.6			65	54
7	2	3.5	0.57	34.8			66	68
8	1.5	2.5	0.6	36.9			79	58
9	1	2	0.5	30			75	65
10	1	4.5	0.22	12.7			106	14
			KNOWN AREA OF ORIGIN		25	102	44	
			STRING METHOD AREA OF ORIGIN		17	95	56	
			HEMOSPAT CALCULATED		21	100	53.3	
			*all numbers are in centimeters					

145

In the above table under location, X is the distance out from the front wall, Y is the distance from the left wall and Z is the distance from the floor. For the known area of origin and the string method area of origin, X, Y, and Z were manually measured. For the HemoSpat® calculated area of origin, X, Y, and Z were computer generated.

Figure 123. Simulation 5.3 computer-generated data.

Figure 124. Simulation 5.3 string method construction.

Table 41. Simulation 5.4 stain coordinate data

SIMULATION #5.4 - STAIN COORDINATE DATA								
VERY HIGH DENSITY BLOOD								
							LOCATION	
BLOOD STAIN		W	L	W/L	ANGLE	X	Y	Z
1		2	4	0.5	30		53	67
2		1	2.5	0.4	23.6		59	63
3		1	2.5	0.4	23.6		59	47
4		1.5	3	0.5	30		79	51
5		2.5	7.5	0.33	19.3		106	21
6		2	3	0.67	42.1		110	36
7		1	3	0.33	19.3		149	60
8		1	3	0.33	19.3		160	62
9		1	4	0.25	14.5		192	78
10		1	5.5	0.18	10.4		206	86
			KNOWN AREA OF ORIGIN		23	104	45	
			STRING METHOD AREA OF ORIGIN		19	110	56	
			HEMOSPAT CALCULATED		20.5	100.6	48.6	
			*all numbers are in centimeters					

In the above table under location, X is the distance out from the front wall, Y is the distance from the left wall and Z is the distance from the floor. For the known area of origin and the string method area of origin, X, Y, and Z were manually measured. For the HemoSpat® calculated area of origin, X, Y, and Z were computer generated.

Figure 125. Simulation 5.4 computer-generated data.

148

Figure 126. Simulation 5.4 string method construction.

Table 42. Simulation 5.5 stain coordinate data

SIMULATION #5.5 - STAIN COORDINATE DATA							LOCATION	
VERY HIGH DENSITY BLOOD								
BLOOD STAIN	W	L	W/L	ANGLE		X	Y	Z
1	1	3	0.33	19.3			50	77
2	1	3	0.33	19.3			34	63
3	1	2.5	0.4	23.6			56	48
4	3	6	0.5	30			106	27
5	2	4	0.5	30			138	62
6	2.5	7	0.36	21.1			157	70
7	1	4	0.25	14.5			175	74
8	1.5	5	0.3	17.5			173	93
9	1	4	0.25	14.5			203	91
10	1	3.5	0.29	16.9			186	78
		KNOWN AREA OF ORIGIN				23	104	45
		STRING METHOD AREA OF ORIGIN				19	101	59
		HEMOSPAT CALCULATED				24	107.3	52.8
		*all numbers are in centimeters						

149

www.manaraa.com

In the above table under location, X is the distance out from the front wall, Y is the distance from the left wall and Z is the distance from the floor. For the known area of origin and the string method area of origin, X, Y, and Z were manually measured. For the HemoSpat® calculated area of origin, X, Y, and Z were computer generated.

Figure 127. Simulation 5.5 computer-generated data.

Figure 128. Simulation 5.5 string method construction.
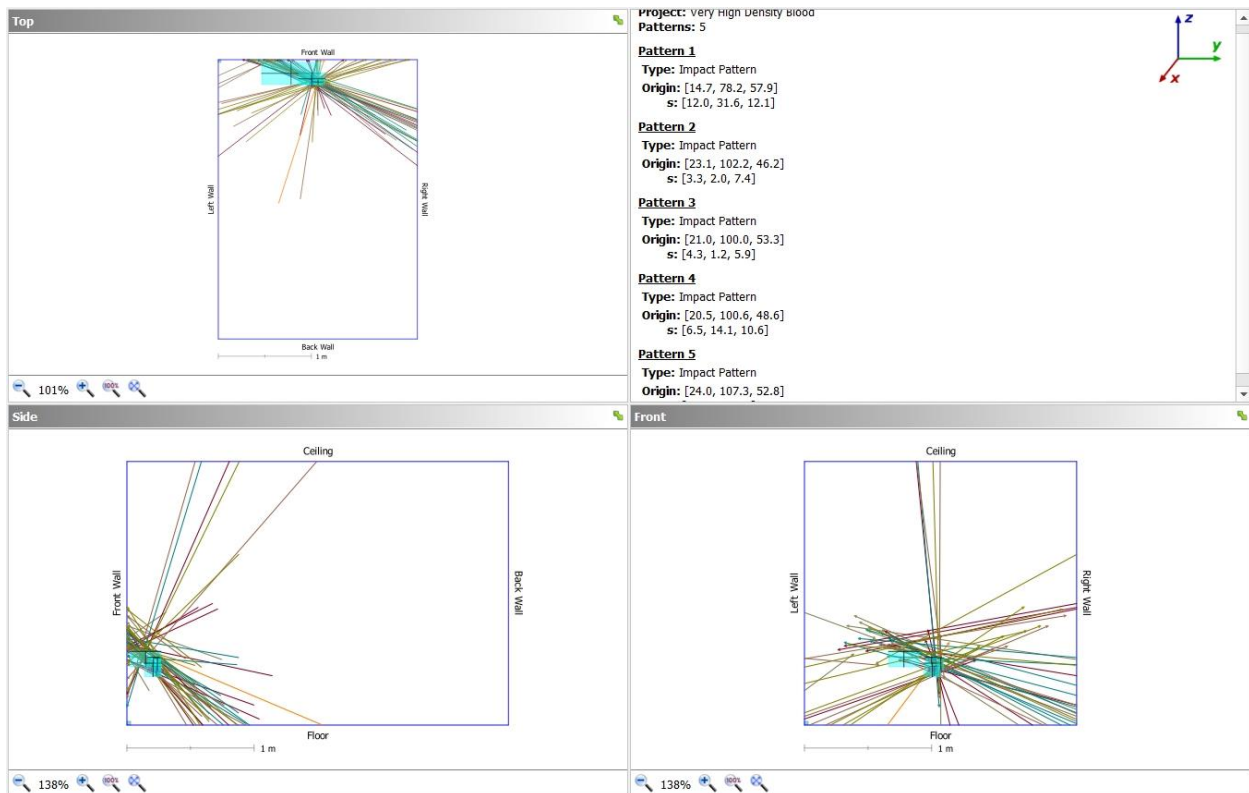
Figure 129. Very high density blood group computer-generated data.

151

Table 43. Mean and SD of simulation sets for HemoSpat® method

HemoSpat®	mean	mean	mean	SD	SD	SD
simulation	x	y	z	x	y	z
1.1-1.5	28.5	120.7	62.1	3.21	4.72	23.47
2.1-2.5	23.2	130.6	62.6	10.61	27.3	7.56
3.1-3.5	31.2	117.8	57.4	7.08	4.76	10.35
4.1-4.5	26.0	103.8	59.0	4.47	2.28	7.0
5.1-5.5	20.6	97.6	51.8	3.50	11.28	4.54

Table 44. Mean and SD of simulation sets for manual string method

String	mean	mean	mean	SD	SD	SD
simulation	x	y	z	x	y	z
1.1-1.5	16.4	123.8	79.8	1.14	8.28	6.49
2.1-2.5	18.0	119.6	76.2	2.54	14.41	7.72
3.1-3.5	17.2	111.2	76.0	2.94	14.14	4.94
4.1-4.5	16.4	112.2	65.6	3.36	13.46	7.63
	17.8	101.8	57.8	0.83	5.35	2.68

Research Questions and Research Hypotheses

The four research questions are:

- RQ2a: To what extent are there differences between the known areas of origin of the bloodstains and the calculated areas of origin of the bloodstains obtained using the manual string approach at the five different blood densities?

- RQ2b: To what extent are there differences between the known areas of origin of the bloodstains and the calculated areas of origin of the bloodstains obtained using the HemoSpat® program at the five different blood densities?

- RQ2c: To what extent are there differences between the calculated areas of origin of the bloodstains obtained using the manual string approach and the HemoSpat® program at the five different blood densities?

- RQ2d: To what extent are the differences between the known areas of origin of the bloodstains and the calculated areas of the bloodstains correlated with the angles of impact?

  The four associated research hypotheses are:

- H2a: There are no differences between the known areas of origin of the bloodstains and the calculated areas of origin of the bloodstains obtained using the manual string approach at the five different blood densities.

- H2b: There are no differences between the known areas of origin of the bloodstains and the calculated areas of origin of the bloodstains obtained using the HemoSpat® program at the five different blood densities.

- H2c: There are no differences between areas of origin of the bloodstains calculated using the manual string approach and the HemoSpat® program.

- H2d: The differences between the known areas of origin of the bloodstains and the calculated areas of origin of the bloodstains are not correlated with the angles of impact.

153

Data Analysis

H2a, H2b, and H2c were tested by determining if the areas of origin of the bloodstains using one method were captured within the 95% CI of the calculated mean areas of origin of the bloodstains using another method. The two sets of 95% CI overlapped with each other, and the 95% CI of the mean differences between the areas obtained with different methods captured zero. H2d was tested by drawing scatterplots to determine if the differences between the calculated areas of origin of the bloodstains minus the known areas of origin of the bloodstains were correlated with the angles of incidence at the five blood densities. Horizontal trend lines reflected no correlation. The effect sizes were indicated by R^2 (i.e., the proportion of the variance in the differences explained by the angles of incidence. $R^2 < 0.04$ reflected a negligible effect size) (Ferguson, 2009).

Hypothesis H2a.

Figure 130 is an error bar chart to determine the extent to which there are differences between the pre-defined known areas of origin of the bloodstains (K) and the calculated areas of origin of the bloodstains (M) obtained using the manual string method at the five different blood densities.

154
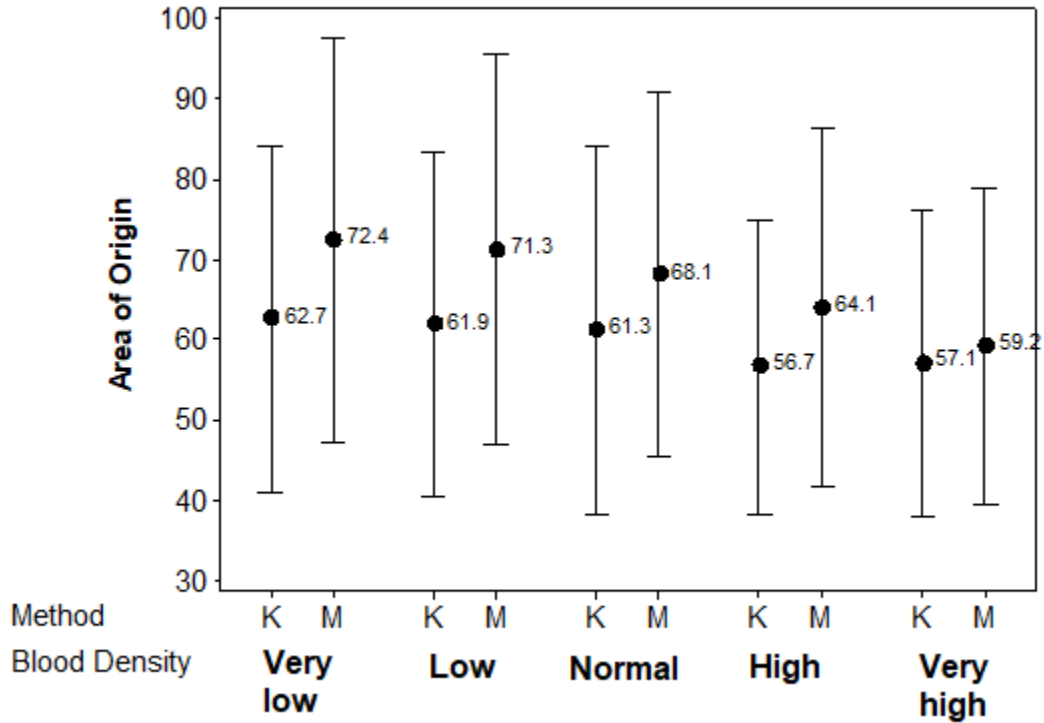
Figure 130. Comparison of the known (K) and calculated areas of origin (M) obtained with the manual string method. Mean areas of origin are represented by circular symbols and the lower and upper bounds of the 95% CIs are represented by I symbols.

The mean known areas of origin ranged from 57.1 at very high blood density to 62.7 at very low blood density. The mean calculated areas of origin ranged from 59.2 at very high blood density to 72.4 at very low blood density. No differences were indicated by the strong overlaps between the lower and upper boundaries of the 95% CI of the known and calculated mean areas of origin at each blood density.

Figure 131 is an error bar chart to determine the extent to which zero was captured within the 95% CI of the differences between the known areas of origin of the bloodstains minus the

areas of origin of the bloodstains obtained using the manual string method at the five blood densities.
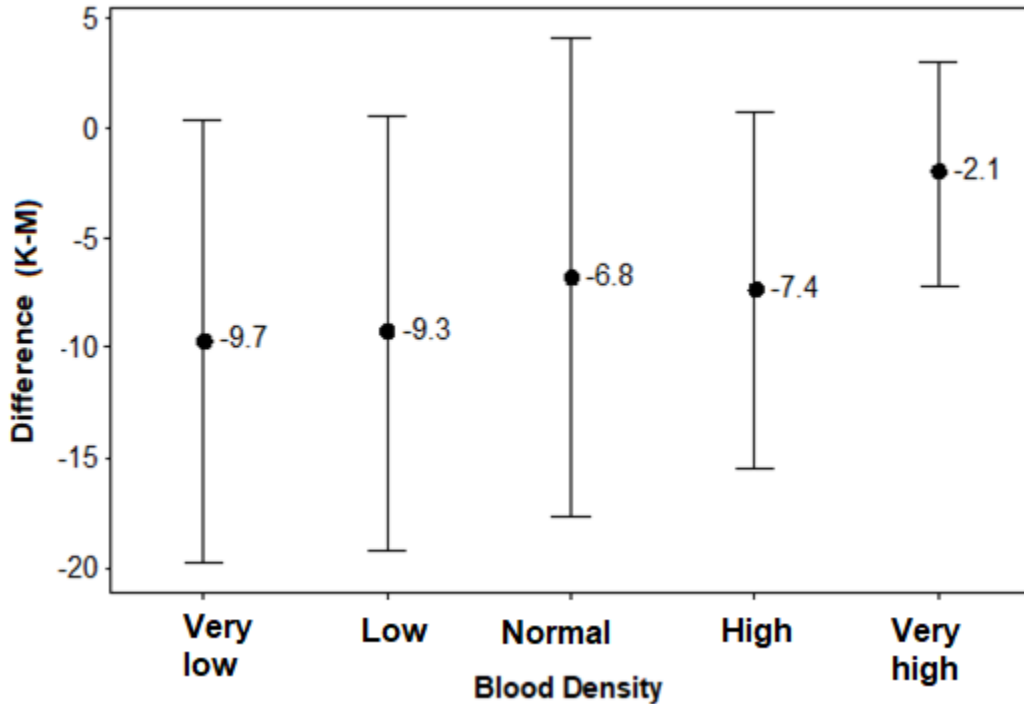
Figure 131. Comparison of mean differences between the known areas of origin minus the areas of origin obtained with the manual string method. Mean differences between areas of origin are represented by circular symbols and the lower and upper bounds of the 95% CIs are represented by I symbols.

The mean differences ranged from -2.1 at very high blood density to -9.7 at very low blood density All of the 95% CI for the mean differences captured zero, implying that the mean differences were not significantly different from zero. Consequently, hypothesis H2a was retained: There were no differences between the known areas of origin of the bloodstains and the

calculated areas of origin of the bloodstains obtained using the manual string approach, at the five different blood densities.

Hypothesis H2b.

Figure 132 is an error bar chart to determine the extent to which there are differences between the pre-defined known areas of origin of the bloodstains (K) and the calculated areas of origin of the bloodstains obtained using the HemoSpat® program (H) at the five different blood densities. The mean known areas of origin ranged from 57.1 at very high blood density to 62.7 at very low blood density. The mean calculated areas of origin ranged from 56.9 at very high blood density to 70.4 at very low blood density. No differences were indicated by the strong overlaps between the lower and upper boundaries of the 95% CI of the known and calculated mean areas of origin at each blood density.
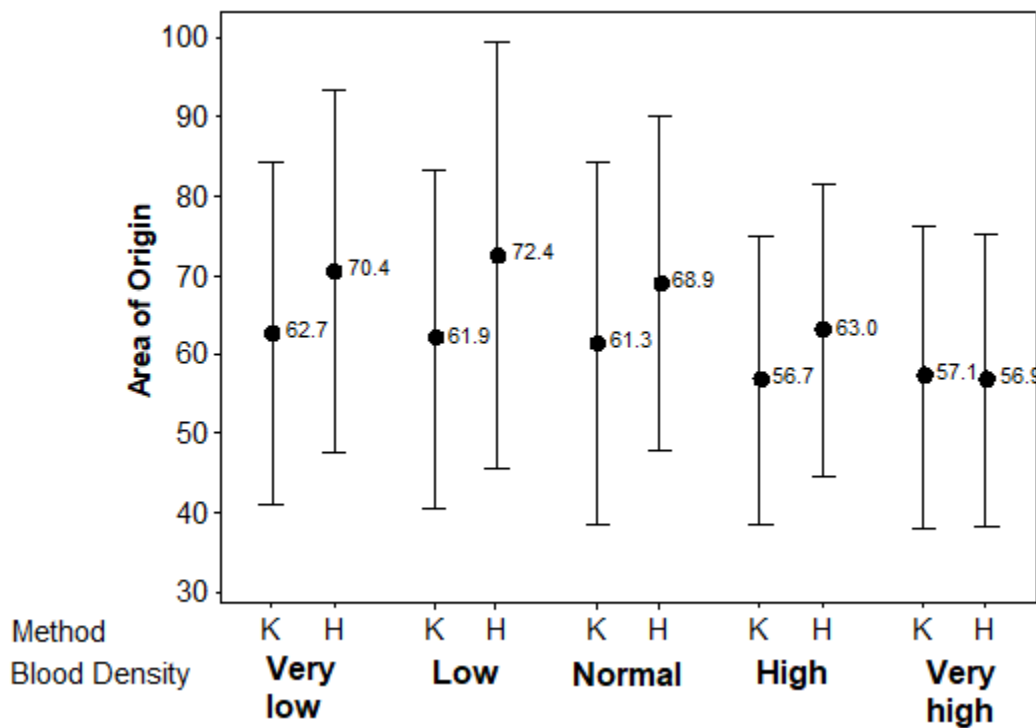
Figure 132. Comparison of the known (K) calculated areas of origin (H) obtained with the HemoSpat® program. Mean areas of origin are represented by circular symbols and the lower and upper bounds of the 95% CIs are represented by I symbols.

Figure 133 is an error bar chart to determine the extent to which zero was captured within the 95% CI of the differences between the known areas of origin of the bloodstains (K) minus the areas of origin of the bloodstains obtained using the HemoSpat® program (H).
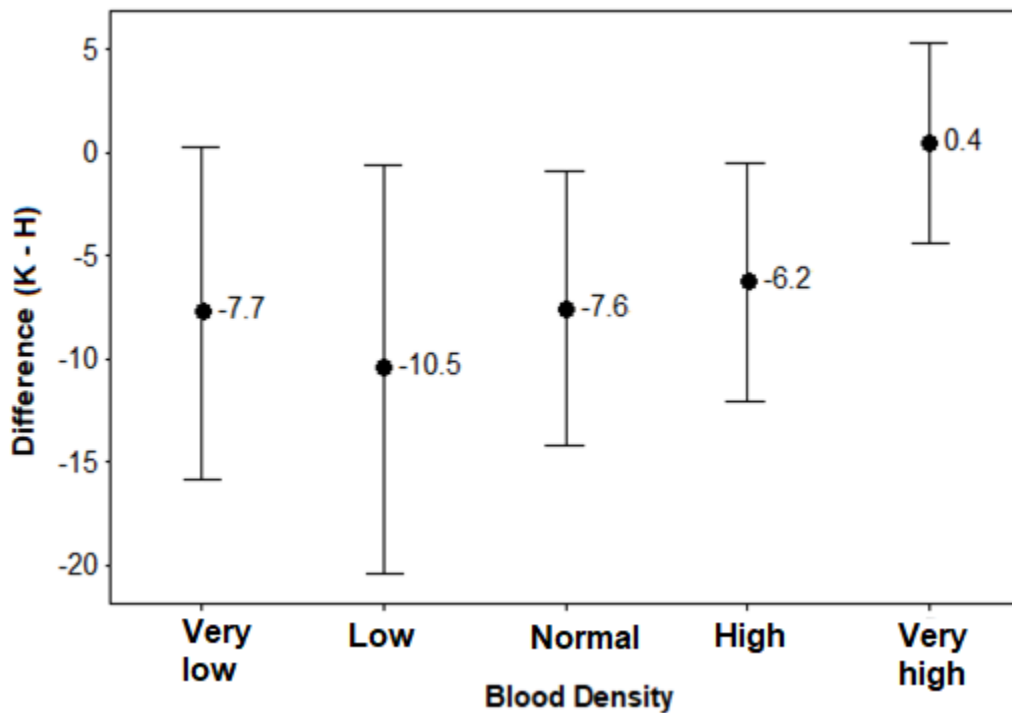
Figure 133. Comparison of differences between the known areas of origin (K) minus the areas of origin obtained with the HemoSpat® program (H). Mean differences between areas of origin are represented by circular symbols and the lower and upper bounds of the 95% CIs are represented by I symbols.

158

The mean differences (K-H) ranged from 0.4 at very high blood density to -10.5 at low blood density. All of the 95% CI for the mean differences captured zero, therefore the mean differences were not significantly different from zero. Consequently, hypothesis H2b was retained; there were no differences between the known areas of origin of the bloodstains and the calculated areas of origin of the bloodstains obtained using the HemoSpat® program, at the five different blood densities.

Hypothesis H2c.

Figure 134 is an error bar chart to determine the extent to which there are differences between the areas of origin of the bloodstains obtained with the manual string method (M) vs. the HemoSpat® program (H) at the five different blood densities. The mean areas of origin obtained with the manual string method ranged from 59.2 at very high blood density to 72.4 at very low blood density. The mean areas of origin obtained with the HemoSpat® program ranged from 56.7 at very high blood density to 70.4 at very low blood density. No differences were indicated by the strong overlaps between the lower and upper boundaries of the 95% CI of the known and calculated mean areas of origin at each blood density.

159
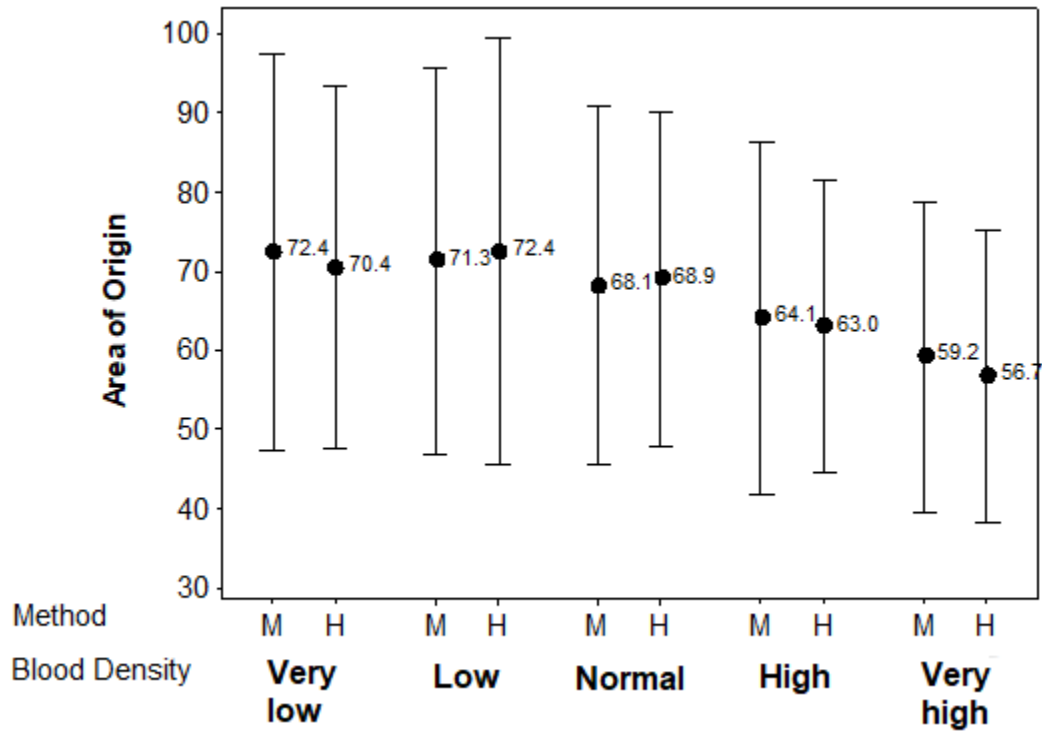
Figure 134. Comparison of areas of origin obtained with the manual string method (M) and the HemoSpat® program (H). Mean areas of origin are represented by circular symbols and the lower and upper bounds of the 95% CIs are represented by I symbols.

Figure 135 is an error bar chart to determine the extent to which zero was captured within the 95% CI of the differences between the areas of origin of the bloodstains obtained using the manual string method (M) minus the areas of origin of the bloodstains obtained using the HemoSpat program (H). The mean differences (M-H) ranged from 2.51 at very high blood density to -1.17 at low blood density. All of the 95% CI for the mean differences captured zero; therefore, the differences were not significantly different from zero.
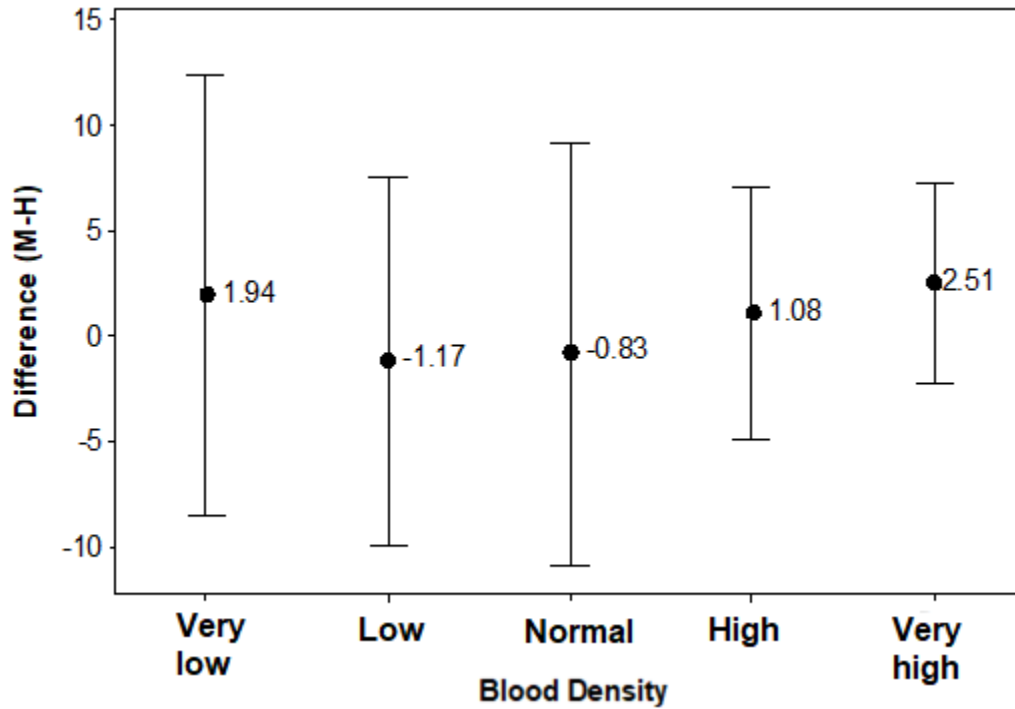
Figure 135. Comparison of differences the areas of origin obtained with the manual string method (M) and the HemoSpat program (H). Mean difference between areas of origin are represented by circular symbols and the lower and upper bounds of the 95% CIs are represented by the I symbol.

Therefore, hypothesis H2c was retained; there were no differences between areas of origin of the bloodstains calculated using the manual string approach and the HemoSpat® program.

Hypothesis H2d.

Figure 136 present scatterplots to determine if the differences between the calculated areas of origin of the bloodstains minus the known areas of origin of the bloodstains are correlated with the angles of impact at the five blood densities (Fisher, R., personal communication 5/12/18).

161
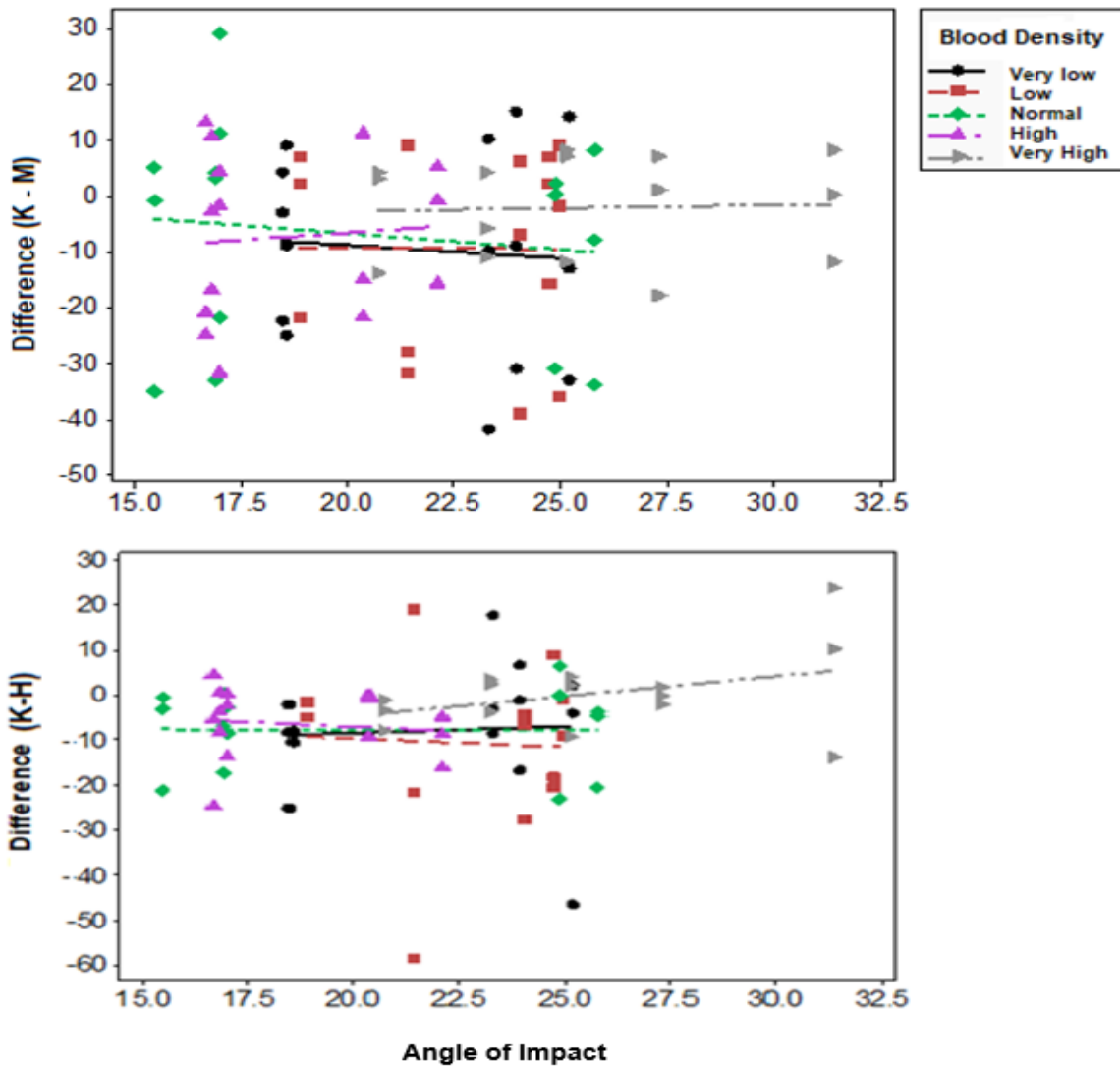
Figure 136. Differences between known (K) and calculated areas of origin using manual string method (M) and HemoSpat® program (H) vs. angles of impact.

The almost horizontal trend lines reflect little or no correlation. $R^2 = 0.0002$ indicated that only 0.02% of the variance in the differences between the known areas and the areas calculated with the manual string method was explained by the angles of impact. $R^2 = 0.017$ indicated that

only 1.7% of the variance in the differences between the known areas and the areas calculated with Hemospat® was explained by the angle of impact**.**

The effect sizes indicated by the very low values of R^2 were negligible. Therefore, hypothesis H2d was retained; the differences between the known areas of origin of the bloodstains and the calculated areas of origin of the bloodstains were not correlated with the angles of impact.

Conclusions

There were no statistically significant differences between the known areas of origin of the bloodstains and the calculated areas of origin of the bloodstains obtained using the manual string approach for the five blood densities. There were no statistically significant differences between the known areas of origin of the bloodstains and the calculated areas of origin of the bloodstains obtained using the HemoSpat® program for the five blood densities. There were no statistically significant differences between areas of origin of the bloodstains calculated using the manual string approach and the HemoSpat® program. The differences between the known areas of origin of the bloodstains and the calculated areas of origin of the bloodstains were not correlated with the angles of impact.

Chapter 4. Study 3: Gunshot Blood Spatter

Purpose and Plan

The purpose of Study 3 was to examine the relationship between the blood density and the distance the blood travelled from the target. The blood densities were measured with the same scale used in Study 1 and Study 2 (1 = very low, 3 = low, 5 = normal, 6 = high, and 7 = very high). A 0.38 caliber revolver was fired into blood samples located on a ballistic gel block

163

target to simulate an exposed area of skin that has blood on its surface. The blood spatter was collected on poster board at five distances from the target (1, 2, 3, 4, and 5). The amount of blood spatter was measured in terms of the number of grids where the blood spatter was observed, at five distances from the target (Table 45).

Table 45. Level designations of end of gun barrel to target

Level Designation	Distance from end of revolver barrel
1	15 cm
2	30 cm
3	45 cm
4	60 cm
5	80 cm

The firearm used was a 0.38 caliber Smith & Wesson Model 15 (Smith & Wesson, Springfield, MA) combat masterpiece 4 inch barrel revolver (Figure 137). The ammunition used was Fiocchi 0.38 special 130 grain, full metal jacket center fire cartridges (Giulio Fiocchi, Lecco, Italy) (Figure 138). The ammunition head stamp was GFL (Giulio Fiocchi, Lecco, Italy) for the ammunition manufacturer. The ammunition manufacturer reported a muzzle velocity of 950 ft/s and a muzzle energy of 260 ft lb (Fiocchi Ammunition).

Figure 137. The 0.38 caliber Smith and Wesson revolver used in simulations.

Figure 138. The 0.38 caliber cartridges used in Study 3.

Device Construction

The site for Study 3 was the farm house that had been previously used for Study 2 testing. The house is set on over 100 acres, and the firing of a revolver did not cause concern to the neighbors. See Figure 65.

Using Charlotte pipe 1 inch PVC piping a structure was built that would allow for 5 levels (distances) of support for poster board measuring 72 cm x 56 cm. This structure had to allow for a bullet stop in its base and for the placement of ballistic gel blocks on top of the bullet stop. The bullet stop consisted of 50 lb bags of sand placed inside of a wooden box. On top of the box were placed 2 ballistic gel blocks, each measuring 10 cm x 22.5 cm x 10 cm, and on top of the 2 ballistic gel blocks was a third ballistic gel block. The third block served as the target. A section of the block measuring 2.0 cm x 2.5 cm x 0.2 cm was cut out of the block so that it would hold 1 mL of blood, essentially on top of the ballistic gel. This simulated uncovered (exposed) skin with blood on its surface. See Figures 139 through 144.

The apparatus was tested to be certain that the sand was sufficient to trap the expended 0.38 caliber projectile. It was found to be satisfactory, and additional sand bags were placed around the base in the event of a ricochet. Below the sand bags was a wooden floor. However, all of the expended bullets were trapped by the sand.

Figure 139. Device to hold poster board sheets.

Figure 140. Device showing ballistic gel target.

167

Figure 141. Close up of the ballistic gel target.

Figure 142. Device showing the slots for poster boards.

168

Figure 143. Device showing relationship between the ballistic gel target and slots for poster board.

Figure 144. Another view of Figure 143.

Simulations

For each simulation the following process was followed:

- The poster board was identified with the blood density number, the position number, and test number. A hole measuring 2.5 cm x 2.5 cm was cut out from the center of the poster board to allow for the gun barrel to be placed through it.

- The designated poster board was placed in the appropriate position on the device (based on the distance from the target).

- The hole in the poster board was positioned over the target by use of a portable laser.

- Once the poster board was set in its position, the blood appropriate sample was removed from the 37 ^{o}C water bath, and a Pasteur pipette was used to withdraw a blood sample aliquot. A 1 mL aliquot of the blood sample was then transferred to the target (the cut out area in the ballistic gel).

- Next, the 0.38 caliber revolver was loaded with one 0.38 special cartridge, and the end of the revolver barrel was positioned inside of the hole in the poster board.

- One shot, using single action to minimize movement of the revolver, was fired into the blood-covered target.

- Once the projectile was fired, the poster board was removed from its designated position, and the blood spatter was allowed to dry.

- Each poster board was photographed to document the blood spatter patterns for each simulation.

The above process was repeated for each of the 50 simulations.

Simulations Documentation and Data Collection

The poster boards from the simulations had varying amounts of blood spatter on them, which could be described based on a visual observation (Figures 145 and 147). However, in order to quantitate the amount of blood spatter on each poster board, it was decided to use a grid system. A sheet of drafting paper measuring 79 cm x 60 cm was used, and a total of 154 equally sized grids, each measuring 5 cm x 5 cm, were drawn onto the tracing paper (Figure 148). The drafting paper was placed over each of the simulation poster boards, and the number of grids that contained any amount of blood spatter were counted (Figures 146 and 149). These data were used to evaluate the impact of the five blood densities on the distance the blood traveled from the target after being struck by a 0.38 caliber bullet, specifically, the distance the blood traveled from the target back towards the revolver (Tables 46-47 and Figure 150).

Figure 145. Simulation very high density blood, level 2-2, blood spatter on poster board.

Figure 146. Grid placed over simulation in Figure 145 to quantify number of grids with blood spatter present.

Figure 147. Simulation very high density blood, level 1-2, blood spatter on poster board.
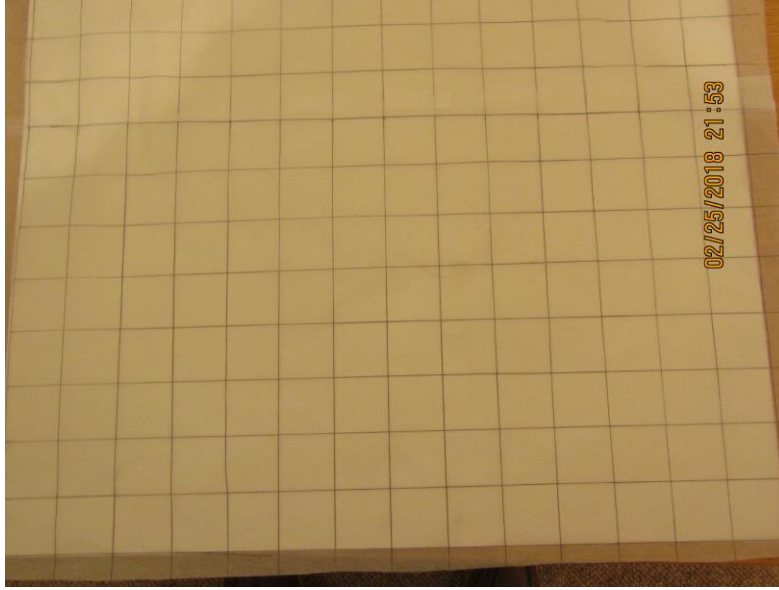
Figure 148. Grid used to count number of quadrants blood spatter was present.
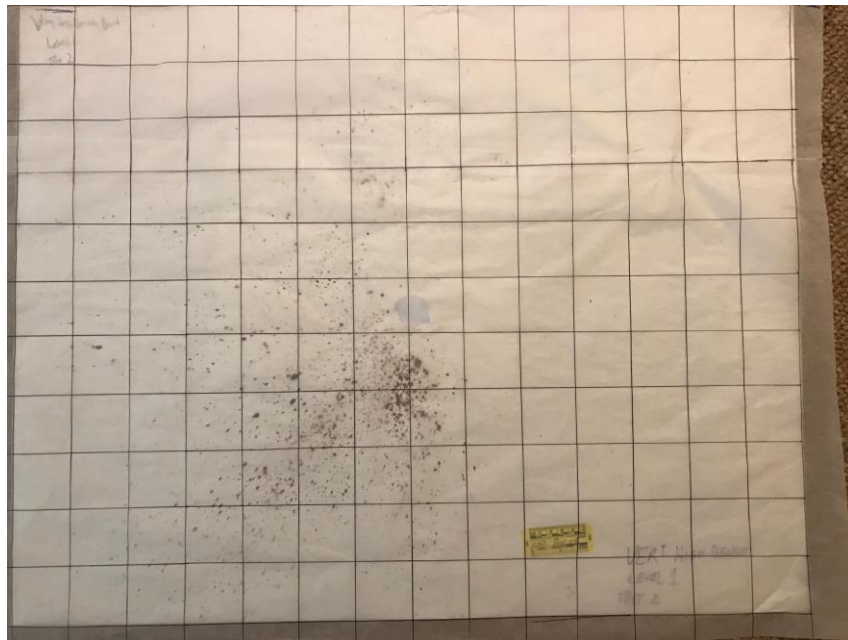
Figure 149. Grid placed over simulation in Figure 147.

173

Table 46. Number of grids at each level by blood density

Levels	VLD	LD	ND	HD	VHD
1	48	68	96	97	89
2	57	82	46	70	66
3	37	48	8	7	14
4	21	5	4	8	23
5	4	11	4	12	8

Table 47. Number of grids by density at each level

Density	Level 1	Level 2	Level 3	Level 4	Level 5
VLD	48	57	37	21	4
LD	68	82	48	5	11
ND	96	46	8	4	4
HD	97	70	7	8	12
VHD	89	66	14	23	8

174
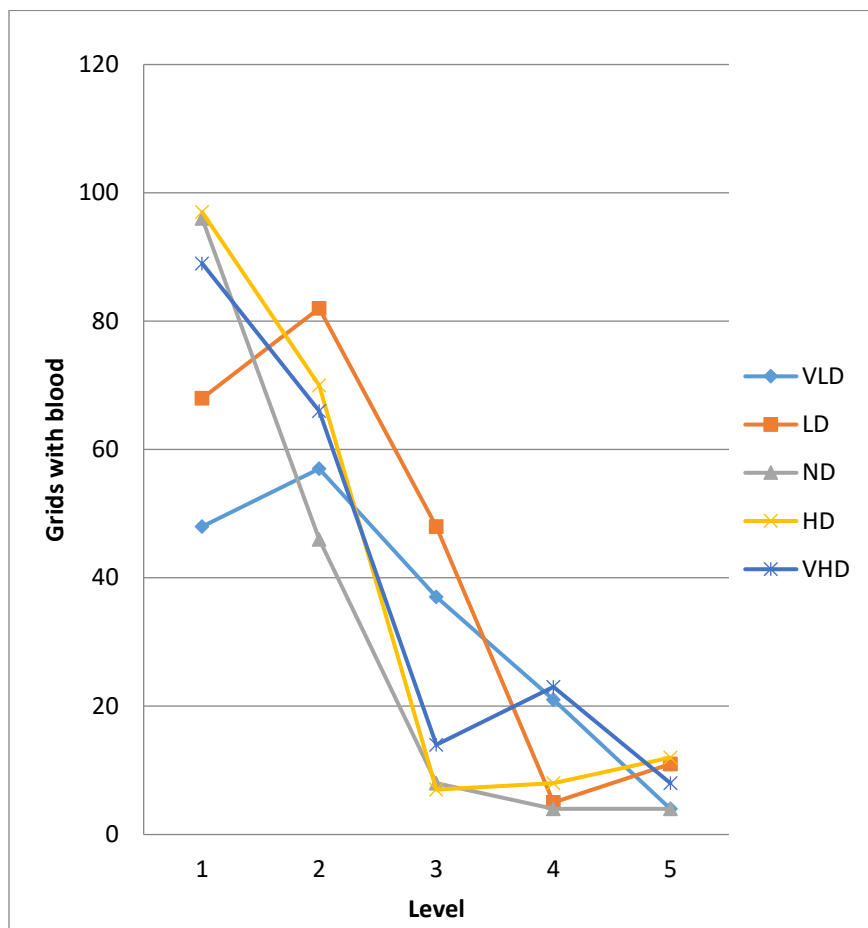
Figure 150. Graph of number of grids with blood spatter to level by density.

Study 3 Research Questions and Hypotheses

RQ3: To what extent is the distance that the blood travels from the target correlated with the blood density?

H3: The distance that the blood travels from the target is correlated with the blood density.

H3 was tested visually by plotting the variations in the amount of blood spatter (number of grids) vs. the blood density, and the distance from the target, and statistically by conducting analysis of covariance (ANCOVA). The purpose of ANCOVA is to determine if the means of a

175

dependent variable are equal across all levels of an independent variable, while statistically controlling for the effects of covariates, confounding, or nuisance variables (Belin & Norman, 2009; Rutherford, 2001). ANCOVA was conducted to exclude the effects of the highly variable amount of blood spatter from the relationship between the distance the blood travelled from the target and the blood density. The distance from the target was the dependent variable. The blood density was the independent variable. The amount of blood spatter was the covariate because it confounded the relationship between the distance travelled and the blood density. The effect size was indicated by η^2; assuming $\eta^2 < 0.04$ was a negligible effect size (Ferguson, 2009).

Data Analysis

This section provides the results of the analysis to address the questions RQ3 and the associated hypotheses H3. Figure 151 plots the variations in the amount of blood spatter (number of grids) vs. the blood density (1 = very low, 3 = low, 5 = normal, 6 = high, and 7 = very high) and the distance from the target (1, 2, 3, 4, and 5). The amount the blood spatter at each of the five blood densities was correlated with the distance from the target. When the distance from the target = 1, the number of grids where blood was observed across the five blood densities was the highest, ranging from 48 to 96. When the distance from the target = 2, the number of grids where blood was observed across the five blood densities was lower, ranging from 57 to 82. When the distance from the target = 3 the number of grids where blood was observed across the five blood densities, was lower, ranging from 7 to 48. When the distance from the target = 4 the number of grids where blood was observed across the five blood densities was lower, ranging from 4 to 23. When the distance from the target = 5, the number of grids where blood was observed across the five blood densities was the least, ranging from 4 to 12.

176
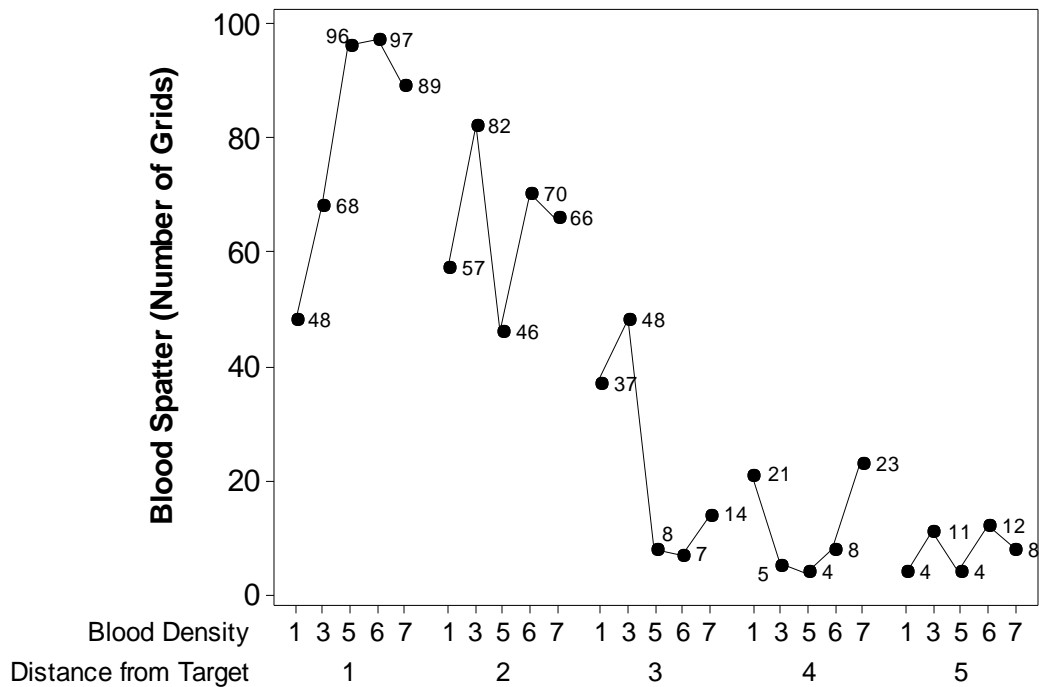
Figure 151. Blood spatter (number of grids) vs. blood density and distance from the target.

Figure 152 is an error bar chart to illustrate the mean amount of blood spatter (number of grids) $\pm$ 95% CI at the five distances from the target across the five blood densities. The mean amount of blood spatter declined systematically with respect to the distance from the target. The mean number of grids where blood was observed ranged from a maximum of 79.6 when the distance from the target = 1 to a minimum of 7.8 grids when the distance from the target = 5. The effect size was $R^2 = 0.753$, implying that 75.3% of the variance in the amount of blood spatter was explained by the distance from the target.

177
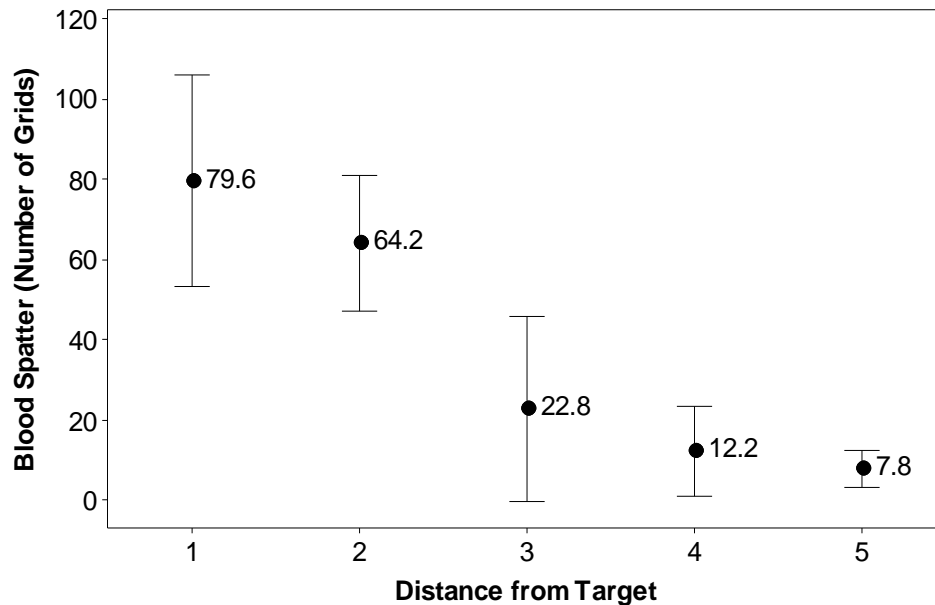
Figure 152. Comparison of the amount of blood spatter vs. distance from target. Mean amount of blood spatter represented by circular symbols and the lower and upper bounds of the 95% CIs are represented by I symbols.

The data presented in Figures 151-152 emphasized that the highly variable amount of blood spatter at each distance from the target confounded the relationship between the distance the blood travelled from the target and the blood density.

Analysis of covariance (ANCOVA) was conducted to exclude the effects of the highly variable amount of blood spatter from the relationship between the distance the blood travelled from the target and the blood density. The distance from the target was the dependent variable. The blood density was the independent variable. The amount of blood spatter was the covariate (i.e., a variable that confounds the relationship between an independent and a dependent variable). ANCOVA was used to control the value of the covariate. Specifically, the amount of blood spatter was held statistically constant with a value of 37.32. Figure 153 illustrates the

178

adjusted mean values ± 95% CI of the distances of the blood spatter travelled from the target, after controlling for the amount of blood spatter, at each of the five blood densities.
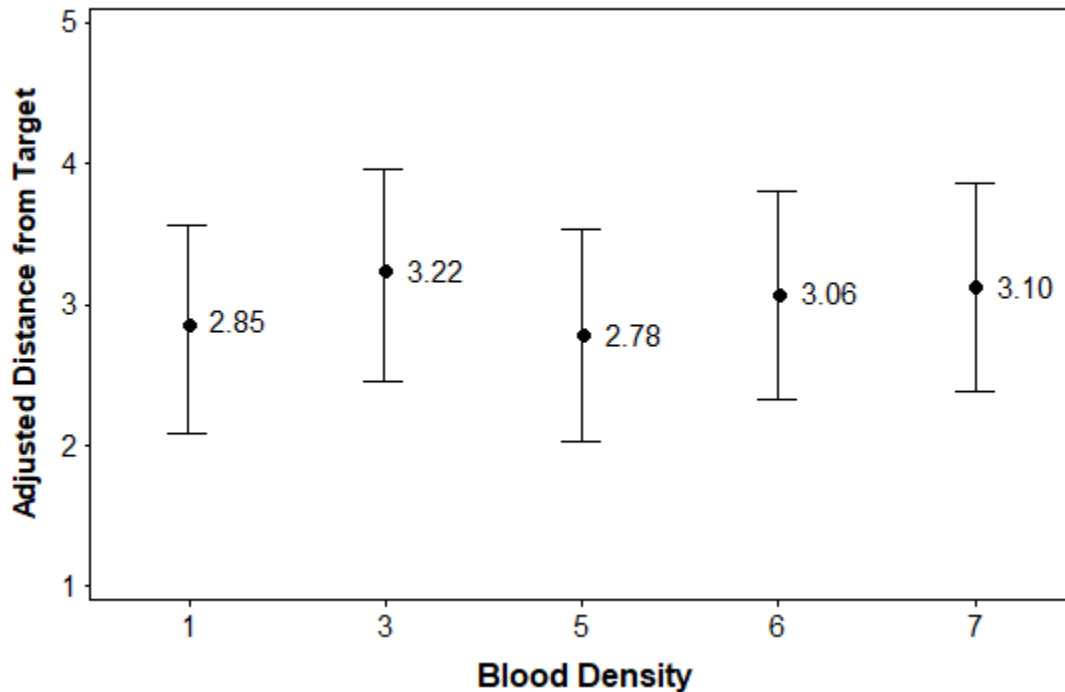
Figure 153. Comparison of adjusted distance blood travelled from target vs. blood density. Adjusted mean values of distance blood traveled to the target represented by circular symbols and the lower and upper bounds of the 95% CI are represented by I symbols.

The mean adjusted distances that the blood travelled from the target, after controlling for the amount of blood scatter, ranged from 2.78 to 3.10. The strongly overlapping 95% CI reflected little difference between the mean differences distances. The effect size ($\eta^2 = 0.053$) was very small (i.e., only 5.3% of the variance was explained). However, this effect size was just above criterion of Ferguson (2009) that the absolute minimum effect size to indicate a practically significant effect is $\eta^2 = 0.04$ (i.e., 4% of the variance is explained).

Because the effect size (indicated by the low value of η^2) was very small, and the confounding effects of the highly variable amounts of blood spatter were high, the correlation between the distance that the blood travelled from the target and the blood density was difficult to evaluate. The results indicated that there was little evidence to support H3: The distance that the blood travels from the target is correlated with the blood density (Fisher R., personal communication 5/13/18).

Conclusions

Is the distance that the blood travels from the target correlated with the blood density? The data indicated that there is no correlation between the blood density and the distance the blood travels from the target after it is impacted with a 0.38 caliber projectile.

Chapter 5. Quality Assurance at the Crime Scene and the Crime Lab

Crime Scene Investigation

Blood pattern analysis is a component of crime scene reconstruction. The manner in which blood was deposited at a crime scene can be a critical part of the overall reconstruction of the sequence of events that occurred before, during, and following the incident being investigated. "Blood pattern analysis is an activity that is subsumed under scientific crime scene investigation and reconstruction." (DeForest, 2018). Blood pattern analysis may be able to provide investigative information which could be helpful to those charged with investigating the incident. Blood pattern evaluation in some cases might have more value than DNA evidence, particularly if there is no issue about the origin of the blood stains.

Unfortunately, very often blood pattern evidence is either overlooked or misinterpreted. The crime scene needs to be evaluated as a whole, not in individual pieces as is often done.

The investigation of a crime scene, making decisions about which items constitute evidence that should be collected for further crime lab evaluation and which items need to be documented, is a very complex process. "Interpreting the physical traces at a potential crime scene is a scientific problem - a very demanding scientific problem! Knowledge of natural phenomena, extensive experience and a high level of proficiency with hypothesis development, hypothesis testing and scientific reasoning are all necessary." (DeForest 2018). In many cases, these decisions are made by individuals who are not trained in criminalistics, but are usually crime scene technicians. These technicians typically receive their direction, i.e., what is evidence and what should be collected, from the investigating officer.

It is imperative that a crime scene investigator evaluate all of the relevant evidence before coming up with a crime scene reconstruction scenario. The investigator must not introduce any potential bias as to what they think occurred and only look for evidence which supports their theory. The crime scene investigator has the task of evaluating which items require further analysis, what needs to be documented, and whether there is a single crime scene or multiple crimes scenes; all of this in a process which provides impartial conclusions, which may be contrary to the direction in which the investigating police agency is pursuing. "The approach to the recognition of relevant physical traces cannot be formulaic. It must be continually developed and refined de novo using the scientific method. In addition to the fundamental science education, the scientific investigator must also have both detailed training and extensive experience with crime scenes." (DeForest, 2018). If the incident is a homicide, then the body of the deceased is evidence, including their clothing and material which may be on the clothing, may be considered a crime scene of its own.

Crime scene investigations cannot be rushed, as they require a very detailed and meticulous evaluation of the evidence or potential evidence and its juxtaposition to other items at the scene.

The individual, evaluating the scene, making the decisions about evidence, documenting, and evaluating all the other myriad of items that require consideration in this very complex exercise of scene reconstruction, should be a highly trained scientist, or more specifically, a criminalist. A criminalist is a generalist who may have additional expertise in a forensic specialty. As a generalist, the criminalist has training and experience in evaluating all of the different types of evidence that may be encountered at a crime scene. He/she formulates decisions on which items should be collected for further testing as well as items needing evaluation at the scene.

Blood pattern analysis requires evaluation at the scene before items are moved and spatial relationships change. A crime scene is a very fragile place, many things can impact how the evidence may be perceived. What has changed since the event took place? Did first responders move certain items and were additional blood patterns created which had nothing to do with the initial scene? There are a variety of ways in which a crime scene can be contaminated or altered. Again, this is a complicated process and must be handled by an appropriate expert, the criminalist.

A Texas homicide case, in which an individual, Joe Bryan, who was convicted of the murder of his wife largely based on blood spatter testimony, is one example of the way in which bloodstain pattern analysis can be misinterpreted by those not appropriately trained. "Through the 1960's, analyzing bloodstain patterns was the province of forensic scientists with years of training in fluid dynamics and high level mathematics." (NY Times, 5/31/18). As bloodstain

pattern analysis became more popular, individuals with little scientific training who have taken a weeklong course became bloodstain pattern analysts, and these "experts" were accepted in many cases by the courts. "An influential state commission said the blood spatter analysis used to convict a former Texas high school principal of murdering his wife in 1985 was "not accurate or scientifically supported" and the expert who testified was entirely wrong. The findings of the Texas Forensic Science Commission, a national leader in forensic science reform, called into question the conviction of Joe Bryan, who has now spent more than 30 years in prison." (Colloff, P., 2018). There is now a Texas statute requiring "that bloodstain pattern analysis be performed by an accredited organization, which should make it harder for prosecutors to introduce testimony by analysts with minimal training and qualifications." (NY Times, 5/31/18).

Crime Scene and Crime Lab Management: The Role of the Criminalist. Who is in Charge?

The concept of crime scene management is an important matter. It means someone has responsibility for the overall crime scene and is making the important decisions about documentation recovery, resources required, how long to maintain the scene, etc. This should be the criminalist (generalist), as this individual is best equipped to make the vital decisions necessary so that a valid crime scene reconstruction is performed. "Scientists with experience at scenes need to have authority over all physical evidence, including the victim's body, if one is present, up until the time it is delivered to the forensic pathologists for autopsy." (DeForest, 2018). This concept runs contrary to most jurisdictions, where the police investigator is in charge of the scene and most likely reluctant to give up this control.

The crime scene - crime lab interaction is the concept of crime scene management should continue with the analysis of the collected evidentiary items from the crime scene or scenes that

183

are linked in some manner. For example, a homicide takes place in a house, the body is transported in a vehicle to a remote area, and the body set on fire. There are at least four connected crime scenes: the house, the vehicle, the site where the body was burned, and of course, the body itself.

The criminalist will interact with the forensic specialists in the crime lab so they both have an understanding of which evidentiary items are important and why. "Think of criminalistics as an orchestra. Each of the specialization areas is required to play a symphony. But a conductor keeps them all together, playing the same orchestral piece, in the same time, and lets each section know when their part is required, when solos begin, when they end. And think of the tools that we acquire, no matter how sophisticated, as a musical instrument." (Hunter, 2000). A review of the scene and how the evidence may help in the scene reconstruction, which is very valuable as compared to just receiving a bag of clothes and performing "standard" testing.

The concept that crime scene management continues with management of the evidentiary analysis at the crime lab would, in my opinion, make the analysis process more efficient and valuable to the criminal justice system.

Very often crime scene technicians, at the request of the investigating officer, will collect a large amount of "evidence" items for fear they might miss something. I call this "evidence pollution." This mass of items is submitted to the crime lab in the typical way and with little to no guidance as to what may be of value forensically. The crime lab scientist will perform their usual testing and write the standard report and will have no idea as to whether their testing was relevant or even evaluated in the full context of a crime scene reconstruction.

The Texas Legislature passed SB-1287, which requires all forensic analysts to be licensed beginning January 1, 2019. Forensic analyst is any person who, on behalf of a crime

184

laboratory accredited by the State, reviews, performs, draws conclusions from, or interprets a forensic analysis for a court or crime laboratory (Tex S.B. 1287). The following forensic disciplines require accreditation: seized drugs testing, toxicology testing, forensic biology, firearms/toolmarks, document examination, materials (trace) analysis, and other disciplines if accredited by a recognized accrediting body and approved by the commission (Adm Code, 651.5). No crime laboratory accreditation is required for the following disciplines: latent print examination, breath specimen testing, and digital evidence testing (Adm Code, 651.6). The Texas statute is generally a step in the right direction. However, if there is no accreditation for a specific analysis, these tests would not be admissible and could lead to an injustice. A novel approach that may exonerate an individual would not be allowed in court.

Outsourcing Forensic Testing

A common situation in the pharmaceutical industry is the outsourcing of bioanalytical testing to a contract research organization (CRO). The primary reason for outsourcing is timelines, the requirement to provide bioanalytical data to regulating agencies, primarily the U.S. FDA, so that companies can submit their applications for new biologic or chemical entities in a timely manner. The lab must meet criteria under the U.S. FDA Good Laboratory Practice (GLP) and Good Clinical Practice (GCP) to perform preclinical and clinical testing. There is a very comprehensive quality process, which is an integral part of the laboratory testing (Organization for Economic Co-operation and Development (OECD) principles of GLP). QA encompasses "those laboratory operations that ensure that quality control procedures are properly implemented; that the accountability of data is maintained; and that every reported result is traceable (i.e., to the date of analysis, the analyst who performed the test, the method used, and

185

the instrument used). The components of a QA program include the use of proper quality control (QC) samples, the use of validated testing procedures, timely evaluation of QC sample results using appropriate statistical processes to detect problems both in individual batches and on an on-going basis, and implementation of necessary corrective actions to eliminate problems." (National Laboratory Certification Program (NLCP), 2000). The quality process includes the following elements:

- Standard operating procedures (SOP)

- Validation protocols

- Sample analysis protocols

- Qualification (validation) of all instruments

- Traceable standards and references

- Each analytical run is independent with separate QC samples, standards, and controls

- Strict criteria for accepting an analytical run

- 100% QC of all data

- All testing is overseen by a project manager, who is a senior scientist and is responsible for approving the analytical runs and data

- Independent QA Group – audit 100% of validation data and at least 10% of all analytical data

    Comparison of the various laboratory types is presented in Table 48. Table 49 compares various aspects of CRO and forensic laboratories.

Table 48. Laboratory testing comparison: clinical, GLP, GCP, and forensic

Lab Type	Purpose of Testing	Results Interpreted by	End User of Data
Clinical	Diagnosis	Physician	Physician
GLP – Bioanalytical Pre-clinical testing	Drug Approval Safety	Study Director	Regulatory Agency
GCP – Bioanalytical Clinical testing Clinical Trials	Drug Approval Safety and Efficacy	Medical Director Principal Investigator	Regulatory Agency
Forensic Lab	Medico-Legal Investigative aids Reconstruction of events	Criminalist Forensic Specialist	Judge, Jury

Table 49. Laboratory comparison bioanalytical CRO to forensic lab

Requirements	CRO Bioanalytical	Forensic Lab
Lab accreditation	Yes, CLIA, GLP, GCP	Yes
Scientist certification	Yes, CLIA	Available
Guidance documents	Yes	Yes
Regulatory inspections	Yes, unannounced	Yes, announced
Client audits	Yes, annually	No
SOPs and procedures	Yes	Yes
QC process	Yes, 100%	Yes
QA internal auditing	Yes	Varies

187

Assay performance criteria	Yes, including reanalysis	Varies
Scientist proficiency	Yes, semi-annual	Varies, accreditation require proficiency
External proficiency	Yes	Varies, accreditation requires proficiency
Blind reanalysis	Yes	No
Double blind reanalysis	Yes	No, difficult to manage
Responsible for oversite	Project Manager	Lab Manager or Criminalist

The QA Department checks for compliance with SOPs and procedures; if there is non-compliance, a deviation report is written. This must be addressed by the lab scientist and project manager and signed by the lab senior management and QA director. All deviations are tracked.

In addition to all of the safeguards built into the testing process, the CRO lab is subject to unannounced inspections by the FDA. A typical FDA audit involves 4-6 auditors and can last several weeks. Besides the audits mandated by regulatory agencies, the lab is also audited by client QA teams at least annually for each client.

The quality system in a U.S. Department of Health and Human (HHS) Services Substance Abuse and Mental Health Services Administration (SAMHSA) approved laboratory performing workplace drug testing is another model of a QA process designed to provide safeguards against inaccurate results. There exists a system of proficiency testing (PT) and QC built into the processes of the SAMHSA-approved lab. Blind testing PT samples submitted quarterly to the lab by HHS are analyzed by the lab following its "normal" testing protocol with results reported back to HHS (Mandatory Guidelines for Federal Workplace Drug Testing Programs, 2017). In addition, HHS requires that open QC samples be included in all analytical

188

runs. Also, double blind samples are prepared, pre-analyzed, and submitted as routine specimens by the client.

In addition to the above QA testing, there is a scheduled audit every six months by auditors who are a combination of contract auditors and HHS staff members.

What Should Be the Model for Forensic Services?

I would propose taking relevant portions from each of the above models to create a comprehensive quality program for forensic labs, which would include the following elements:

1. Crime scene investigation under the control of the criminalist /generalist.

2. Lab testing performed and results reviewed under the direction of criminal/generalist.

3. SOPs providing general guidance, allowing for "non-standard" evidence.

4. 100% QC of all data by a 2nd party.

5. A separate and independent QA Department to oversee all aspects of quality, including conducting QA audits of all reports and all lab operations.

6. Incorporation of blind QC samples into all runs.

7. Double blind submissions, similar to blind proficiency samples that are received from a 3rd party. Though this would be difficult to manage, in the case of CDS (controlled dangerous substances) it is doable using pretested samples that are scheduled for destruction. For other testing a contractor would need to simulate a case and associated evidence and submit as routine evidence.

8. Inspections by regulatory agencies resulting with real ramifications if problems are found. These inspections would include unannounced site visits performed by professionals that are not other lab directors.

9. Auditing of court testimony by lab management or the criminalist/generalist to ensure the testimony is consistent with the results. This is best accomplished by reviewing testimony transcripts.

10. The forensic labs should be independent and separate from the police department and/or prosecutor's office. It should include equal fee-based access to its testing services by both the prosecution and defense. The question of payment for an indigent defendant is a significant issue. "A strong recommendation of the NAS (National Academy of Science) report, published in 2009, was that forensic labs establish independence from law enforcement." (Rudin & Inman, 2015). "The scientific analysis of forensic evidence can be essential to solving crimes, but as long as the process is controlled by the police and prosecutors, and not scientists, there will never be adequate oversight" (NY Times, 2018).

11. Outsourcing the appropriate routine testing to a CRO to ensure timely reporting and to ease the testing burden on the forensic lab. The outsourced forensic labs should have all of the quality procedures proposed above.

There are many similarities between a regulated bioanalytical lab and a forensic lab. Both work with non-standard material, such as a new biological or chemical entity in the case of a bioanalytical laboratory and evidentiary items (there is no standard evidence) for the forensic lab. Both are intellectual endeavors requiring a creative, scientific thought processes within a regulatory or legal framework. Each involves scientific problem-solving which drives the approach to cases. Technology serves as only a tool is the problem-solving endeavor.

Chapter 6. Research Conclusions

The goal of this research was to determine if change in the physical property of blood had an impact on blood stain patterns in forensic investigations.

Study 1 was designed to determine if a change in the physical property of human blood would impact the geometry of resultant blood stains when blood, dropping only under the influence of gravity, impacts a surface at various angles.

The conclusions from Study 1 were that there is an impact on blood stain geometry and other aspects of the blood stains, including color and presence of tails. However, there is no effect on the calculated angles of impact. The comparison of normal human blood to very high density and very low density samples did not show a statistically significant difference on the calculated angle of impact.

The purpose of Study 2 was to determine if changes in the physical properties of human blood had an impact on the determination of area of origin from blood spatter that was produced by striking a blood-covered target with a baseball bat. A comparison was made between the determination of the area of origin using a manual string method and using a commercially available software program, HemoSpat®.

The conclusions reached from Study 2 were that there is no difference between the blood densities in determining the area of origin. Additionally, both the manual method and the computer program method were equivalent. The area of origin terminology was used in this dissertation to describe the location of the blood source at the time the blood spatter was produced. The volume of origin terminology better describes the physical situation as the origin is defined in three dimensions (x, y, and z) rather than in two dimensions.

191

The purpose of Study 3 was to determine if blood of different densities traveled further when a target with blood on its surface was struck by a 0.38 caliber projectile.

The Study 3 conclusion was there is no statistical difference in the distance the blood traveled.

Chapter 7. Contribution to the Field of Forensic Science and Criminal Justice

This research intended to answer or clarify a number of questions related to bloodstain pattern analysis (BPA). These questions include:

- When the physical characteristics of an individual's blood are outside of the normal range, as in some blood disorders and other disease conditions, how does this impact bloodstain patterns from that individual's blood? Is there the potential to misinterpret the bloodstain patterns and could this result in crime scene reconstruction errors?

- Are the differences from normal blood statistically significant given the errors in manual measurements as well as in bloodstain selection?

- This research included recommendations for a quality assurance process at crime scenes with a focus on BPA. The key elements of a QA program were discussed. A critical component in the process is the role of a criminalist/generalist, who has the ability to review the evidence and reach an independent conclusion regarding the BPA. This quality process extends to the nature and extent of documentation and preservation that is reasonable and expected. The need for a criminalist's review is to answer the question has all the evidence been recognized? Additionally, the criminalist is part of the decision making process as to what is relevant and should be further evaluated. Crime scene reconstruction must consider all of the evidence and not only the evidence that may support a particular theory of the crime. The

192

hypothesis will be tested against the observations (evidence) and modified if the data do not fit. Of course, this assumes that all of the "relevant" evidence has been identified, documented, and collected where possible.

- This research utilized digital measuring and computer assisted data analysis in the bloodstain pattern examinations. This research provided a better understanding of the value of this technology and suggested enhancements that could provide more complete analysis, especially of physical parameters that are assumed to be relatively constant in a narrow window of inter-personal variation.

- This research has shown that there is not material or statistically significant impact on BPA on bloodstain patterns when the physical properties of the blood are outside of the normal range. That finding is still an important contribution to the field and adds to the scientific validity of bloodstain pattern analysis.

- In Daubert vs. Merrell Dow Pharmaceuticals (Daubert), The United States Supreme Court considered the question of the admissibility of novel scientific evidence. The Supreme Court suggested factors that should be used to determine the reliability of a scientific theory or technique. These are known as the Daubert Factors, and they are the following.
  - Has the scientific theory or technique been tested and are the methods based on a testable hypothesis?
  - Has the scientific theory or technique been subjected to peer review and publication?
  - What are the known or potential error rates of the theory or technique when applied?
  - Do standards and controls exist and are they maintained?

193

o Has the theory or technique been generally accepted in the relevant scientific community? (Foster & Huber, 1999; James & Nordby, 2003; Saferstein, 2005; Willis et al., 2001; FBI Lab, 2008; and Daubert vs. Merrell, 1993).

The research in this thesis has added to the scientific knowledge regarding BPA. An evaluation of error rates is also a component of this research. The quality assurance recommendations in the thesis should serve to complement the standard and control requirements within the Daubert Factors. In summary, this research should provide additional data to complement the scientific validity of conclusions reached based on bloodstain pattern analysis.

Chapter 8. Future Work and Additional Areas for Research

There are many areas of additional research and study needed when it comes to scientific scene reconstruction and blood pattern analysis. The first is a better understanding of the training and educational requirements to prepare individuals for this complex task. This could be at a minimum university-based master's level formal educational program. The second is technology that will assist in evaluating items that may provide additional information about the incident, such as the color and geometry of bloodstains. More efficient software for scene documentation, including individual stain coordinates, would be valuable. A new device that may assist in crime scene documentation is the Leica ScanStation (Leica Geosystems AG, Hexagon, Stockholm, Sweden). The ScanStation measures everything within its line of sight instead of only what an investigator thinks is important at the time. At a later date, investigators can view the scene to examine any geospatial relationships that become relevant (Leica Geosystems, 2018).

Research in the development of techniques to analyze bloodstains for therapeutic agents that the individual had in their blood at the time the bloodstain was produced could be very

194

useful in cases where a body has been removed from the scene of a homicide. From this analysis, one may be able to discern medical conditions that the individual may have, which could be of value as investigative aids. More research into the role of a criminalist/generalist in crime scene management and in overall case management is needed to maximize the potential evidence available and to put it in the appropriate perspective without preconceived theories of the crime. All of the above would help in demonstrating that bloodstain pattern analysis is a "legal" science and meets the Daubert benchmarks.

APPENDIX

Anton Paar DMA 35 Density Instrument Specifications

FINAL INSPECTION	DMA 35 Version 3 Standard	Anton Paar
Cat.No: 84138	Ser. No.	82040116

Serial Numbers

Ser. No. instrument	82040116
Ser. No. main board	21795428
Ser. No. coil print	21848261

Functional Test

Display	✓	Pipette-style pump	✓
Keyboard	✓	Infrared interface	✓
Store button	✓	Acoustic signal	✓
Optical	✓	Accessories	✓

Labels

Type plate	✓
Batterie plate	✓
ISO17025 calibration	

Calibration

	Temperature [°C]	Density [g/cm³]
Deionized water	39,7	0,9924
Deionized water	21,1	0,9982
Deionized water	12,3	0,9997
Air	21,5	0,0012
n-Heptane	20,9	0,6834

n-Heptane	455236254	11.05.2016

Firmware

Version	v1.90

Specifications according to the inspection schedule fulfilled	
Date:	
Controller:	

Tel.: +43 (0)316 257-0
www.anton-paar.com

Created on 22.04.2006 09:55
Created by Edelsbrunner-TI

C88AF01-D
Page 1 of 1

ADVIA Instrument Print outs

HEADER

Aspiration Date/Time	09/02/2016 10:36:29 A
Sample Type	PATIENT
SID	2
Sample Selectivity	CBC/DIFF/RETIC
Age & Sex	
Instrument Number	Advia 120
Sequence	37
Species	Human

Routine Retic

Retic	1.94	* L	17.6	* x10^6 cells/uL
CHr		H	32.2	* pg
CHm			30	* pg

Routine CBC

WBC	L	0.63	*	x10^3 cells/uL
RBC	L	0.91	*	x10^6 cells/uL
HGB	L	2.6	*	g/dL
HCT	L	8.0	*	%
MCV		87.8	*	fL
MCH		28.4	*	pg
MCHC		32.3	*	g/dL
CHCM		35.3	*	g/dL
CH		30.9	*	pg
RDW		13.0	*	%
HDW		2.94	*	g/dL
PLT	L	38		x10^3 cells/uL
MPV	H	16.3		fL

Routine WBC Differential

	%		#	
WBC		L	0.63	x10^3 cells/uL
Neut	54.4	L	0.34	x10^3 cells/uL
Lymph	32.1	L	0.20	x10^3 cells/uL
Mono	5.2		0.03	x10^3 cells/uL
Eos	4.5		0.03	x10^3 cells/uL
Baso	0.7		0.00	x10^3 cells/uL
LUC	3.2		0.02	x10^3 cells/uL
MPXI			5.6	
WBCP			0.70	x10^3 cells/uL

Morphology Flags

MICRO	
MACRO	
HYPO	
HYPER	
ANISO	
HC VAR	
LEFT SHIFT	+
BLASTS	++
ATYPS	
NRBC	
IG	++
LARGE PLT	+++
PLT CLUMPS	
MPO DEF	
RBC FRAG	
RBC Ghosts	

Additional Routine Parameters

%Blast Suspect	7.4	
%Hyper	2.7	
%Hypo	0.6	
%Macro	0.4	
%Micro	0.6	
RBC Fragments	0.00	x10^3 cells/uL
RBC Ghosts	0.00	x10^3 cells/uL
Neut X		
Neut Y		
MNx	14.5	
MNy	11.5	
MNN	48.3	
%NMN	50.6	
Cellular HGB	2.8	g/dL

Sample/System Flags

B-NV	U
CHC/MCHC	CHOM HCT HD2/V HGB MCH MCHC MCV RBC RDW CH CHDW
RTC-L	CHOMg CHCMr Chg CHr MCVg MCVr RDWg RDWr #RETIC %RETIC CHDWg CHDWv

HEADER

Aspiration Date/Time	09/02/2016 10:37:44 A
Sample Type	PATIENT
SID	3
Sample Selectivity	CBC/DifF/RETIC
Age & Sex	
Instrument Number	Advia 120
Sequence	38
Species	Human

FOR LABORATORY USE ONLY

Morphology Flags

MICRO	
MACRO	
HYPO	
HYPER	
ANISO	
HC VAR	
LEFT SHIFT	+
BLASTS	+
ATYPS	++
NRBC	
IG	+++
LARGE PLT	+++
PLT CLUMPS	
MPO DEF	
RBC FRAG	
RBC Ghosts	

Routine Retic

	%	#	
Retic	1.77	23.3	x10⁹ cells/L
Chr		H 32.9	pg
CHm		30.4	pg

Routine CBC

WBC	L	0.90	x10³ cells/µL
RBC	L	1.92	x10⁶ cells/µL
HGB	L	3.9	g/dL
HCT	L	11.7	%
MCV		88.9	fL
MCH		29.4	pg
MCHC		33.0	g/dL
CHCM		34.8	g/dL
CH		30.9	pg
RDW		12.9	%
HDW		2.66	g/dL
PLT	L	39	x10³ cells/µL
MPV	H	15.6	fL

Routine WBC Differential

	%		#	
WBC		L	0.90	x10³ cells/µL
Neut	61.6	L	0.56	x10³ cells/µL
Lymph	19.4	L	0.17	x10³ cells/µL
Mono	6.3	L	0.06	x10³ cells/µL
Eos	2.3		0.02	x10³ cells/µL
Baso	0.9		0.01	x10³ cells/µL
LUC	9.5	H	0.09	x10³ cells/µL
LI				
MPXI	5.8			
WBCP	1.05			x10³ cells/µL

Sample/System Flags

B-NV LI
PX-NV #LUC %LUC #LYMPH %LYMPH WBCP #NEUT %NEUT #MONO
%MONO #EOS %EOS %NEUTu #NEUTu %LYMPHu #LYMPHu
%MONOu #MONOu %EOSu #EOSu %LUCu #LUCu

Additional Routine Parameters

%Blast Suspect	4.8	
%Hyper	1.8	
%hypo	0.7	
%Macro	0.5	
%Micro	0.5	
RBC Fragments	0.00	x10⁶ cells/µL
RBC Ghosts	0.00	x10⁴ cells/µL
Neut X	64.8	
Neut Y	75.9	
MNx	14.0	
MNy	12.5	
%MN	55.0	
%PMN	44.0	
Cellular HGB	4.1	g/dL

Plot labels: Perox, RBC V/HC, Baso, Retic Scatter Absorption, Perox Rate, Baso Rate, RBC Rate, Platelet X, Retic Rate, HGB Trans

HEADER

Aspiration Date/Time	09/02/2016 10:38:45 A
Sample Type	PATIENT
SID	
Sample Selectivity	CBC/DIFF/RETIC
Age & Sex	
Instrument Number	Advia 120
Sequence	39
Species	Human

FOR LABORATORY USE ONLY

Morphology / flags

MICRO	
MACRO	
HYPO	
HYPER	
ANISO	
HC VAR	
LEFT Shift Y	*
BLASTS	++
ATYPS	
NRBC	
IG	+++
LARGE PLT	+++
PLT CLUMPS	
MPO DEF	
RBC FRAG	
RBC Ghosts	

Routine Retic

	%	#	
Retic	1.69	29.2	x10⁹ cells/L
Chr		H 32.3	pg
C-Hm		30.5	pg

Routine CBC

		#	
WBC	L	1.17	x10³ cells/µL
RBC	L	1.72	x10⁶ cells/µL
HGB	L	5.0	g/dL
HCT	L	15.4	%
MCV		89.5	fL
MCH		29.1	pg
MCHC	L	32.6	g/dL
CHCM		34.5	g/dL
CH		30.8	pg
RDW		12.9	%
HDW		2.56	g/dL
PLT	L	37	x10³ cells/µL
MPV	H	16.9	fL

Routine WBC Differential

	%		#	
WBC				x10³ cells/µL
Neut	53.9	L	0.63	x10³ cells/µL
Lymph	31.5	L	0.37	x10³ cells/µL
Mono	6.7	L	0.08	x10³ cells/µL
Eos	3.4		0.04	x10³ cells/µL
Baso	0.9		0.01	x10³ cells/µL
LUC	3.6		0.04	x10³ cells/µL
LI			5.4	
MPXI				
WBCP			1.24	x10³ cells/µL

Additional Routine Parameters

%Blast Susped	6.8	
%Hyper	1.5	
%Hypo	0.9	
%Macro	0.5	
%Micro	0.5	
RBC Fragments	0.00	x10⁶ cells/µL
RBC Ghosts	0.00	x10⁶ cells/µL
Neut X	68.6	
Neut Y	70.1	
MNx	13.5	
MNy	12.5	
%MN	52.7	
%PMN	46.2	
Cellular HGB	5.3	g/dL
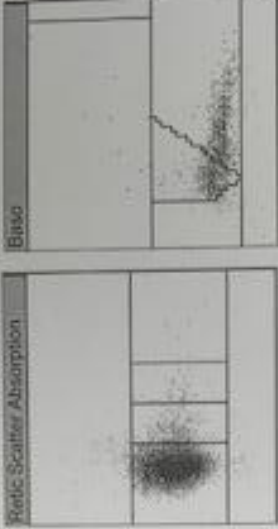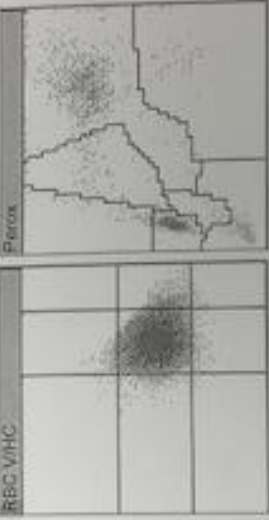
Sample/System Flags

B-NV   LI

CHCM/CE CHCM HCT HDW HGB MCH MCHC MCV RBC RDW CH CHDW

Perox

RBC V/HC

Baso

Retic Scatter Absorption

Baso Rate

Perox Rate

Retic Rate

RBC Rate

Platelet X

HGB Trans

Perox | **Baso** | **RBC V/HC** | **Retic Scatter Absorption**

Perox Rate | **Baso Rate** | **RBC Rate** | **Retic Rate** | **HGB Trans.** | **Platelet X**

HEADER

Aspiration Date/Time	09/02/2016 10:40:04 A
Sample Type	PATIENT
SID	
Sample Selectivity	CBC/DIFF/RETIC
Age & Sex	
Instrument Number	Advia 120
Sequence	46
Species	Human

FOR LABORATORY USE ONLY

Routine Retic

	%	#	
Retic	1.87	65.0	x10^9 cells/L
CHr		H 32.6	pg
CHm		30.3	pg

Routine CBC

WBC	L 2.36	x10^3 cells/µL	
RBC	L 3.47	x10^6 cells/µL	
HGB	L 10.4	g/dL	
HCT	L 32.5	%	
MCV	93.5	fl	
MCH	30.0	pg	
MCHC	L 32.1	g/dL	
CHCM	L 32.5	g/dL	
CH	30.3	pg	
RDW	12.8	%	
HDW	2.67	g/dL	
PLT	L 22	x10^3 cells/µL	
MPV	10.5	fl	

Routine WBC Differential

	%	#	
WBC		L 2.36	x10^3 cells/µL
Neut	53.5	L 1.27	x10^3 cells/µL
Lymph	31.2	L 0.74	x10^3 cells/µL
Mono	6.7	L 0.16	x10^3 cells/µL
Eos	3.3	0.08	x10^3 cells/µL
Baso	H 2.4	0.06	x10^3 cells/µL
LUC	2.9	0.07	x10^3 cells/µL
LI		L 1.74 *	
MPXI	5.6		
WBCP		2.54	x10^3 cells/µL

Morphology Flags

MICRO	
MACRO	
HYPO	
HYPER	
ANISO	
HC VAR	
LEFT SHIFT	++
BLASTS	
ATYPS	
NRBC	
IG	+++
LARGE PLT	
PLT CLUMPS	
MPO DEF	
RBC FRAG	
RBC Ghosts	

Sample/System Flags

B-NV LI

Additional Routine Parameters

%Blast Suspect	4.4	
%Hyper	0.2	
%Hypo	3.4	
%Macro	1.5	
%Micro	0.2	
RBC Fragments	0.00	x10^6 cells/µL
RBC Ghosts	0.01	x10^6 cells/µL
Neut X	64.6	
Neut Y	73.3	
MNx	13.0	
MNy	12.5	
%MN	56.5	
%PMN	41.1	
Cellular HGB	10.6	g/dL

HEADER
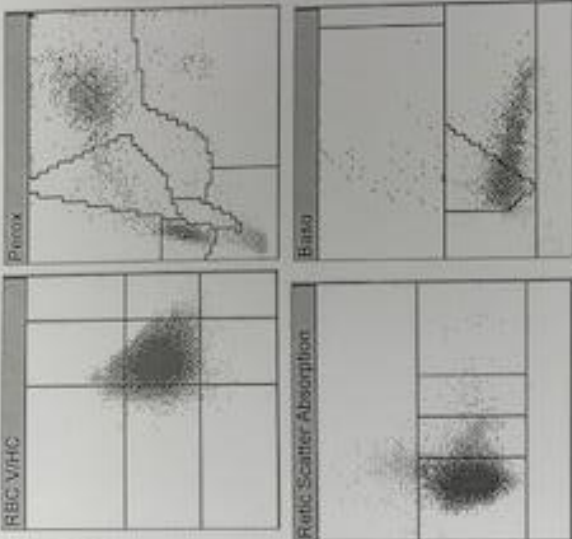
Aspiration Date/Time	09/02/2016 10:41:12 A
Sample Type	PATIENT
SID	6
Sample Selectivity	CBC/DIFF/RETIC
Instrument Number	Advia 120
Sequence	41
Species	Human

Age & Sex

FOR LABORATORY USE ONLY

Routine Retic

Retic		1.43	%
Chr		32.6	pg
Chcm		30.4	pg
#		100.6	x10⁴ cells/µL

Routine CBC

WBC	L	4.61	x10³ cells/µL
RBC	H	7.02	x10⁶ cells/µL
HGB	H	20.9	g/dL
HCT	H	67.0	%
MCV		95.4	fL
MCH		29.8	pg
MCHC	L	31.2	g/dL
CHCM	L	31.9	g/dL
CH		30.3	pg
RDW		13.1	%
HDW		2.83	g/dL
PLT	L	26	x10³ cells/µL
MPV		10.8	fL

Routine WBC Differential

		%	#	
WBC	L		4.61	x10³ cells/µL
Neut		52.4	2.52	x10³ cells/µL
Lymph		34.6	1.68	x10³ cells/µL
Mono		6.3	0.30	x10³ cells/µL
Eos		3.2	0.15	x10³ cells/µL
Baso	H	1.7	0.08	x10³ cells/µL
LUC		1.7	0.08	x10³ cells/µL
MPXI		2.04	*	
WBCP		-0.9	4.63	x10⁴ cells/µL

Morphology Flags

MACRO	
MICRO	
HYPO	*
HYPER	
ANISO	
MICRO	
RC VAR	
LEFT SHIFT	*
BLASTS	
ATYPS	
NRBC	
IG	+++
LARGE PLT	
PLT CLUMPS	
MPO DEF	
RBC FRAG	
RBC Ghosts	

Sample/System Flags

B-NV U

Additional Routine Parameters

%Blast Suspect	2.8	
%Hyper	0.1	
%Hypo	5.8	
%Macro	2.5	
%Micro	0.2	
RBC Fragments	0.00	x10⁴ cells/µL
RBC Ghosts	0.01	x10⁴ cells/µL
Neut X	61.2	
Neut Y	74.1	
MNv	15.9	
MNy	13.5	
%MN	62.8	
%PMN	35.1	
Cellular HGB	21.3	g/dL
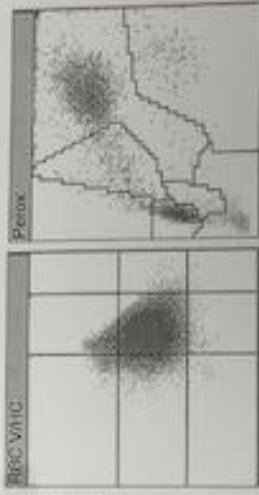
#6

HEADER

Aspiration Date/Time	09/02/2016 10:42:41.A
Sample Type	PATIENT
SID	7
Sample Selectivity	CBC/DIFF/RETIC
Age & Sex	
Instrument Number	Advia 120
Sequence	42
Species	Human

FOR LABORATORY USE ONLY

Routine Retic

Retic		1.44	x10^6 cells/L
CHr		H	32.5	pg
CHm			30.4	pg

Routine CBC

WBC		5.28	x10^3 cells/µL
RBC	H	7.64	x10^6 cells/µL
HGB	H	23.0	g/dL
HCT	H	75.0	%
MCV		95.5	fL
MCH		30.1	pg
MCHC	L	31.5	g/dL
CHCM	L	31.7	g/dL
CH		30.2	pg
RDW		13.0	%
HDW		2.63	g/dL
PLT	L	28	x10^3 cells/µL
MPV		9.5	fL

Routine WBC Differential

		%	#	
WBC			5.28	x10^3 cells/µL
Neut		54.3	2.87	x10^3 cells/µL
Lymph		29.9	1.58	x10^3 cells/µL
Mono		6.7	0.35	x10^3 cells/µL
Eos		2.8	0.15	x10^3 cells/µL
Baso	H	4.2	0.22	x10^3 cells/µL
LUC		2.3	0.12	x10^3 cells/µL
LI	L	1.38*		
MPXI		-2.6		
WBCP			5.34	x10^3 cells/µL

Morphology Flags

MICRO	
MACRO	+
HYPO	+
HYPER	
ANISO	
HC VAR	
LEFT SHIFT	***
BLASTS	
ATYPS	
NRBC	
IG	***
LARGE PLT	
PLT CLUMPS	
MPO DEF	
RBC FRAG	
RBC Ghosts	

System/System Flags

(I=IV/ U)

Additional Routine Parameters

%Blast Suspect	2.5	
%Hyper	0.1	
%Hypo	6.5	
%Macro	2.5	
%Micro	0.2	
RBC Fragments	0.00	x10^6 cells/µL
RBC Ghosts	0.01	x10^6 cells/µL
Neut X	60.1	
Neut Y	74.3	
MNx	14.0	
MNy	13.5	
%MN	56.6	
%PMN	38.8	
Cellular HGB	23.2	g/dL

204

Sample 1

Total

Smithers Avanza

Aspiration Date/Time	10/26/2017 09:26:56 A
Sample Type	PATIENT
SID	1
Sample Selectivity	CBC/DIFF
Age & Sex	U
Instrument Number	Advia 120
Sequence	86
Species	Human

FOR LABORATORY USE ONLY

Perox

Baso

RBC V/HC

Platelet X

Perox Rate

Baso Rate

RBC Rate

HGB Trans

Routine CBC

WBC	L	0.05	x10³ cells/µL
RBC	L	0.85	x10⁶ cells/µL
HGB	L	2.7	g/dL
HCT	L	7.4	%
MCV		87.4	fl
MCH	H	31.8	pg
MCHC		36.4	g/dL
CHCM		36.8	g/dL
CH		32.0	pg
RDW	H	20.9	%
HDW	H	3.30	g/dL
PLT	L	31	x10³ cells/µL
MPV		10.3	fl

Morphology Flags

MICRO	
MACRO	+
HYPO	
HYPER	++
ANISO	++
HC VAR	
LEFT SHIFT	
BLASTS	++
ATYPS	
NRBC	
IG	
LARGE PLT	
PLT CLUMPS	
MPO DEF	
RBC FRAG	
RBC Ghosts	

Additional Routine Parameters

%Blast Suspect	4.5	
%Hyper	8.2	
%Hypo	0.6	
%Macro	3.4	
%Micro	2.1	
RBC Fragments	0.00	x10⁶ cells/µL
RBC Ghosts	0.01	x10⁶ cells/µL
Neut X		
Neut Y		
MNx	13.0	
MNy	6.0	
%MN	18.2	
%PMN	68.2	
Cellular HGB	2.7	g/dL

Routine WBC Differential

		%		#	
WBC			L	0.05	x10³ cells/µL
Neut	L	51.3	L	0.03	x10³ cells/µL
Lymph		23.1	L	0.01	x10³ cells/µL
Mono	H	17.9	L	0.01	x10³ cells/µL
Eos		5.1		0.00	x10³ cells/µL
Baso	H	6.8		0.00	x10³ cells/µL
LUC		2.6		0.00	x10³ cells/µL
LI			L	1.82	
MPXI			H	12.2	
WBCP				0.04	x10³ cells/µL

Sample/System Flags

B-NO	#BASO %Baso WBC WBCB WBCu %BASOu #BASOu.
B-SUSP	#BASO %Baso #LUC %LUC #LYMPH %LYMPH %LYMPHu #LYMPHu %BASOu #BASOu %LUCu #LUCu
PX-NO	#LUC %LUC #LYMPH %LYMPH WBCP #NEUT %NEUT #MONO %MONO #EOS %EOS %NEUTu #NEUTu %LYMPHu #LYMPHu %MONOu #MONOu %EOSu #EOSu #LUCu #LUCu
PLTORN	CHCM HCT HDW MCH MCHC MCV MPV PCT PDW PLT RBC RDW

Sample # 1

Tube 1

Smithers Avanza

Aspiration Date/Time	10/26/2017 09:06:06 A
Sample Type	PATIENT
SID	1
Sample Selectivity	CBC/Diff
Age & Sex	
Instrument Number	Advia 120
Sequence	75
Species	Human
FOR LABORATORY USE ONLY	

Routine CBC

WBC	L	0.07	* x10³ cells/µL
RBC	L	0.82	* x10⁶ cells/µL
HGB	L	2.7	* g/dL
HCT		7.1	* %
MCV	H	87.0	fL
MCH	H	33.0	pg
MCHC	H	37.9	g/dL
CHCM		36.8	g/dL
CH		31.8	pg
RDW	H	21.7	%
HDW	H	3.31	g/dL
PLT	L	36	* x10³ cells/µL
MPV		9.7	* fL

Additional Routine Parameters

%Blast Suspect	1.6	
%Hyper	7.9	
%Hypo	0.9	
%Macro	3.7	
%Micro	2.3	
RBC Fragments	0.00	x10³ cells/µL
RBC Ghosts	0.01	x10³ cells/µL
Neut X		
Neut Y		
MNx	13.5	
MNy	12.5	
%MN	9.5	
%PMN	41.3	
Cellular HGB	2.6	g/dL

Morphology Flags

MICRO	
MACRO	+
HYPO	+
HYPER	++
ANISO	
RC VAR	
LEFT SHIFT	
BLASTS	++
ATYPS	
NRBC	
IG	++
LARGE PLT	
PLT CLUMPS	
MPO DEF	
RBC FRAG	
RBC Ghosts	

Routine WBC Differential

	%		#		
WBC			0.07	* L	x10³ cells/µL
Neut	45.3		0.03	* L	x10³ cells/µL
Lymph	34.0		0.02	* L	x10³ cells/µL
Mono	H 15.1		0.01	* L	x10³ cells/µL
Eos	3.8		0.00	*	x10³ cells/µL
Baso	H 3.2		0.00	*	x10³ cells/µL
LUC	1.9		0.00	*	x10³ cells/µL
U			2.21		
MPXI			L -21.5		
WBCP			0.06	*	x10³ cells/µL

Sample/System Flags

B-NO	#BASO %Baso WBC WRBC WRBCB WRBCu %BASOu #BASOu
B-SUSP	#BASO %Baso #LUC %LUC #LYMPH %LYMPH %LYMPHu #LYMPHu %LYMPHu %BASOu %LUCu #LUCu
PX-NO	#LUC %LUC #LYMPH %LYMPH WBCP #NEUT %NEUT #MONO %MONO #EOS %EOS %NEUTu #NEUTu %LYMPHu #LYMPHu %MONOu #MONOu %EOSu #EOSu %LUCu #LUCu
	PLTOR CHCM HGT HDW MCH MCHC MCV MPV PCT PDW PLT RBC RDW

Perox

Baso

RBC V/HC

Platelet X

Baso Rate

Perox Rate

RBC Rate

HGB Trans

Sample 2   Table 1

Smithers Avanza

Aspiration Date/Time	10/26/2017 09:07:41 A
Sample Type	PATIENT
SID	2
Sample Selectivity	CBC/DIFF
Age & Sex	
Instrument Number	Advia 120
Sequence	76
Species	Human

FOR LABORATORY USE ONLY

Routine CBC

WBC	L	0.06	x10³ cells/µL
RBC	L	1.41	x10⁶ cells/µL
HGB	L	4.8	g/dL
HCT	L	12.4	%
MCV		88.0	fL
MCH	H	33.7	pg
MCHC	H	38.3	g/dL
CHCM		36.2	g/dL
CH		31.7	pg
RDW	H	20.4	%
HDW		3.15	g/dL
PLT	L	33	x10³ cells/µL
MPV		11.0	fL

Routine WBC Differential

		%		#	
WBC			L	0.06	x10³ cells/µL
Neut		47.6	L	0.03	x10³ cells/µL
Lymph		33.3	L	0.02	x10³ cells/µL
Mono		8.3	L	0.01	x10³ cells/µL
Eos	H	9.5		0.01	x10³ cells/µL
Baso	H	3.7		0.00	x10³ cells/µL
LUC		1.2		0.00	x10³ cells/µL
MPXI		2.39			
WBCP		-0.9			
				0.10	x10³ cells/µL

Additional Routine Parameters

%Blast Suspect	1.9	
%Hyper	6.2	
%Hypo	0.6	
%Macro	3.4	
%Micro	1.9	
RBC Fragments	0.00	x10⁶ cells/µL
RBC Ghosts	0.01	x10⁶ cells/µL
Neut X		
Neut Y		
MNx	16.0	
MNy	12.5	
%MN	13.0	
%PMN	75.9	
Cellular HGB	4.5	g/dL

Morphology Flags

MACRO	*
MACRO	
HYPO	+
HYPER	+
ANISO	++
HC VAR	
LEFT SHIFT	
BLASTS	++
ATYPS	
NRBC	
IG	
LARGE PLT	
PLT CLUMPS	
MPO DEF	
RBC FRAG	
RBC Ghosts	

Sample/System Flags

B-SAT	WBCB WBC WBCu
B-SUSP	#BASO %Baso #LUC %LUC #LYMPH %LYMPH %LYMPHu #LYMPHu %BASOu %LUCu #BASOu #LUCu
CHCMCE	CHCM HCT HDW HGB MCH MCHC MCV RBC RDW CH CHDW
WBC-CE	WBC WBCu
PX-NO	#LUC %LUC #LYMPH %LYMPH WBCP #NEUT %NEUT #MONO %MONO #EOS %EOS %NEUTu #NEUTu %LYMPHu #LYMPHu %MONOu #MONOu %EOSu #EOSu %LUCu #LUCu
PLTORN	CHCM HCT HDW MCH MCHC MCV MPV PCT PDW PLT RBC RDW

Sample 2

Smithers Avanza

Aspiration Date/Time	10/26/2017 09:25:59 A
Sample Type	PATIENT
SID	2
Sample Selectivity	CBC/DIFF
Age & Sex	U
Instrument Number	Advia 120
Sequence	85
Species	Human

Routine CBC

WBC	L	0.07	x10^3 cells/µL
RBC	L	1.41	x10^6 cells/µL
HGB	L	4.7	g/dL
HCT	L	12.4	%
MCV		88.3	fL
MCH	H	33.7	pg
MCHC	H	38.1	g/dL
CHCM		36.0	g/dL
CH		31.6	pg
RDW	H	19.9	%
HDW		3.08	g/dL
PLT	L	28	x10^3 cells/µL
MPV		10.8	fL

Routine WBC Differential

		%		#	
WBC			L	0.07	x10^3 cells/µL
Neut	L	33.8	L	0.02	x10^3 cells/µL
Lymph	H	51.5	L	0.03	x10^3 cells/µL
Mono		7.4		0.00	x10^3 cells/µL
Eos		4.4		0.00	x10^3 cells/µL
Baso	H	3.3		0.00	x10^3 cells/µL
LUC		2.9		0.00	x10^3 cells/µL
LI		2.46			
MPXI		-7.7			
WBCP				0.08	x10^3 cells/µL

Morphology Flags

MICRO	+
MACRO	
HYPO	+
HYPER	++
ANISO	
HC VAR	
LEFT SHIFT	
BLASTS	
ATYPS	
NRBC	
IG	
LARGE PLT	
PLT CLUMPS	
MPO DEF	+
RBC FRAG	
RBC Ghosts	

Additional Routine Parameters

%Blast Suspect	0.0	
%Hyper	5.5	
%Hypo	0.6	
%Macro	3.2	
%Micro	1.7	
RBC Fragments	0.00	x10^3 cells/µL
RBC Ghosts	0.01	x10^3 cells/µL
Neut X	14.5	
Neut Y		
MNx	14.5	
MNy	12.5	
%MN	15.0	
%PMN	78.3	
Cellular HGB	4.5	g/dL

Perox

Baso

RBC V/HC

Platelet X

Perox Rate

RBC Rate

Baso Rate

HGB Trans

Sample/System Flags

B-NO #BASO %Baso WBC WBCB WBCu %BASOu #BASOu
B-SUSP #BASO %Baso #LUC %LUC #LYMPH %LYMPHu
%LYMPHu %BASOu #BASOu %LUCu #LUCu
CHCMCE CHCM HCT HDW HGB MCH MCHC MCV RBC RDW CH CHDW
MPO-D #LUC %LUC #LYMPH %LYMPH %LYMPHu #NEUT #MONO
%MONO #EOS %EOS %NEUTu #NEUTu %LYMPHu #LYMPH
%MONOu #MONOu %EOSu #EOSu %LUCu #LUCu
PX-NO #LUC %LUC #LYMPH %LYMPH WBCP #NEUT %NEUT #MONO
%MONO #EOS %EOS %NEUTu #NEUTu %LYMPHu #LYMPHu
%MONOu #MONOu %EOSu #EOSu %LUCu %LUCu #LUCu

Sample 3

Tube 1

Smithers Avanza

Aspiration Date/Time	10/26/2017 09:09:15 A
Sample Type	PATIENT
SID	3
Sample Selectivity	CBC/DIFF
Age & Sex	U
Instrument Number	Advia 120
Sequence	77
Species	Human
	FOR LABORATORY USE ONLY

Routine CBC

WBC	L	0.95	x10³ cells/µL
RBC	L	3.71	x10⁶ cells/µL
HGB	L	11.8	g/dL
HCT	L	34.1	%
MCV		91.8	fl
MCH	H	31.9	pg
MCHC		34.7	g/dL
CHCM		33.4	g/dL
CH		30.5	pg
RDW	H	17.6	%
HDW		2.84	g/dL
PLT	L	25	x10³ cells/µL
MPV		9.7	fl

Routine WBC Differential

	%		#	
WBC		L	0.95	x10³ cells/µL
Neut	42.5	L	0.40	x10³ cells/µL
Lymph	39.1	L	0.37	x10³ cells/µL
Mono	H 10.7	L	0.10	x10³ cells/µL
Eos	3.3		0.03	x10³ cells/µL
Baso	1.1		0.01	x10³ cells/µL
LUC	3.3		0.03	x10³ cells/µL
LI			2.86	
MPXI			-3.2	
WBCP			0.93	x10³ cells/µL

Additional Routine Parameters

%Blast Suspect	2.9
%Hyper	1.3
%Hypo	2.0
%Macro	3.4
%Micro	1.0
RBC Fragments	0.00 x10⁶ cells/µL
RBC Ghosts	0.02 x10⁶ cells/µL
Neut X	56.1
Neut Y	68.9
MNx	14.5
MNy	6.0
%MN	38.9
%PMN	59.6
Cellular HGB	11.4 g/dL

Morphology Flags

MICRO	
MACRO	+
HYPO	
HYPER	+
HC VAR	
LEFT SHIFT	
BLASTS	
ATYPS	
NRBC	
IG	
LARGE PLT	
PLT CLUMPS	
MPO DEF	
RBC FRAG	
RBC Ghosts	

Perox

Baso

RBC V/HC

Platelet.X

Baso Rate

Perox Rate

RBC Rate

HGB Trans

Sample/System Flags

Sample 3

Smithers Avanza

Aspiration Date/Time	10/26/2017 09:28:55 A
Sample Type	PATIENT
SID	3
Sample Selectivity	CBC/DIFF
Age & Sex	U
Instrument Number	Advia 120
Sequence	87
Species	Human

Routine CBC

WBC	L	0.84	x10³ cells/µL
RBC	L	3.69	x10⁶ cells/µL
HGB	L	11.9	g/dL
HCT	L	33.9	%
MCV		91.8	fL
MCH	H	32.2	pg
MCHC		35.1	g/dL
CHCM		33.7	g/dL
CH		30.8	pg
RDW	H	17.6	%
HDW		2.87	g/dL
PLT	L	18	x10³ cells/µL
MPV		10.4	fL
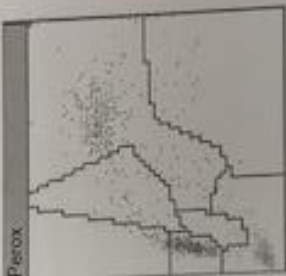
Routine WBC Differential

	%		#		
WBC			L	0.84	x10³ cells/µL
Neut	L	34.9	L	0.29	x10³ cells/µL
Lymph	H	50.0	L	0.42	x10³ cells/µL
Mono		5.7	L	0.05	x10³ cells/µL
Eos		3.4		0.03	x10³ cells/µL
Baso		0.4		0.00	x10³ cells/µL
LUC	H	5.7		0.05	x10³ cells/µL
LI		1.96			
MPXI		-7.1			
WBCP		0.75			x10³ cells/µL

Additional Routine Parameters

%Blast Suspect	2.7	
%Hyper	1.5	
%Hypo	1.7	
%Macro	3.4	
%Micro	1.0	
RBC Fragments	0.00	x10⁶ cells/µL
RBC Ghosts	0.02	x10⁶ cells/µL
Neut X	59.9	
Neut Y	70.3	
MNx	15.5	
MNy	14.5	
%MN	38.9	
%PMN	60.1	
Cellular HGB	11.4	g/dL

Morphology Flags

MICRO	
MACRO	*
HYPO	
HYPER	*
ANISO	*
HC VAR	
LEFT SHIFT	
BLASTS	*
ATYPS	*
IG	
NRBC	
LARGE PLT	
PLT CLUMPS	
MPO DEF	
RBC FRAG	
RBC Ghosts	

Sample/System Flags

PX-NV #LUC %LUC #LYMPH %LYMPH WBCP #NEUT %NEUT #MONO %MONO #EOS %EOS #NEUTu %NEUTu #LYMPHu %LYMPHu %MONOu #MONOu %EOSu #EOSu %LUCu #LUCu

Perox

Baso

Tube 2

RBC V/HC

Platelet X

Perox Rate

Baso Rate

RBC Rate

HGB Trans

Sample 4

Tube 1

Smithers Avanta

Aspiration Date/Time	10/26/2017 09:10:18 A
Sample Type	PATIENT
SID	4
Sample Selectivity	CBC/DIFF
Age & Sex	U
Instrument Number	Advia 120
Sequence	78
Species	Human

FOR LABORATORY USE ONLY

Routine CBC

WBC	L	3.36	x10³ cells/µL
RBC	H	7.60	x10⁶ cells/µL
HGB	H	23.5	g/dL
HCT	H	72.8	%
MCV		95.7	fL
MCH		30.8	pg
MCHC	L	32.2	g/dL
CHCM	L	30.8	g/dL
CH		29.5	pg
RDW	H	15.0	%
HDW		2.42	g/dL
PLT	L	32	x10³ cells/µL
MPV		10.6	fL

Routine WBC Differential

	%		#		
WBC			L	3.36	x10³ cells/µL
Neut	42.1	*L		1.41	*L	x10³ cells/µL
Lymph	41.7	*		1.40	*	x10³ cells/µL
Mono	H	9.5	*	0.32	*	x10³ cells/µL
Eos		3.0	*	0.10	*	x10³ cells/µL
Baso	H	1.8	*	0.06	*	x10³ cells/µL
LUC		2.0	*	0.07	*	x10³ cells/µL
LI				2.44	*	
MPXI				-7.4		
WBCP				3.34	*	x10³ cells/µL

Additional Routine Parameters

%Blast Suspect	2.1	
%Hyper	0.2	
%Hypo	10.2	
%Macro	3.9	
%Micro	0.7	
RBC Fragments	0.06	x10⁶ cells/µL
RBC Ghosts	0.03	x10⁶ cells/µL
Neut X	58.9	
Neut Y	71.5	
MNx	17.6	
MNy	14.8	
%MN	34.6	
%PMN	63.2	
Cellular HGB	22.4	g/dL

Morphology Flags

MICRO	+
MACRO	++
HYPO	
HYPER	
ANISO	
HC VAR	
LEFT SHIFT	+
BLASTS	
ATYPS	
NRBC	+
IG	
LARGE PLT	
PLT CLUMPS	+
MPO DEF	
RBC FRAG	
RBC Ghosts	

Sample/System Flags

B-NV   U
N-RBC   #BASO %Baso #LUC %LUC #LYMPH %LYMPH WBC WBCB
            WBCu WBCP #NEUT %NEUT #MONO %MONO #EOS %EOS
            %hRBC #NRBC %NEUTu #NEUTu %LYMPHu #LYMPHu
            %MONOu #MONOu %EOSu #EOSu %BASOu #BASOu %LUCu
            #LUCu

PLT-CL MPV PCT PDW PLT WBCP

Sample 4

Sample 5

Tube 1

Smithers Avanza

Aspiration Date/Time	10/26/2017 09:22:36 A
Sample Type	PATIENT
SID	5
Sample Selectivity	CBC/DIFF
Age & Sex	
Instrument Number	Advia 120
Sequence	83
Species	Human
FOR LABORATORY USE ONLY	

Routine CBC

WBC	L	3.62	x10³ cells/µL
RBC	H	8.13	x10⁶ cells/µL
HGB	H	24.6	g/dL
HCT	H	78.8	%
MCV		96.9	fL
MCH		30.2	pg
MCHC	L	31.2	g/dL
CHCM	L	30.4	g/dL
CH		29.3	pg
RDW	H	15.0	%
HDW	H	2.37	g/dL
PLT	L	54	x10³ cells/µL
MPV		9.6	fL

Routine WBC Differential

		%			#	
WBC			L	3.62		x10³ cells/µL
Neut		41.2	L	1.49		x10³ cells/µL
Lymph		43.1		1.56		x10³ cells/µL
Mono	H	10.0		0.36		x10³ cells/µL
Eos		3.3		0.12		x10³ cells/µL
Baso	H	8.8		0.32		x10³ cells/µL
LUC		2.4	H	0.09		x10³ cells/µL
LI				2.11		
MPXI				-9.5		
WBCP				3.41		x10³ cells/µL

Additional Routine Parameters

%Blast Suspect	6.1	
%Hyper	0.1	
%Hypo	13.1	
%Macro	4.7	
%Micro	0.6	
RBC Fragments	0.01	x10⁶ cells/µL
RBC Ghosts	0.04	x10⁶ cells/µL
Neut X	50.5	
Neut Y	70.7	
MNx	2.1	
MNy	3.7	
%MN	29.0	
%PMN	60.4	
Cellular HGB	24.0	g/dL

Morphology Flags

MICRO	
MACRO	+
HYPO	+++
HYPER	
ANISO	
HC VAR	
LEFT SHIFT	+
BLASTS	**
ATYPS	
NRBC	+
IG	
LARGE PLT	
PLT CLUMPS	
MPO DEF	
RBC FRAG	
RBC Ghosts	

Sample/System Flags

B-NV	LI
B-SUSP	#BASO %Baso #LUC %LUC #LYMPH %LYMPH %LYMPHu #LYMPHu %BASOu #BASOu %LUCu #LUCu
N-RBC	#BASO %Baso #LUC %LUC #LYMPH %LYMPH WBC WBCB WBCu WBCP #NEUT %NEUT #MONO %MONO #EOS %EOS %NRBC #NRBC %NEUTu #NEUTu %LYMPHu #LYMPHu %MONOu #MONOu %EOSu #EOSu %BASOu #BASOu %LUCu #LUCu
NRPXNV	#BASO %Baso #LUC %LUC #LYMPH %LYMPH WBC #NEUT %NEUT #MONO %MONO #EOS %EOS %NRBC #NRBC
NR-LPD	#BASO %Baso #LUC %LUC #LYMPH %LYMPH WBC #NEUT #NEUT %MONO #MONO #EOS %EOS %NRBC #NRBC

Sample 5

Tube 2

Smithers Avanza

Aspiration Date/Time	10/25/2017 09:34:20 A
Sample Type	PATIENT
SID	5
Sample Selectivity	CBC/DIFF
Age & Sex	U
Instrument Number	Advia 120
Sequence	91
Species	Human

FOR LABORATORY USE ONLY

Routine CBC

WBC	L	4.05	x10³ cells/µL
RBC	H	7.99	x10⁶ cells/µL
HGB	H	24.5	g/dL
HCT	H	77.6	%
MCV		97.0	fL
MCH		30.7	pg
MCHC	L	31.6	g/dL
CHCM	L	30.3	g/dL
CH		29.3	pg
RDW	H	15.0	%
HDW		2.36	g/dL
PLT	L	69	x10³ cells/µL
MPV		9.7	fL

Morphology Flags

MICRO	
MACRO	+
HYPO	+++
HYPER	
ANISO	
HC VAR	
LEFT SHIFT	+
BLASTS	
ATYPS	++
NRBC	+
IG	
LARGE PLT	
PLT CLUMPS	
MPO DEF	
RBC FRAG	
RBC Ghosts	

Additional Routine Parameters

%Blast Suspect	6.7	
%Hyper	0.1	
%Hypo	13.8	
%Macro	4.8	
%Micro	0.6	
RBC Fragments	0.01	x10⁶ cells/µL
RBC Ghosts	0.04	x10⁶ cells/µL
Neut X	56.2	
Neut Y	69.9	
MNx	17.8	
MNy	14.3	
%PMN	45.6	
%PMN	48.7	
Cellular HGB	23.5	g/dL

Routine WBC Differential

	%		#	
WBC			4.05	x10³ cells/µL
Neut	L	34.5	L 1.40	x10³ cells/µL
Lymph		44.5	1.80	x10³ cells/µL
Mono	H	12.5	0.51	x10³ cells/µL
Eos		5.9	0.24	x10³ cells/µL
Baso	H	3.4	0.14	x10³ cells/µL
LUC		2.6	0.11	x10³ cells/µL
LI			2.19	
MPXI			-8.3	
WBCP			3.85	x10³ cells/µL

Sample/System Flags

B-NV	U
B-SUSP	#BASO %Baso #LUC %LLUC #LYMPH %LYMPH %LLYMPH #LYMPHu #LYMPHu %BASOu #BASOu %LUCu #LUCu
N-RBC	#BASO %Baso #LUC %LLUC #LYMPH %LYMPH WBC %BCB WBCu WBCP #NRBC #NEUTu #NEUTu %LYMPHu #LYMPHu %MNRBC #MONOu #MONOu %EOSu #EOSu %BASOu %BASOu #LUCu #LUCu
NR-LPD	#BASO %Baso #LUC %LLUC #LYMPH %LYMPH WBC #NEUT %NEUT #MONO %MONO #EOS %EOS %NRBC #NRBC

Porox

Baso

RBC V/HC

Platelet X

Perox Rate

RBC Rate

Baso Rate

HGB Trans

Certificates of Analysis

BioreclamationIVT
The complete resource for all biologicals

Certificate of Analysis

PRODUCT: HUMAN SERUM	
CATALOG # HMSRM	
ANTICOAGULANT:	
NONE LOT#: BRH1399238	
STORAGE TEMPERATURE: -20 ^{0}C OR COLDER	

COA DATE: 19OCT2017

PURCHASE   VISA
ORDER:

PROJECT   1268023
NUMBER:

VOLUME   100 ML
SHIPPED:

PRESENTATION: 1 LOT OF 100 ML (1 X 100 ML) OF HUMAN SERUM RECOVERED FROM WHOLE
                             BLOOD DONATIONS

FILTRATION: NONE

EXPIRATION: 31OCT2019

BIOHAZARD INFO: THIS MATERIAL SHOULD BE HANDLED AS IF CAPABLE

OF TRANSMITTING INFECTIOUS AGENTS. PLEASE USE UNIVERSAL PRECAUTIONS.

NO TEST METHOD CAN PROVIDE

TOTAL ASSURANCE THAT HEPATITIS B VIRUS, HEPATITIS C VIRUS, HUMAN

IMMUNODEFICIENCY VIRUS, OR OTHER INFECI'IOUS AGENTS ARE ABSENT. THUS,

ALL BIOLOGICAL PRODUCI'S THAT WE

PROVIDE SHOULD BE HANDLED AT THE BIO-SAFETY LEVEL 2 AS RECOMMENDED BY THE CDC/NIH MANUAL "BIOSAFETY IN MICROBIOLOGICAL

216

AND BIOMEDICAL LABORATORIES, FROM POTENTIALLY INFECTIOUS HUMAN SERUM OR BLOOD SPECIMENS"

THE MATERIAL LISTED ON THIS CERTIFICATE OF ANALYSIS HAS BEEN

TESTED IN ACCORDANCE WITH FDA REGULATIONS AND FOUND TO BE

NEGATIVE FOR HIV ^{1}/2 AB AND HCV AB AND NON-REACTIVE FOR HBSAG, HIV-I

RNA, HCV RNA, HBV DNA AND STS.

THIS PRODUCT IS BEING SOLD FOR RESEARCH AND OR MANUFACTURING PURPOSES ONLY. IT IS NOT TO
BE USED IN HUMANS OR ANIMALS AND FURTHER MANUFACTURING THA T WILL RESULT IN A FINISHED PRODUCT THAT CONTAINS VIABLE LEUKOCYTES IS' PROHIBITED. FOR IN VITRO USE ONLY. THE USER
ASSUMES ALL RESPONSIBILITY FOR ITS USAGE AND DISPOSAL. IN ACCORDANCE WITH ALL REGULA TIONS.

PRODUCT: HUMAN RED BLOOD CELLS CATALOG # HMRBCNAHP ANTICOAGULANT: SODIUM HEPARIN
LOT#: BRH1399239

STORAGE TEMPERATURE: 4^0C

COA DATE: 190CT2017
PURCHASE ORDER: VISA
PROJECT NUMBER: 1268023
VOLUME SHIPPED: 75 ML
PRESENTATION: 1 LOT OF 75 ML (1 X 75 ML) OF
                                              HUMAN
                                              RED BLOOD CELLS
EXPIRATION: 19NOV2017
BIOHAZARD INFO: THIS MATERIAL SHOULD BE HANDLED AS IF CAPABLE

OF TRANSMITTING INFECTIOUS AGENTS. PLEASE USE UNIVERSAL PRECAUTIONS.

NO TEST METHOD CAN PROVIDE

TOTAL ASSURANCE THAT HEPATITIS B VIRUS, HEPATITIS C VIRUS, HUMAN

IMMUNODEFICIENCY VIRUS, OR OTHER INFECTIOUS AGENTS ARE ABSENT.

THUS, ALL BIOLOGICAL PRODUCTS THAT WE

PROVIDE SHOULD BE HANDLED AT THE BIO-SAFETY LEVEL 2 AS

RECOMMENDED BY THE CDC/NIH MANUAL "BIOSAFETY IN MICROBIOLOGICAL

AND BIOMEDICAL LABORATORIES, FROM POTENTIALLY INFECTIOUS HUMAN

SERUM OR BLOOD SPECIMENS"

THE MATERIAL LISTED ON THIS CERTIFICATE OF ANALYSIS HAS BEEN

TESTED IN ACCORDANCE WITH FDA REGULATIONS AND FOUND TO BE

NEGATIVE FOR HIV AB AND HCV AB AND NON-REACTIVE FOR HBSAG, HIV-I RNA,

HCV RNA, HBV DNA, "'NV RNA, ANTI-T. CRUZI, ZIKA VIRUS RNA AND STS.

THIS PRODUCT IS' BEING SOLD FOR RESEARCH AND OR MANUFACTURING
PURPOSES ONLY. IT IS NOT TO
BE USED IN HUMANS OR ANIMALS AND FURTHER MANUFACTURING THA T
WILL RESUL T IN A FINISHED PRODUCT THAT CONTAINS VIABLE LEUKOCYTES IS
PROHIBITED. FOR IN VITRO USE ONLY. THE USER
ASSUMES ALL RESPONSIBILITY FOR ITS USAGE AND DISPOSAL IN
ACCORDANCE WITH ALL REGULATIONS.

Certificate of Analysis

6

PRODUCT: HUMAN WHOLE BLOOD
CATALOG # HMWBNAHP
ANTICOAGULANT: SODIUM HEPARIN
LOT#: BRH1399237
STORAGE TEMPERATURE: 4 ^{0}C

COA DATE: 19OCT2017
PURCHASE ORDER: VISA
PROJECT NUMBER: 1268023
VOLUME SHIPPED: 100 ML
PRESENTATION: 1 LOT OF 100 ML (1 X 100 ML) OF HUMAN
                       WHOLE BLOOD
EXPIRATION: 19NOV2017
BIOHAZARD INFO: THIS MATERIAL SHOULD BE HANDLED AS IF CAPABLE

OF TRANSMITTING INFECTIOUS AGENTS. PLEASE USE UNIVERSAL PRECAUTIONS.

NO TEST METHOD CAN PROVIDE

TOTAL ASSURANCE THAT HEPATITIS B VIRUS, HEPATITIS C VIRUS, HUMAN

IMMUNODEFICIENCY VIRUS, OR OTHER INFECTIOUS AGENTS ARE ABSENT.

THUS, ALL BIOLOGICAL PRODUCTS THAT WE

PROVIDE SHOULD BE HANDLED AT THE BIO-SAFETY LEVEL 2 AS

RECOMMENDED BY THE CDC/NIH MANUAL "BIOSAFETY IN MICROBIOLOGICAL

AND BIOMEDICAL LABORATORIES, FROM POTENTIALLY INFECTIOUS HUMAN

SERUM OR BLOOD SPECIMENS"

THE MATERIAL LISTED ON THIS CERTIFICATE OF ANALYSIS HAS BEEN

TESTED IN ACCORDANCE WITH FDA REGULATIONS AND FOUND TO BE

219

NEGATIVE FOR HIV ^{1}/2 AB AND HCV AB AND NON-REACTIVE FOR HBSAG, HIV-I

RNA, HCV RNA, HBV DNA, WNV RNA, ANTI-T. CRUZI, ZIKA VIRUS RNA AND STS.

THIS PRODUCT IS BEING SOLD FOR RESEARCH AND OR MANUFACTURING PURPOSES ONLY. IT IS NOT TO
BE USED IN HUMANS OR ANIMALS AND FURTHER MANUFACTURING THAT WILL RESULT IN A FINISHED PRODUCT THAT CONTAINS VIABLE LEUKOCYTES IS PROHIBITED. FOR IN VITRO USE ONLY. THE USER
ASSUMES ALL RESPONSIBILITY FOR ITS USAGE AND DISPOSAL IN ACCORDANCE WITH ALL REGULATIONS.

```
PRODUCT: HUMAN SERUM
CATALOG # HMSRM
ANTICOAGULANT:
NONE LOT#: BRH1215150
STORAGE TEMPERATURE: -20 $^0$C OR COLDER
```

COA DATE: 31AUG2016

PURCHASE ORDER:

PROJECT NUMBER: 1216074

VOLUME SHIPPED: 25 ML

PRESENTATION: 1 LOT OF 25 ML (1 X 25 ML) OF

HUMAN SERUM RECOVERED FROM WHOLE

BLOOD DONATIONS

FILTRATION: NONE

EXPIRATION: 31AUG2018

BIOHAZARD INFO: THIS MATERIAL SHOULD BE HANDLED AS IF

CAPABLE OF TRANSMITTING INFECTIOUS AGENTS. PLEASE USE

UNIVERSAL PRECAUTIONS. NO TEST METHOD CAN PROVIDE

TOTAL ASSURANCE THAT HEPATITIS B VIRUS, HEPATITIS C VIRUS, HUMAN IMMUNODEFICIENCY VIRUS, OR OTHER INFECTIOUS AGENTS ARE ABSENT. THUS, ALL BIOLOGICAL PRODUCTS THAT WE

PROVIDE SHOULD BE HANDLED AT THE BIO-SAFETY LEVEL 2 AS RECOMMENDED BY THE CDC/NIH MANUAL "BIOSAFETY IN MICROBIOLOGICAL AND BIOMEDICAL LABORATORIES, FROM POTENTIALLY INFECTIOUS HUMAN SERUM OR BLOOD SPECIMENS"

THE MATERIAL LISTED ON THIS CERTIFICATE OF ANALYSIS HAS BEEN TESTED IN ACCORDANCE WITH FDA REGULATIONS AND FOUND TO BE NEGATIVE FOR HIV ^{1}/2 AB AND HCV AB AND NON-REACTIVE FOR HBSAG, HIV-I RNA, HCV RNA, HBV DNA AND STS.

THIS PRODUCT IS BEING SOLD FOR RESEARCH AND OR MANUFACTURING PURPOSES ONLY. IT IS' NOT TO

BE USED IN HUMANS OR ANIMALS AND FURTHER MANUFACTURING THAT WILL RESULT IN A FINISHED PRODUCT THATCONTAINS' VIABLE LEUKOCYTES IS PROHIBITED. FOR IN VITRO USE ONLY. THE USER

221

ACCORDANCE WITH ALL REGULA TIONS.

1   T 516 483   4683 E

rx.4

PRODUCT: HUMAN RED BLOOD CELLS (SODIUM HEPARIN)

BRH1215151 STORAGE TEMPERATURE: 4 ^{0}C

COA DATE: 31AUG2016
PURCHASE ORDER: VISA
PROJECT NUMBER: 1216074
VOLUME SHIPPED: 25 ML
PRESENTATION: 1 LOT OF 25 ML (1 X 25 ML) OF HUMAN
                         RED BLOOD CELLS (SODIUM HEPARIN)
EXPIRATION: 30SEP2016
BIOHAZARD INFO: THIS MATERIAL SHOULD BE HANDLED AS IF
CAPABLE OF TRANSMITTING INFECTIOUS AGENTS. PLEASE USE
UNIVERSAL PRECAUTIONS. NO TEST METHOD CAN PROVIDE
TOTAL ASSURANCE THAT HEPATITIS B VIRUS, HEPATITIS C VIRUS,
HUMAN IMMUNODEFICIENCY
VIRUS, OR OTHER INFECTIOUS AGENTS ARE ABSENT. THUS, ALL

BIOLOGICAL PRODUCTS THAT WE

PROVIDE SHOULD BE HANDLED AT THE BIO-SAFETY LEVEL 2 AS

RECOMMENDED BY THE CDC/NIH MANUAL "BIOSAFETY IN MICROBIOLOGICAL AND BIOMEDICAL LABORATORIES, FROM POTENTIALLY INFECTIOUS HUMAN SERUM OR BLOOD SPECIMENS"

THE MATERIAL LISTED ON THIS CERTIFICATE OF ANALYSIS HAS BEEN TESTED IN ACCORDANCE WITH FDA REGULATIONS AND FOUND TO BE NEGATIVE FOR HIV AB AND HCV AB AND NON-REACTIVE FOR HBSAG, HIV-I RNA, HCV RNA, HBV DNA, WNV RNA, ANTI-T. CRUZI AND STS.

THIS PRODUCT IS BEING SOLD FOR RESEARCH AND OR MANUFACTURING PURPOSES ONLY. IT IS' NOT TO BE USED IN HUMANS OR ANIMALS AND FURTHER MANUFACTURING THAT WILL RESULT IN A FINISHED PRODUCT THAT CONTAINS' VIABLE LEUKOCYTES IS PROHIBITED. FOR IN VITRO USE ONLY. THE USER ASSUMES' ALL RESPONSIBILITY FOR ITS USAGE AND DISPOSAL IN ACCORDANCE WITH ALL REGULATIONS.

Certificate of Analysis

```
PRODUCT: HUMAN WHOLE BLOOD
CATALOG # HMWBNAHP
ANTICOAGULANT: SODIUM HEPARIN
LOT#: BRH1215149
STORAGE TEMPERATURE: 4°C
```

COA DATE: 31AUG2016

PURCHASE ORDER: VISA

PROJECT   1216074

NUMBER:

VOLUME SHIPPED: 50 ML

PRESENTATION: 1 LOT OF 50 ML (1 X 50 ML) OF

HUMAN

WHOLE BLOOD

EXPIRATION: 30SEP2016

BIOHAZARD INFO:THIS MATERIAL SHOULD BE HANDLED AS IF CAPABLE

OF TRANSMITTING

INFECTIOUS AGENTS. PLEASE USE UNIVERSAL PRECAUTIONS. NO

TEST METHOD CAN PROVIDE

TOTAL ASSURANCE THAT HEPATITIS B VIRUS, HEPATITIS C VIRUS,

HUMAN IMMUNODEFICIENCY VIRUS, OR OTHER INFECTIOUS AGENTS

ARE ABSENT. THUS, ALL BIOLOGICAL PRODUCTS THAT WE

PROVIDE SHOULD BE HANDLED AT THE BIO-SAFETY LEVEL 2 AS

RECOMMENDED BY THE CDC/NIH MANUAL "BIOSAFETY IN

MICROBIOLOGICAL AND BIOMEDICAL LABORATORIES, FROM

POTENTIALLY INFECTIOUS HUMAN SERUM OR BLOOD SPECIMENS"

224

THE MATERIAL LISTED ON THIS CERTIFICATE OF ANALYSIS HAS BEEN

TESTED IN ACCORDANCE WITH FDA REGULATIONS AND FOUND TO BE

NEGATIVE FOR HIV ^{1}/2 AB AND HCV AB AND NON-REACTIVE FOR HBSAG,

HIV-I RNA, HCV RNA, HBV DNA, WNV RNA, ANTI-T. CRUZI AND STS.

THIS PRODUCT IS BEING SOLD FOR RESEARCH AND OR
MANUFACTURING PURPOSES' ONLY. IT IS NOT TO
BE USED IN HUMANS OR ANIMALS AND FURTHER MANUFACTURING THAT WILL RESULT IN A FINISHED
PRODUCT THAT CONTAINS VIABLE LEUKOCYTES IS PROHIBITED. FOR IN VITRO USE ONLY. THE USER
ASSUMES ALL RESPONSIBILITY FOR ITS USAGE AND DISPOSAL IN ACCORDANCE WITH ALL

225

CERTIFICATE OF ANALYSIS

DATE: 27NOV2018

HUMAN RED BLOOD CELLS
Product Number: HUMANRBCNHUZN

Lot Number(s):	BRH1596631
Expiration Date:	27DEC2018
Storage Conditions:	4°C
Anticoagulant:	SODIUM HEPARIN

PROJECT DETAILS

Purchase Order:	VISA
Sales Order Number:	S10018022278
Presentation:	1 INDIVIDUAL DONOR OF 1 UNIT (1 X APPROX. 150-175 ML) OF HUMAN RED BLOOD CELLS

GENDER	AGE	RACE
MALE	37	BLACK

BIOHAZARD INFO: THIS MATERIAL SHOULD BE HANDLED AS IF CAPABLE OF TRANSMITTING INFECTIOUS AGENTS. PLEASE USE UNIVERSAL PRECAUTIONS. NO TEST METHOD CAN PROVIDE TOTAL ASSURANCE THAT HEPATITIS B VIRUS, HEPATITIS C VIRUS, HUMAN IMMUNODEFICIENCY VIRUS, OR OTHER INFECTIOUS AGENTS ARE ABSENT. THUS, ALL BIOLOGICAL PRODUCTS THAT WE PROVIDE SHOULD BE HANDLED AT THE BIO-SAFETY LEVEL 2 AS RECOMMENDED BY THE CDC/NIH MANUAL "BIOSAFETY IN MICROBIOLOGICAL AND BIOMEDICAL LABORATORIES, FROM POTENTIALLY INFECTIOUS HUMAN SERUM OR BLOOD SPECIMENS"

THIS PRODUCT IS BEING SOLD FOR RESEARCH AND/OR MANUFACTURING PURPOSES ONLY. THE BIOLOGICAL SAMPLES SUPPLIED BY BIOIVT, OR ANY MATERIAL ISOLATED FROM THE SAMPLES, ARE FOR IN-VITRO RESEARCH USE ONLY AND ARE NOT TO BE USED AS A SOURCE OF MATERIAL FOR CLINICAL THERAPIES. HUMAN MATERIAL MAY BE USED IN VIVO IN ANIMALS. THE USER ASSUMES ALL RESPONSIBILITY FOR ITS USAGE AND DISPOSAL, IN ACCORDANCE WITH ALL REGULATIONS.

THE MATERIAL LISTED ON THIS CERTIFICATE OF ANALYSIS HAS BEEN TESTED IN ACCORDANCE WITH FDA REGULATIONS AND FOUND TO BE NEGATIVE FOR HIV ½ AB AND HCV AB AND NON-REACTIVE FOR HBSAG, HIV-1 RNA, HCV RNA, HBV DNA, WNV RNA, ANTI-T. CRUZI, ZIKA VIRUS RNA AND STS.

BIOIVT WARRANTS THAT AT THE TIME OF SHIPMENT THE PRODUCT IS FREE FROM DEFECTS IN MATERIAL AND WORKMANSHIP AND CONFORMS TO SPECIFICATIONS WHICH ACCOMPANY THE PRODUCT. BIOIVT MAKES NO OTHER WARRANTY, EXPRESSED OR IMPLIED, INCLUDING ANY WARRANTY OF MERCHANTABILITY OR FITNESS FOR ANY PARTICULAR PURPOSE OR PERFORMANCE.

*As of March 5th, 2018, "BioIVT" will replace the current brand of BioreclamationIVT and those of each of its affiliates and subsidiaries: IVT Holdings Inc., Asterand Bioscience, Inc., Asterand UK Acquisition limited, Asterand US Acquisition Corporation, Labquote.com LLC, ILSBio LLC, Seratrials LLC, Sera Laboratories International Ltd., Translational Cell Science LLC, Bioreclamation-IVT India Private Limited, In Vitro Inc., In Vitro GmbH, Qualyst Holdings LLC, Qualyst Transporter Solutions LLC

North America & Asia Pacific ☐ 516-483-1196 @ customerservice@bioivt.com PO Box 770, Hicksville NY 11802-0770,U.S.A.

Europe, Middle East & Africa ☐ 44 (0) 1444 250010 @ cseurope@bioivt.com West Sussex RH15 9TN, U.K.

www.bioivt.com

REGULA TIONS.

BIOIVT
ELEVATING SCIENCE™

CERTIFICATE OF ANALYSIS

DATE: 27NOV2018

HUMAN SERUM
Product Number: HUMANSRMUNN

Lot Number(s):   BRH1596630
Expiration Date: 30NOV2023
Storage Conditions: -20°C OR COLDER
Anticoagulant: NONE

PROJECT DETAILS

Purchase Order:	VISA
Sales Order Number:	S10018022278
Total Volume Shipped:	50 ML
Presentation:	1 LOT OF 50 ML (1 X 50 ML) OF HUMAN SERUM RECOVERED FROM WHOLE BLOOD DONATIONS. THIS MATERIAL HAS NOT GONE THROUGH A FREEZE/THAW PRIOR TO SHIPMENT.
Filtration:	None

LOT#	GENDER	AGE	RACE
BRH1596630	MALE	41	BLACK
	FEMALE	23	BLACK

BIOHAZARD INFO: THIS MATERIAL SHOULD BE HANDLED AS IF CAPABLE OF TRANSMITTING INFECTIOUS AGENTS. PLEASE USE UNIVERSAL PRECAUTIONS. NO TEST METHOD CAN PROVIDE TOTAL ASSURANCE THAT HEPATITIS B VIRUS, HEPATITIS C VIRUS, HUMAN IMMUNODEFICIENCY VIRUS, OR OTHER INFECTIOUS AGENTS ARE ABSENT. THUS, ALL BIOLOGICAL PRODUCTS THAT WE PROVIDE SHOULD BE HANDLED AT THE BIO-SAFETY LEVEL 2 AS RECOMMENDED BY THE CDC/NIH MANUAL "BIOSAFETY IN MICROBIOLOGICAL AND BIOMEDICAL LABORATORIES, FROM POTENTIALLY INFECTIOUS HUMAN SERUM OR BLOOD SPECIMENS"

THIS PRODUCT IS BEING SOLD FOR RESEARCH AND/OR MANUFACTURING PURPOSES ONLY. THE BIOLOGICAL SAMPLES SUPPLIED BY BIOIVT, OR ANY MATERIAL ISOLATED FROM THE SAMPLES, ARE FOR IN-VITRO RESEARCH USE ONLY AND ARE NOT TO BE USED AS A SOURCE OF MATERIAL FOR CLINICAL THERAPIES. HUMAN MATERIAL MAY BE USED IN VIVO IN ANIMALS. THE USER ASSUMES ALL RESPONSIBILITY FOR ITS USAGE AND DISPOSAL, IN ACCORDANCE WITH ALL REGULATIONS.

THE MATERIAL LISTED ON THIS CERTIFICATE OF ANALYSIS HAS BEEN TESTED IN ACCORDANCE WITH FDA REGULATIONS AND FOUND TO BE NEGATIVE FOR HIV ½ AB AND HCV AB AND NON-REACTIVE FOR HBSAG, HIV-1 RNA, HCV RNA, HBV DNA AND STS.

BIOIVT WARRANTS THAT AT THE TIME OF SHIPMENT THE PRODUCT IS FREE FROM DEFECTS IN MATERIAL AND WORKMANSHIP AND CONFORMS TO SPECIFICATIONS WHICH ACCOMPANY THE PRODUCT. BIOIVT MAKES NO OTHER WARRANTY, EXPRESSED OR IMPLIED, INCLUDING ANY WARRANTY OF MERCHANTABILITY OR FITNESS FOR ANY PARTICULAR PURPOSE OR PERFORMANCE.

*As of March 5th, 2018, "BioIVT" will replace the current brand of BioreclamationIVT and those of each of its affiliates and subsidiaries: IVT Holdings Inc., Asterand Bioscience, Inc., Asterand UK Acquisition limited, Asterand US Acquisition Corporation, Labquote.com LLC, ILSBio LLC, Seratrials LLC, Sera Laboratories International Ltd., Translational Cell Science LLC, Bioreclamation-IVT India Private Limited, In Vitro Inc., In Vitro GmbH, Qualyst Holdings LLC, Qualyst Transporter Solutions LLC

North America & Asia Pacific	☎ 516-483-1196 @ customerservice@bioivt.com PO Box 770, Hicksville NY 11802-0770,U.S.A.	Europe, Middle East & Africa	☎ 44 (0) 1444 250010 @ cseurope@bioivt.com West Sussex RH15 9TN, U.K.

@ www.bioivt.com

Comparison of Measurements – Caliper vs. Caliper 4X Magnification

	bloodstain measurements with caliper							bloodstain measurements 400% on screen with caliper				
very high density								very high density				
7.1 10 degrees	W	L	W/L	Angle				7.1 10 degrees	W	L	W/L	Angle
1	4.37	31.63	0.14	8.04				1	12.76	93.87	0.14	8.04
2	4.43	30.87	0.14	8.04				2	11.96	93.64	0.13	7.46
3	4.57	30.65	0.15	8.62				3	11.77	93.85	0.13	7.46
4	4.63	31.24	0.15	8.62				4	12.14	92.66	0.13	7.46
5	4.51	31.39	0.14	8.04				5	11.24	91.75	0.12	6.89
6	4.75	30.86	0.15	8.62				6	11.82	92.57	0.13	7.46
7	4.49	30.98	0.14	8.04				7	11.54	93.08	0.12	6.89
8	4.39	31.39	0.14	8.04				8	11.96	91.07	0.13	7.46
9	4.41	30.51	0.14	8.04				9	11.48	92.68	0.12	6.89
10	4.62	30.79	0.15	8.62				10	11.82	91.10	0.13	7.46
mean	4.51	31.03	0.14	8.27				mean	11.84	92.61	0.13	7.35
SD	0.123	0.364	0.00516	0.299				SD	0.414	1.06	0.00632	0.362
RSD	2.74%	1.17%	3.59%	3.62%				RSD	3.50%	1.14%	4.94%	4.94%
7.1 55 degrees								7.1 55 degrees				
1	11.51	14.45	0.80	53.13				1	31.51	38.76	0.81	54.09
2	11.39	14.65	0.78	51.26				2	30.32	39.23	0.77	50.35
3	11.71	14.08	0.83	56.09				3	30.26	38.43	0.79	52.18
4	11.72	14.41	0.81	54.09				4	30.65	38.84	0.79	52.18
5	11.73	14.29	0.82	55.08				5	30.07	38.52	0.78	51.26
6	12.03	13.81	0.87	60.46				6	30.09	38.40	0.78	51.26
7	11.56	14.42	0.80	55.13				7	30.31	38.49	0.79	52.18
8	11.58	14.34	0.81	54.09				8	31.25	38.63	0.81	54.09
9	11.83	14.23	0.83	56.09				9	30.30	38.67	0.78	51.26
10	11.17	14.46	0.77	50.35				10	30.01	38.42	0.78	51.26
mean	11.62	14.31	0.81	54.58				mean	30.47	38.63	0.79	52.01
SD	0.239	0.233	0.0282	2.81				SD	0.511	0.256	0.0131	1.23
RSD	2.06%	1.63%	3.47%	5.15%				RSD	1.68%	0.66%	1.67%	2.38%
7.1 90 degrees								7.1 90 degrees				
1	13.33	13.90	0.96	73.73				1	45.07	45.95	0.98	78.52
2	13.67	14.12	0.97	75.93				2	44.03	45.42	0.97	75.93
3	14.04	14.43	0.97	75.93				3	44.52	45.44	0.98	78.52
4	13.64	14.11	0.97	75.93				4	43.70	45.72	0.96	73.73
5	14.05	14.19	0.99	81.89				5	43.94	45.87	0.96	73.73
6	13.95	13.91	1.00	90.00				6	44.04	46.16	0.95	71.80
7	13.91	14.46	0.96	73.73				7	43.92	46.04	0.95	71.80
8	14.16	14.32	0.99	81.89				8	45.38	45.50	1.00	90.00
9	14.10	14.45	0.98	78.52				9	43.90	45.30	0.97	75.93
10	13.61	14.11	0.96	73.73				10	44.09	46.00	0.96	73.73
mean	13.86	14.20	0.97	78.13				mean	44.25	45.74	0.97	76.37
SD	0.269	0.209	0.0143	5.18				SD	0.554	0.305	0.0154	5.35
RSD	1.94%	1.47%	1.47%	6.64%				RSD	1.25%	0.67%	1.60%	7.01%

	bloodstain measurements with caliper						bloodstain measurements 400% on screen with caliper				
normal density	W	L	W/L	Angle			normal density	W	L	W/L	Angle
5.1 10 degrees							5.1 10 degrees				
1	5.06	31.75	0.16	9.20			1	17.35	110.59	0.16	9.20
2	5.12	31.88	0.16	9.20			2	17.49	114.72	0.15	8.62
3	5.07	33.97	0.15	8.62			3	16.90	125.44	0.13	7.46
4	5.51	32.13	0.17	9.78			4	17.98	122.77	0.15	8.62
5	5.18	32.02	0.16	9.20			5	15.21	125.58	0.12	6.89
6	5.14	32.07	0.16	9.20			6	16.24	124.17	0.13	7.46
7	4.93	33.78	0.15	8.62			7	17.21	121.11	0.14	8.04
8	5.28	32.40	0.16	9.20			8	16.57	120.17	0.14	8.04
9	5.17	31.56	0.16	9.20			9	16.38	120.48	0.14	8.04
10	5.35	31.28	0.17	9.78			10	16.54	118.22	0.14	8.04
mean	5.18	32.28	0.16	9.20			mean	16.78	120.32	0.14	8.04
SD	0.164	0.895	0.00666	0.386			SD	0.780	4.782	0.0115	0.667
RSD	3.17%	2.77%	4.17%	4.20%			RSD	4.65%	3.97%	8.25%	8.31%
5.3 55 degrees							5.3 55 degrees				
1	14.94	19.73	0.76	49.46			1	65.93	87.56	0.75	48.59
2	15.22	19.61	0.78	51.26			2	64.54	87.63	0.74	47.73
3	15.01	18.99	0.79	52.18			3	67.67	86.84	0.78	51.26
4	14.90	19.36	0.77	50.35			4	65.45	86.90	0.75	48.59
5	15.09	19.09	0.79	52.18			5	65.83	85.84	0.77	50.35
6	15.28	18.61	0.82	55.08			6	66.55	87.62	0.76	49.46
7	15.20	19.09	0.80	53.13			7	64.89	85.98	0.75	48.59
8	15.41	19.07	0.81	54.09			8	65.90	86.69	0.76	49.46
9	15.34	19.51	0.79	52.18			9	66.06	86.40	0.76	49.46
10	15.21	19.21	0.79	52.18			10	66.55	86.20	0.77	50.35
mean	15.16	19.22	0.79	52.21			meab	65.93	86.76	0.76	49.38
SD	0.17	0.332	0.0176	1.65			SD	0.886	0.672	0.0119	1.055
RSD	1.12%	1.73%	2.23%	3.16%			RSD	1.34%	0.77%	1.58%	2.14%
5.5 90 degrees							5.5 90 degrees				
1	16.39	16.69	0.98	78.52			1	42.60	43.95	0.97	75.93
2	16.31	16.78	0.97	75.93			2	42.29	43.52	0.97	75.93
3	16.45	16.44	1.00	90.00			3	42.86	43.98	0.97	75.93
4	16.12	16.70	0.97	75.93			4	43.07	42.86	1.00	90.00
5	16.56	17.31	0.96	73.73			5	42.42	44.31	0.96	73.73
6	16.18	16.86	0.96	73.73			6	43.03	44.43	0.97	75.93
7	16.31	16.61	0.98	78.52			7	41.83	43.28	0.97	75.93
8	16.59	16.65	1.00	90.00			8	42.75	44.25	0.97	75.93
9	16.47	16.81	0.98	78.52			9	43.15	43.54	0.99	81.89
10	16.57	16.74	0.99	81.89			10	43.79	43.67	1.00	90.00
mean	16.39	16.75	0.98	79.68			mean	42.77	43.77	0.98	79.12
SD	0.163	0.226	0.0144	5.97			Sd	0.539	0.497	0.0141	6.096
RSD	1.00%	1.35%	1.48%	7.49%			RSD	1.26%	1.14%	1.45%	7.71%

229

	bloodstain measurements with caliper						bloodstain measurements 400% on screen with caliper				
very low density	W	L	W/L	Angle			very low density		W	L	W/L	Angle
1.5 10 degrees							1.5 10 degrees					
1	4.95	43.14	0.11	6.31			1		14.30	102.74	0.14	8.04
2	5.27	42.64	0.12	6.89			2		15.30	103.42	0.15	8.62
3	5.17	44.02	0.12	6.89			3		14.51	103.36	0.14	8.04
4	5.37	42.41	0.13	7.46			4		14.36	99.69	0.14	8.04
5	5.04	43.34	0.12	6.89			5		14.72	108.42	0.14	8.04
6	5.39	43.82	0.12	6.89			6		14.04	108.6	0.13	7.46
7	5.23	43.10	0.12	6.89			7		14.00	106.00	0.13	7.46
8	5.17	41.97	0.12	6.89			8		15.01	105.85	0.14	8.04
9	5.08	41.17	0.12	6.89			9		14.47	106.80	0.14	8.04
10	5.58	43.01	0.13	7.46			10		13.44	102.92	0.13	7.46
mean	5.22	42.86	0.12	6.95			mean		14.41	104.78	0.14	7.92
SD	0.186	0.853	0.00567	0.325			SD		0.529	2.827	0.00632	0.366
RSD	3.50%	1.99%	4.69%	4.69%			RSD		3.67%	2.70%	4.58%	4.63%
1.4 55 degrees							1.4 55 degrees					
1	13.60	17.40	0.78	51.26			1		50.16	66.34	0.76	49.46
2	14.00	17.42	0.80	53.13			2		50.72	65.89	0.77	50.35
3	14.08	16.52	0.85	58.21			3		51.51	65.61	0.79	52.18
4	14.04	16.86	0.83	56.09			4		51.75	65.28	0.79	52.18
5	13.77	17.33	0.79	52.18			5		50.45	65.59	0.77	50.35
6	14.09	17.59	0.80	53.13			6		51.41	64.55	0.80	53.13
7	14.01	17.28	0.81	54.09			7		50.72	66.70	0.76	49.46
8	13.61	16.93	0.80	53.13			8		51.65	65.51	0.79	52.18
9	13.72	17.51	0.78	51.26			9		51.15	65.81	0.78	51.26
10	13.93	17.25	0.81	54.09			10		52.20	64.87	0.80	53.13
mean	13.88	17.20	0.80	53.66			mean		51.17	65.61	0.78	51.37
SD	0.192	0.335	0.0217	2.14			SD		0.645	0.635	0.0152	1.39
RSD	1.38%	1.95%	2.70%	4.00%			RSD		1.26%	0.97%	1.95%	2.72%
1.2 90 degrees							1.2 90 degrees					
1	17.30	18.11	0.96	73.73			1		67.92	69.46	0.98	78.52
2	17.18	17.68	0.97	75.93			2		68.55	69.53	0.99	81.89
3	17.28	17.50	0.99	81.89			3		68.05	69.20	0.98	78.52
4	17.64	17.59	1.00	90.00			4		65.90	68.58	0.96	73.73
5	17.33	17.45	0.99	81.89			5		65.89	68.94	0.96	73.73
6	17.25	17.62	0.98	78.52			6		67.32	68.89	0.98	78.52
7	17.44	17.77	0.98	78.52			7		67.36	69.47	0.97	73.73
8	17.26	17.96	0.96	73.73			8		66.96	68.42	0.98	78.52
9	17.58	18.04	0.97	75.93			9		66.46	68.44	0.97	73.73
10	16.98	17.78	0.96	73.73			10		67.33	68.59	0.98	78.52
mean	17.32	17.75	0.98	78.39			mean		67.17	68.95	0.98	76.94
SD	0.191	0.225	0.0142	5.12			SD		0.889	0.439	0.00971	2.94
RSD	1.11%	1.27%	1.47%	6.54%			RSD		1.32%	0.64%	1.00%	3.83%

Digital Caliper Specifications

CARE & MAINTENANCE

1. Keep body face clean; prevent liquid material from getting into slider to destroy electronics
2. Face should be cleaned with a clean, dry, lint-free cloth. Lubricate body with a few drops of clock oil. Acetone & alcohol must not be used.
3. Keep battery compartment clean and free of corrosion.

TROUBLESHOOTING

PROBLEM:	SOLUTION:
Display cannot count	Battery voltage is under 1.45V. Remove cover and replace battery.
Every second 5 digits Jump simultaneously	Faulty circuit. Remove battery, after 30 sec. put battery back into compartment.
Display shows 000.00 Or IN 00.000	Function buttons and sliders signal end may have shorted out. Remove the cover, put the button springs in place with rubber covers. Contact must be unobstructed.
Function buttons not active	Springs or rubber covers may be out of shape due to excessive pressing. See solution above for tips.
Reading error for full Length is ≥ 0.1mm .	Sensor may have dirt or deposits in it Remove cover and slider assembly. Blow off sensor face with clean pressurized air (≥51kg/cm squared), clean with a dry, lint-free cloth.
No display on LCD screen	1.) Poor battery contact. Check battery compartment, clean if necessary. 2.) Battery voltage is under 1.3V. Replace with correct battery.

AUTO POWER-OFF
Digital Caliper

OWNER'S MANUAL
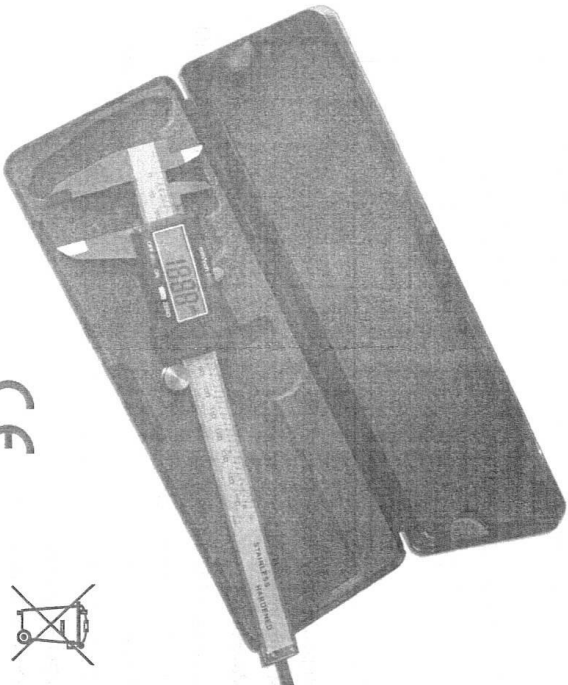
FOR YOUR SAFETY, and CARE OF THIS TOOL.
Please read these instructions carefully and retain them for future use.

03.04.0487ECC

CE

TUV SUD
Product Service

In accordance with th European Directiv ROHS 2002/95/CE

D4 06 07 60503 00

231

CALIPER FEATURES

Metric/Inch change over (True conversion)

Data output socket

Battery compartment cover

Zero setting (zero setting at any position within the measuring range)

On/Off switch

CALIPER APPLICATIONS

Measurements of external dimensions
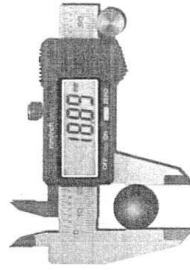
Measurements of internal dimensions
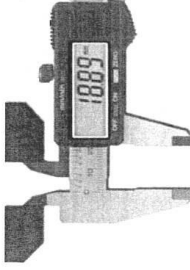
Measurements of depth
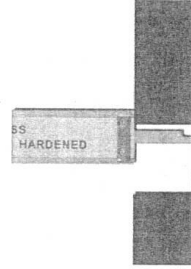
Measurements of steps

A 0-20.00

B 0-20.02
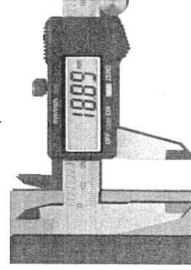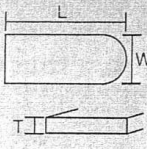
Differential method measurement (Application of zero setting)

SPECIFICATIONS AND FUNCTIONS

Your digital caliper was constructed with quality materials and workmanship and will Give you many years of trouble free use when cared for as described in the "Care & Maintenance" section.

Measuring Range:	Resolution:
0 - 150mm / 0 - 6"	0.01mm / 0.0005"
0 - 200mm / 0 - 8"	0.01mm / 0.0005"
0 - 300mm / 0 - 12"	0.01mm / 0.0005"

Measuring Range:	Accuracy:
0 - 200mm / 0 - 8"	0.03mm / 0.001"
200- 300mm / 8 - 12"	0.04mm / 0.0015"

Repeatability: 0.01 mm or 0.0005"

Maximum measuring speed: 1.5m/sec or 60"/sec.

Measuring system: Non-contaction linear CAP measuring system

Display: LCD display, minus sign "-", character in 6.35mm/0.25" height for 5 digits, small digit "5" and "IN" sign for inch measuring unit.

Battery: One silver oxide battery 1.5V for one year of continuous use. Low battery warning by flashing display.

Operating temperature: 0 ℃ ~ +40 ℃

Storage temperature: -20 ℃ ~ +70 ℃

Influence of humidity: Not important within 0 to 80% of relative humidity.

Data output: Serial output for interface with host computer or printer

Data processing interface (option): Functions:

Data storage, processing & printing, with software of quality control

Auto power off

232

www.manaraa.com

Metal Rule Grade Specifications

Metal Rules Grade 1 of JIS B7516-2005(abstract)
as of June, 2016

Standard	Grade 1 of JIS B7516—2005					
Material	SUS420 J2 of JIS G 4305 or that equivalent or superior to this in quality.					
Hardness of Material	Hv400 min					
Size	Nominal Size	Overall Length(L) Size	Tolerance	Thickness(T) Size	Tolerance	Width(W) Size	Tolerance

Nominal Size	Overall Length(L) Size	Tolerance	Thickness(T) Size	Tolerance	Width(W) Size	Tolerance
150	175		0.5		15	
300	335		1.0		25	
600	640	±5mm	1.2	±10%	30	±2%
1,000	1,050		1.5		35	
1,500	1,565		2.0		40	
2,000	2,065		2.0		40	

Unit : mm

Flatness of Scale Face	The scale face shall be flat to a level of no hindrance to measurements.

Straightness of Scale Side Face

Nominal Size	Straightness	Nominal Size	Straightness
150	0.23 max	1,000	0.40 max
300	0.26 max	1,500	0.50 max
600	0.32 max	2,000	0.60 max

Unit : mm

Squareness of Scale End Face	The squareness of the scale end face of a rule in respect of its scale side shall be 0.035mm max per 10mm length of the end face.

Tolerance of Length (*Temperature at 20°C)

Length	Tolerance
500 max	±0.15
over 500 ~ 1,000 max	±0.20
over 1,000 ~ 1,500 max	±0.25
over 1,500 ~ 2,000 max	±0.30

Unit : mm

Conversion table

Items	Inch/Conversion Chart (TAP DRILL WW.UNC)	Length	Width	Weight	Volume
Hard Chrome Finish 15cm	●				
30cm	●				
60cm	●				
1m	●				
Metric x Shaku 15cm left		●	●		
30cm left		●	●		
60cm left		●	●	●	
1m left		●	●	●	●
1m right	●				
Polish Finish 15cm	●				
30cm	●				
60cm	●				
1m	●				
Pickup 10cm		●			
15cm		●	●		
30cm		●	●		
60cm		●	●	●	
1m		●	●	●	●
With Scale Stopper 15cm	●				
30cm	●				
1mm Dividing 15cm	●				
30cm	●				
60cm	●				
1m	●				
Mini 15cm	●				

■Material Less than 2m : Stainless steel SUS420J2   Over 3m : Stainless steel SUS304
(SUS means STELL STAINELSS—rust-resistant.   Hv means HARD VICKERS —unit for hardness.)
All of our stainless rules are registered as Japanese Industrial Standard (JIS) under the specifications above. Although some of rules exceed JIS specifications due to unusual graduations, shapes, or sizes, all of our products, regardless of registration, have gone through strict product inspections based on the JIS specifications above to provide safe, high quality products. SUS420J2 has baking finish. SUS304 doesn't have baking finish.
Length tolerance over 3m : 3m±0.5mm, 4m±0.65mm, 5m±0.8mm, 6m±0.95mm

Digital Angle Finder Specifications
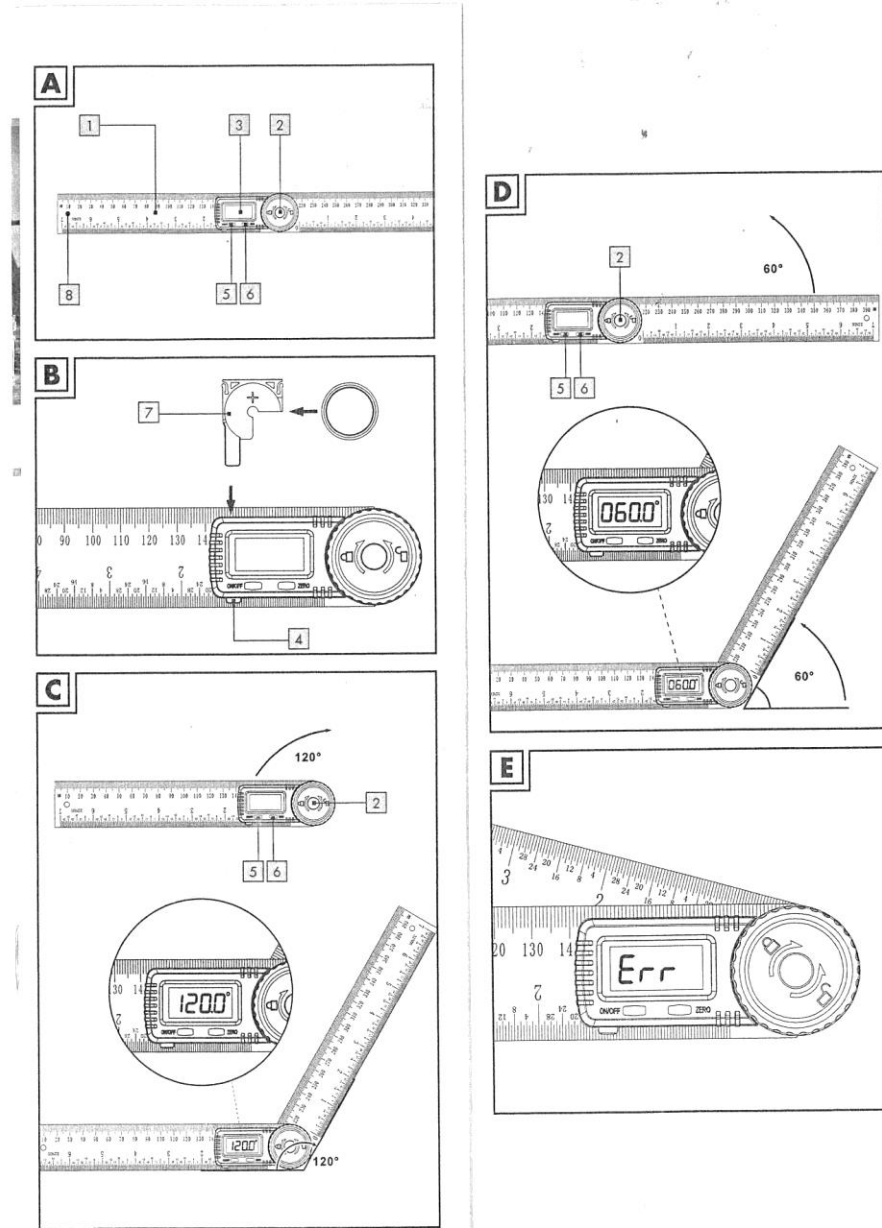
DIGITAL ANGLE FINDER

● **Introduction**

We congratulate you on the purchase of your new product. You have chosen a high quality product. The instructions for use are part of the product. They contain important information concerning safety, use and disposal. Before using the product, please familiarise yourself with all of the safety information and instructions for use. Only use the product as described and for the specified applications. If you pass the product on to anyone else, please ensure that you also pass on all the documentation with it.

● **Intended use**

Only for private use.
Not for commercial use.

● **Scope of delivery**

1 x Angle Ruler
1 x Battery
1 x Instruction for use

● **Description of parts**

1 Measuring ruler
2 Locking knob
3 LCD display
4 Battery compartment button
5 ON/OFF button
6 ZERO button
7 Battery receptacle
8 Hanging hole

● **Technical data**

Measurement unit:	degrees (°)
Measuring range:	0 - 360°
Resolution:	0.1°
Accuracy:	± 0.3°
Measuring system:	Liner capacitive measuring system
Display:	LCD display
Operating temperature:	+5 °C - +40 °C
Influence of humidity:	within a range from 0 % to 80 % relative humidity irrelevant
Battery:	3 V === (Direct current) CR2032 (included)

6

HORUSDY®
Professional Tools
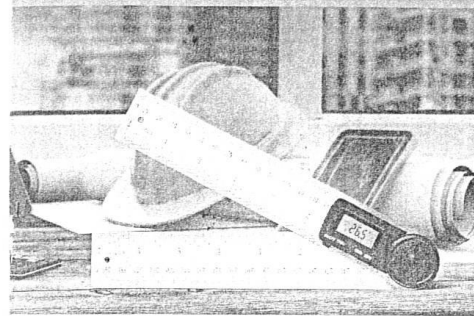
DIGITAL ANGLE FINDER

USER MANUAL

Manufacturers Reference Number: T97352

235

Digital Angle Finder Calibration Data

		60 degrees	30 degrees	90 degrees
		measurements taken from constructed triangles using digital angle finder		
		30,60,90 right triangle		
		60 degrees	30 degrees	90 degrees
	1	59.7	29.6	89.6
	2	59.6	29.8	89.9
	3	59.8	29.8	90.0
	4	59.6	30.3	89.1
	5	59.6	30.00	89.7
mean		59.7	29.9	89.6
SD		0.0894	0.264	0.350
RSD		0.15%	0.88%	0.39%
error		0.57%	0.33%	0.44%
		equilateral triangle		
		60 degrees		
	1	59.0		
	2	59.4		
	3	59.7		
	4	59.6		
	5	59.7		
mean		59.5		
SD		0.294		
RSD		0.50%		
error		0.87%		

		isosceles right triangle		
		45 degrees	45 degrees	90 degrees
	1	44.4	44.6	89.6
	2	44.3	44.9	90.5
	3	44.3	44.7	90.6
	4	44.6	44.8	90.7
	5	44.5	44.7	90.1
mean		44.4	44.7	90.3
SD		0.130	0.114	0.452
RSD		0.29%	0.25%	0.50%
error		1.29%	0.58%	0.33%
		3,4,5 right triangle		
		53.1 degrees	36.9 degrees	90 degrees
	1	52.7	36.5	89.6
	2	52.6	36.4	89.7
	3	52.8	36.5	90.1
	4	52.9	36.4	90.0
	5	53.0	36.7	90.1
mean		52.8	36.5	89.9
SD		0.158	0.122	0.234
RSD		0.30%	0.34%	0.26%
error		0.56%	1.08%	0.11%

Triangles Used For Digital Angle Finder Calibrations

EQUILATERAL △

30, 60, 90 RT △

239
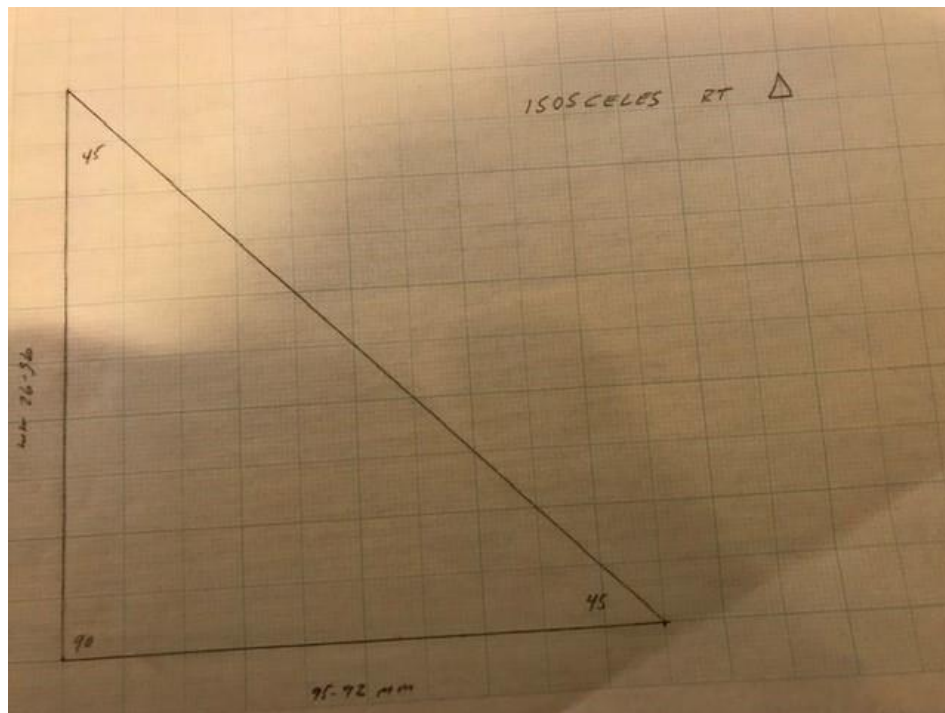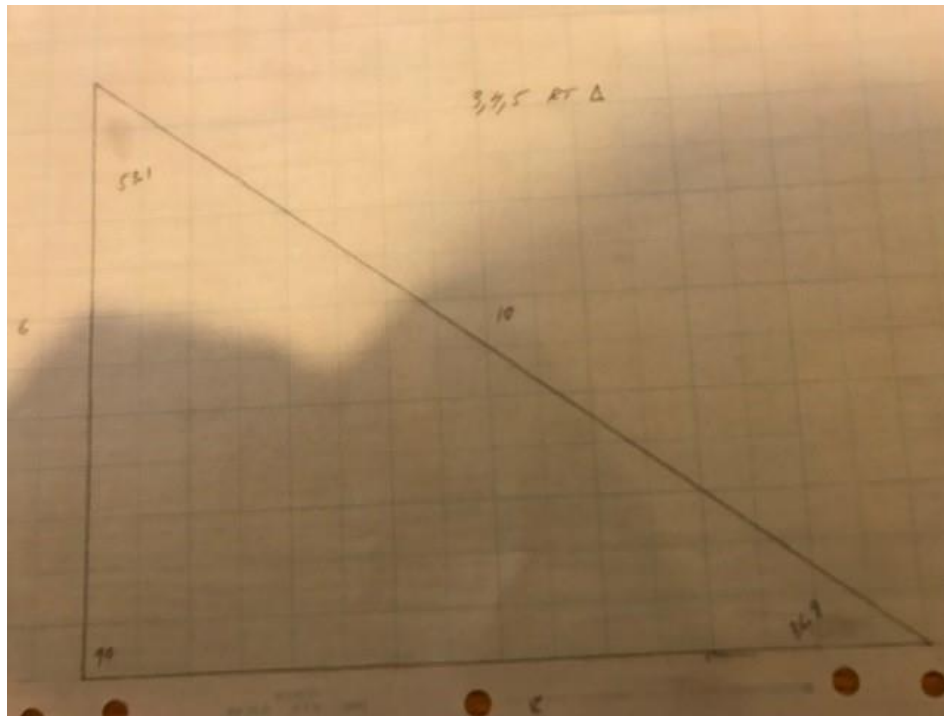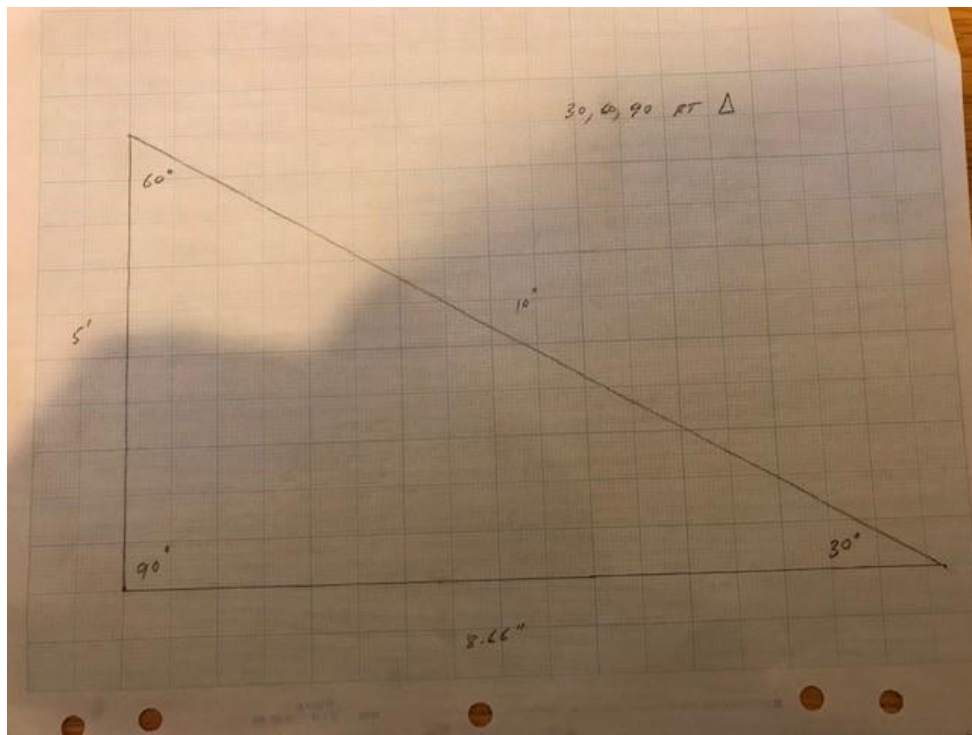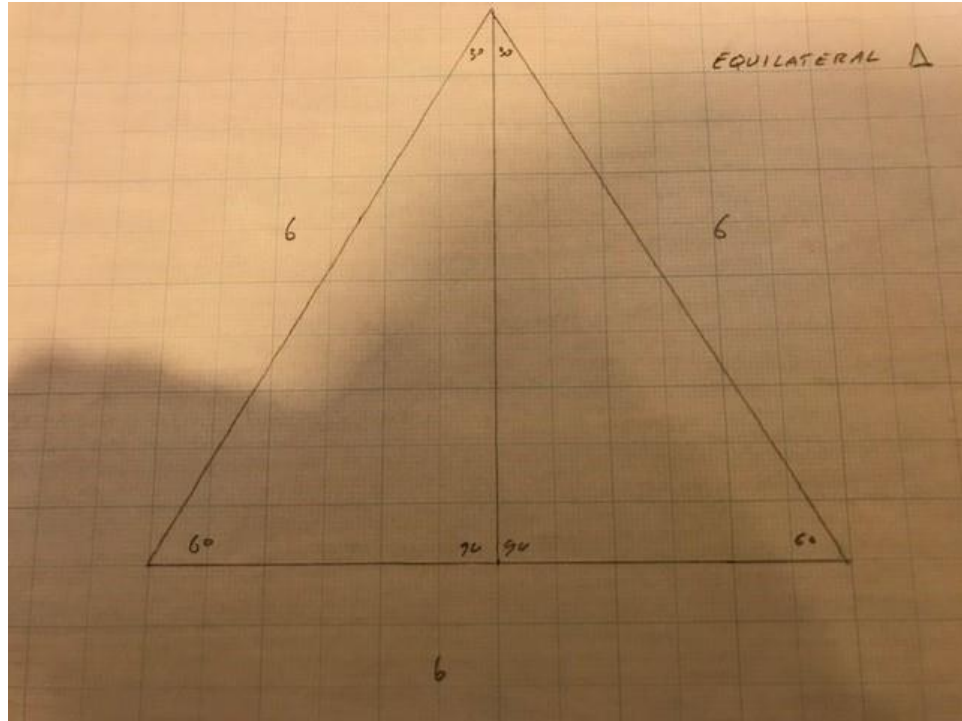
Study 1 Bloodstain Photographs

The number designations for the bloodstain pictures is the following

Impact angle, number indicating stain density, number of bloodstain in the sequence.

1: very low density

2: low density

3: normal density

4: high density

5: very high density

Example

10° 1-1
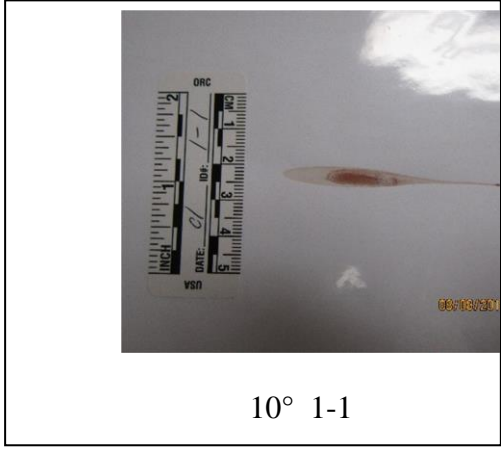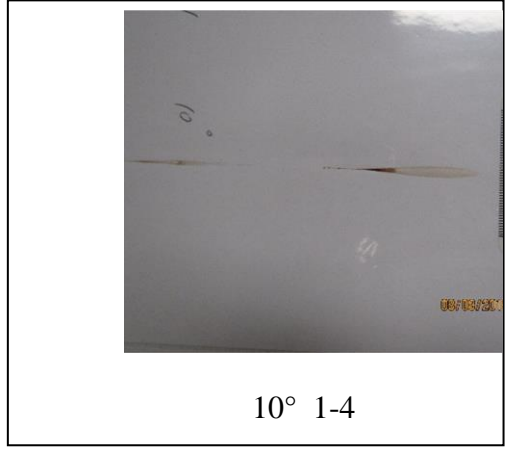
10° 1-1

10° 1-4

10° 1-2

10° 1-5

10° 1-3

10° 1-6

241
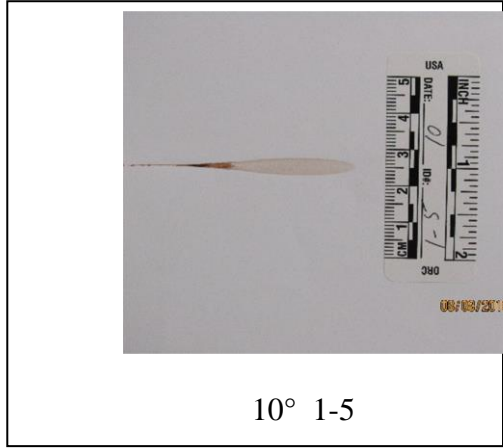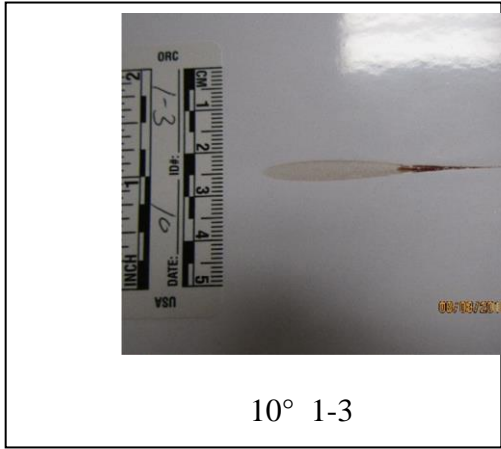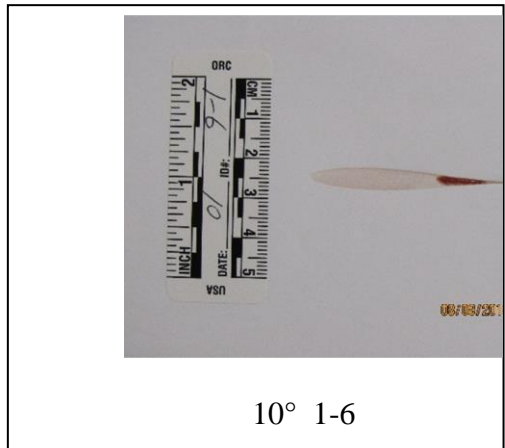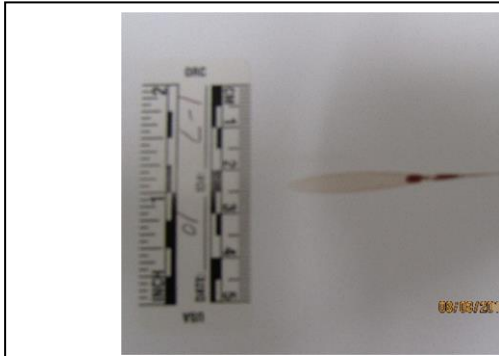
10° 1-7

10° 1-10

10° 1-8

10° 1-9

242
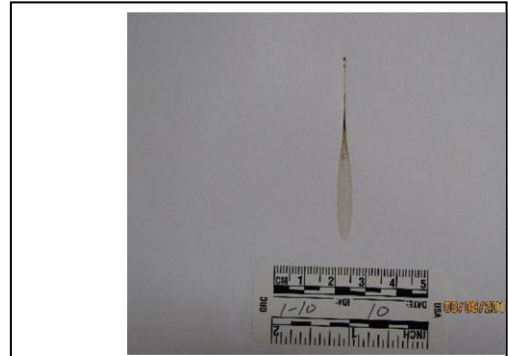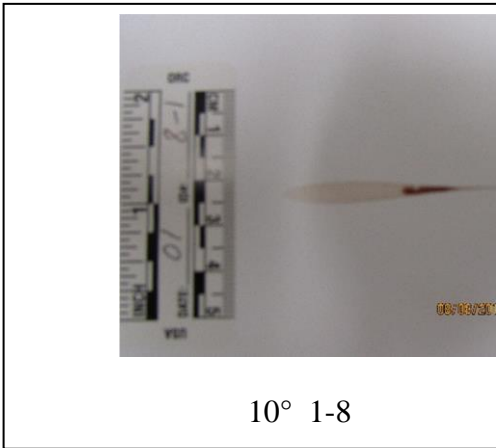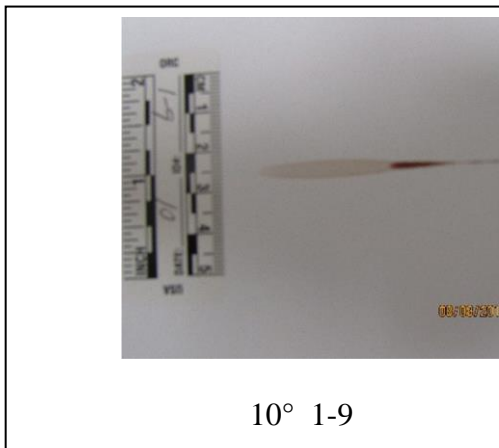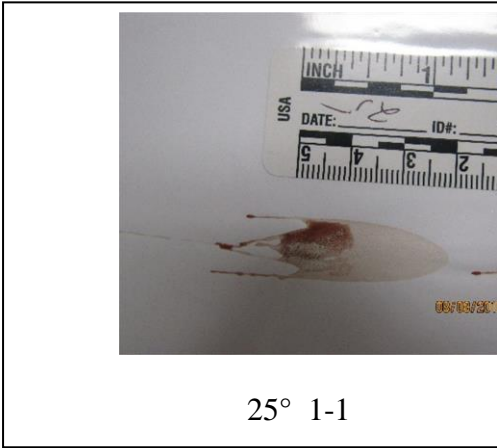
25° 1-1

25° 1-4

25° 1-2

25° 1-5

25° 1-3

25° 1-6

243

25° 1-7

25° 1-10

25° 1-8

25° 1-9

40° 1-1

40° 1-2

40° 1-3

40° 1-4

40° 1-5

40° 1-6

40° 1-7

40° 1-10

40° 1-8

40° 1-9
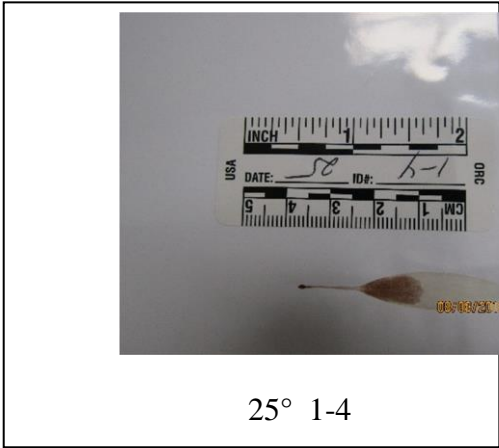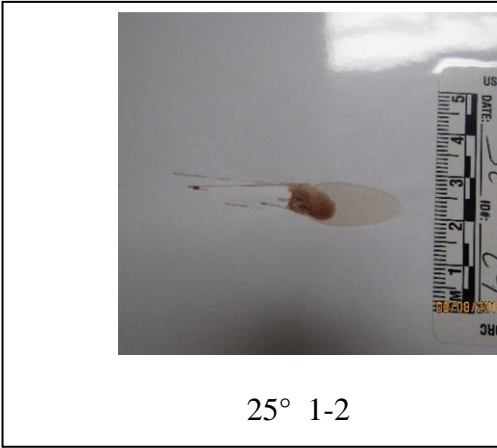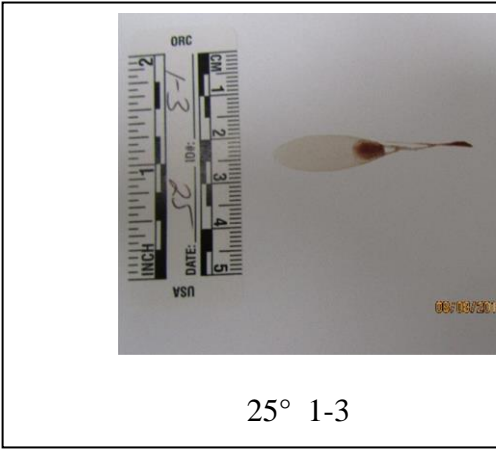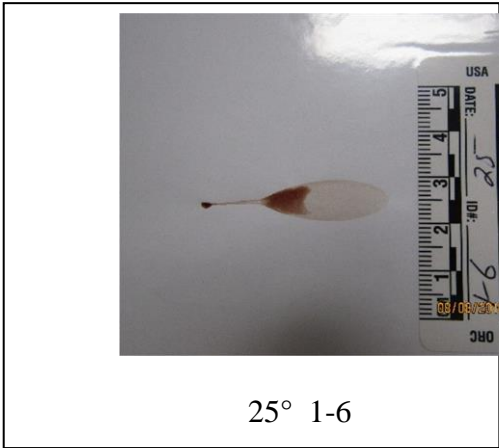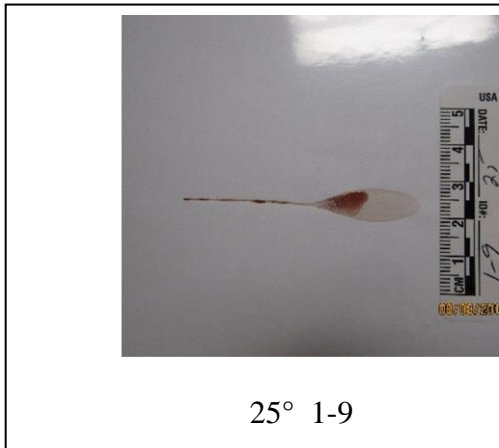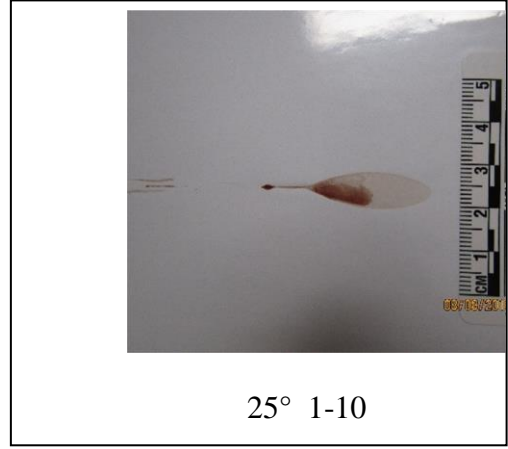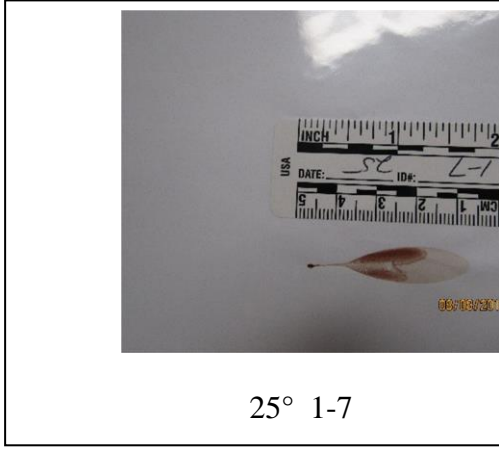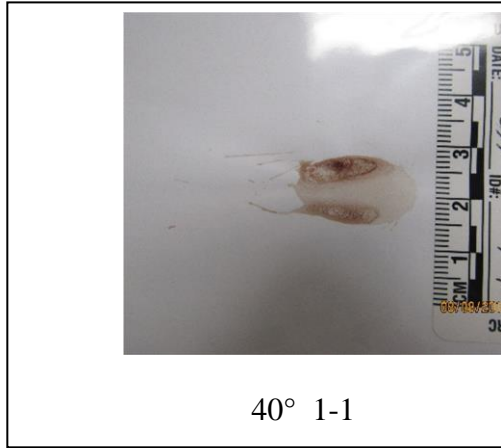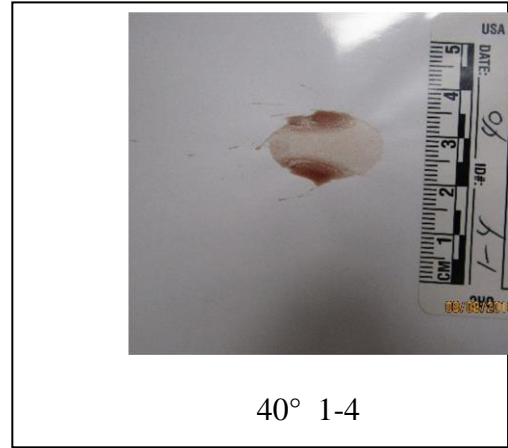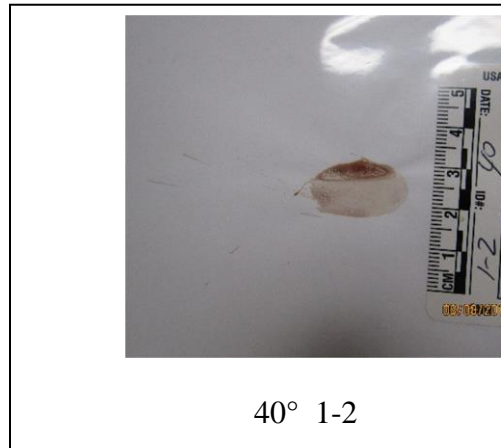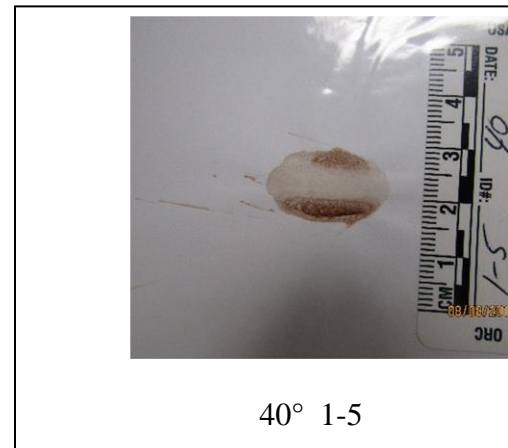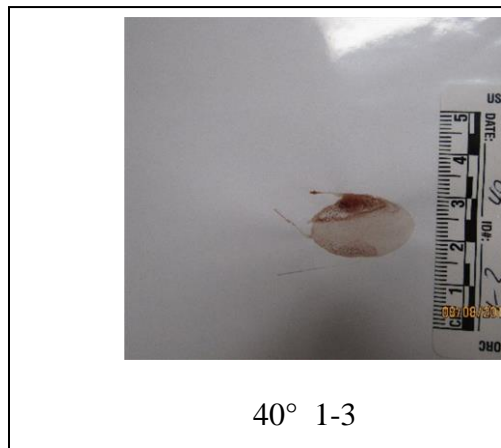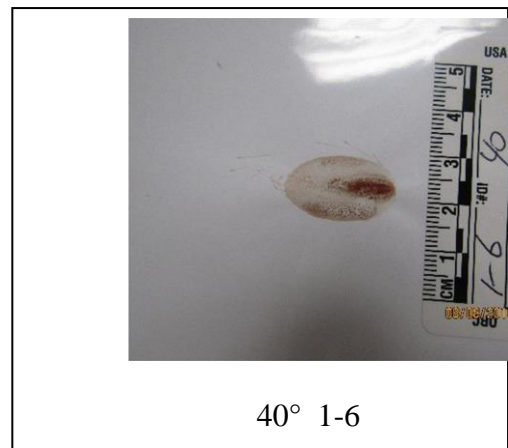
246
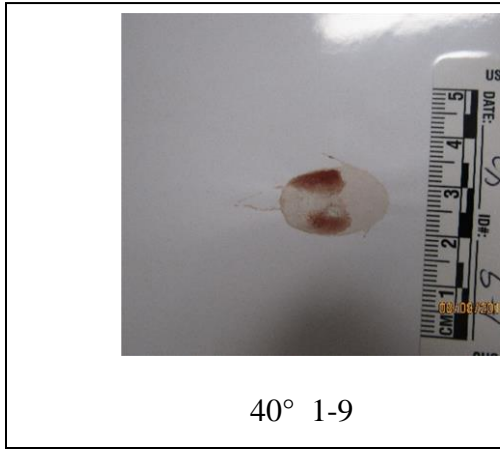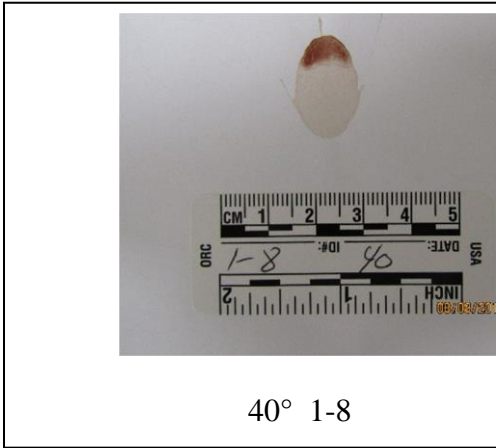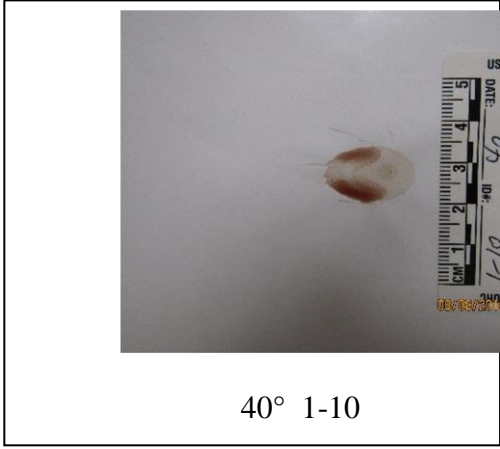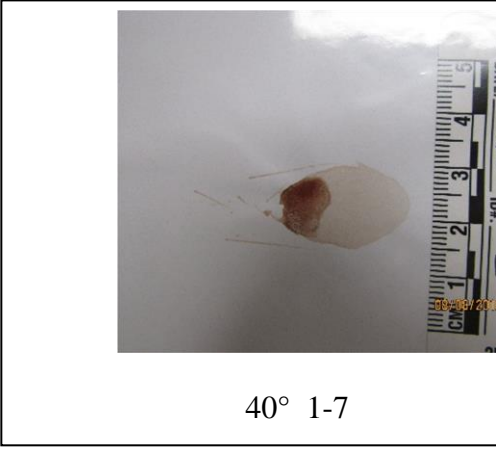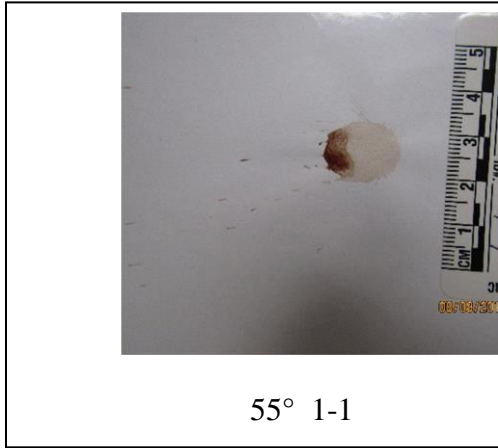
55° 1-1
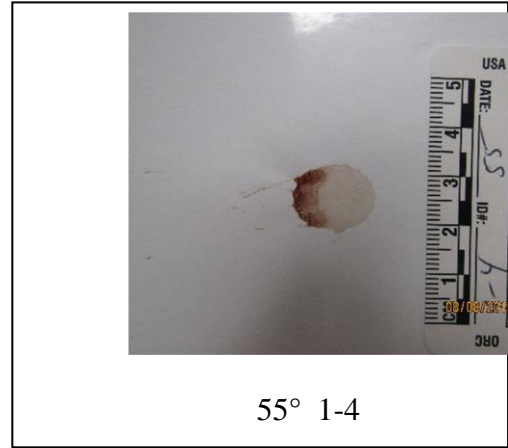
55° 1-4
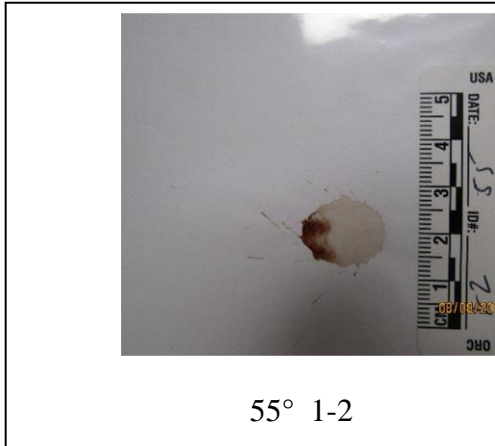
55° 1-2

55° 1-5

55° 1-3

55° 1-6

55° 1-7

55° 1-10

55° 1-8

55° 1-9
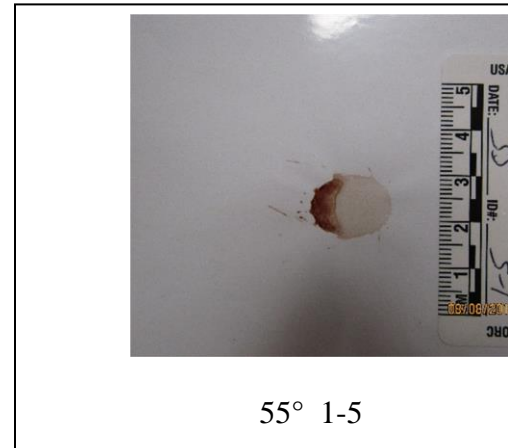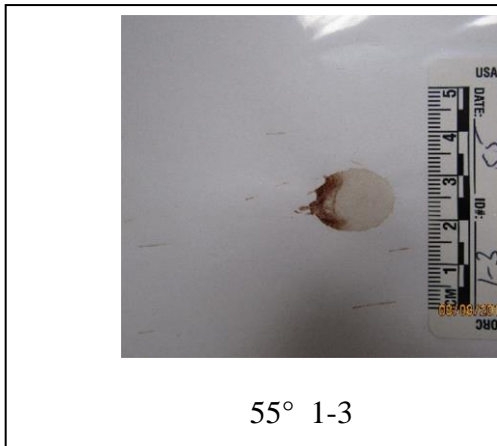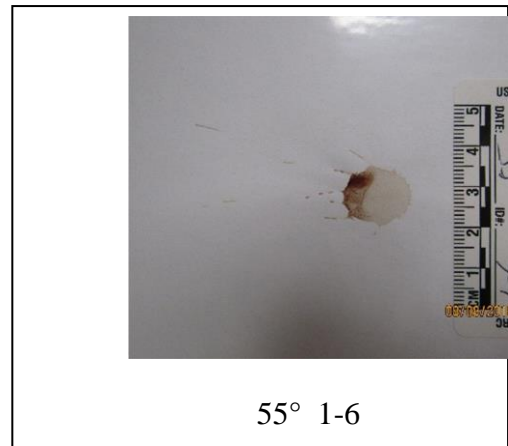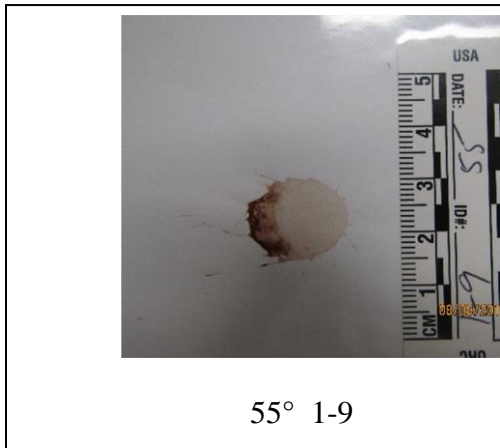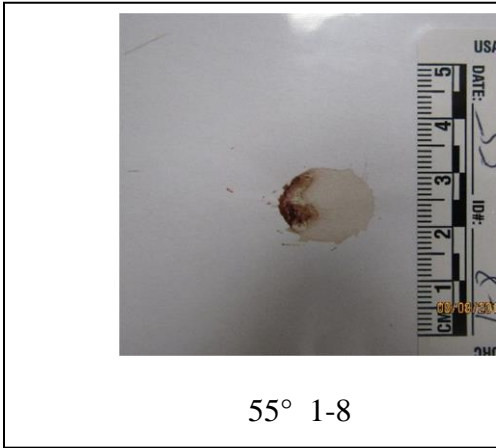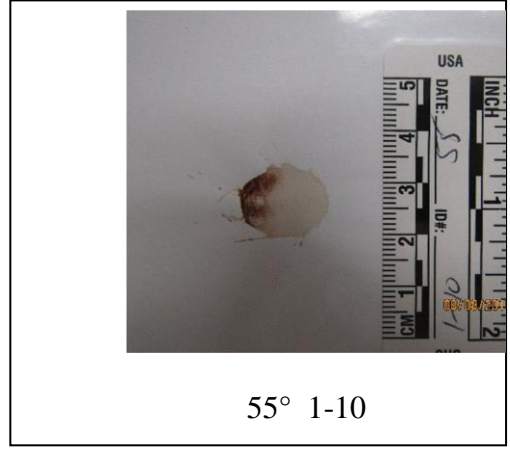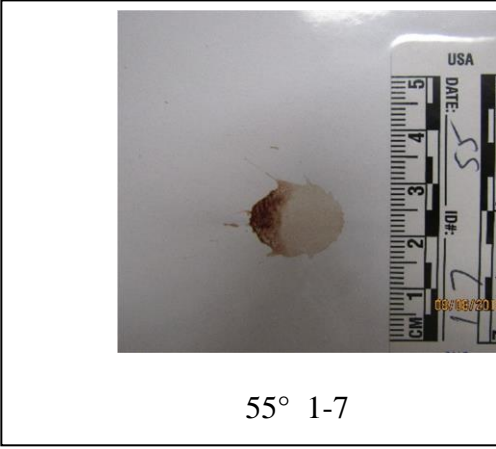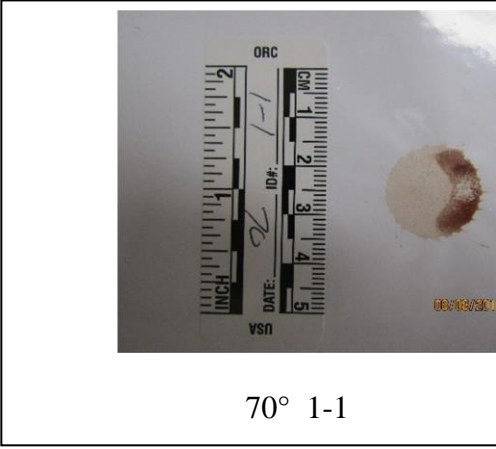
70° 1-1
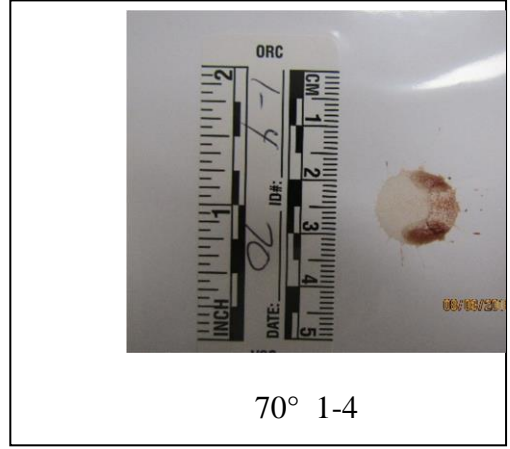
70° 1-4

70° 1-2

70° 1-5

70° 1-3

70° 1-6

70° 1-7

70° 1-10

70° 1-8

70° 1-9

250
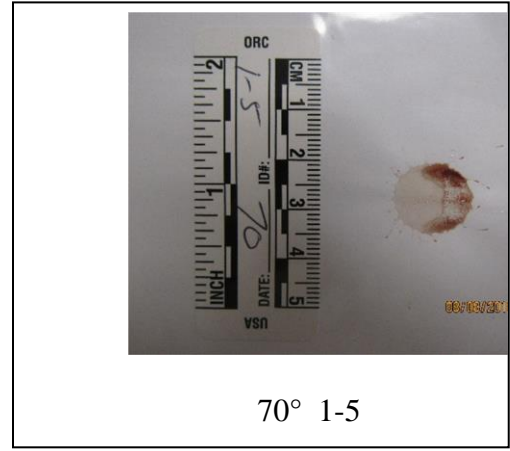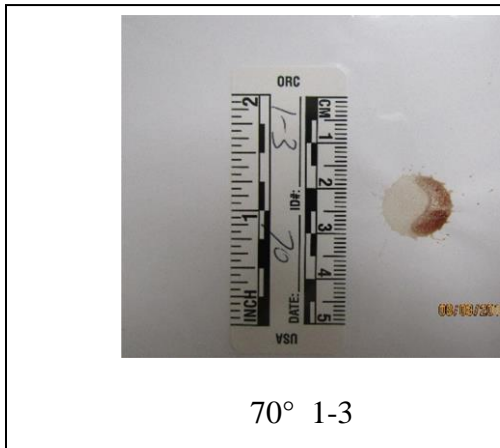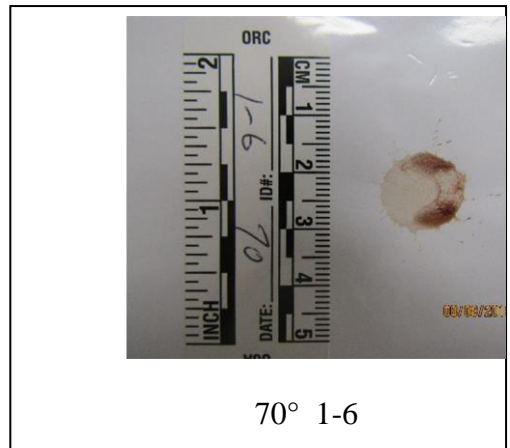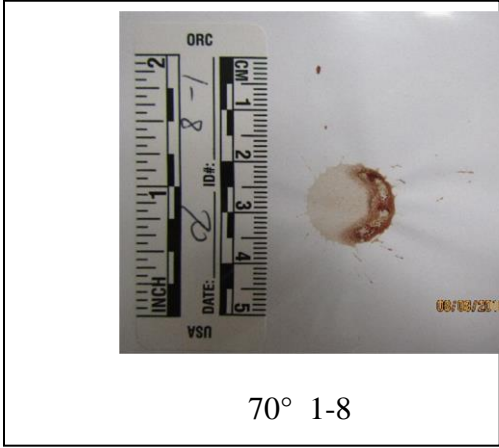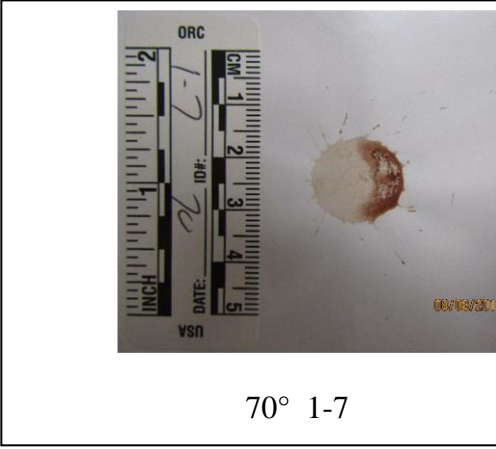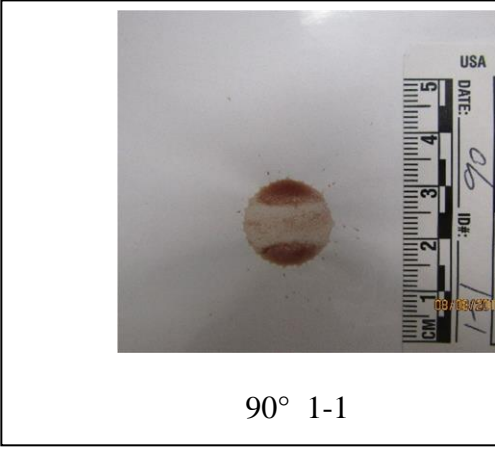
90° 1-1
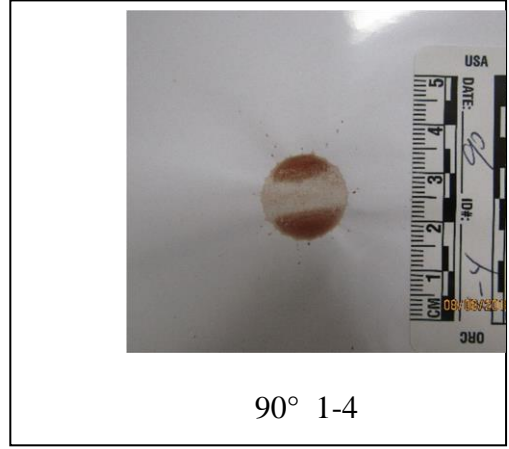
90° 1-4

90° 1-2

90° 1-5

90° 1-3

90° 1-6

251

90° 1-7

90° 1-10

90° 1-8

90° 1-9

10° 3-1

10° 3-4

10° 3-2

10° 3-5

10° 3-3

10° 3-6

253

10° 3-7

10° 3-10

10° 3-8

10° 3-9

254

25° 3-1

25° 3-2

25° 3-3

25° 3-4

25° 3-5

25° 3-6

255
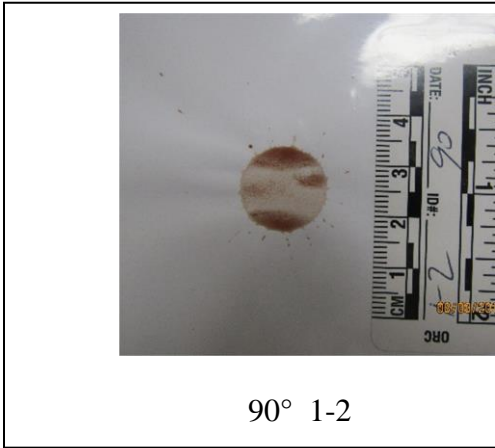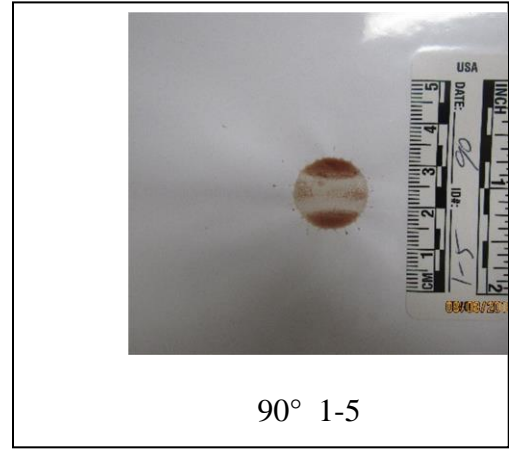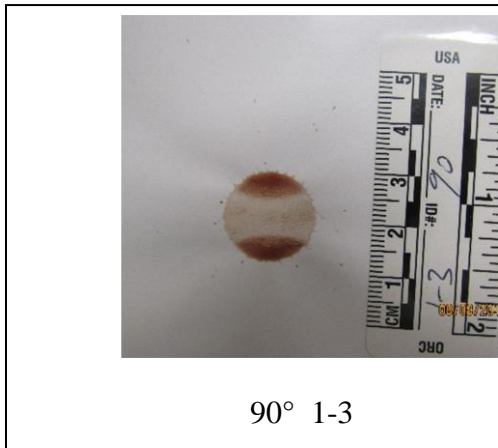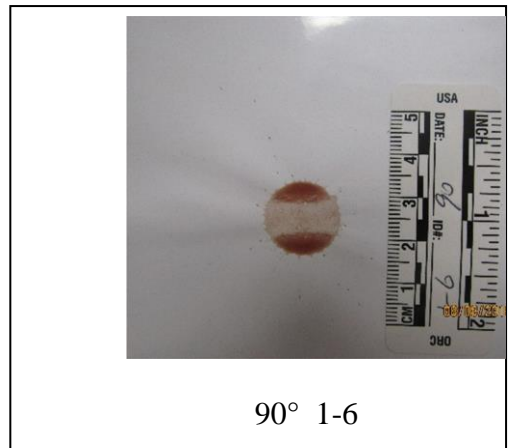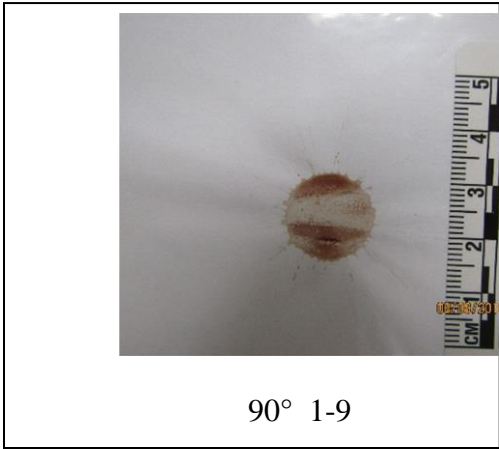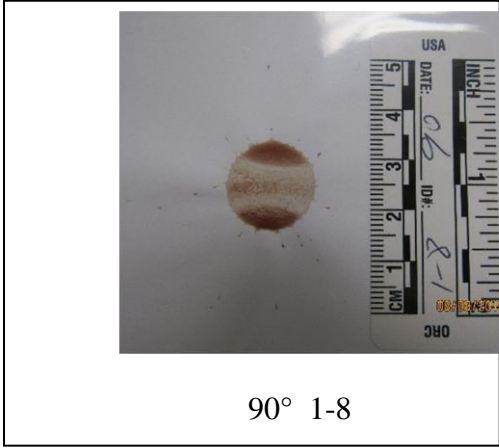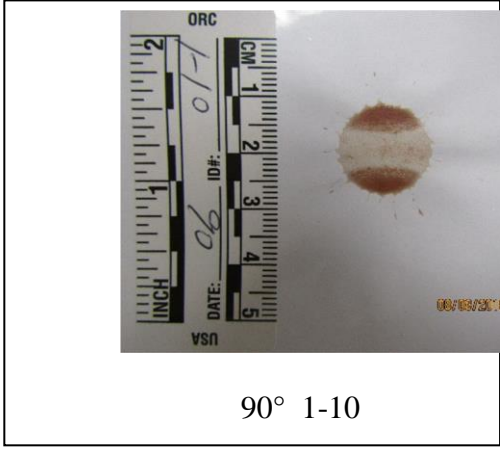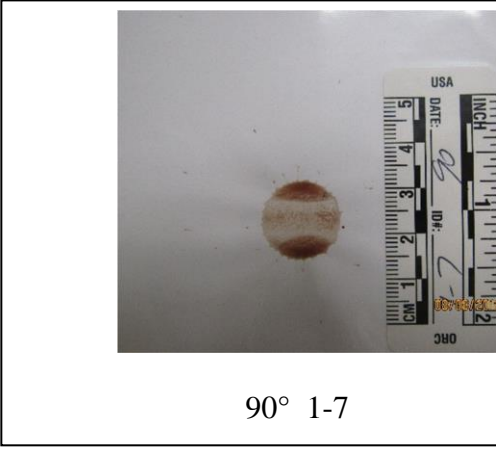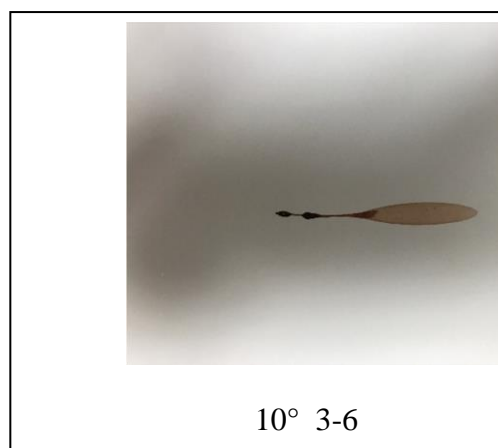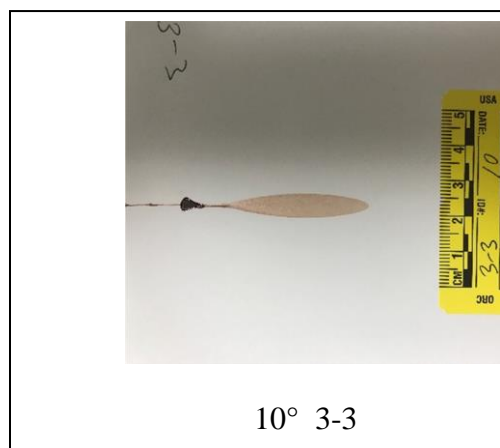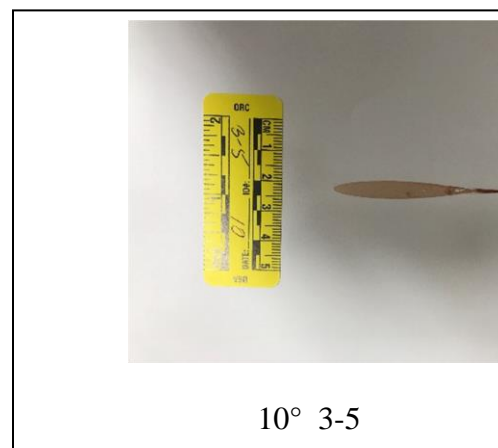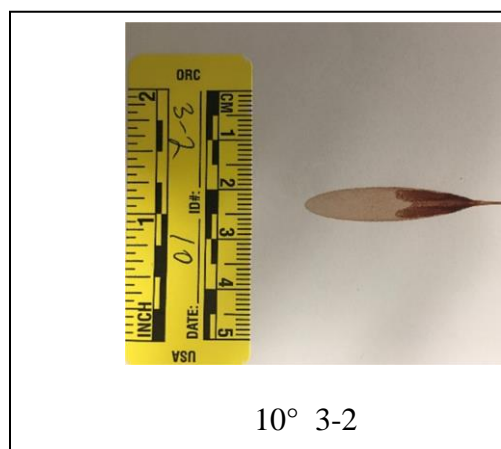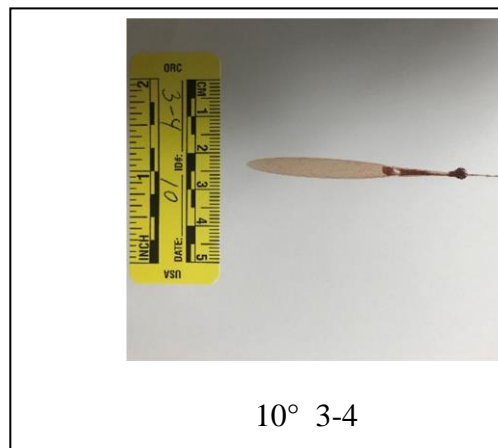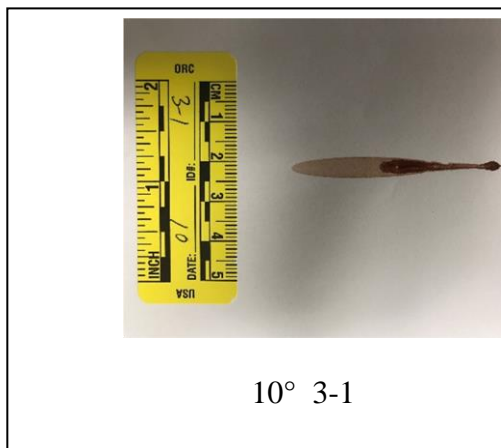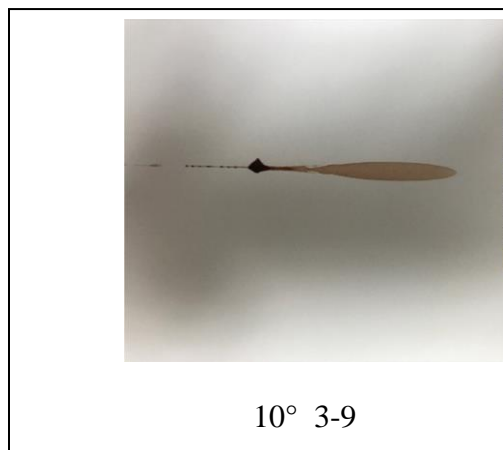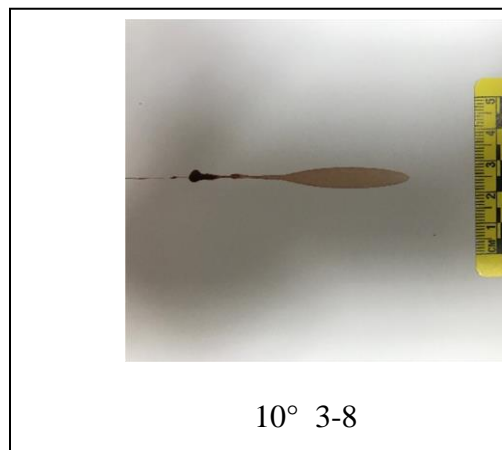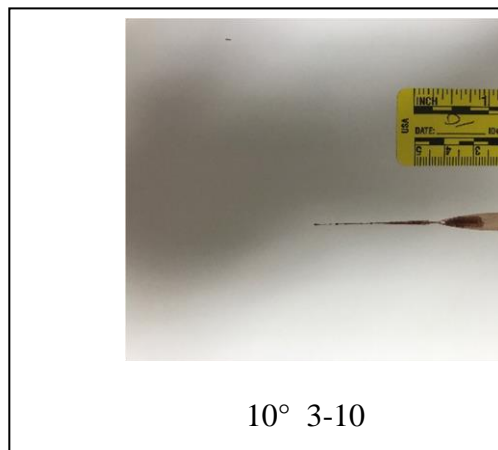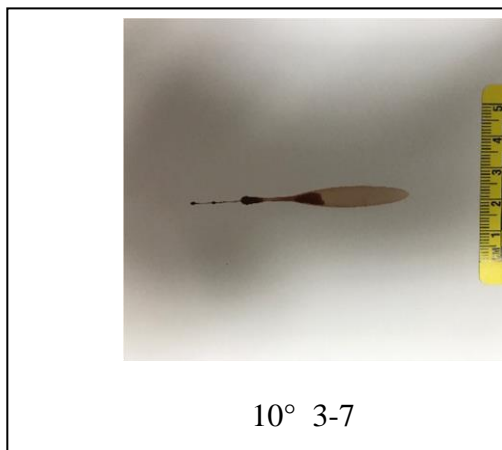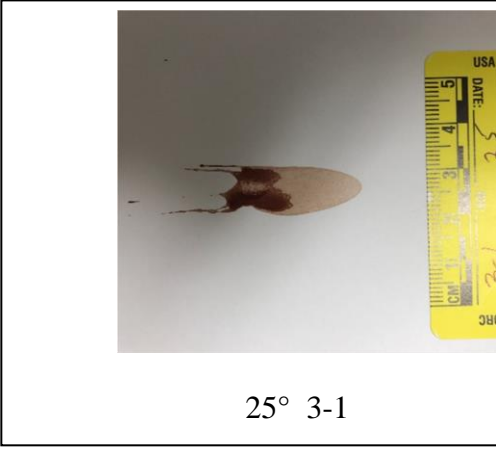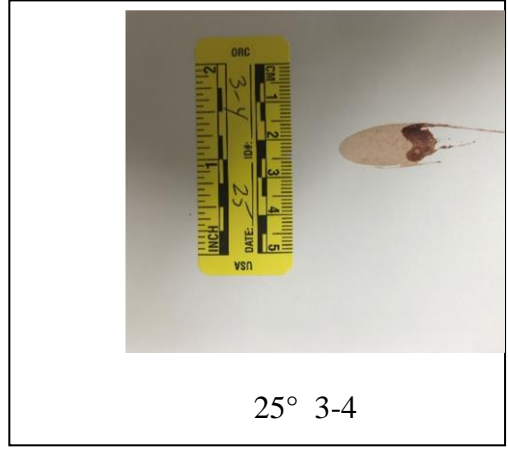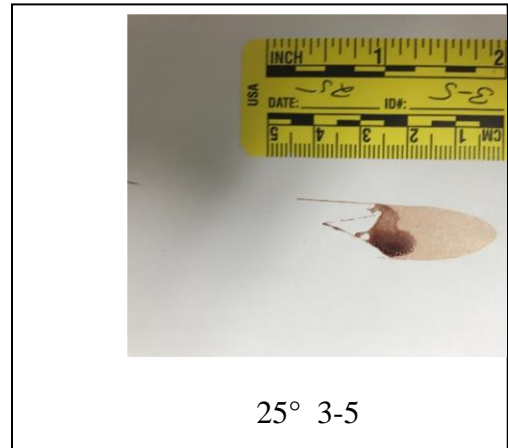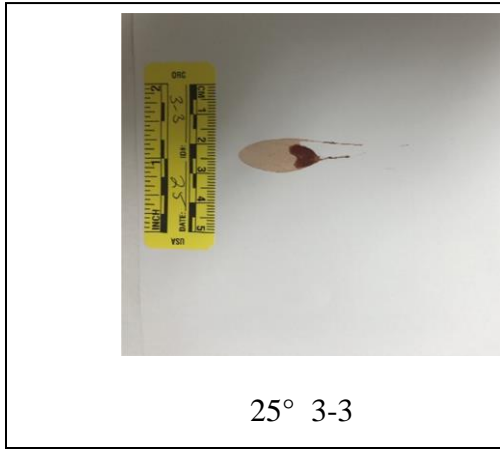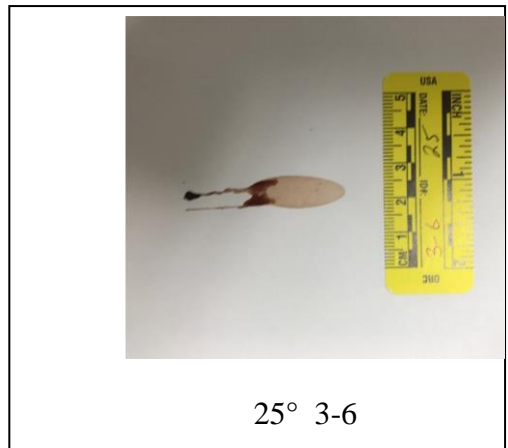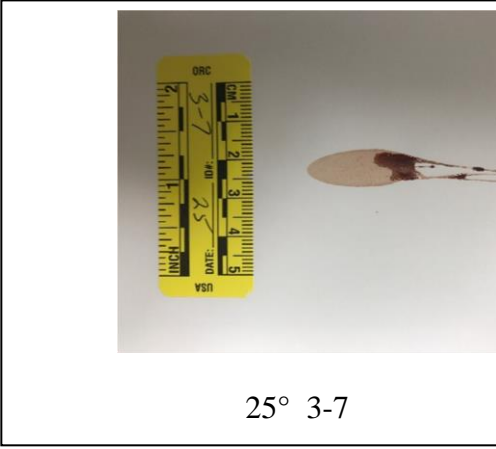
25° 3-7
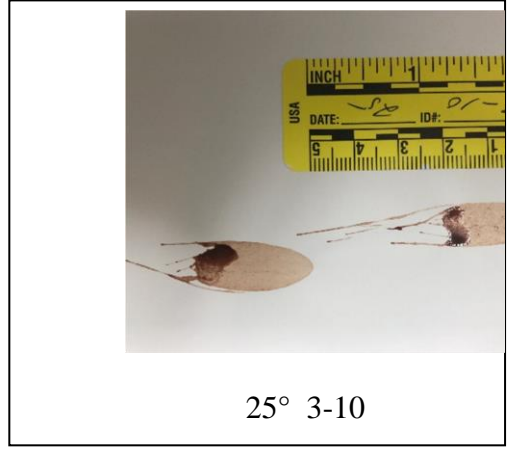
25° 3-10
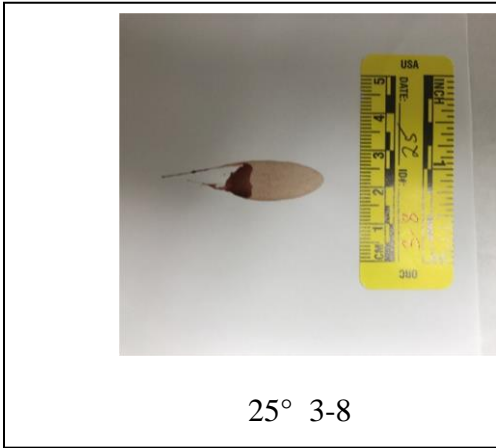
25° 3-8
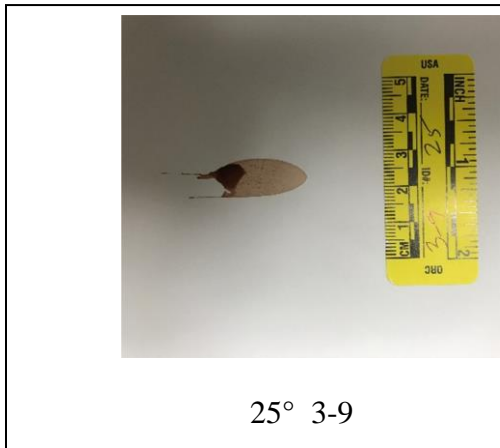
25° 3-9
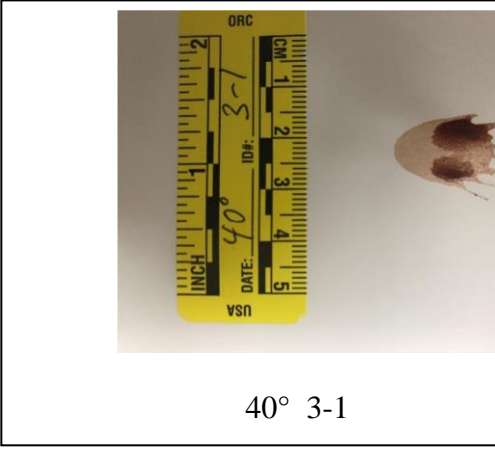
40° 3-1

40° 3-4

40° 3-2

40° 3-5

40° 3-3

40° 3-6

257

40° 3-7

40° 3-10

40° 3-8

40° 3-9

258

55° 3-1

55° 3-4

55° 3-2

55° 3-5

55° 3-3

55° 3-6

55° 3-7

55° 3-10

55° 3-8

55° 3-9
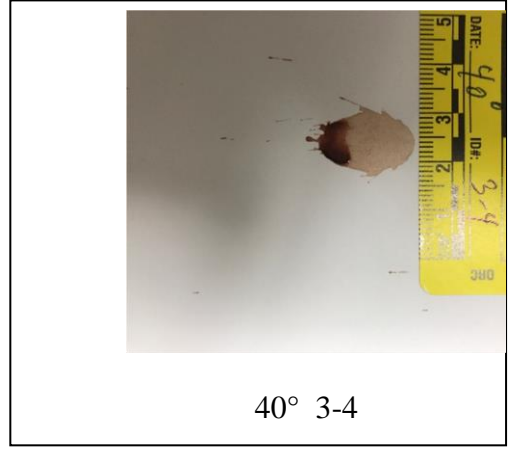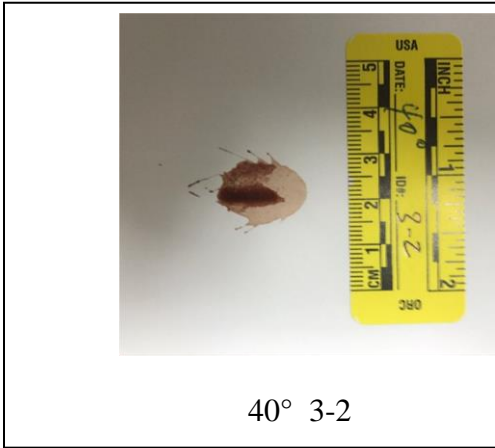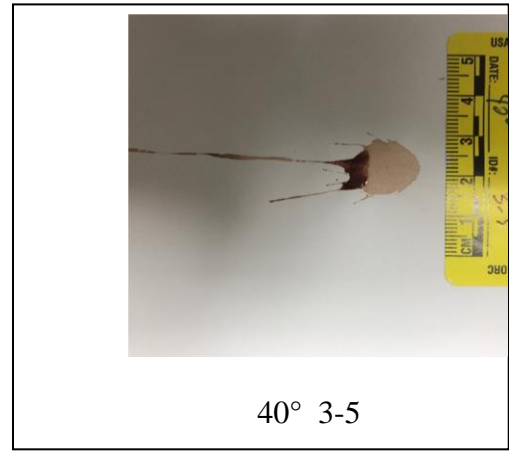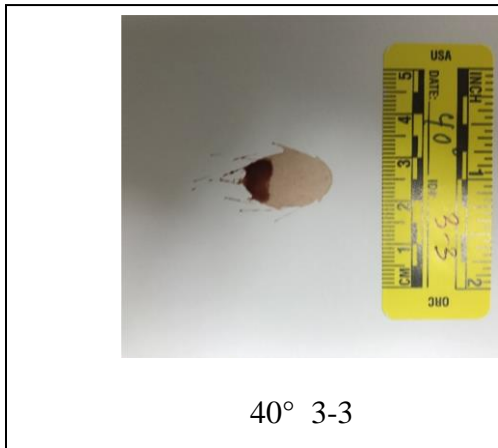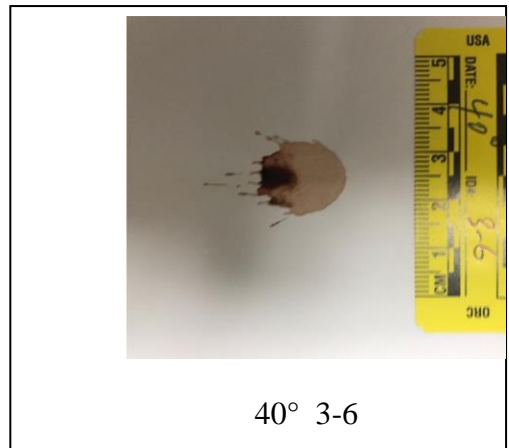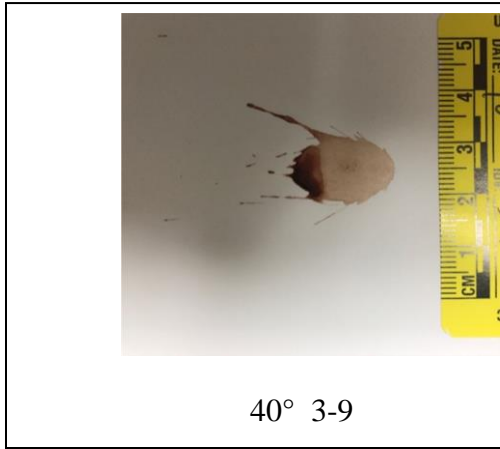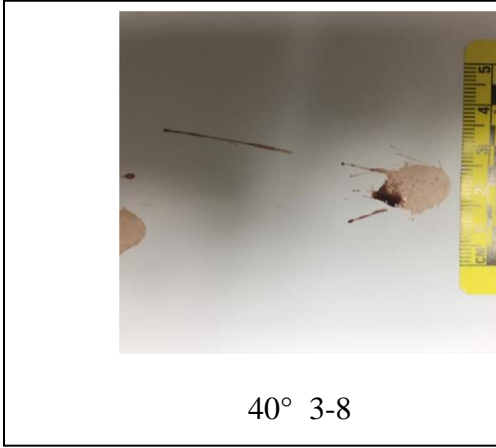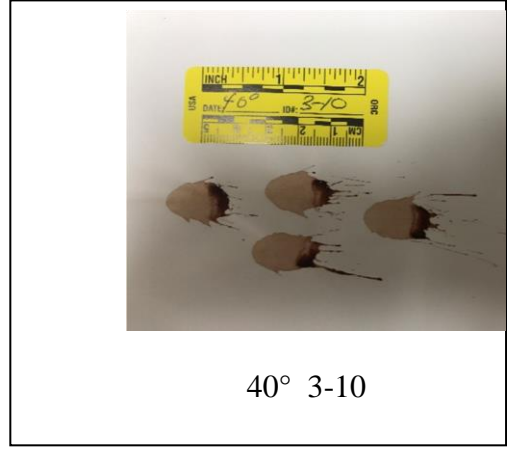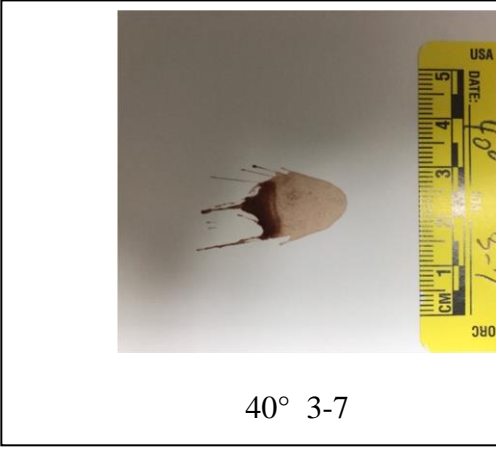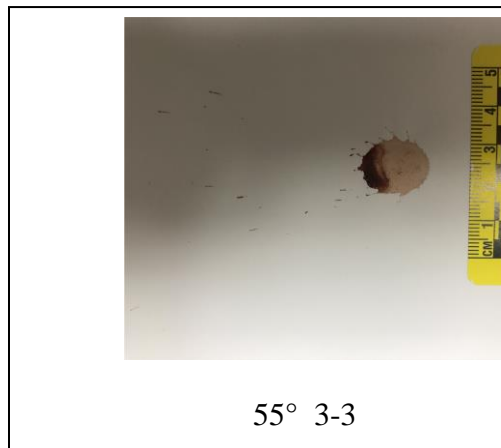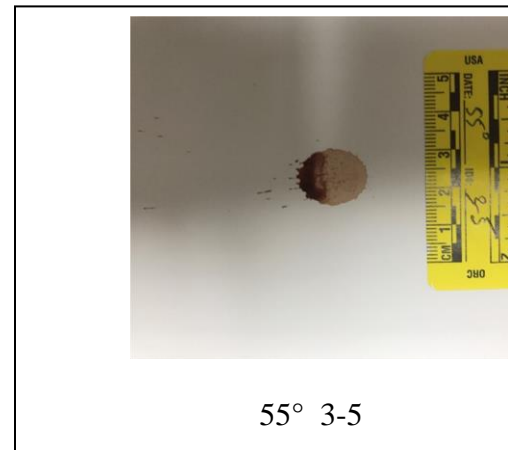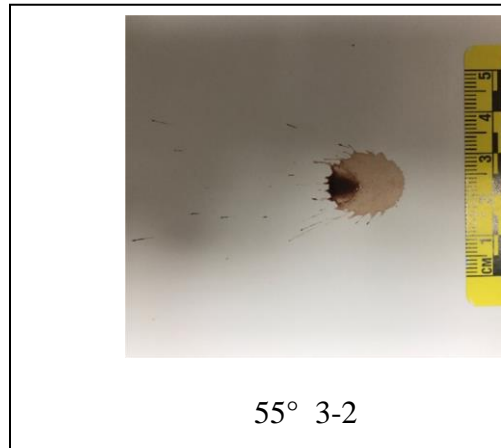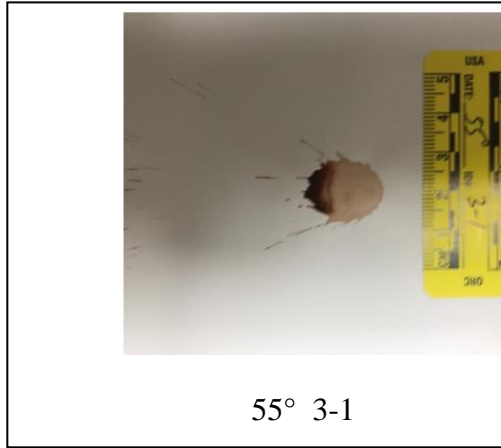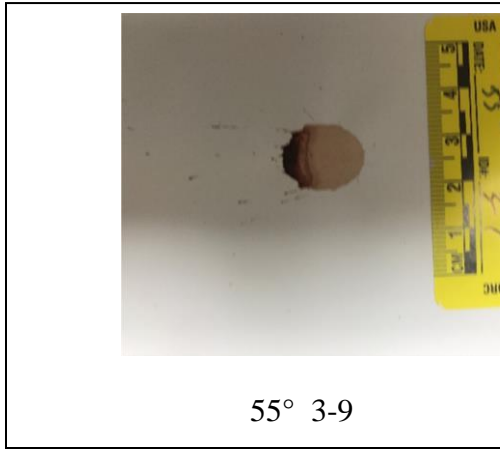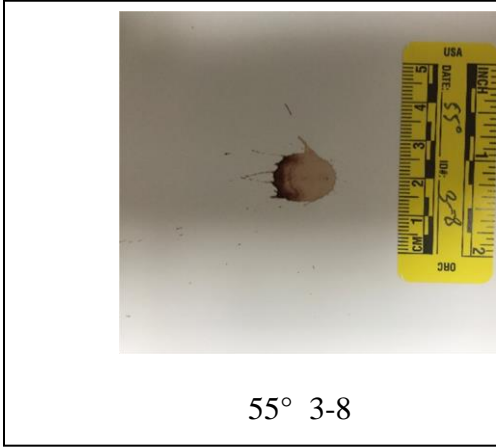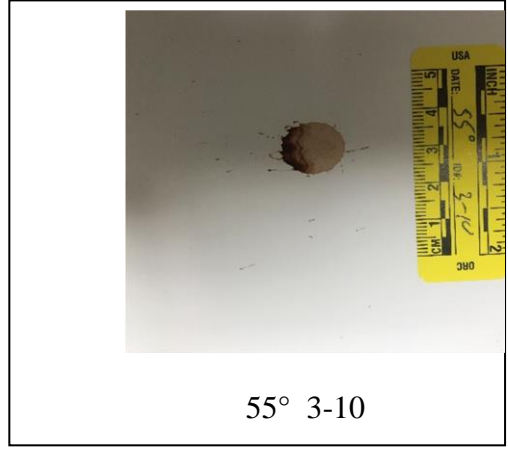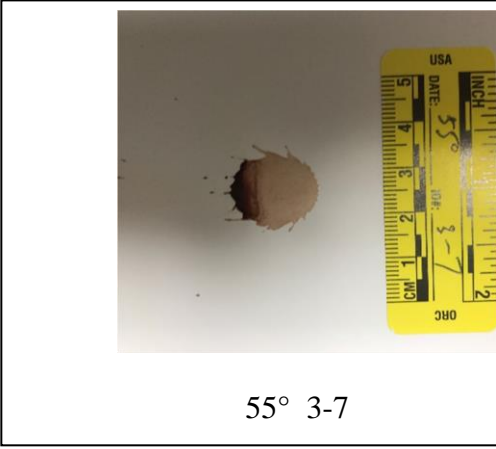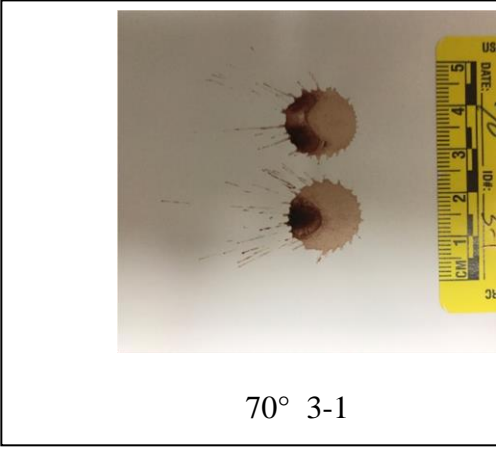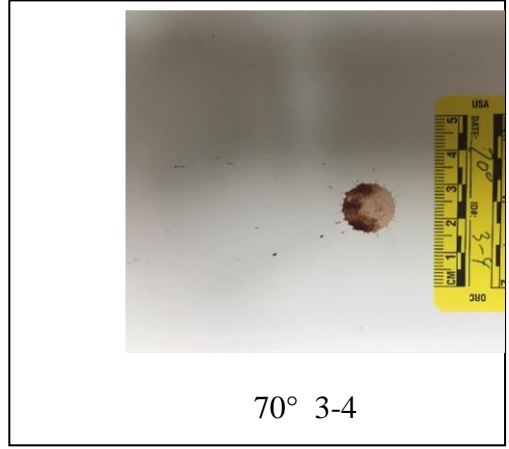
70° 3-1

70° 3-4
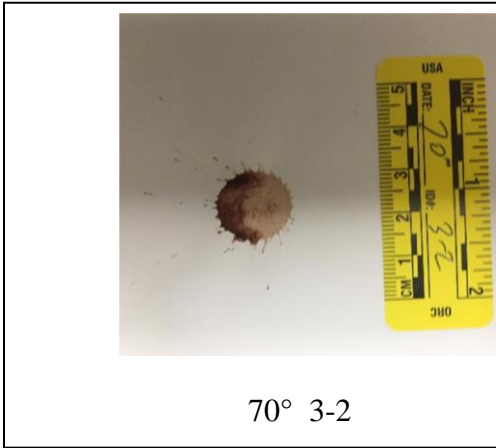
70° 3-2

70° 3-5

70° 3-3

70° 3-6

261
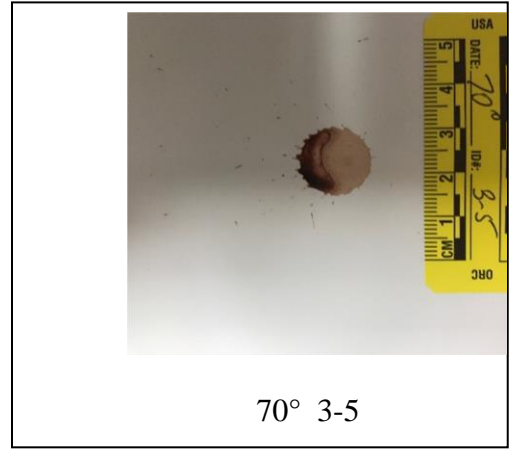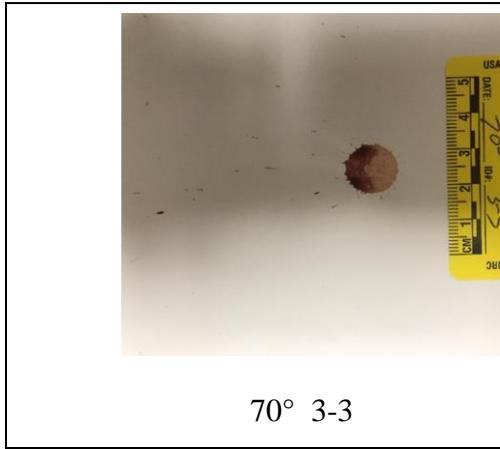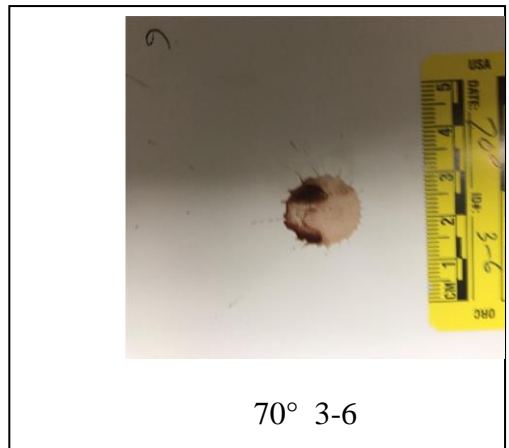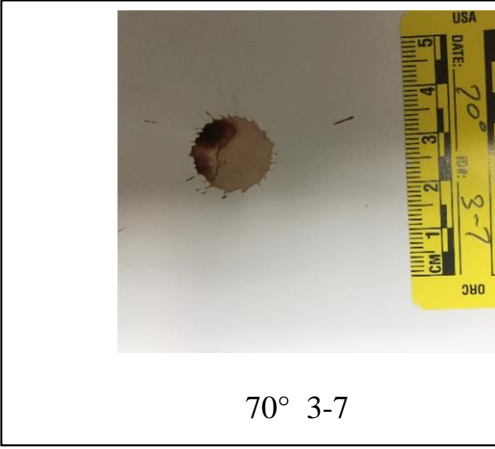
70° 3-7

70° 3-10

70° 3-8

70° 3-9

262
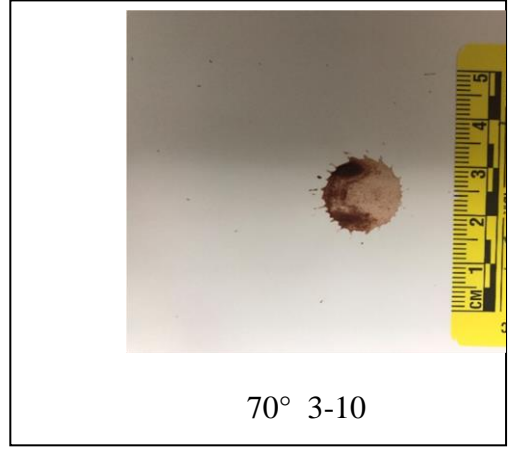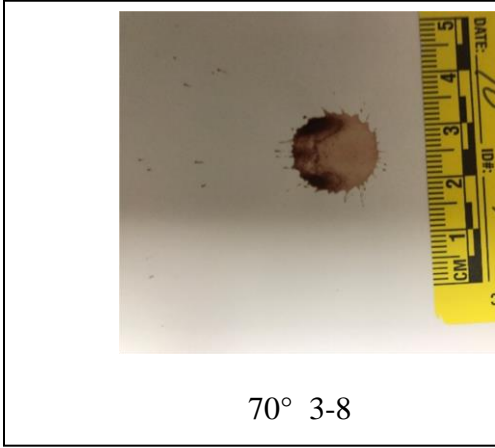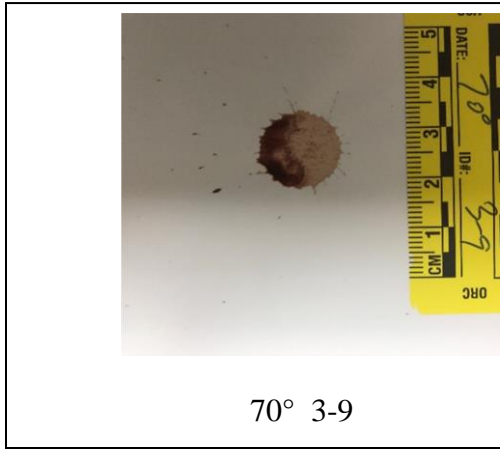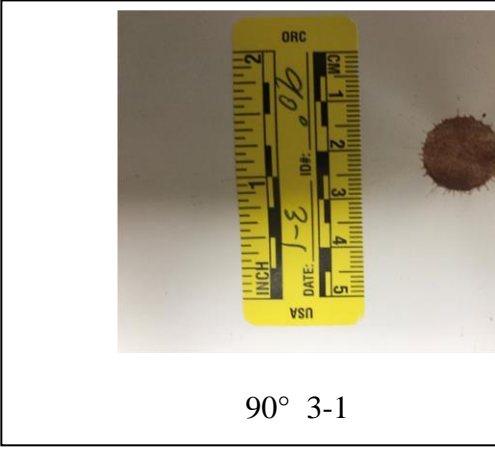
90° 3-1

90° 3-4

90° 3-2

90° 3-5

90° 3-3

90° 3-6

263

90° 3-7

90° 3-10

90° 3-8

90° 3-9

264

10° 5-1

10° 5-4

10° 5-2

10° 5-5

10° 5-3

10° 5-6

265
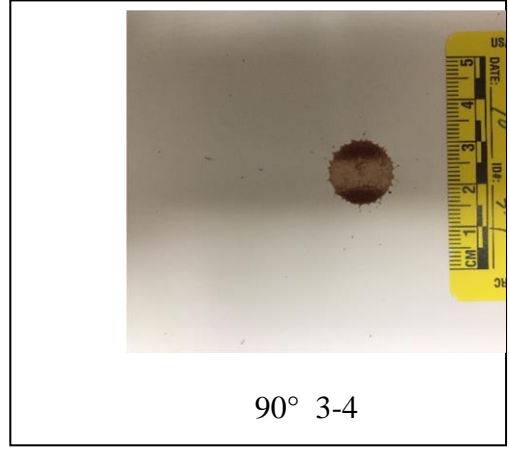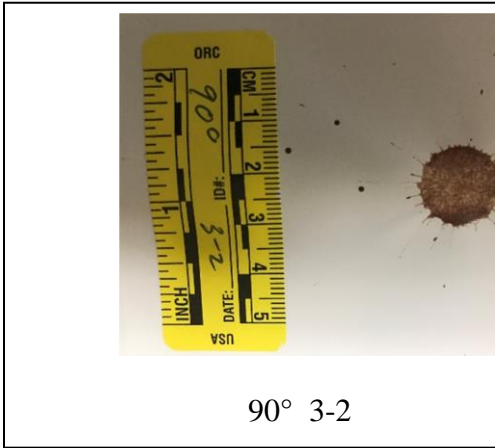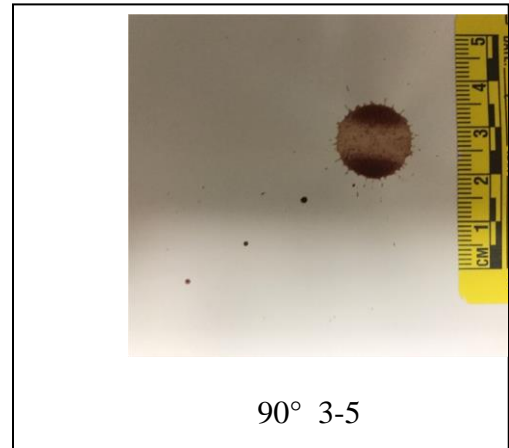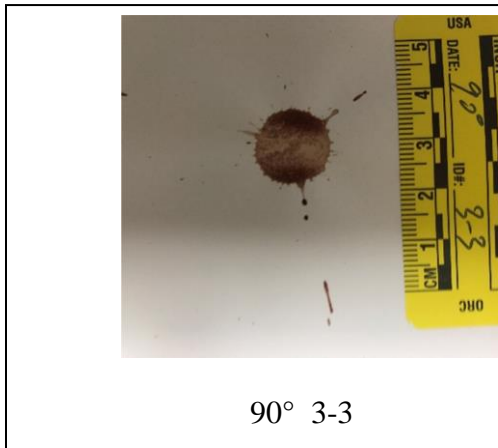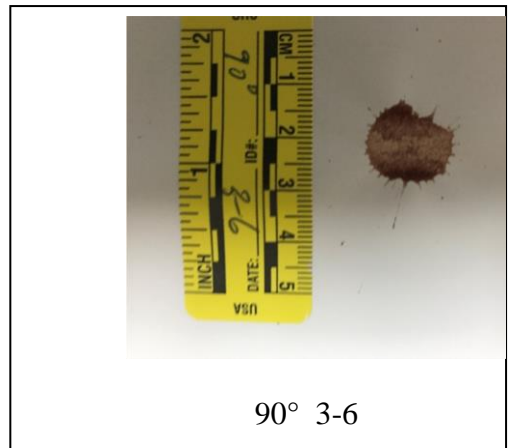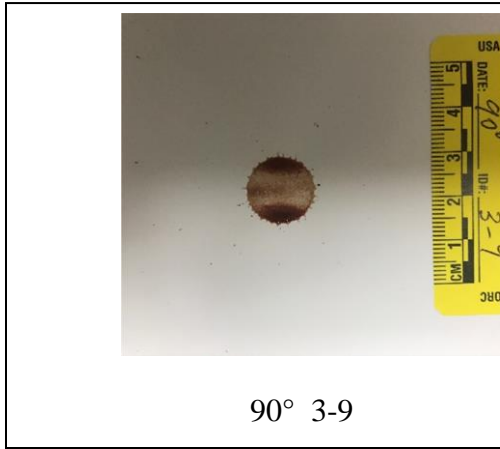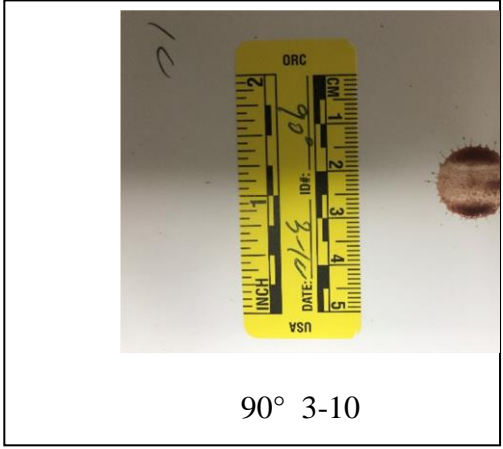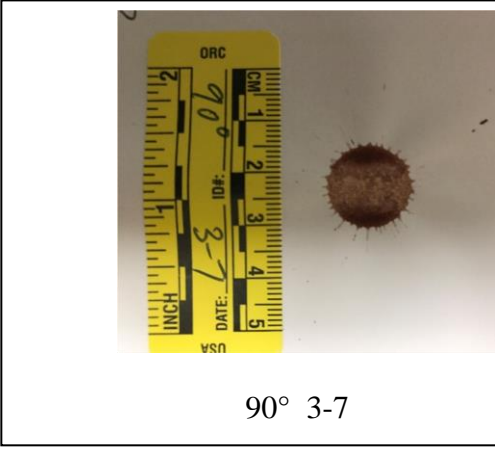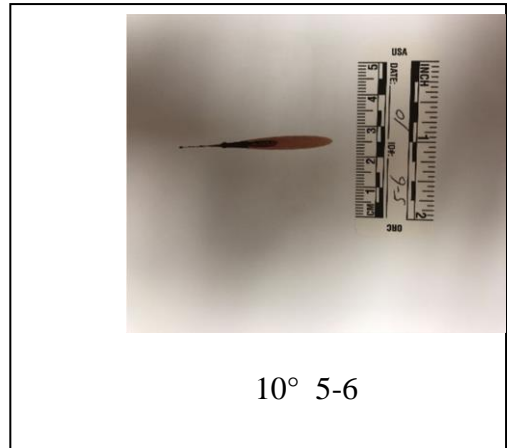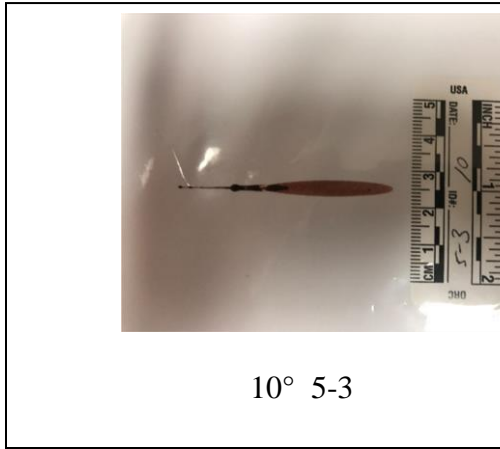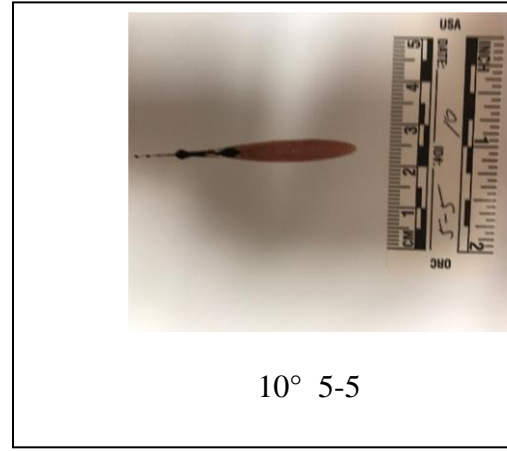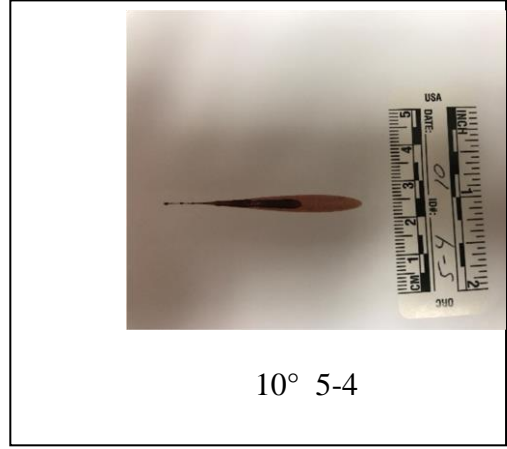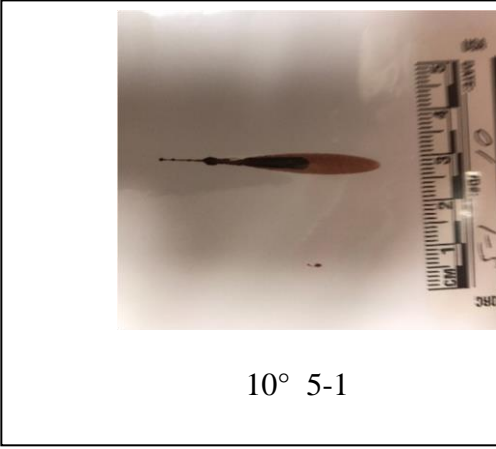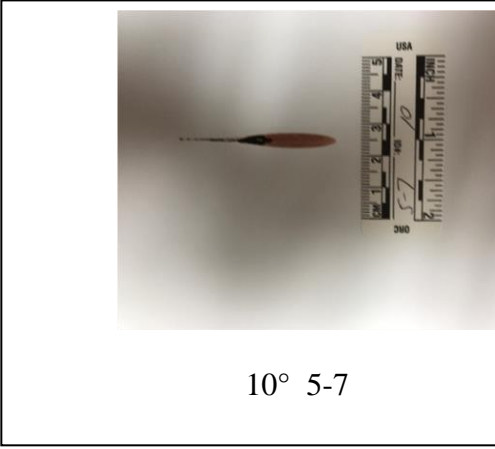
10° 5-7
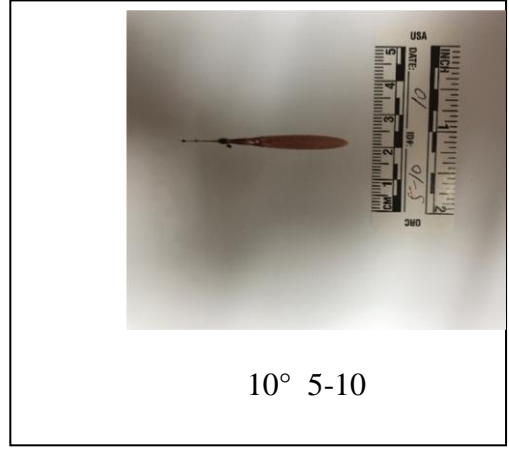
10° 5-10
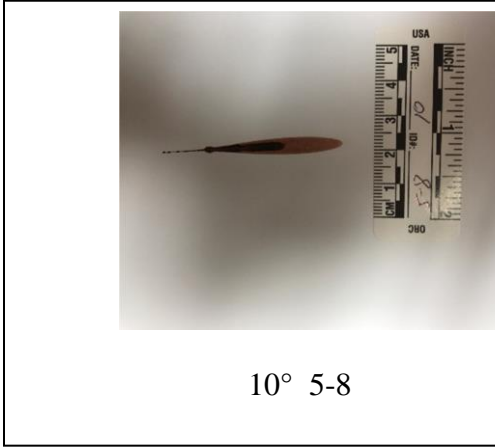
10° 5-8
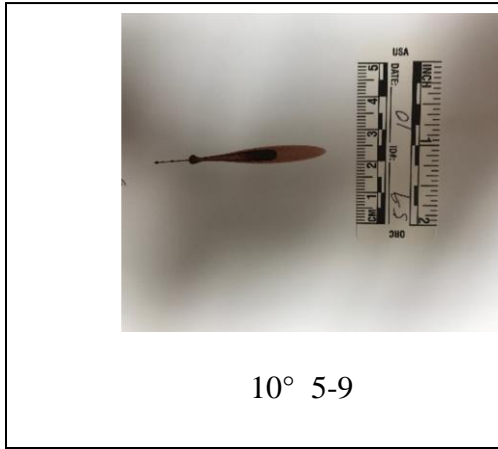
10° 5-9
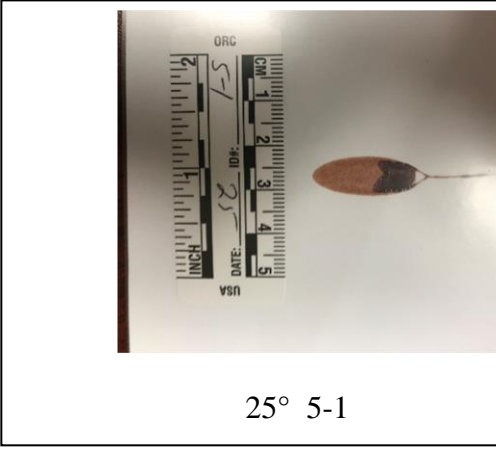
25° 5-1
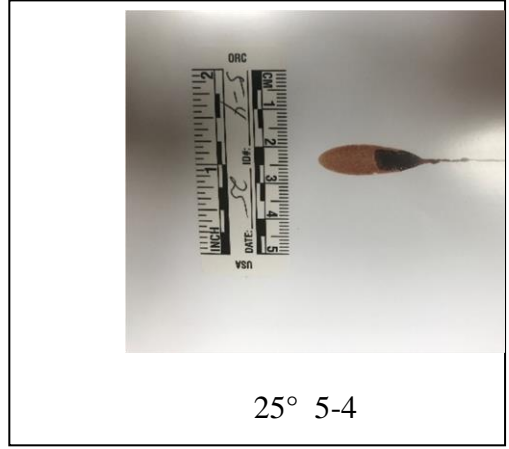
25° 5-4
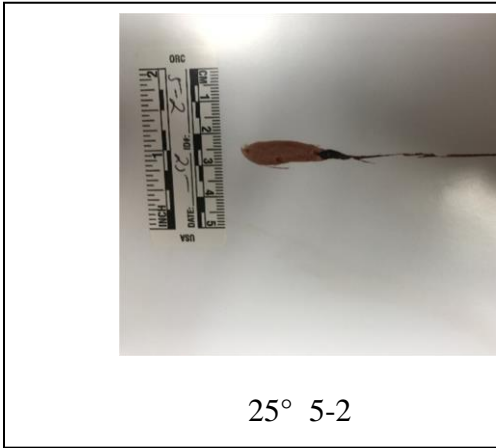
25° 5-2

25° 5-5

25° 5-3

25° 5-6

25° 5-7

25° 5-10

25° 5-8

25° 5-9

268
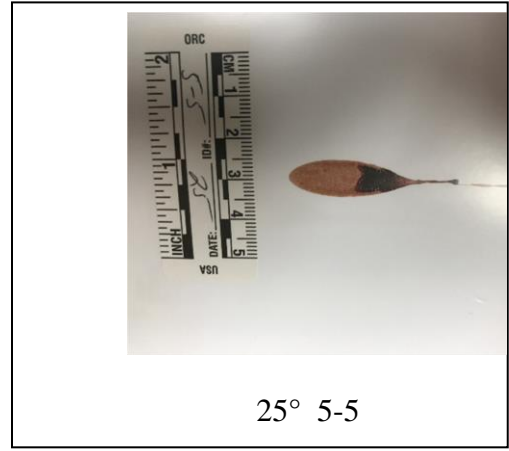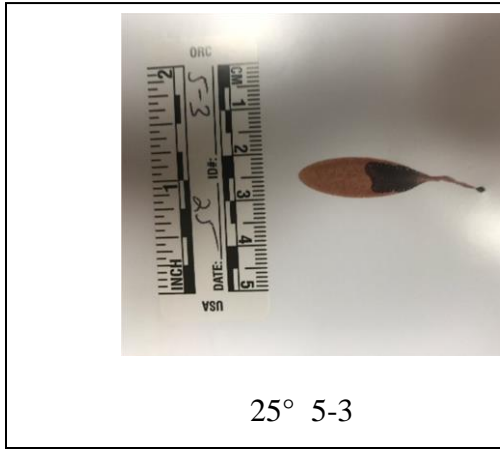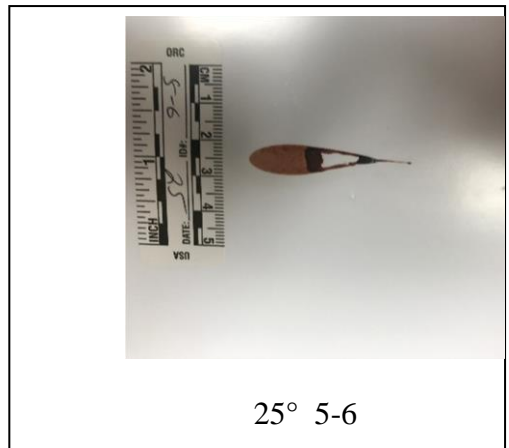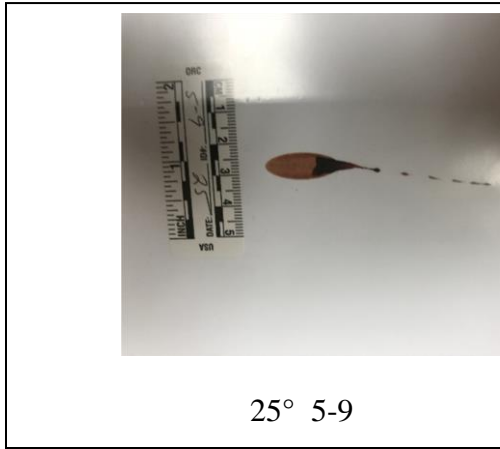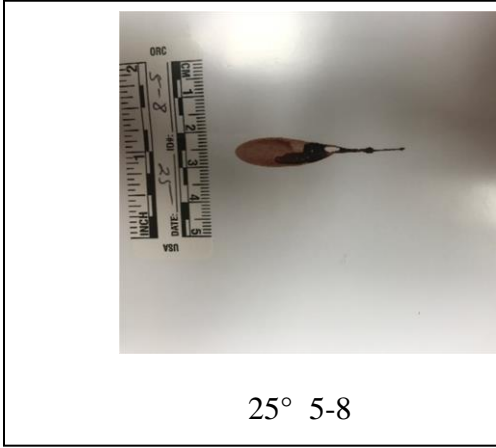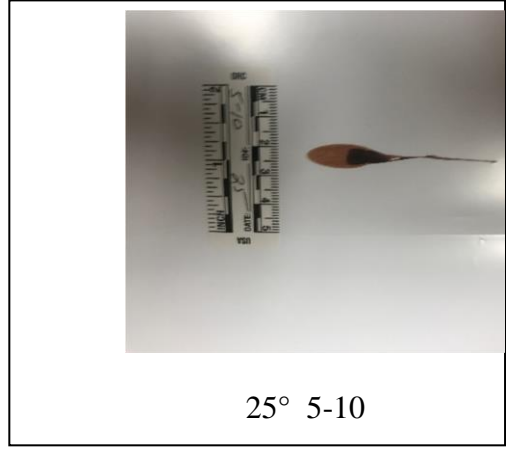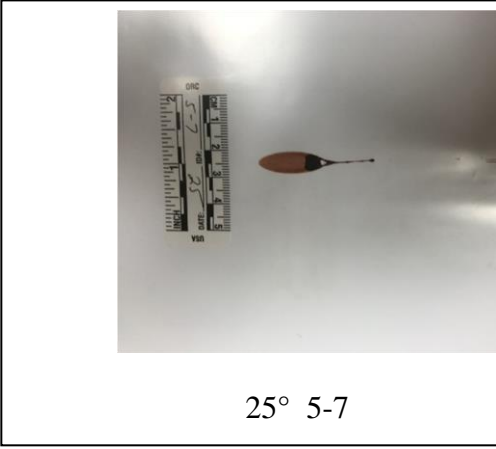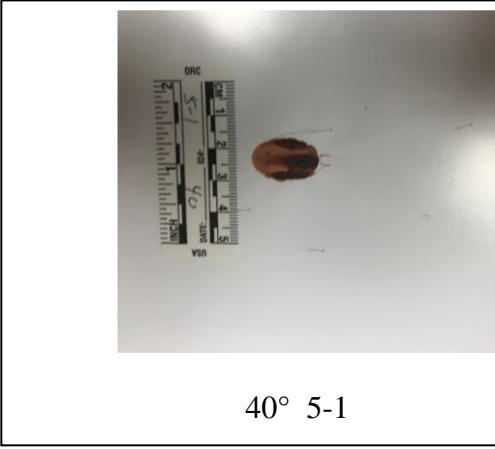
40° 5-1
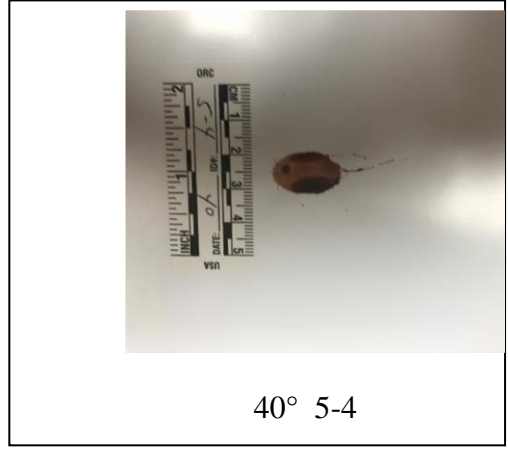
40° 5-4
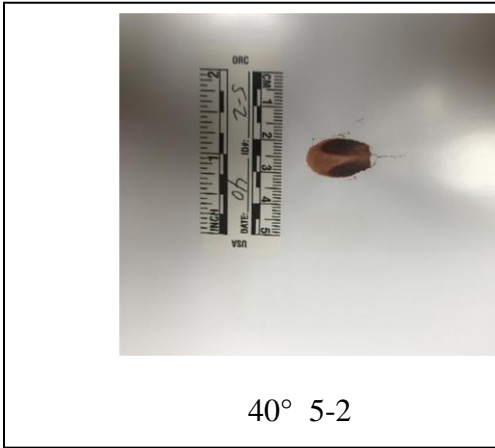
40° 5-2

40° 5-5

40° 5-3

40° 5-6

269

40° 5-7

40° 5-10

40° 5-8

40° 5-9
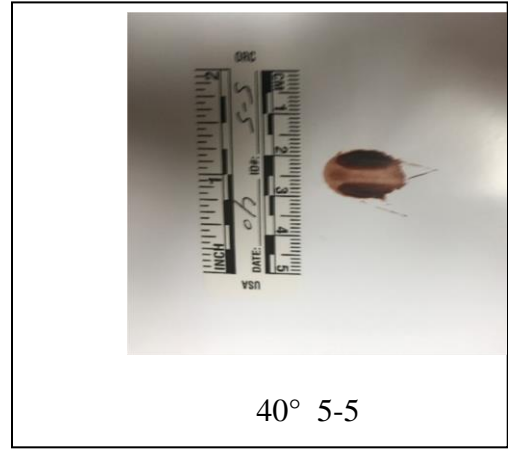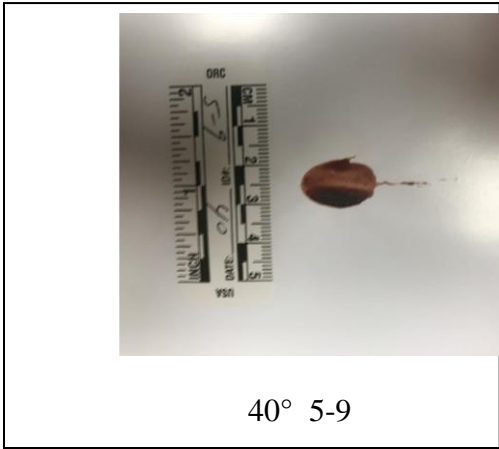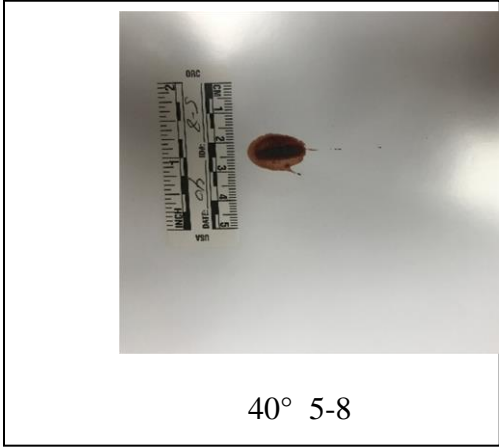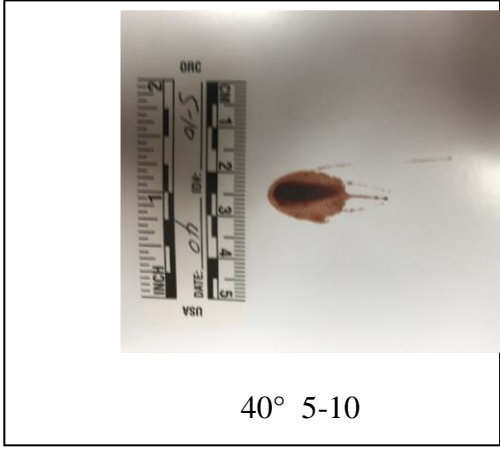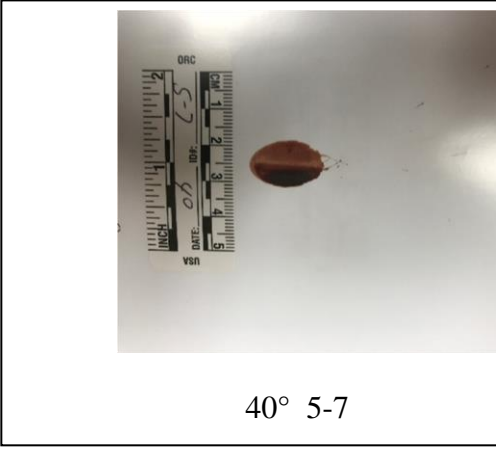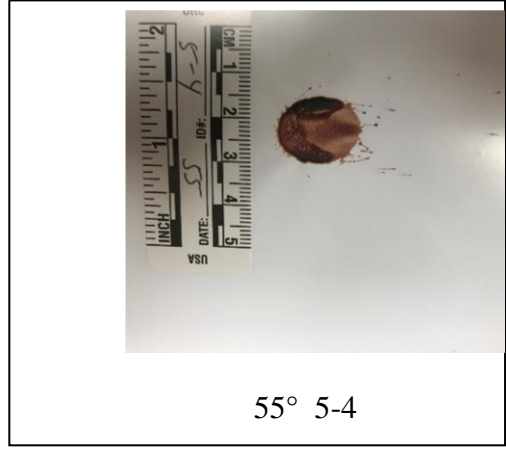
55° 5-1

55° 5-4
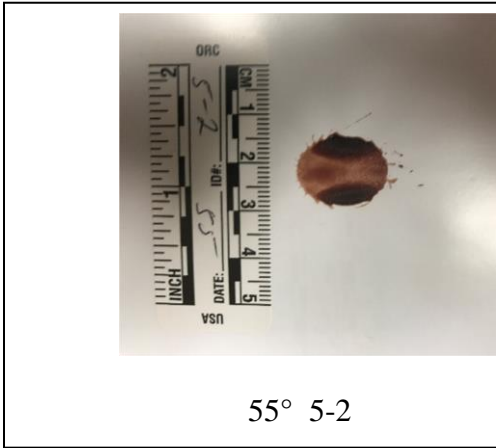
55° 5-2
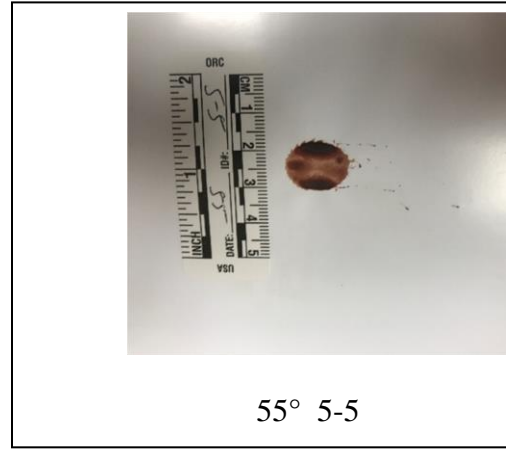
55° 5-5
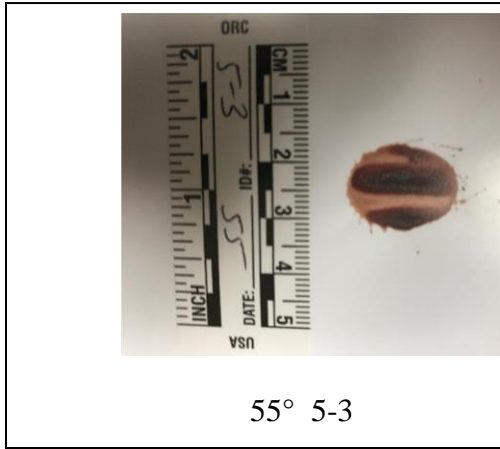
55° 5-3
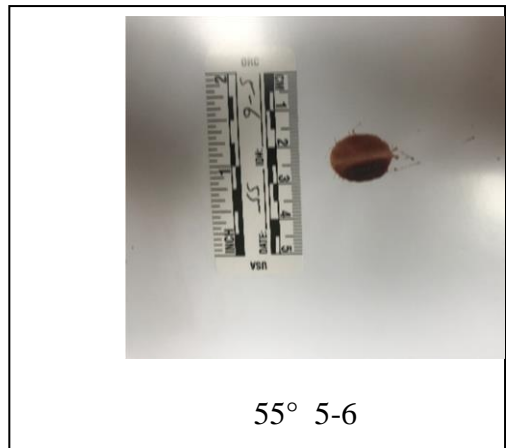
55° 5-6

55° 5-7

55° 5-10

55° 5-8

55° 5-9

70° 5-1

70° 5-2

70° 5-3

70° 5-4

70° 5-5

70° 5-6

273

70° 5-7

70° 5-10

70° 5-8

70° 5-9

274
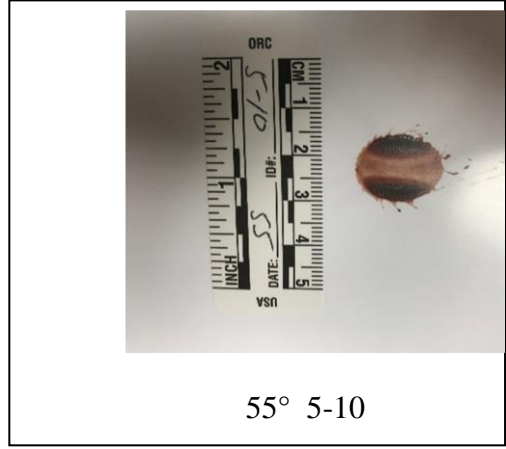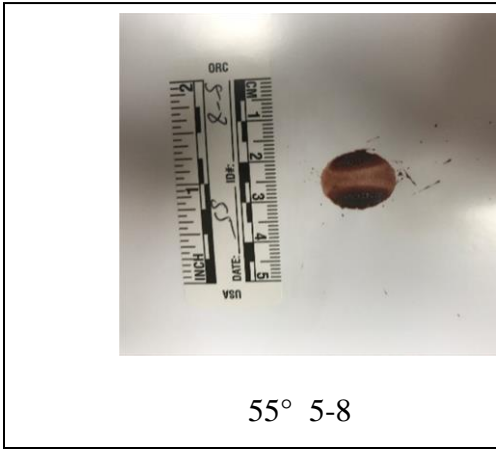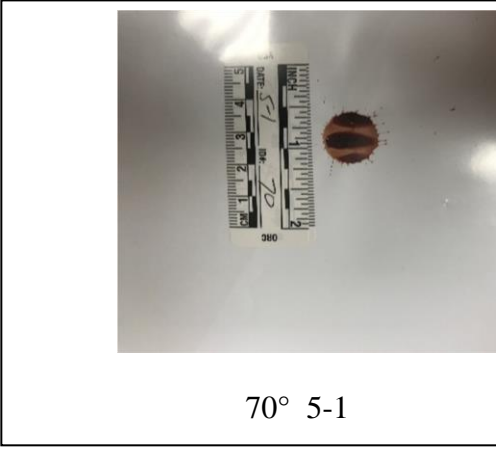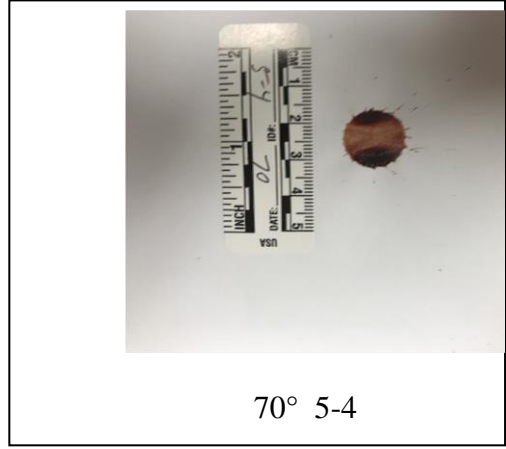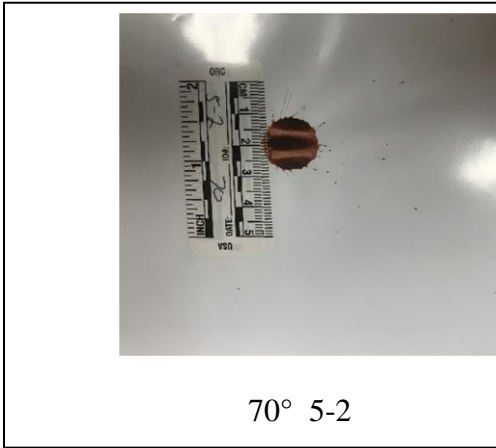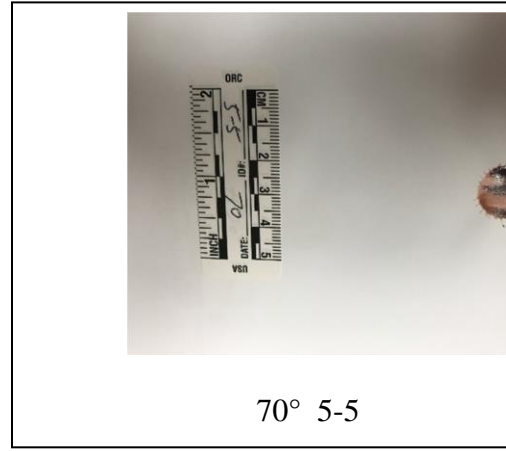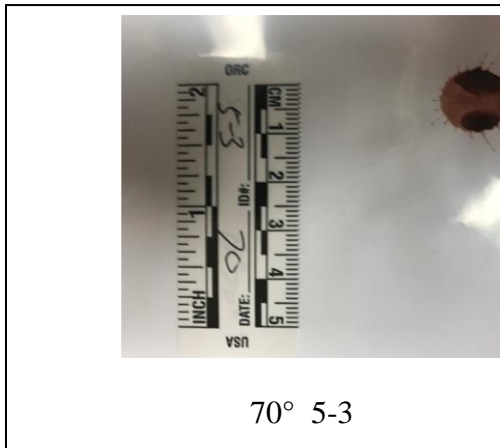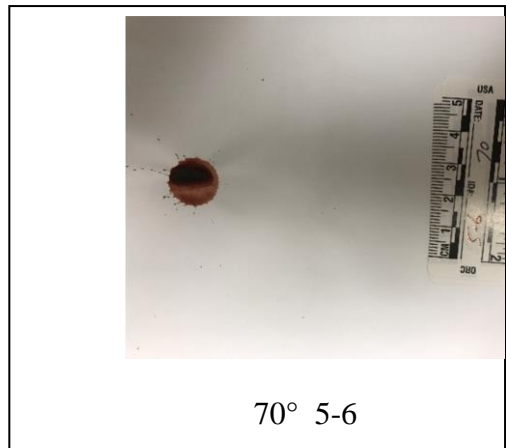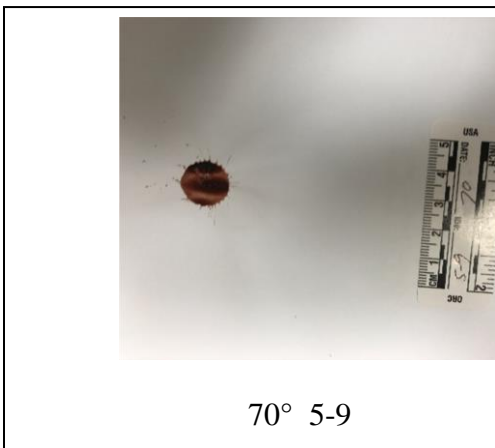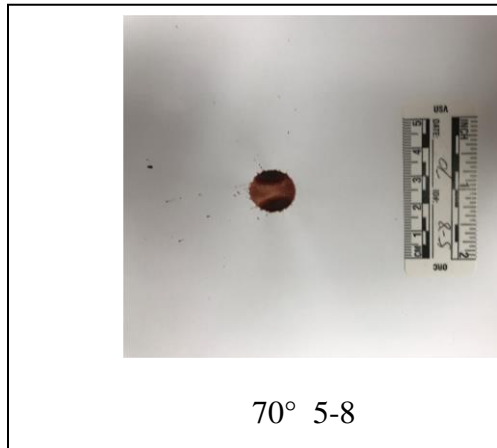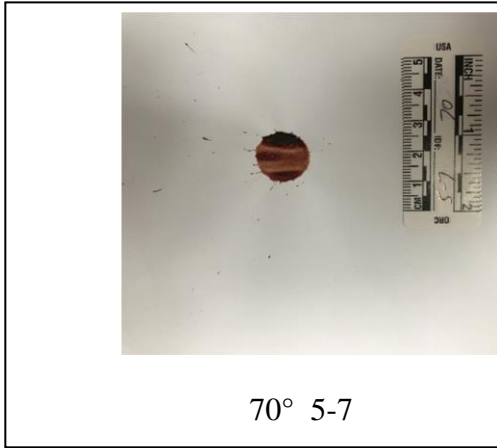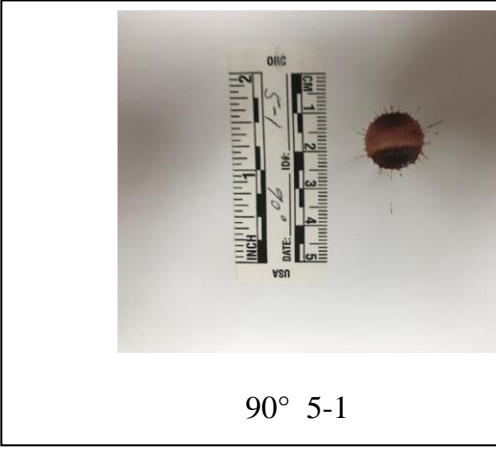
90° 5-1

90° 5-4

90° 5-2

90° 5-5

90° 5-3

90° 5-6

90° 5-7

90° 5-10

90° 5-8

90° 5-9

276

10° 6-1

10° 6-4

10° 6-2

10° 6-5

10° 6-3

10° 6-6

277

10° 6-7

10° 6-10

10° 6-8

10° 6-9

25° 6-1

25° 6-2

25° 6-3

25° 6-4

25° 6-5

25° 6-6

279

25° 6-7

25° 6-10

25° 6-8

25° 6-9
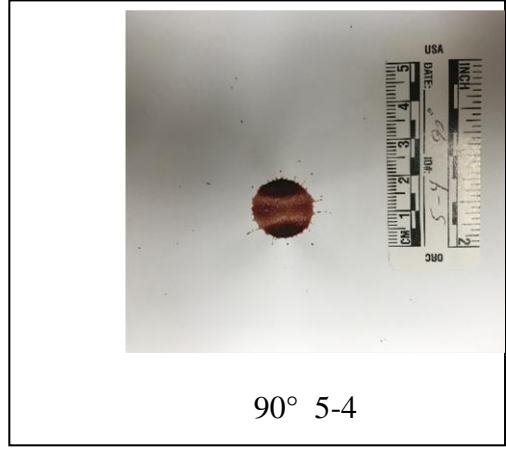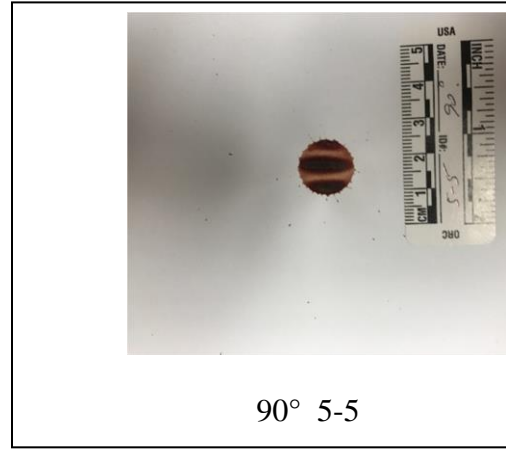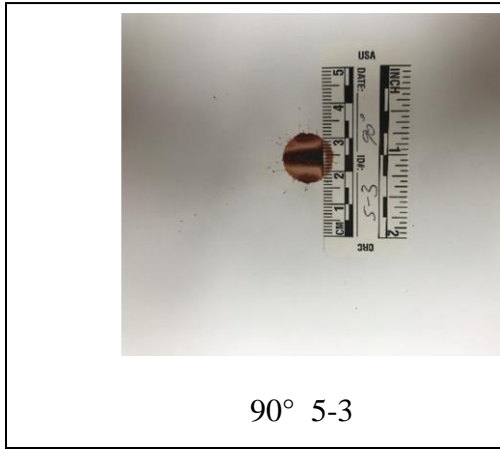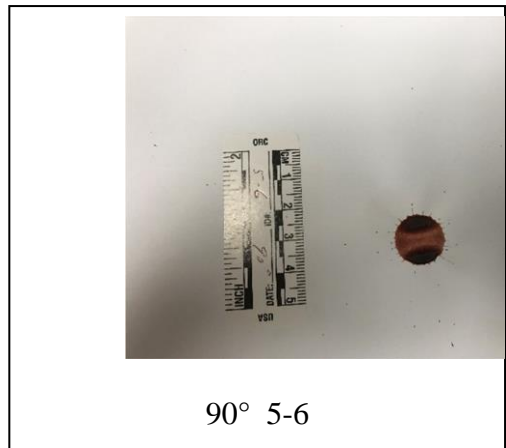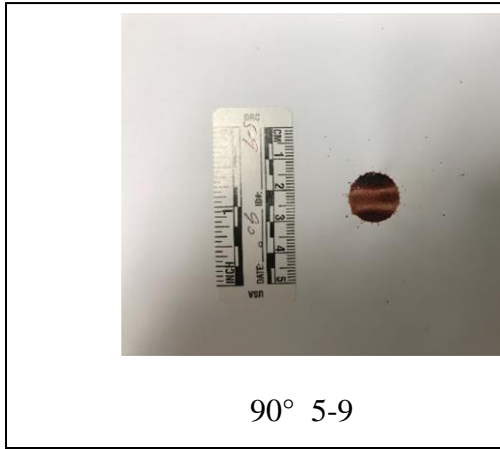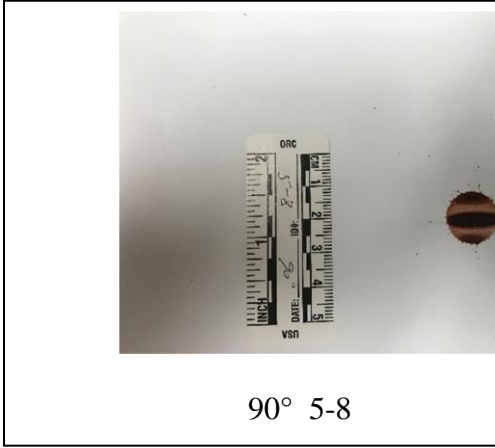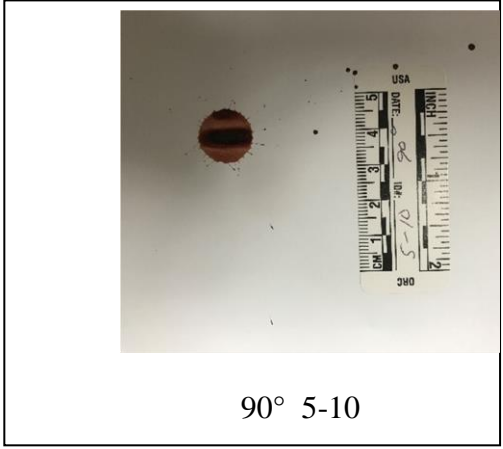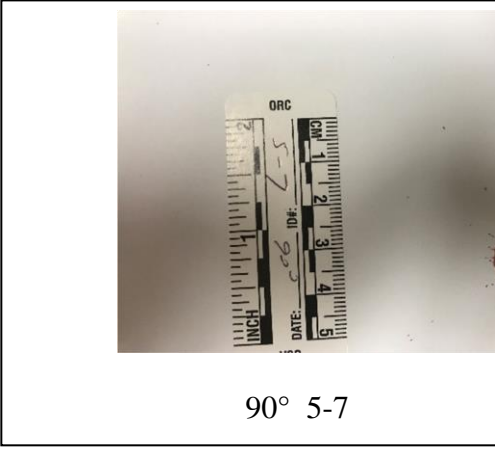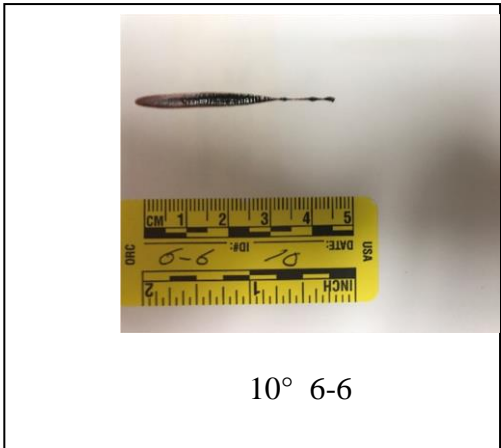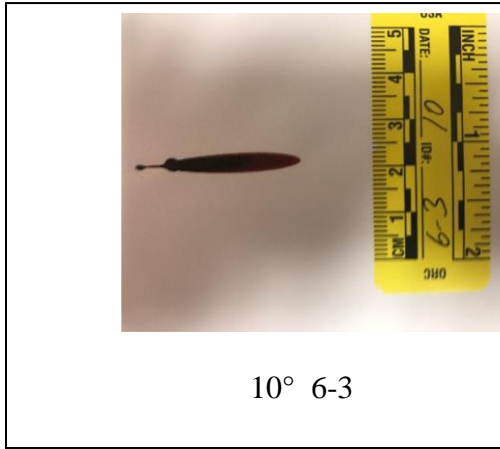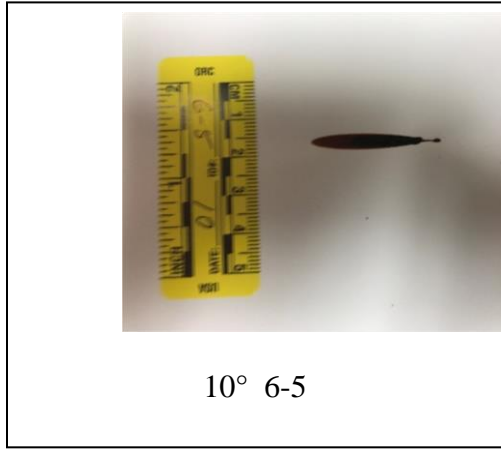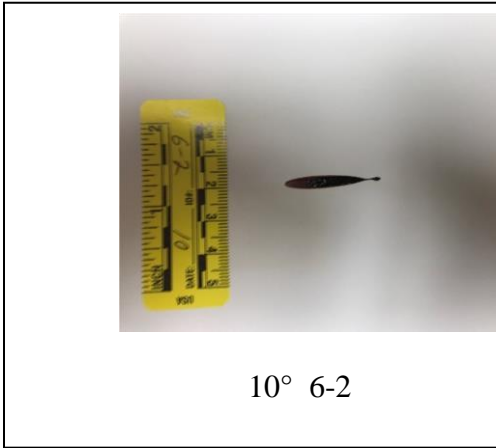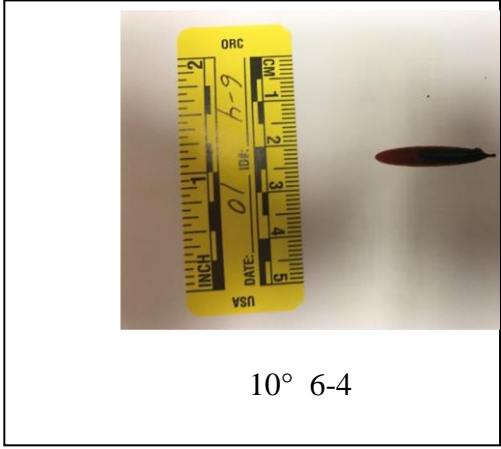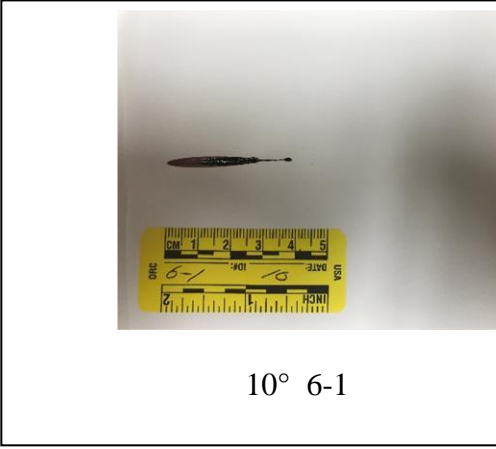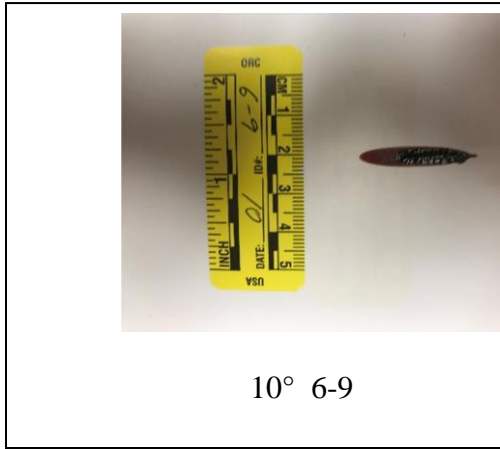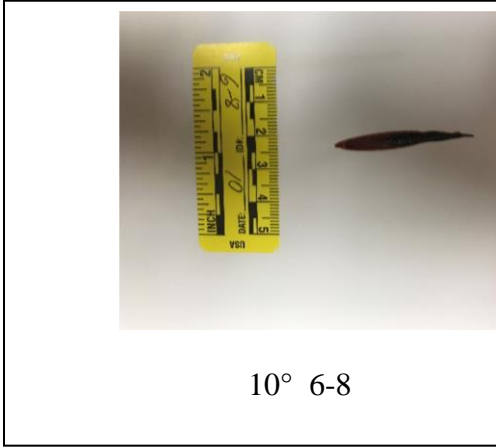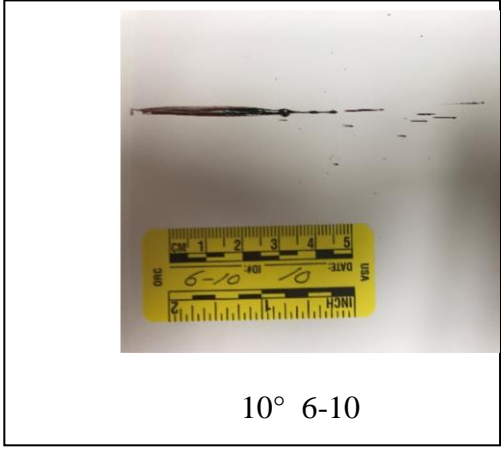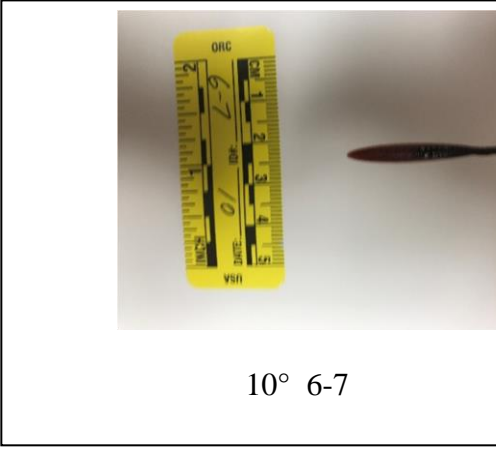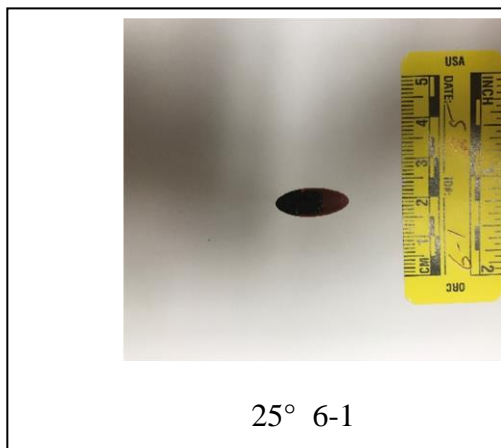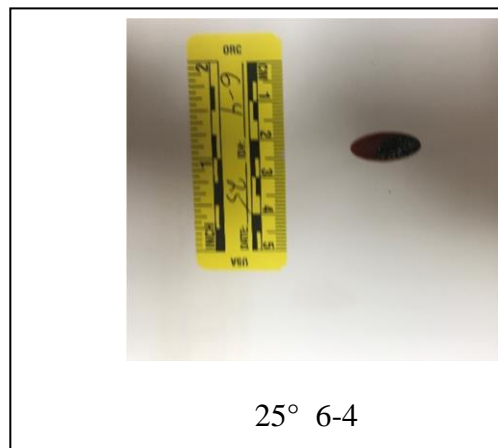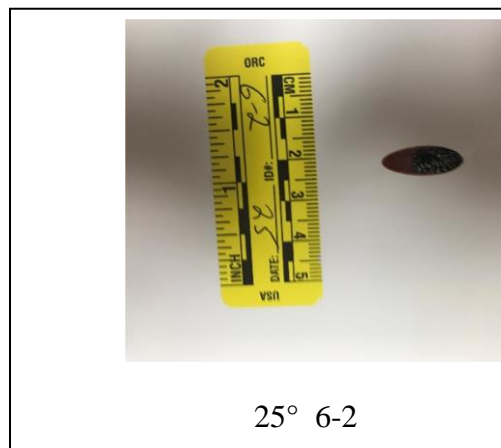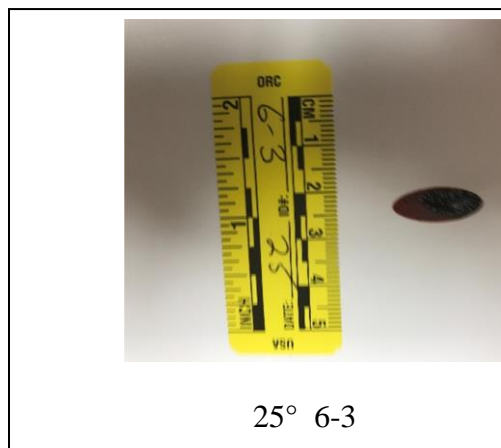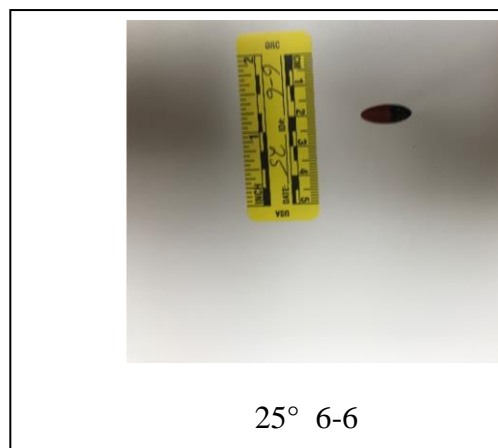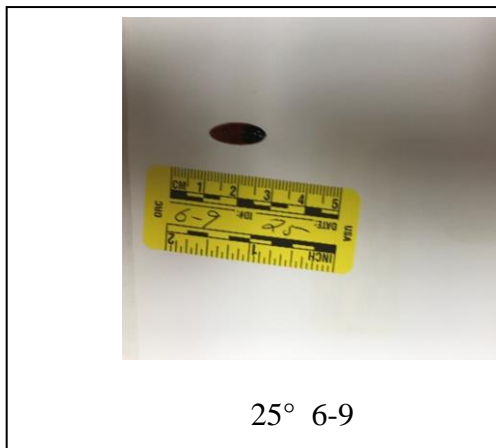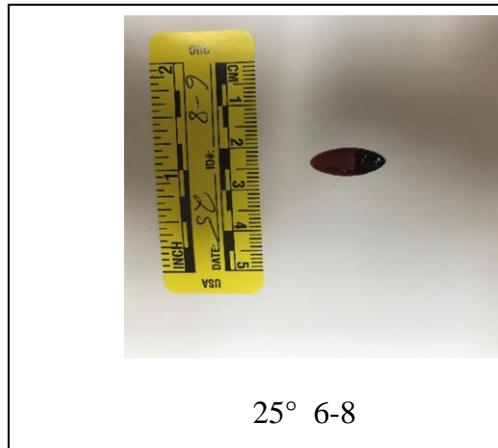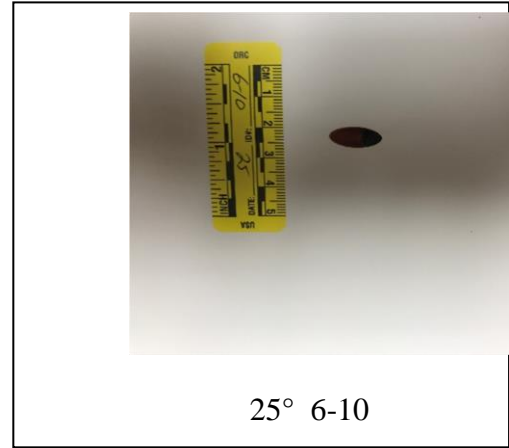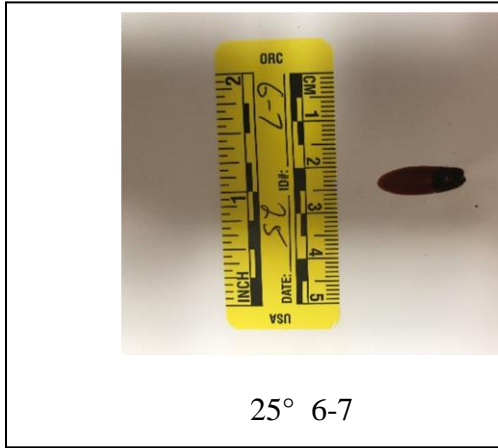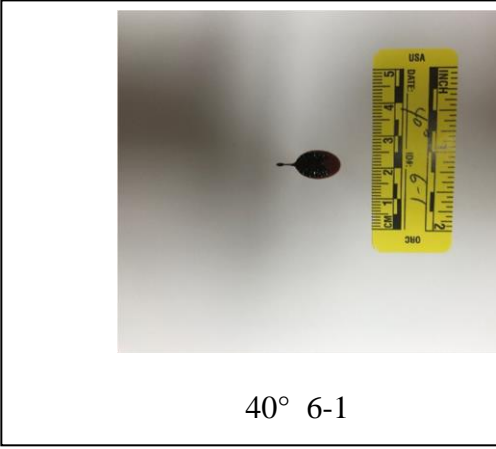
40° 6-1
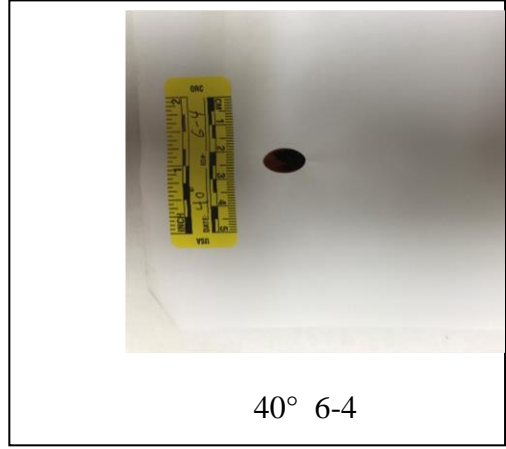
40° 6-4
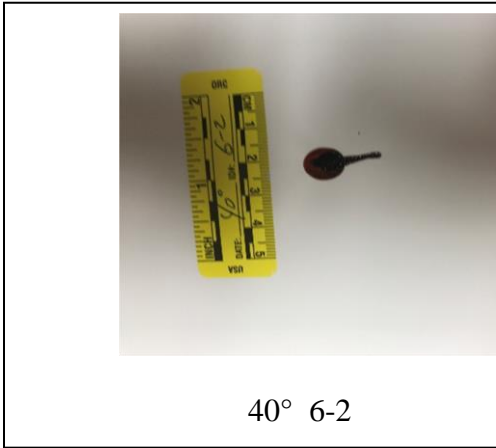
40° 6-2

40° 6-5

40° 6-3

40° 6-6

40° 6-7

40° 6-10

40° 6-8

40° 6-9

282
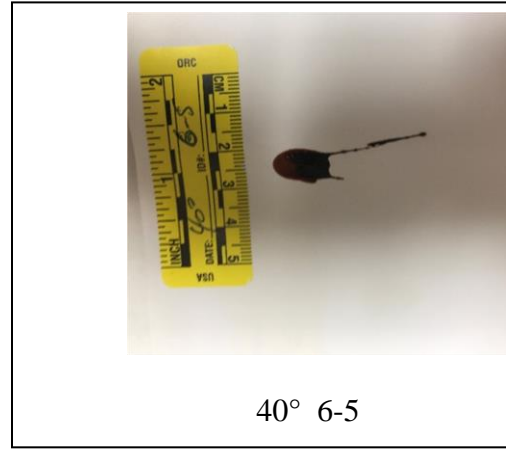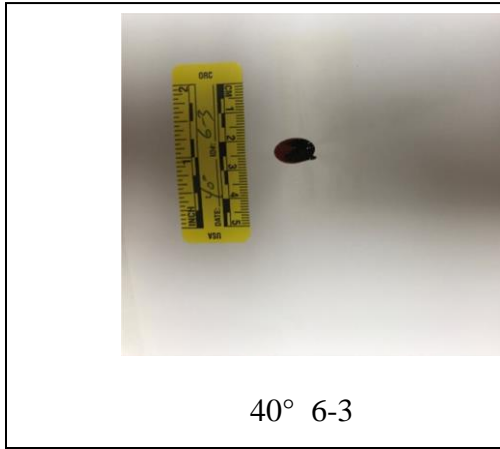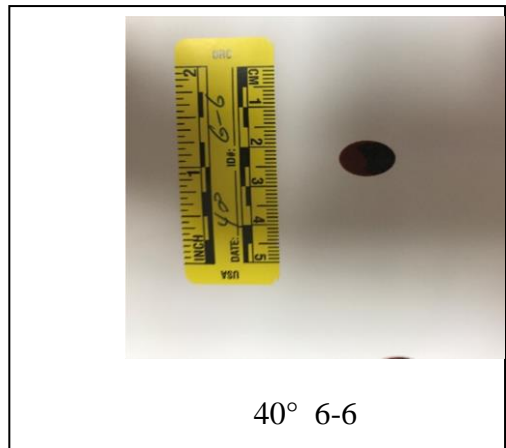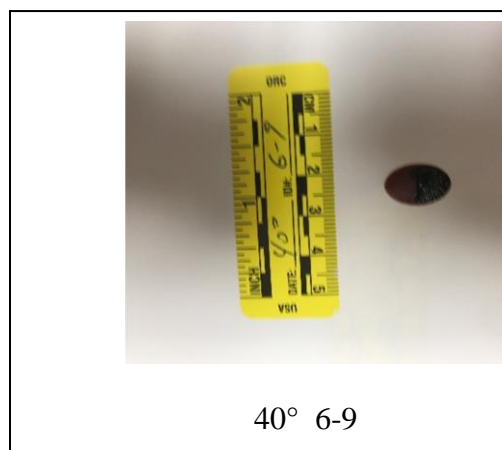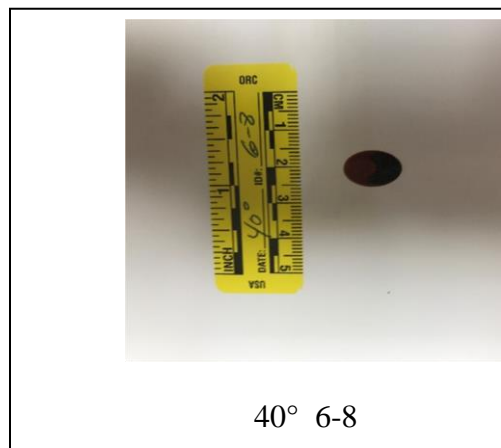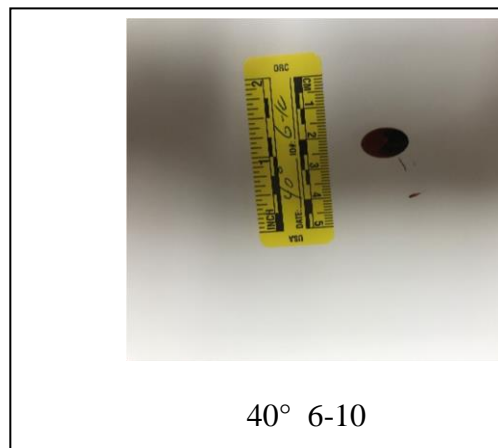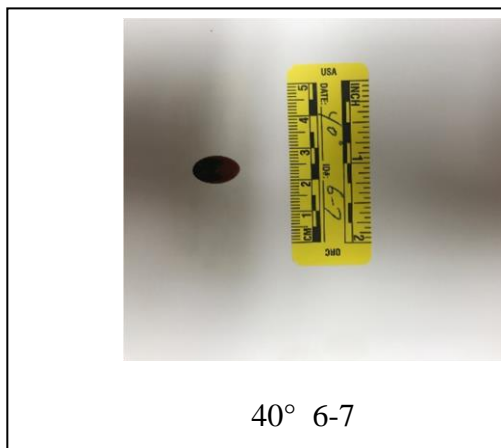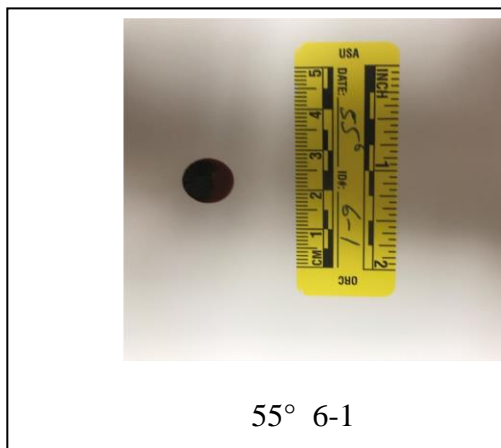
55° 6-1

55° 6-4

55° 6-2

55° 6-5

55° 6-3

55° 6-6

283

55° 6-7

55° 6-10

55° 6-8

55° 6-9

284
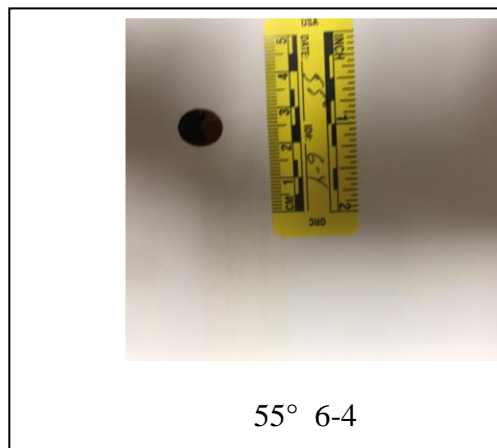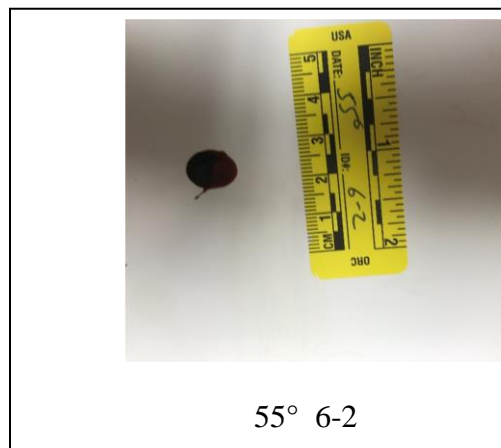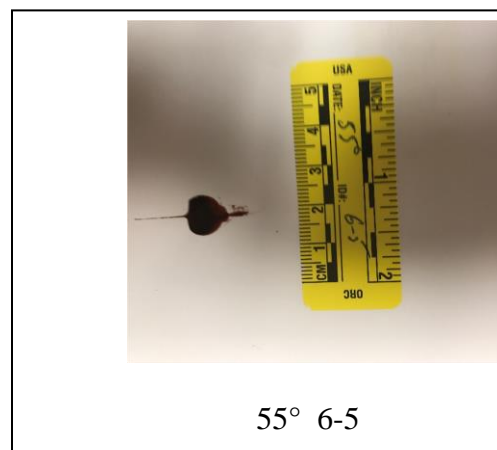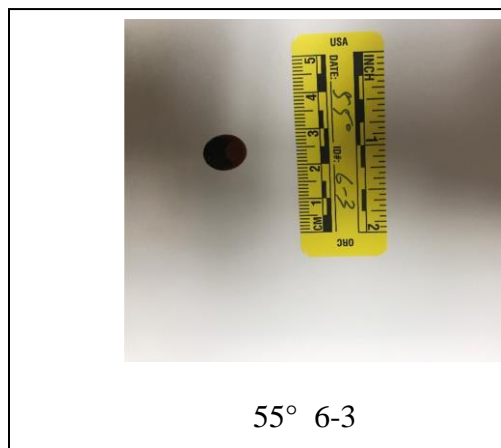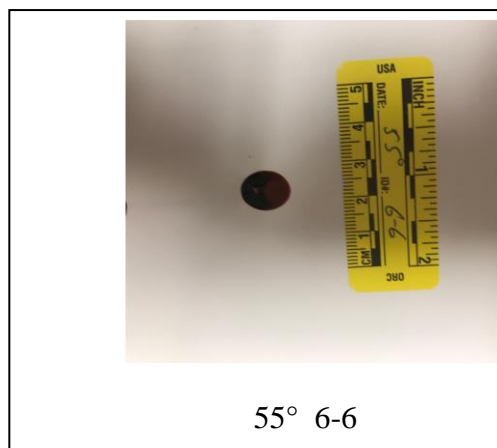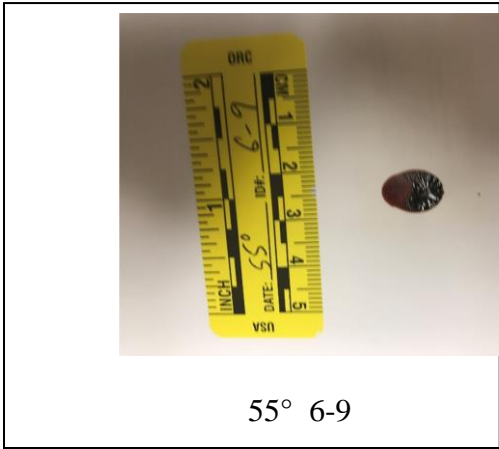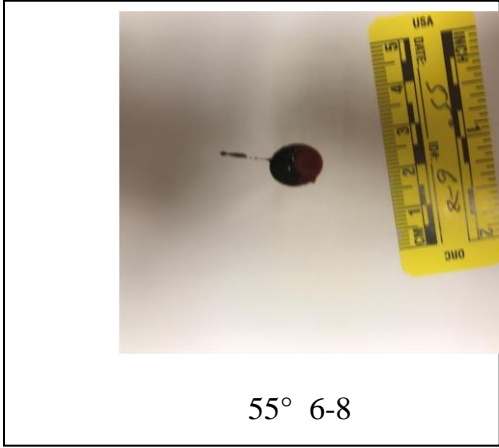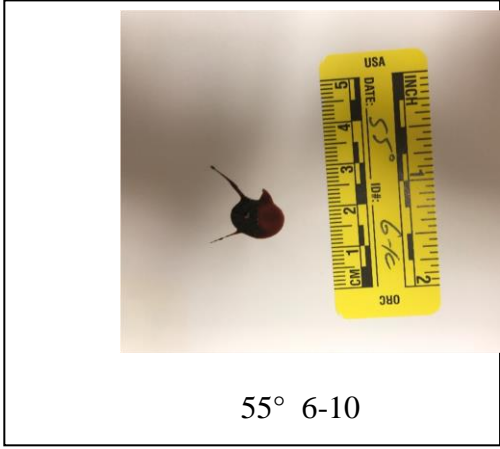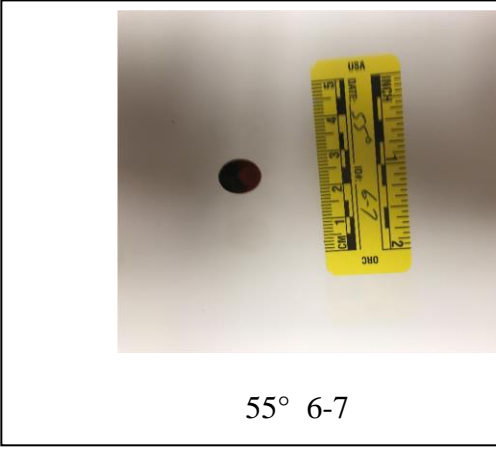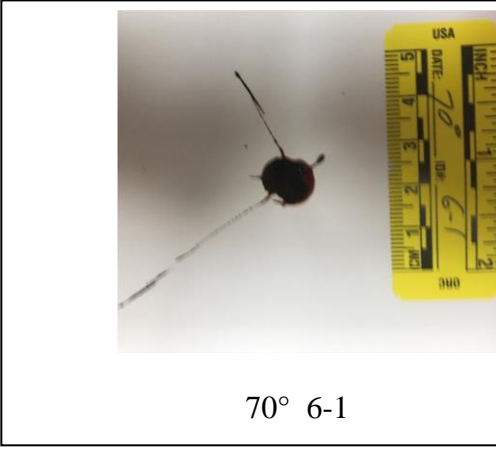
70° 6-1
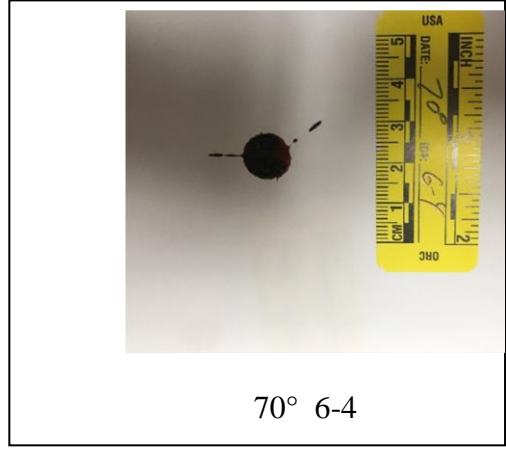
70° 6-4
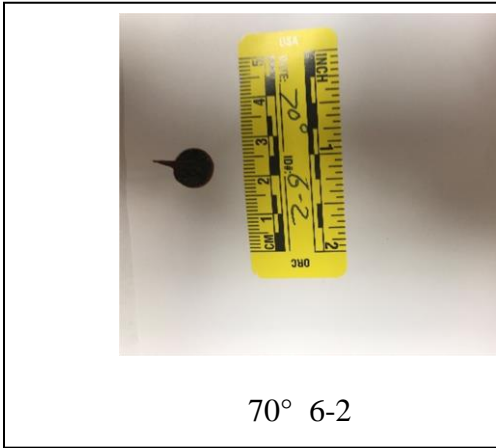
70° 6-2

70° 6-5

70° 6-3

70° 6-6

285

70° 6-7

70° 6-10

70° 6-8

70° 6-9
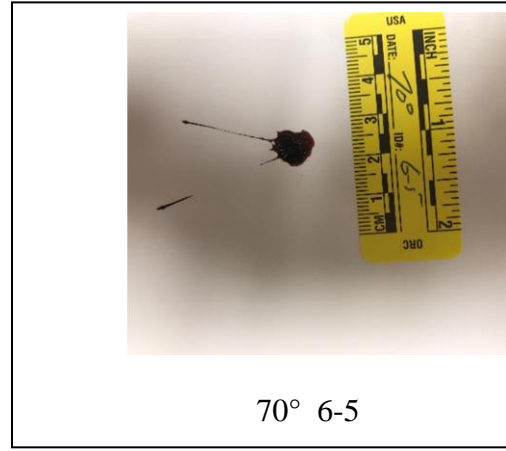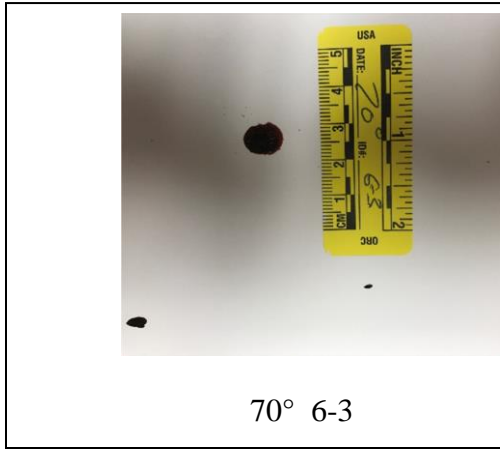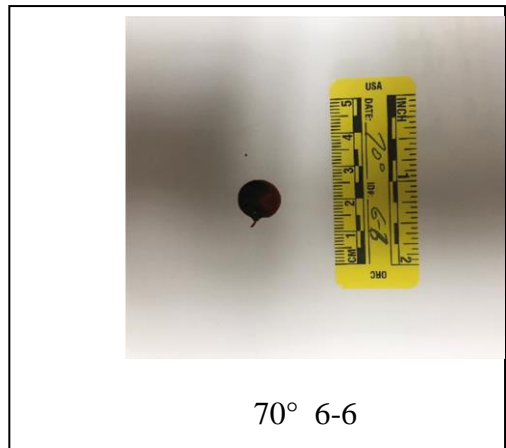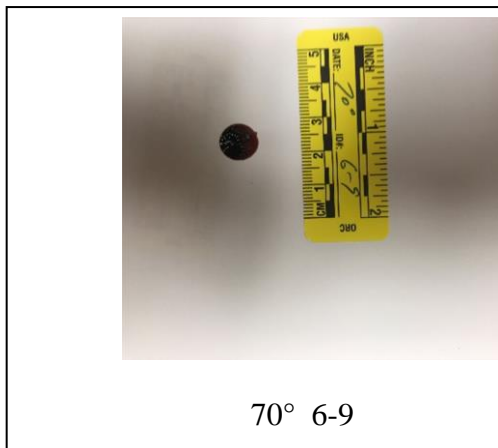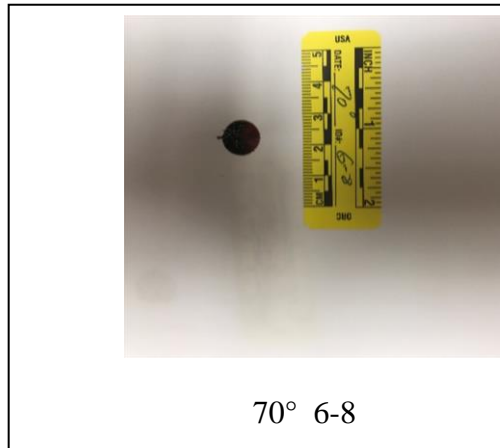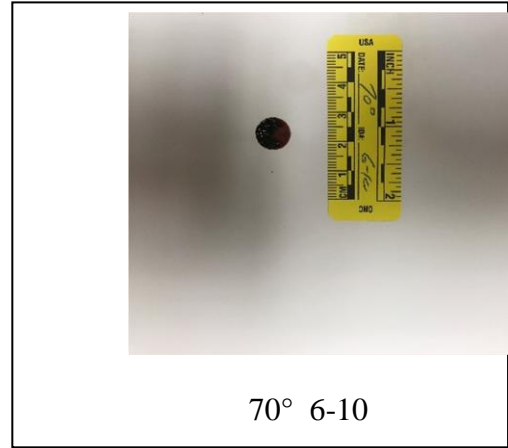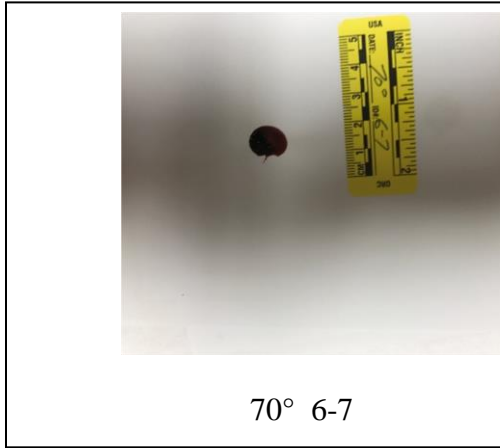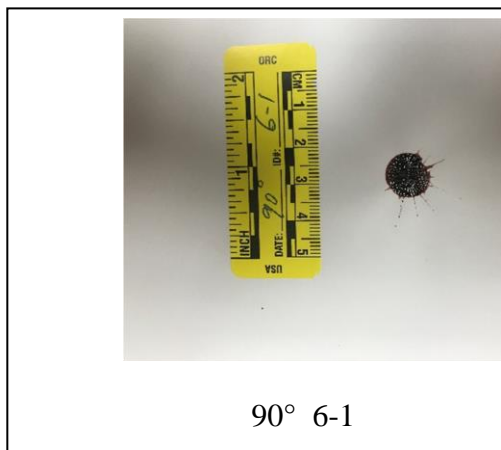
90° 6-1
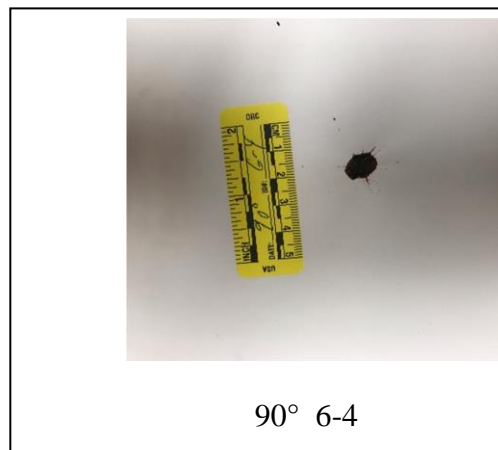
90° 6-4
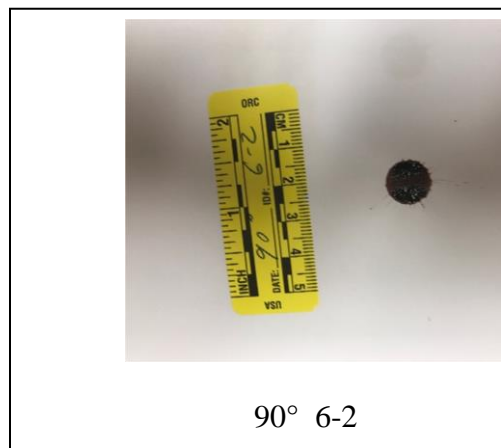
90° 6-2

90° 6-5

90° 6-3

90° 6-6

90° 6-7

90° 6-10

90° 6-8

90° 6-9

288
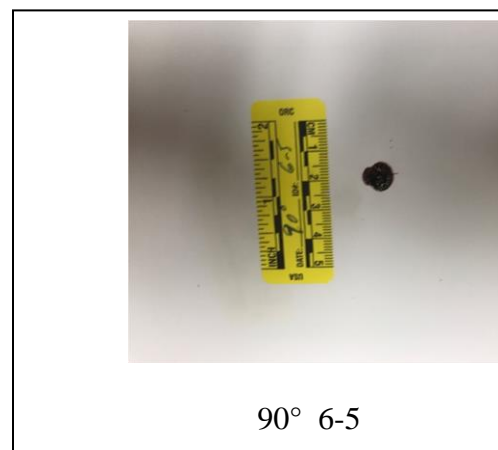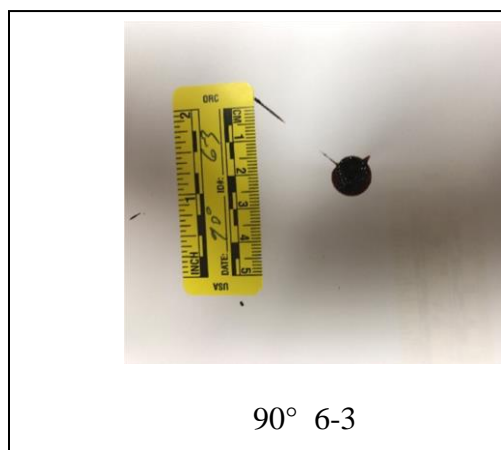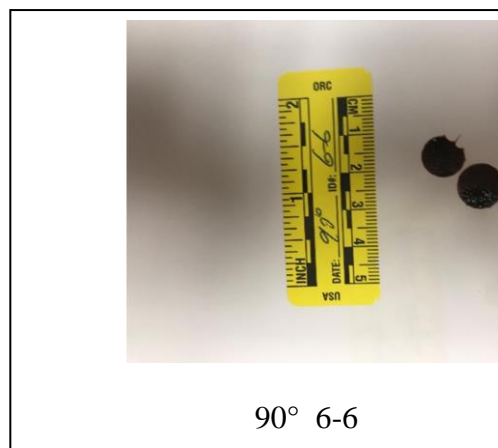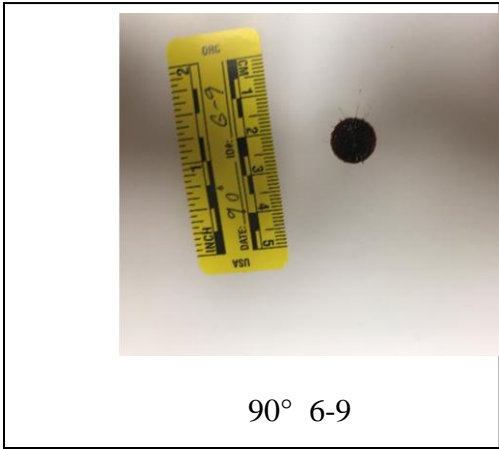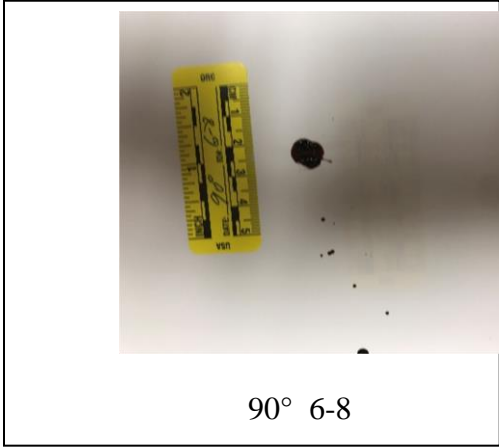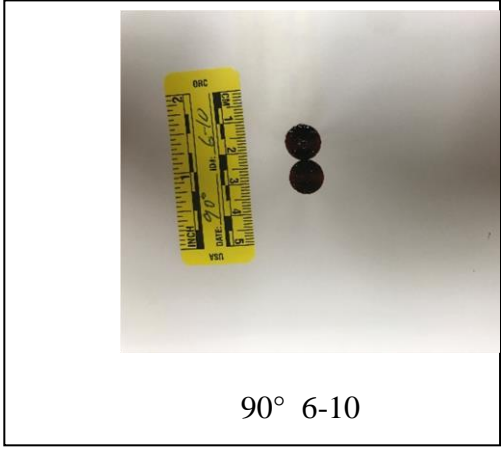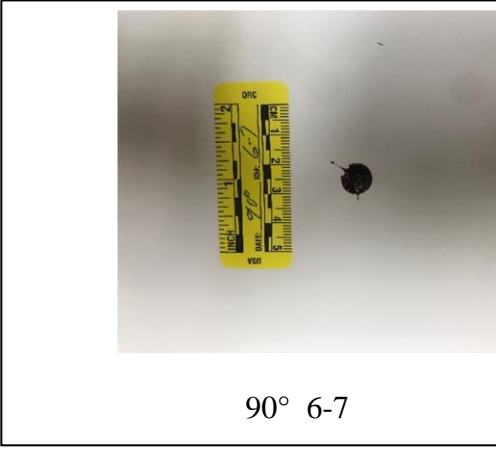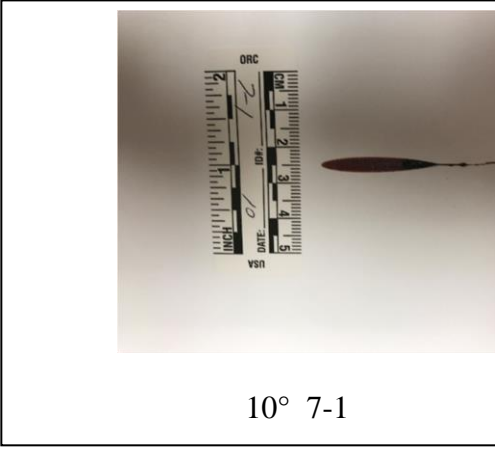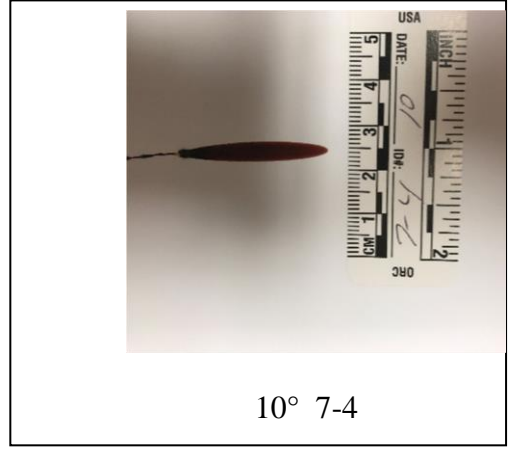
10° 7-1

10° 7-4

10° 7-2

10° 7-5

10° 7-3

10° 7-6

289
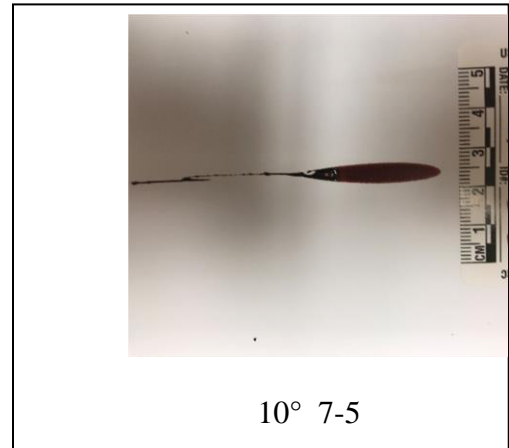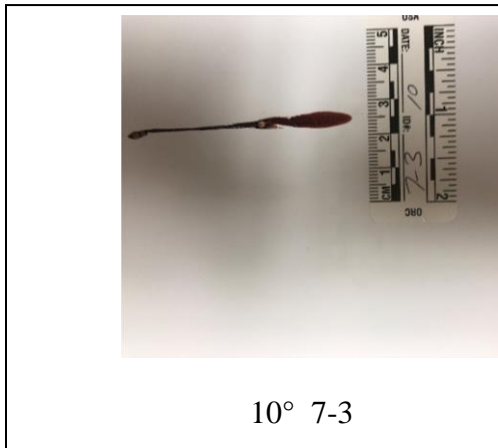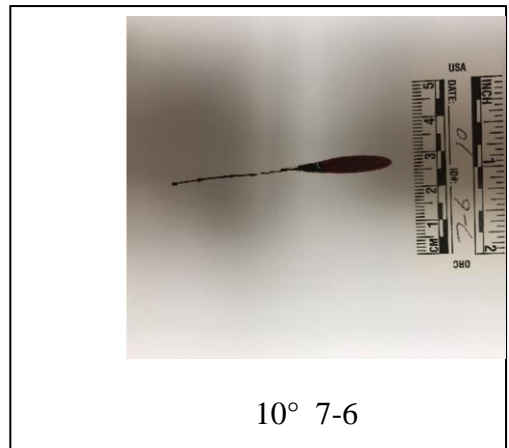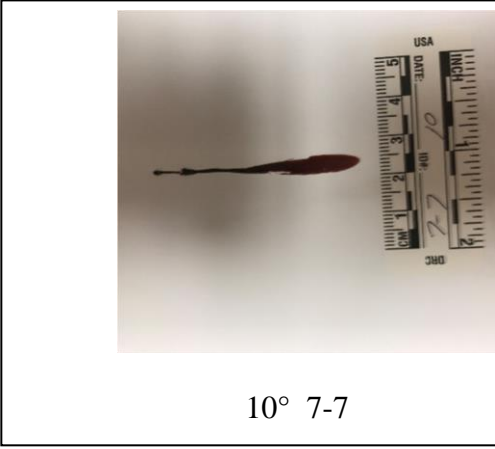
10° 7-7

10° 7-10

10° 7-8

10° 7-9

290
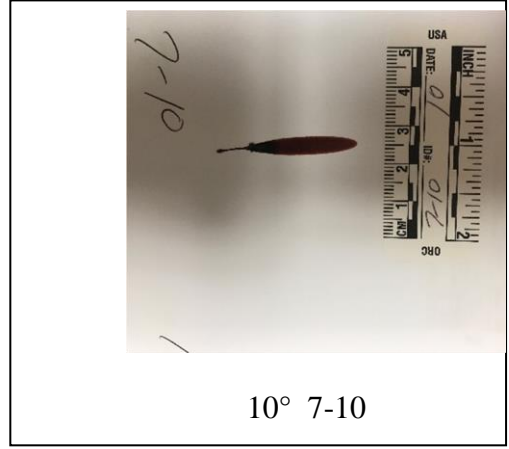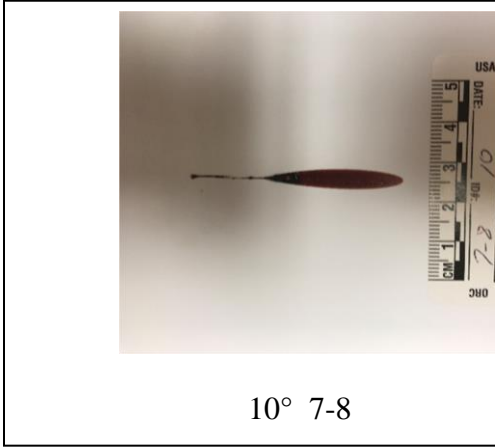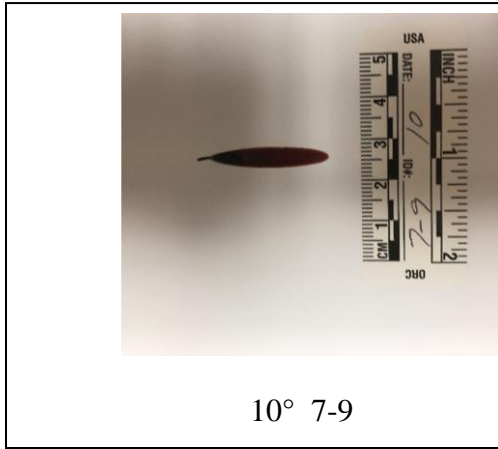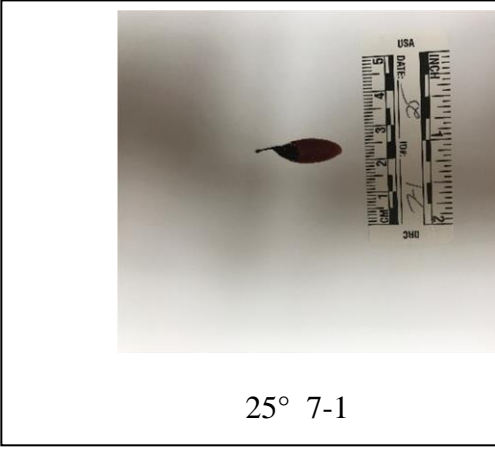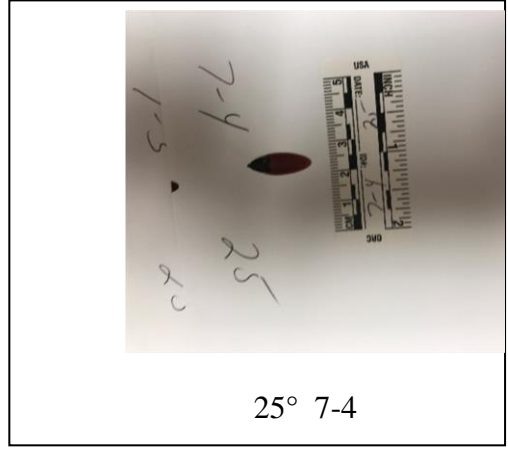
25° 7-1

25° 7-4

25° 7-2

25° 7-5

25° 7-3

25° 7-6

291

25° 7-7

25° 7-10

25° 7-8

25° 7-9

40° 7-1

40° 7-4

40° 7-2

40° 7-5

40° 7-3

40° 7-6

293

40° 7-7

40° 7-10

40° 1-8
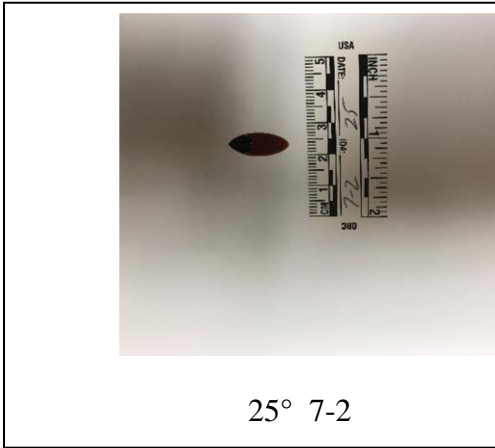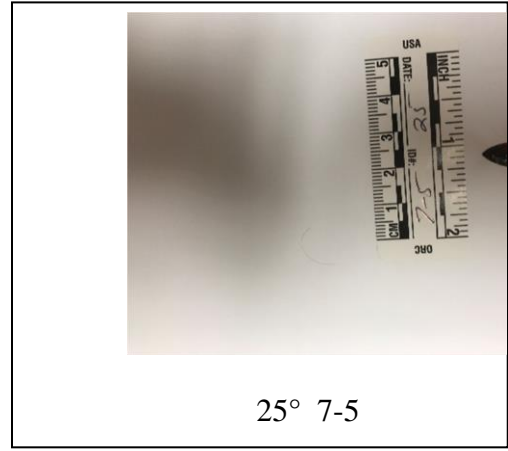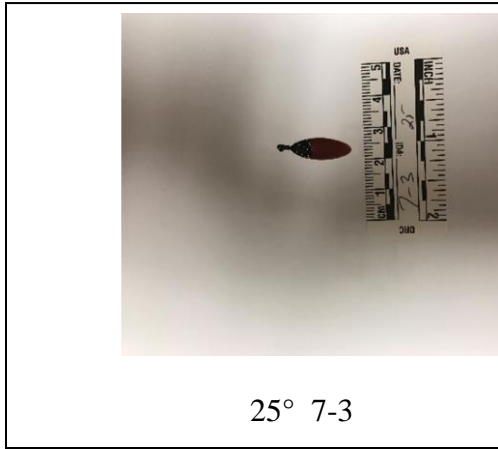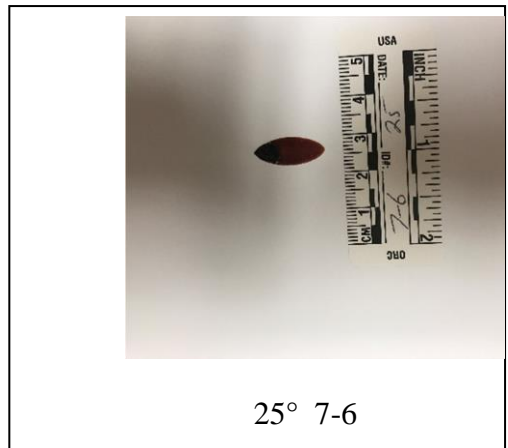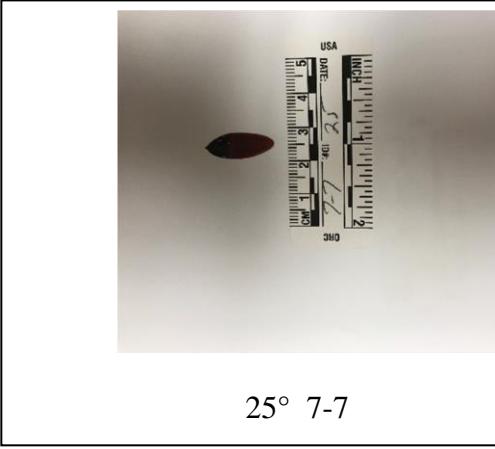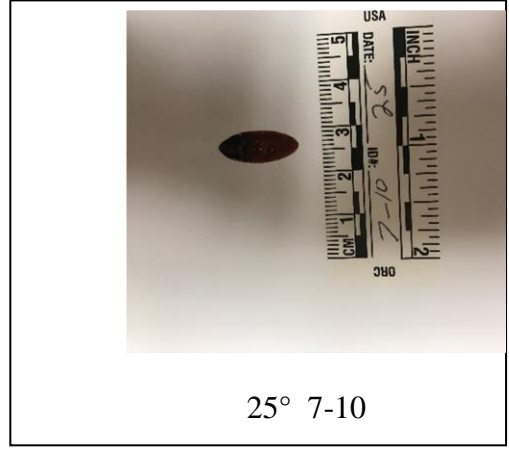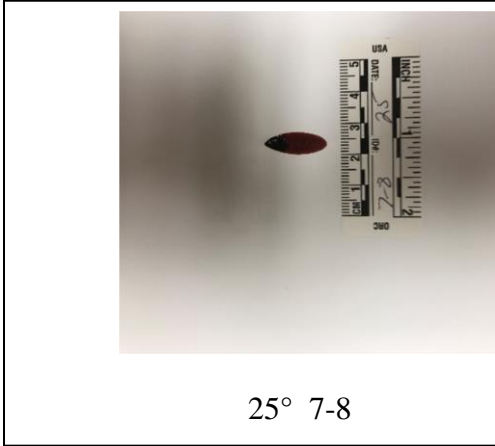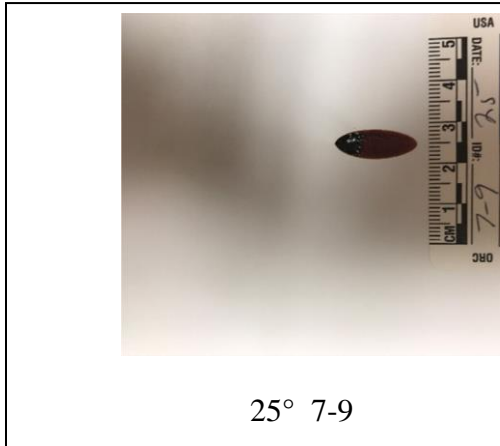
40° 7-9
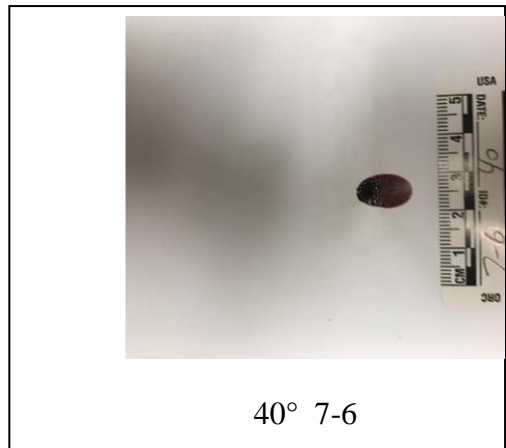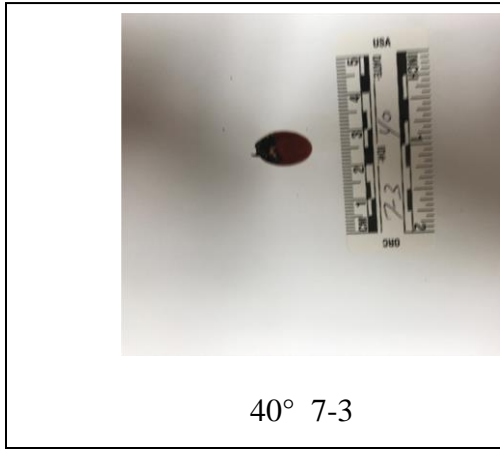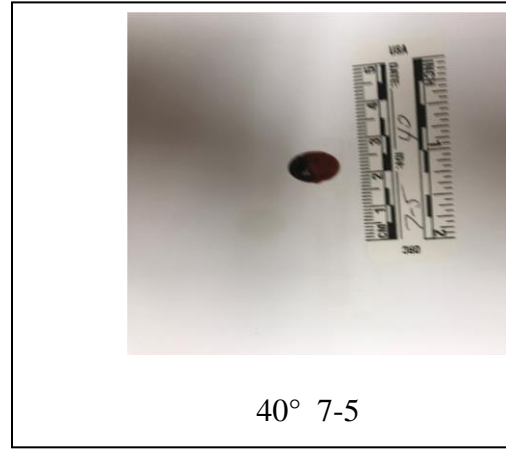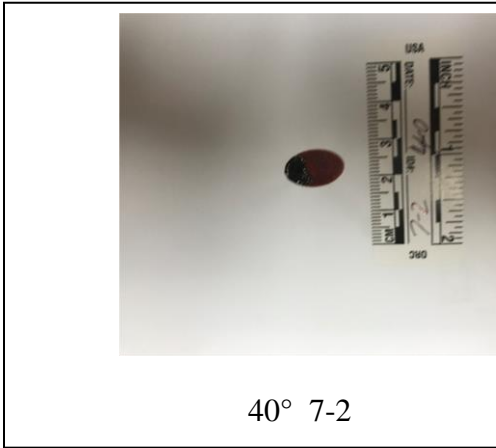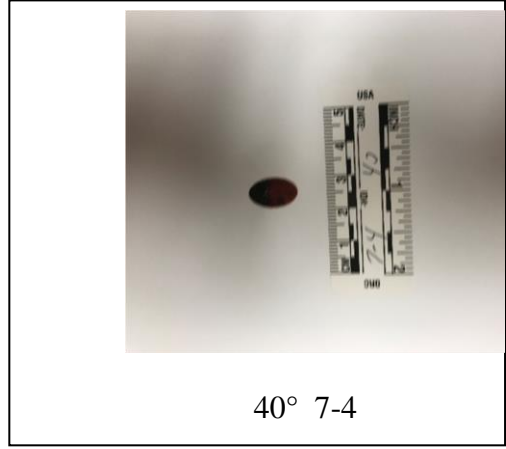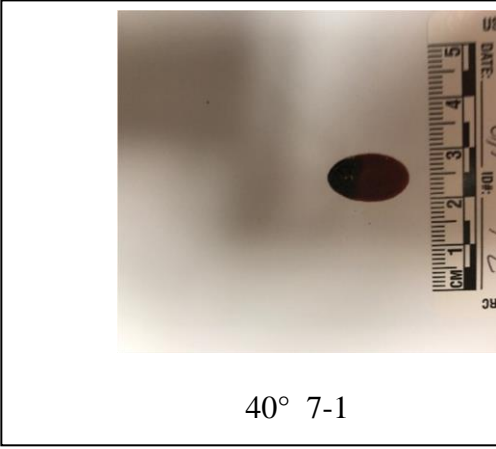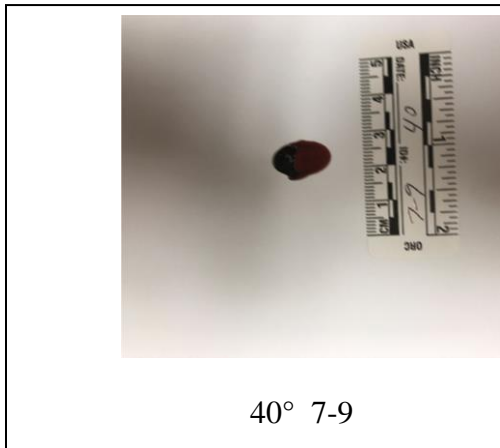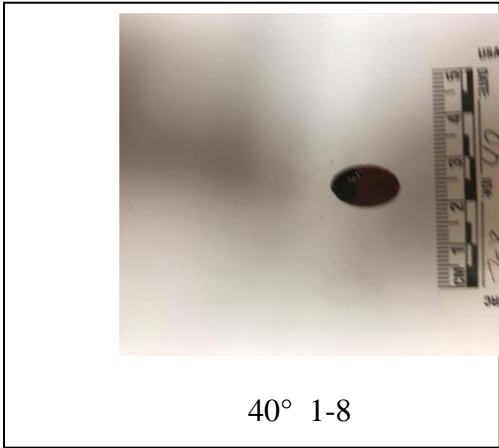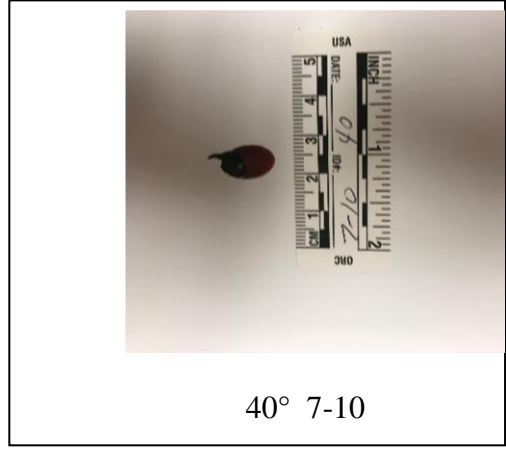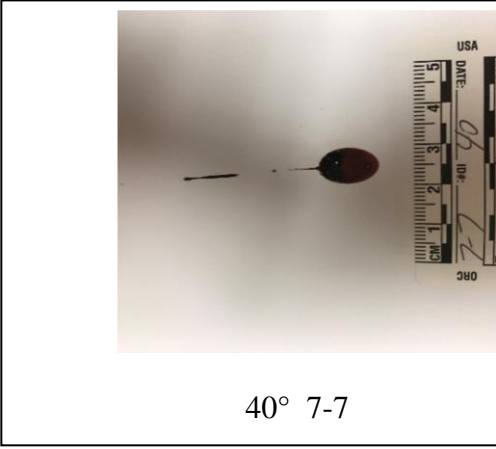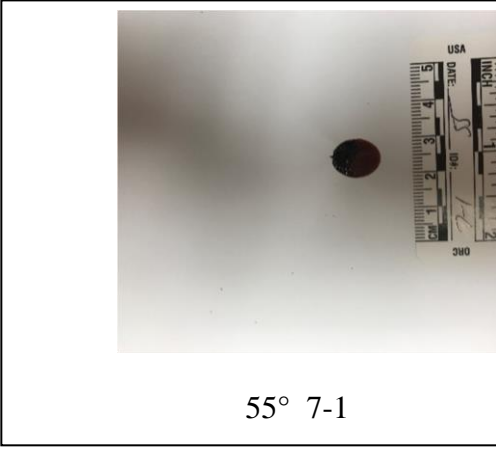
55° 7-1

55° 7-4

55° 7-2

55° 7-5

55° 7-3

55° 7-6

295

55° 7-7

55° 7-10

55° 7-8

55° 7-9

296

70° 7-1

70° 7-2

70° 7-3

70° 7-4

70° 7-5

70° 7-6

297

70° 7-7

70° 7-10

70° 7-8

70° 7-9

298
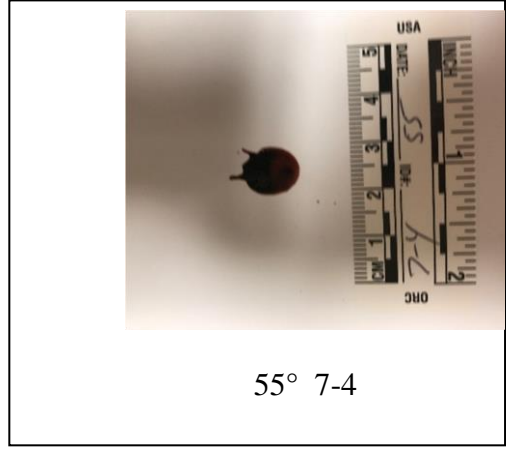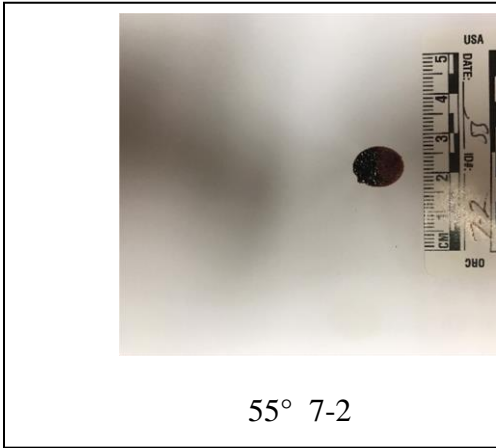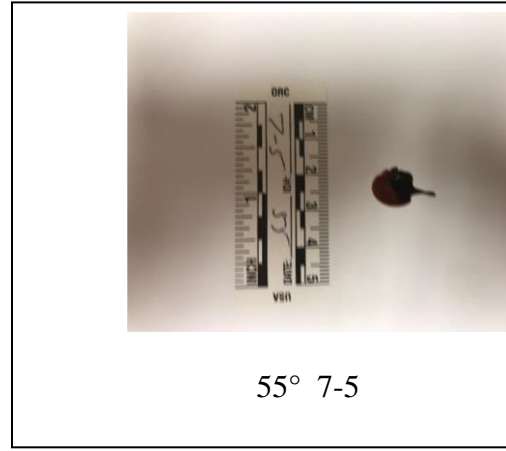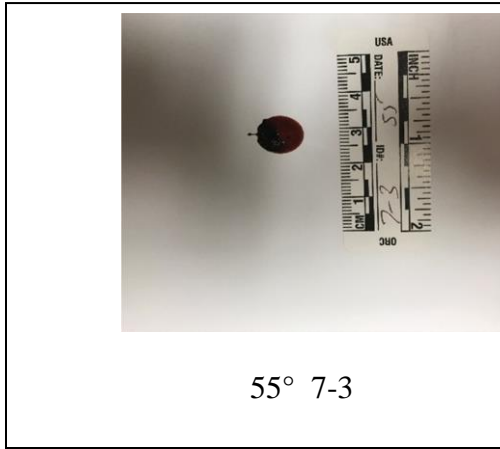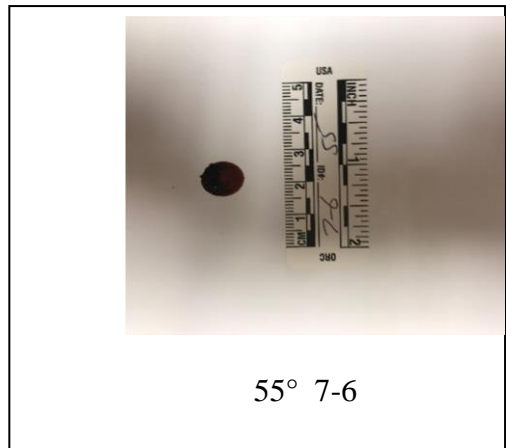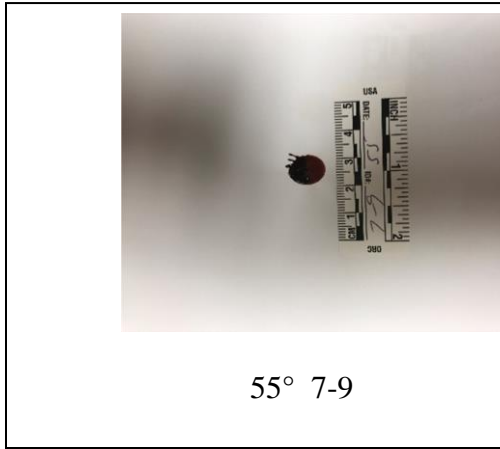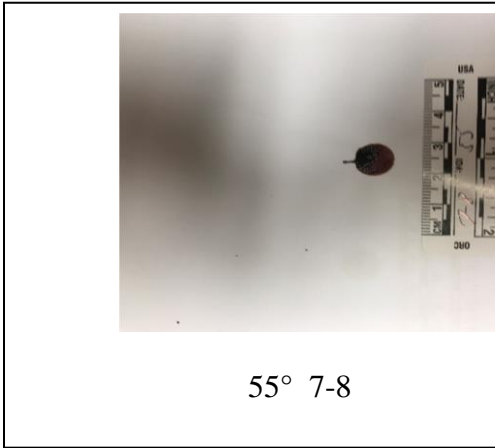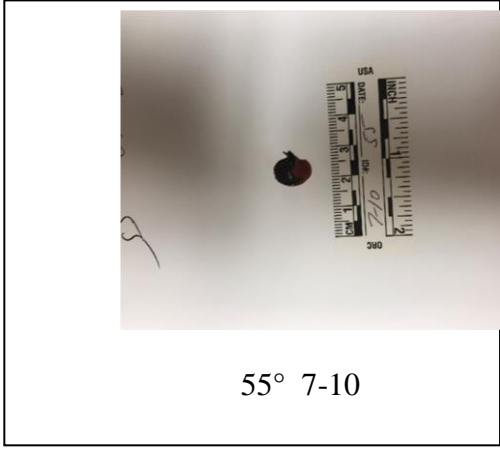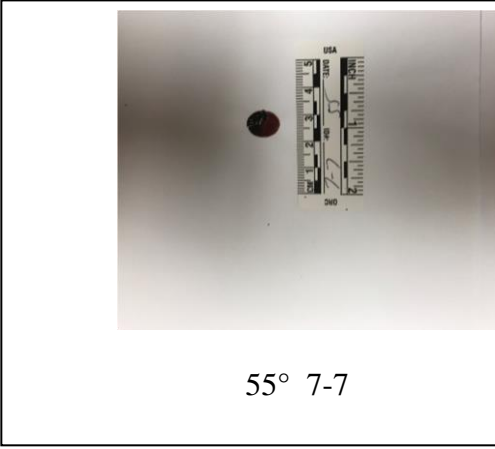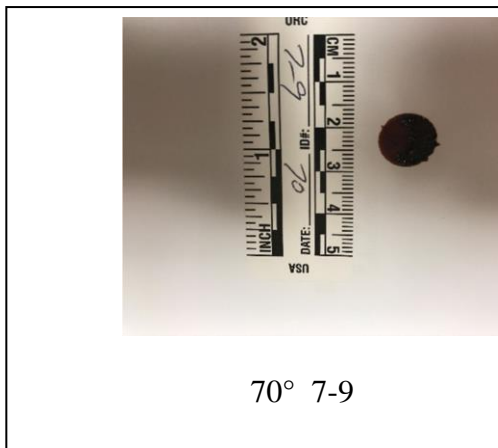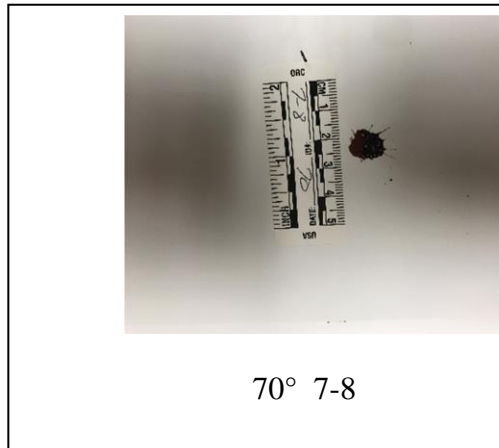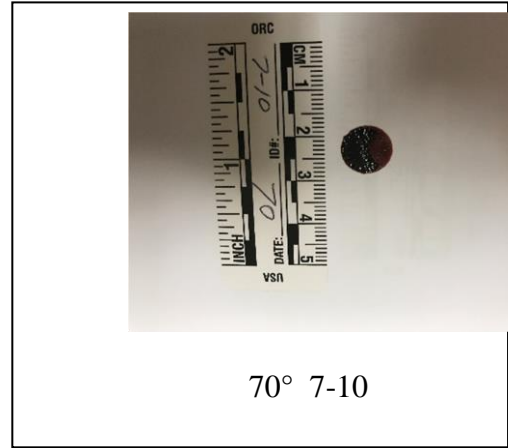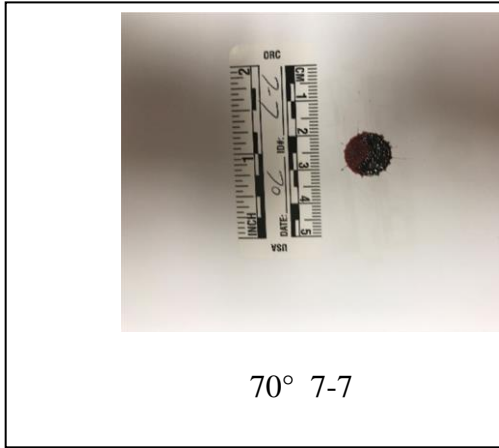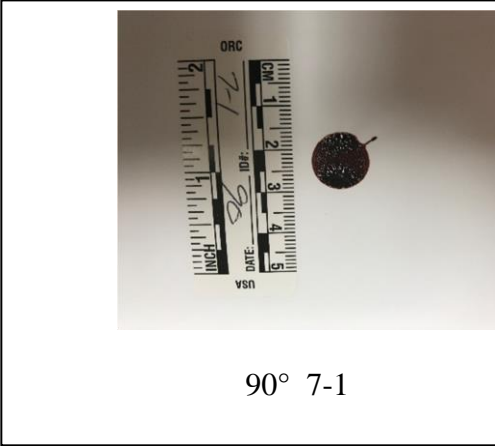
90° 7-1
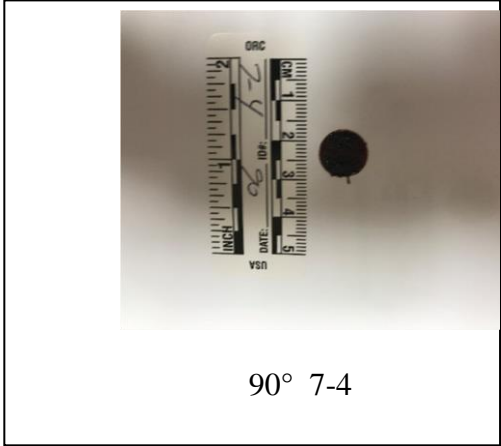
90° 7-4
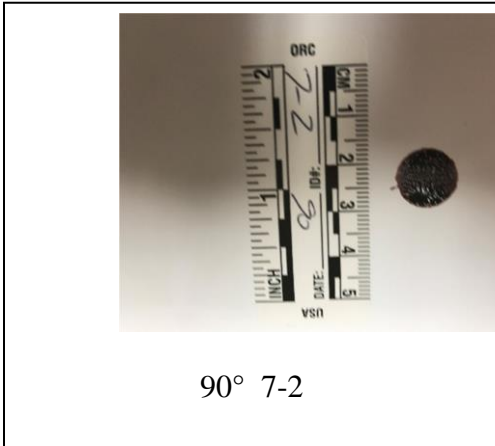
90° 7-2

90° 7-5

90° 7-3

90° 7-6

90° 7-7

90° 7-10

90° 7-8

90° 7-9
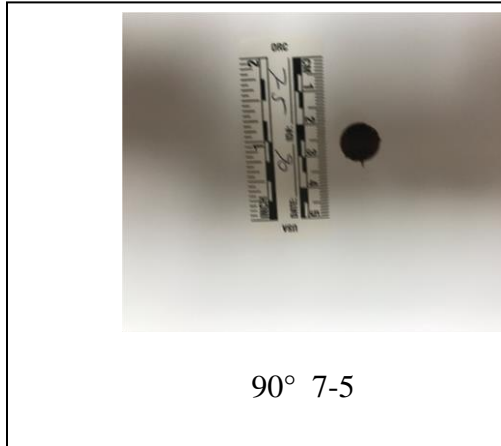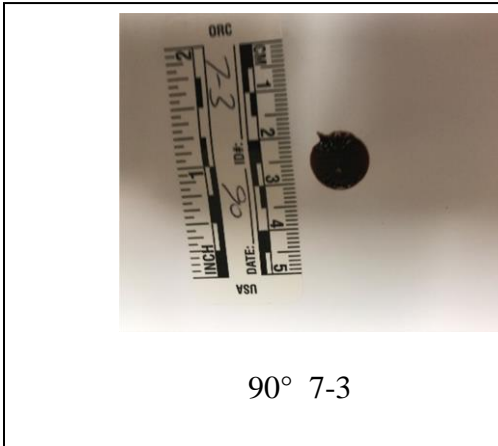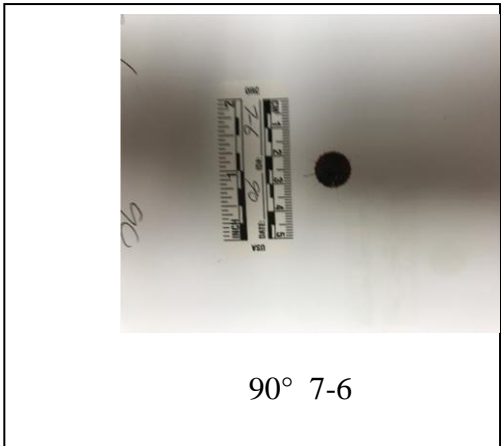
Confidence Interval Explanation and Example

The formula to calculate a 95% confidence interval is:

$$M \pm t_{(N-1)} \times SE$$

where M = mean value of a sample of data; $t_{(N-1)}$ is the critical value of the *t* statistic at *p* = .05 when the sample size is N; SE is the standard error of the mean, given by $\sigma/\sqrt{N}$, (where σ = standard deviation of the sample of data).
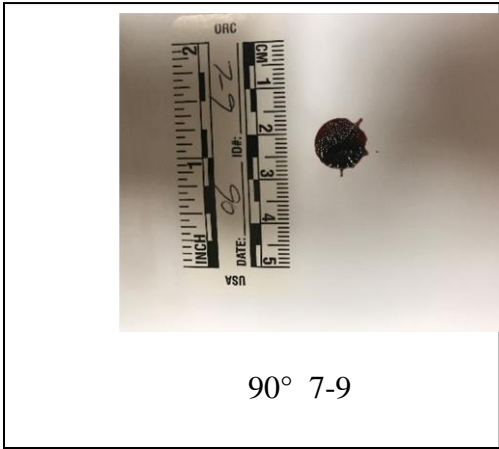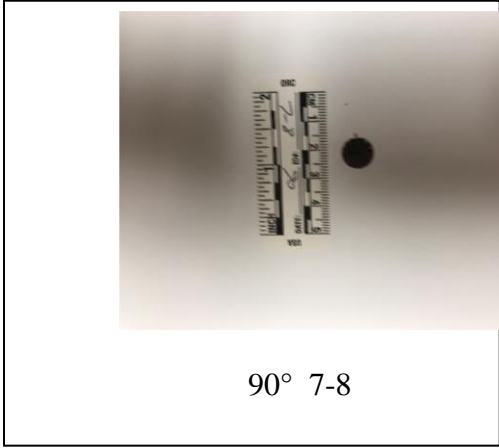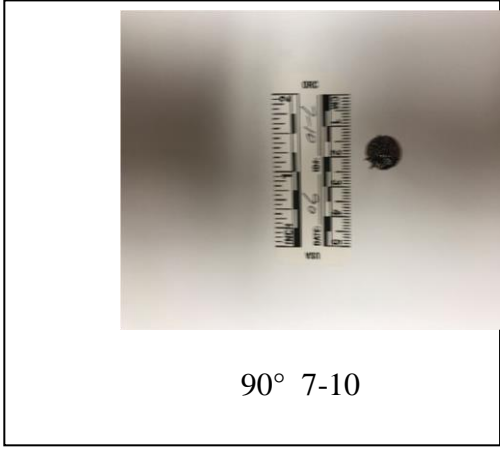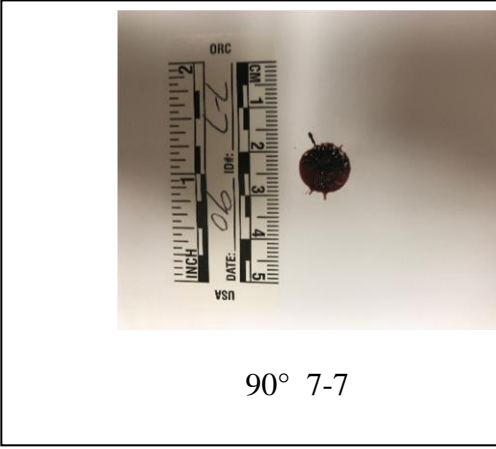
For example, the known mean location of the (area) volume of origin and the 95% CI of the mean at Blood Density = 1 is calculated using data for five sets of observations (numbered by 1.1, 1.2, 1.3, 1.4, and 1.5) at points x, y, and z as follows:

Blood Density	Observation	Point	Known Area of Origin (cm)
1	1.1	x	31.00
1	1.1	y	119.00
1	1.1	z	45.00
1	1.2	x	31.00
1	1.2	y	119.00
1	1.2	z	45.00
1	1.3	x	28.00
1	1.3	y	119.00
1	1.3	z	45.00
1	1.4	x	24.00
1	1.4	y	108.00
1	1.4	z	47.00
1	1.5	x	24.00
1	1.5	y	108.00
1	1.5	z	47.00
Calculation of 95% CI of mean			
	Sample size	N	15.00
	Mean	M	62.67
	Standard Deviation	σ	38.96
	Standard Error	$\sigma/\sqrt{N}$	10.06

t test statistic at p = .05			2.14
t x Standard Error			21.58
Lower limit of 95% CI	M - (t x Standard Error)		41.09
Upper limit of 95% CI	M + (t x Standard Error)		84.24

The mean (M = 62.67) and the 95% CI (lower limit = 41.09; upper limit = 84.24) of the known area of origin at points x, y, and z using Blood Density = 1 calculated in the above table are represented by the first point and vertical bar on the extreme left-hand side of the interval plot shown below (labelled Method = K and Blood Density = 1 on the horizontal axis)
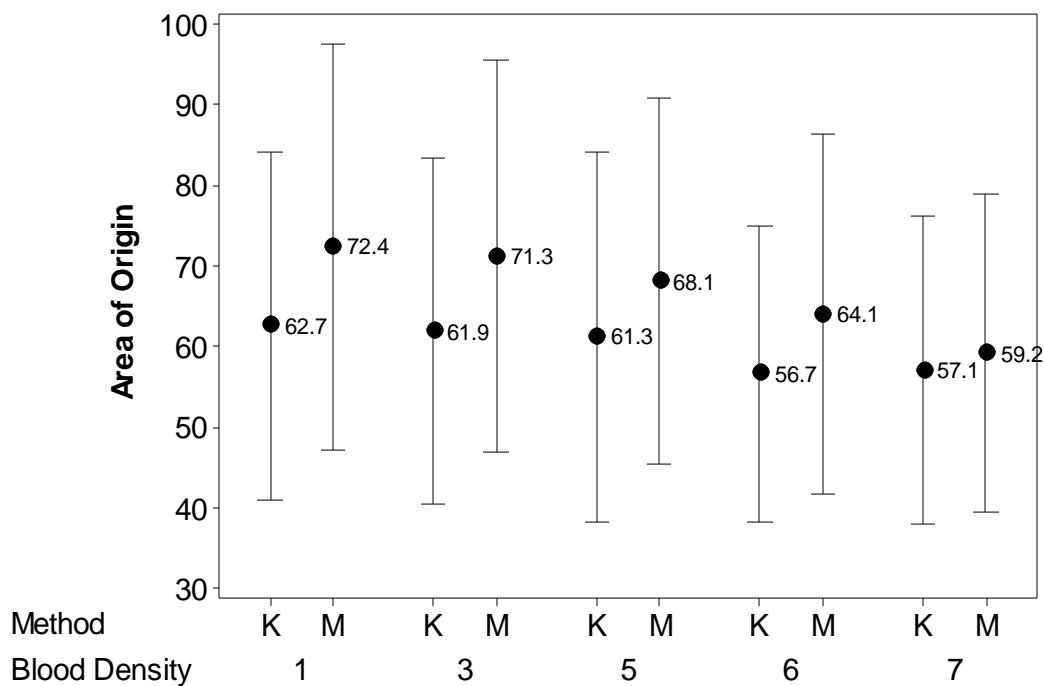
Confirmation of Polymer Composition by FT-IR

Confirmation of Polymer Composition by FT-IR employing Thermo Fisher Nicolet 6500 with spectra taken in transmission mode and displayed as absorbance vs. cm^{-1} all spectra collected at 4 cm^{-1} resolution, 32 scans, auto gain.
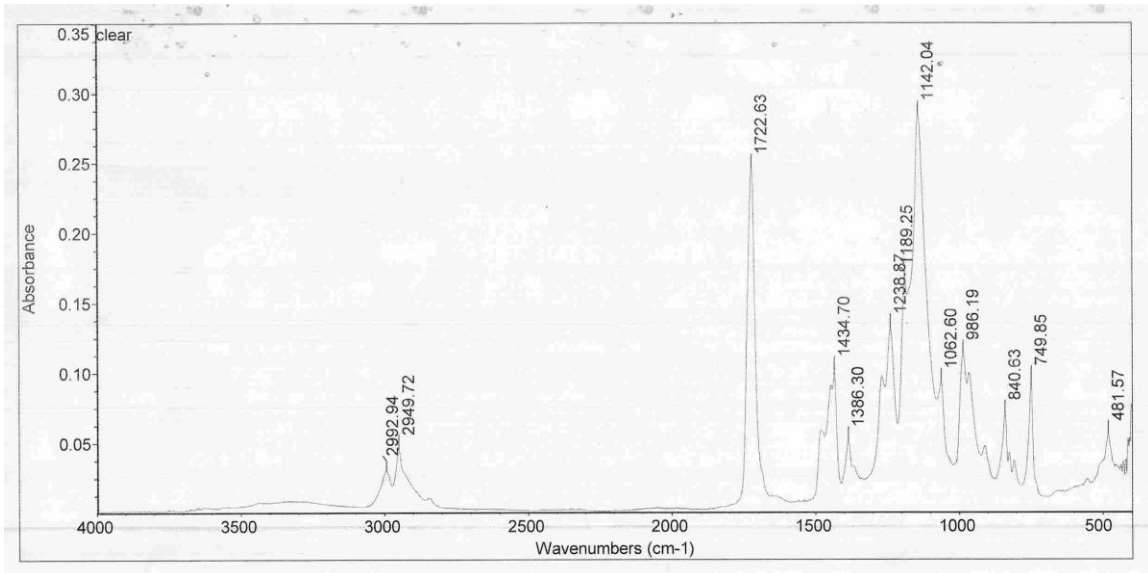
Omnic (Themo-Fisher software) search of data base HR Nicolet Sampler and Hummel Polymer libraries returned Polymethylmethacrylate (acrylic) top two hits match values 83.8 and 76.5
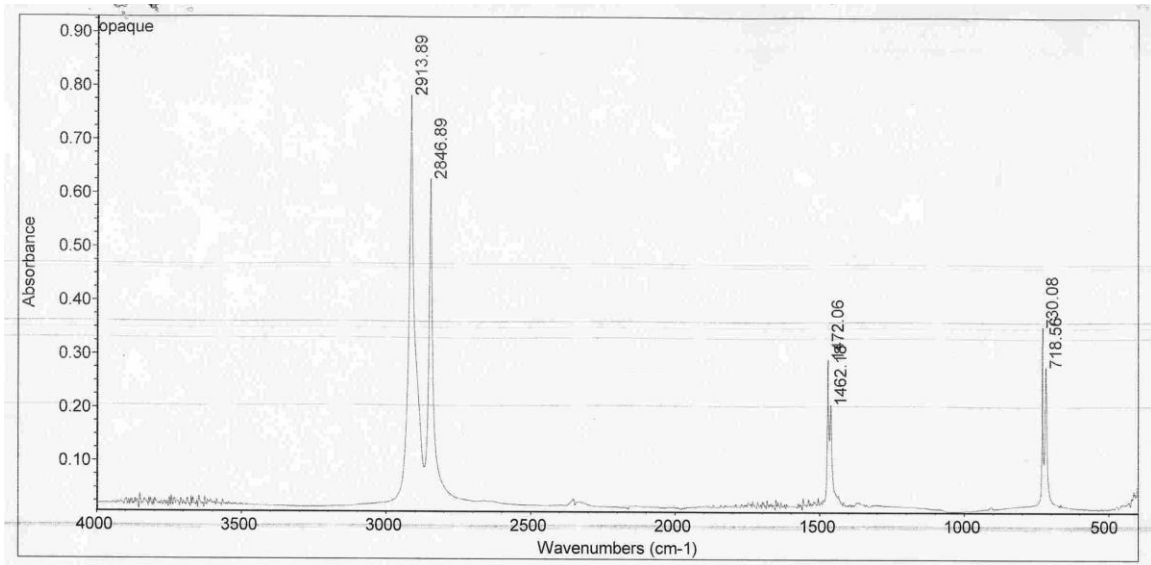
303

Omnic (Themo-Fisher software) search of data base HR Nicolet Sampler and Hummel

Polymer libraries returned Polyethylene top two hits match values 82.8 and 69.1

304
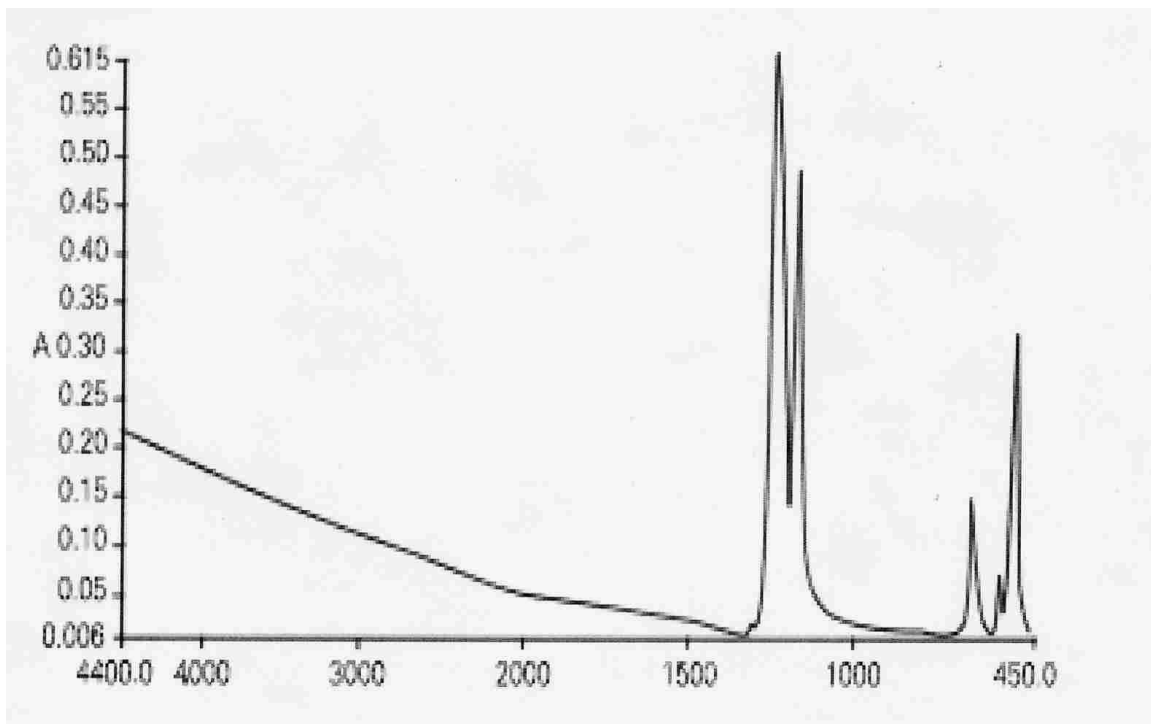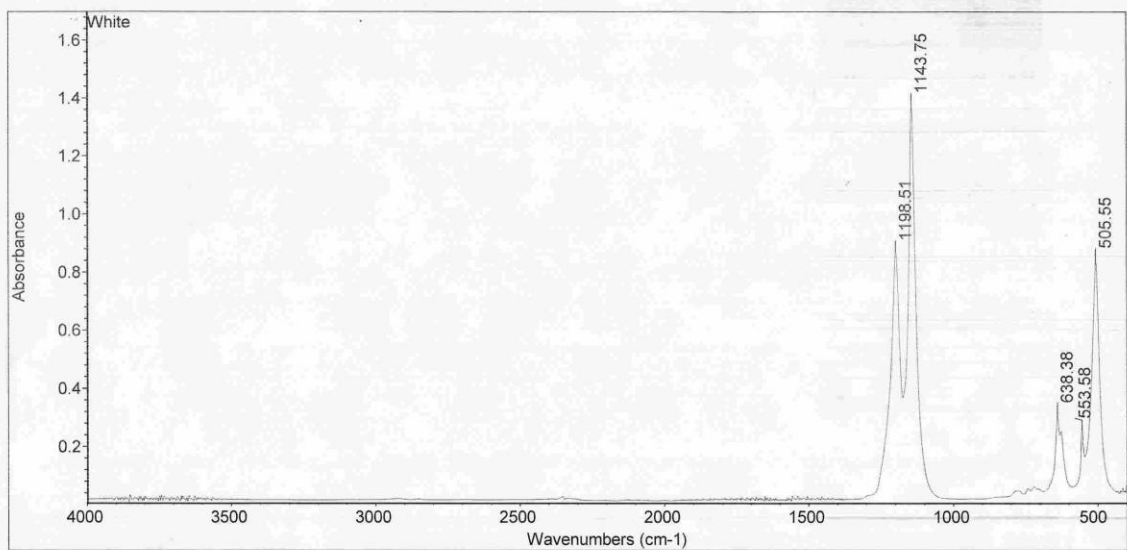
Top spectra collected from employed polymer material bottom spectra from Internet

PTFE sample card from International Crystal.net Note excellent agreement.

305

Take away. Polymer materials purchased for and used for blood contact angle

measurements are what supplier claimed.

Contact Angle on Various Polymer Substrates

Polymer Sample	CA for Probe Liquid			
	W	G	F	EG
PTFE	106.96	88.40	83.68	72.00
PP	97.15	85.39	81.73	59.57
PE	89.10	74.25	69.08	55.45
PS	84.80	76.75	70.15	61.78
PMMABA	79.19	70.51	62.95	57.01
PMMA	77.53	75.22	57.45	53.62
PET	75.63	67.58	62.87	50.93
PVDF	77.65	65.35	69.07	57.77

References

Adams, B.D., Baker, R., Lopez, J.A. & Spencer, S. (2009). Myeloproliferative disorders and the hyperviscosity syndrome. *Emergency Medicine Clinical North America*, 27(3), 459-76.

Adamson A.W., Gast A.P.(1997) *Physical chemistry of surfaces,* 6th ed. Wiley Intersciences, NY.

Aimram, A.N., Afthanorhan, A., & Razali, N.H.M. (2015). Moderated mediation using partial least squares structural equation modeling. *Elixir Statistics, 80*, 31035-31039.

Ansell, J., Hirsch, J., Hylek, E. (2008). Pharmacology and management of the vitamin K antagonist. *American College of Chest Physicians Evidence-Based Clinical Practice Guidelines,* 8th Edition, Chest 133 (6 Suppl), 160S – 198S.

Anton Paar, DMA 35, Instruction Manual, Document # C761B001ML-C, 11/14/2012.

Bad Blood (Editorial). (2018, May 31). NY Times. Retrieved from http://www.nytimes.com/2018/05/31/opinion/blood-spatter-evidence.html

Baron, R. M., & Kenny, D. A. (1986). The moderator-mediator variable distinction in social psychological research: Conceptual, strategic, and statistical considerations. Journal of *Personality and Social Psychology, 51,* 1173-1182.

Baskurt, O.K. % Meiselman, H.J. (2003). Blood rheology and hemodynamics. *Seminars in Thrombosis and Hemostasis,* Vol.29, No.5.

Belin, T.R., Normand, S-L, T. (2009). The role of ANCOVA in analyzing experimental data. *Psychiatric Anals, 39*, 753-760.

Bevel, T. & Gardner, R.M., (2002). *Bloodstain Pattern Analysis with an Introduction to Crime Scene Reconstruction,* 2nd ed., *CRC Press.*

Brodbeck, S. (2012). Introduction to bloodstain pattern analysis, *SIAK – Journal – Journal for Police Science and Practice,* Volume 2, 51-57.

Brownson, D. A. C., & Banks, C. E., (2010), Crime scene investigation: The effect of drug contaminated bloodstains on bloodstain pattern analysis. *Analytical Methods*, 2, 1885-1889.

Carter, A.L., Forsythe-Erman, J., Hawkes, V., Illes, M., Laturnus, P., Lefebvre, G., Stewart, C. & Yamashita, B. (2006), Validation of the backtrack suite of programs for bloodstain pattern analysis. *Journal of Forensic Identification*, 56, (2).

Chaplin, M. (2007). Water structure and science: Hydrocolloid rheology, Retrieved from http://www.lsbu,ac.uk/water/hyrhe.html

Ciofalo, M., Collins, W.M., & Hennessy, T.R. (2002). Nanoscale fluid dynamics in physiological processes: A review study. *Advances in Computational Bioengineering*, WIT Press, Southampton, U.K.

Colloff, P., (2018). "Influential Texas Commission Says Blood-Spatter Testimony in Joe Bryan's Murder Case Was 'Not Accurate or Scientifically Supported' " *ProPublica*.

Colquhoun, D. (2017). The reproducibility of research and the misinterpretation of p- values. Royal Society Open Science. doi: 10.1098/rsos.171085.

Dailey, J.F. (2001). *Blood*, 2nd ed. Medical Consulting Group: Ipswich, MN.

Das R., Collins A., Verma A., Fernandez J., Taylor M. (2015). Evaluation simulant materials for understanding cranial backspatter from a ballistic projectile. *J. Forensic Sciences*, 60; 627-637.

Daubert v. Merrell Dow Pharmaceuticals, (1993) 509 U.S. 579, 113 S. Ct. 2786, 125 L.Ed. 2d 469.

Davies, H.T.O. & Crombie, I.K. (2009). What are confidence intervals and p-values? Retrieved from http://grunigen.lib.uci.edu/sites/all/docs/gm/what_are_conf_inter.pdf

DeForest, Peter (2018), Physical aspects of blood traces as a tool in crime scene investigations. *The CAC News*, 3rd Quarter 2018.

DeForest, Peter, Gaensslen, R.E. & Lee, Henry (1983). *Forensic science, an introduction to criminalistics,* McGraw-Hill, NY.

Deshmukah, R. R., Arolkar G.A. & Parab, S.S. (2012). Studies in dielectric properties of various polymers and its correlation with surface free energy, *International Journal of Chemical and Physical Sciences,* Vol. 1, No. 2.

Dillard, C.R. & Goldberg, D.E. (1978). *Chemistry: reactions, structure and properties*, 2nd ed. McMillan Publishing, NewYork, N.Y.

Eckmann, D.M., Bowers, S., Stecker, M. & Cheung, A.T. (2000). Hematocrit, volume expander, temperature and shear rate effects on blood viscosity. *Anesthetic Analogy,* 91: 539-45.

309

Edwards, J. R., & Lambert L. S. (2007). Methods for integrating moderation and mediation: A general analytical framework using moderated path analysis. *Psychological Methods, 12*, 1-22.

El-Sayed, M., Brownson, D.A.C. & Banks, C.E. (2011). Crime scene investigation II: The effect of warfarin on bloodstain pattern analysis. *Analytical Methods*, 3, 1521-1524.

Fassot, G., Henseler, J., & Coelho, P.S. (2016). Testing moderating effects in PLS path models with composite variables. *Industrial Management and Data Systems, 116*, 1887-1900.

Ferguson, C.F. (2009). An effect size primer: a guide for clinicians and researchers. *Professional Psychology: Research and Practice, 40*, 532-538.

FBI Laboratory (2008). Scientific working group on bloodstain pattern analysis: topics to consider in preparation for an admissibility hearing on bloodstain pattern analysis. *Forensic Science Communications,* Vol.10, No.4.

Ron Fisher, 2018, Personal Communication – Statistics Consultant.

Flocchi Ammunition (2018). Retrieved from http://www.FiocchiGFL.IT

Foster, K. & Huber, P. (1999). *Judging science, scientific knowledge and the federal courts,* MIT Press, Cambridge, MA.

Freedman, M.D. (1992). Oral anticoagulants: pharmacodynamics, clinical indications and adverse effects. *Journal of Clinical Pharmacology, 32 (3)*, 196-200.

Hair, J. F., Hult, G. T. M., Ringle, C. M., & Sarstedt, M. (2017). *A primer on partial least squares structural equation modeling (PLS-SEM)*, 2nd ed., Thousand Oaks, CA: Sage.

Hakim, N. & Liscio, E. (2015). Calculating point of origin of blood spatter using laser scanning technology, *Journal of Forensic Science,* Vol.60, No. 2.

Halsey, L.G., Curran-Everett, D., Vowler, S.L., & Drummon G.B. (2015). The fickle p-value generates irreproducible results. *Nature Methods, 12,* 179-185.

Hampton, H. & Havel, J. (2014). *Introductory to biological statistics*. Longrove, Il. Waveland Press.

Harmening, D. (1997) *Clinical hematology and fundamentals of hemostasis*, Philadelphia, F.A. Davis Company.

Hayes, A. F. (2013). *Introduction to mediation, moderation, and conditional process analysis. A regression based approach*. New York, NY: Guildford Press.

310

Hemingway, T.J. (2014). Hyperviscosity syndrome. Retrieved from
    htttp://emedicine.medscape.com/article/780258-overview

Holbrook, A.M., Pereira, J.A., Labiris, R., McDonald, H., Douketis, J.D., Crowther, M. & Wells,
    P.S. (2005). Systematic overview of warfarin and its drug and food interactions. *Archives
    of Internal Med*icine, 165 (10), 1095-106.

Hrncir E., Rosina J (1997). Surface tension of blood. *Physiological Research,* 46, 319-321.

Hubbard, R., & Lindsay, R.M. (2008). Why p-values are not a useful measure of evidence in
    statistical significance testing. *Theory & Psychology, 18,* 69-88.

Hunter, Carol (2000), Criminalistics in the New Millennium. *CAC News,* 1st Quarter, 2000.

James, S.H., Kish, P.E. & Sutton, T.P. (2005). *Principles of bloodstain pattern analysis: theory
    and practice*. CRC Press, Boca Raton, FL.

James, S. & Nordby, J. Ed (2003). *Forensic science, an introduction to scientific and
    investigative technique,* CRC Press, Boca Raton.

Jose, P.E. (2013). *Doing statistical mediation and moderation.* New York, NY: Guilford Press.

Kesmarky, G., Kenyeres, P., Rabai, M. & Toth, K. (2008). Plasma viscosity: A forgotten
    variable. *Clinical Hemorheology and Microcirculation*, 39, 243-246.

Kirk, P. (1953). *Crime investigation, physical evidence and the police laboratory*. Interscience
    Publishers, N.Y., N.Y. p.4.

Klabunde, R.E. (2004). *Cardiovascular physiology concepts,* Lippincott, Williams &
    Wilkins, London, U.K.

Kock, N. (2015). *Hypothesis testing with confidence intervals and p-values*. Laredo, TX:
    ScriptWarp Systems.

Laturnus, P. (1994). Measurement survey. *International Association of Bloodstain Pattern
    Analysts News*, 10 (3), 14-27.

Leica Geosystems Crime Scene Investigation (2018). Retrieved from http:// psg.leica-
    geosystems.us/page/applications/crime-scene-investigation

MacDonell, H.L. & Bialousz, L.F. (1971). *Flight characteristics and stain patterns of human
    blood*. National Institute of Law Enforcement and Criminal Justice, Law Enforcement
    Assistance Administration, Washington, D.C.

MacDonell, H.L. (1971), "Interpretation of bloodstains – physical considerations," in *Legal Med.
    Ann.*, ed Wecht, C., New York, Appleton-Century Crofts, pp. 91-136.

311

Mandatory Guidelines for Federal Workplace Drug Testing Programs: Final Rule, Fed. Reg, 82 FR 7920-2017.

Marasini, D., Quatto, P., & Ripamonti, E. (2016). The use of p-values in applied research: interpretation and new trends. S*tatistica, 4,* 315-325. Retrieved from http://rivista-statistica.unibo.it/article/download/6439/6498

Marieb, E. (2003). *Human anatomy and physiology.* 6th ed. Pearson, Benjamin, Cummings, Upper Saddle River, N.J.

Mark, D.B., Lee, K.L., & Harrell, F.E. (2016). Understanding the role of p-values and hypothesis tests in clinical research. *JAMA Cardiology*, 1(9), 1048-54.doi:10.1001/jamacardio. 2016.3312.

Mark H., Workman, Jr., J. (2018). Outliers, Part III. Dealing with outliers. *Spectroscopy,* 33(10): 23-25.

McGregor R.G. (2018). Best practices for viscosity measurement in QC labs. *American Laboratory*, October: 34-36.

Minitab (2016). Getting started with Minitab 17. Retrieved from http://www.minitab.com/uploadedFiles/Documents/getting-started/Minitab 17_GettingStarted-en.pdf

Mukherjee, N., Bansal, B., & Chen, X.D., (2005) Measurement of surface tension of homogenised milks. *International Journal of Food Engineering*, Vol. 1, 2:2.

National Laboratory Certification Program (2000), Guidance Document for Laboratories and Inspectors, OMB 0930-0158.

Neitzel GP, Smith M (2017). The fluid dynamics of droplet impact on inclined surfaces with application to forensic blood spatter analysis. *Office of Justice Programs' National Criminal Justice Reference Service.*

Nuzzo, R. (2014). Scientific method: statistical errors. P-values, the 'gold standard' of statistical validity, are not as reliable as many scientists assume. *Nature*, 506, 150-152.

OECD Principles of Good Laboratory Practice (Revised 1997), OECD-1.1998 and 21 CFR Part 58, *GLP for Non-Clinical Lab Studies*.

Panagiotakos, D.B. (2008). The value of p-values in biomedical research. *Open Cardiovascular Medicine, 2,* 97-99. doi: 10.2174/1874192400802010097.

Peck, R., Olsen, C., & Devore, J. (2016). *Introduction to statistics and data analysis*. 5th Ed. Boston, MA: Cengage Learning.

Pizzola, P., Roth, S. & De Forest, P. (1986). Blood droplet dynamics – I, *Journal of Forensic Sciences,* Vol. 31, No.1, 36-49.

Pizzola, P.A., Roth, S., Deforest, P.R. (1986a) Blood droplet dynamics – II, *Journal of Forensic Sciences,* 31: 50-64.

Raymond, M. A., Smith, E.R, & Liesegand, J. (1996a). Oscillating blood droplets: Implications for crime scene reconstruction. *Science and Justice* 36 (3): 166-171.

Raymond, M.A. (1997). *Oscillating Blood Droplets: Implications for Crime Scene Reconstruction*. PhD thesis, La Trobe University, Melbourne, Vic.

Raymond, M.A., Hall, N.M.G. & Jones, M.K. (2001). Bloodstain pattern interpretation. *In Expert Evidence*, Vol. 3, Freckelton, I, & Selby, H, Editors. Law Book Company, Sydney, NSW.

Raymond, M.A., Smith, E.R. & Liesegang, J. (1996). The physical properties of blood – forensic considerations. *Science & Justice*, 36, 153-160.

Raymond, T. (1997). Crime scene reconstruction from bloodstains. *Australian Journal of Forensic Sciences,* 29(2): 69-78.

Rodak, B. (2002). *Hematology: Clinical Principals and Applications,* 2nd ed. W.B. Saunders Publishing Company, Philadelphia, PA.

Rogers, N. (2009). *Hematocrit implications for bloodstain pattern analysis*. MS thesis, University of Western Australia, Perth.

Rosencranz, R. & Bogen, S, (2006). Clinical laboratory measurement of serum, plasma & blood viscosity, *Journal of Clinical Pathology,* 125 (SUP 1) S78-S86.

Rudin, Norah and Inman, Keith (2015), Could your lab be next? A sentinel event in the profession of forensic science, *CAC News*, 4th Quarter 2015.

Rutherford, A. (2001). *Introducing ANOVA and ANCOVA: A GLM approach*. Thousand Oaks, CA: Sage.

Saferstein, R. Ed (2005) *Forensic Science Handbook, Vol. II,* Prentice Hall, Upper Saddle River, N.J.

Slemko, J. (2018, December 15). Bloodstain Tutorial. Retrieved from http://www.bloodspatter.com/bloodstain-tutorial-page-2

Sullivan, G.M., & Feinn, R. (2012). Using effect size—or why the p-value is not enough. *Journal of Graduate Medical Education, 4(3),* 279-282.

Szucs, D., & Ioannidis, J.P.A. (2017). When null hypothesis significance testing is unsuitable for research: A reassessment. *Frontiers of Human Neuroscience, 11*, 390. doi: 10.3389/fnhum.2017.00390.

Tefferi, A. (2003). A contemporary approach to the diagnosis and management of polycythemia vera. *Current Hematology Reports*, 2 (3), 237- 41.

Texas Admin. Code ch. 651 §651.5. Forensic Disciplines and Procedures Subject to Commission Accreditation. Retrieved from http://texreg.sos.state.tx.us/public/readtac$ext.TacPage?sl=R&app=9&p_dir=&p_rloc=&p_t

Texas Admin. Code ch. 651 §651.6. Forensic Disciplines and Procedures to Which Commission Accreditation Does Not Apply by Statute. Retrieved from http://texreg.sos.state.tx.us/public/readtac$ext.TacPage?sl=R&app=9&p_dir=&p_rloc=&p_t

Texas Forensic Science Commission Forensic Analyst Licensing Program. Retrieved from http://www.txcourts.gov/fsc/licensing

Thornton, J. & Kirk, P. (1974). *Crime investigation,* 2nd Ed*.,* Wiley & Sons, N.Y.

Vogel, S. (1996). *Life in moving fluids. The physical biology of flow*. 2nd ed. Princeton University Press, Princeton, N.J.

Walitza, E. (1980). *On the rheology of blood and synovial fluids.* John Wiley & Sons.

Willis, C., Piranian, A., Donaggio, J., Barnett, R. & Rowe, W. (2001). Errors in the estimation of the distance of fall and angle of impact blood drops, *Journal Science International,* 123, 1-4.

Wonder, A.Y. (2001). *Blood dynamics*. Academic Press, London.

Wong, K. (2016). Mediation analysis, moderation analysis, and higher order construct modeling in partial least squares structural equation modeling (PLS-SEM): a B2B example using SmartPLS. *Marketing Bulletin, 26,* 1-21.

Woodward, H.E. (1912). *A Study of the Surface Tension of Blood Serum by the Drop Weight Method.* PhD thesis, Columbia University, New York, New York.

Wu, A. H. B. Ed (2006). *Tietz clinical guide to laboratory tests*, 4th Ed. W. B. Saunders Co., St. Louis, MO.

Zaitsev, Sergei Yu, (2018). Dynamic surface tension measurements for animal blood analysis and correlations with related biochemical parameters, *Colloids Interfaces*, 2,5.

315